

2004

THE INTERFERENCE FREE DETERMINATION OF SELENIUM IN ENVIRONMENTAL AND CLINICAL SAMPLES BY ICP-MS

Turner, Justine Clare

<http://hdl.handle.net/10026.1/2491>

<http://dx.doi.org/10.24382/4991>

University of Plymouth

All content in PEARL is protected by copyright law. Author manuscripts are made available in accordance with publisher policies. Please cite only the published version using the details provided on the item record or document. In the absence of an open licence (e.g. Creative Commons), permissions for further reuse of content should be sought from the publisher or author.

**THE INTERFERENCE FREE DETERMINATION OF
SELENIUM IN ENVIRONMENTAL AND CLINICAL
SAMPLES BY ICP-MS**

by

Justine Clare Turner

A thesis submitted to the University of Plymouth
in partial fulfilment for the degree of

DOCTOR OF PHILOSOPHY

Department of Environmental Sciences
Faculty of Science

In collaboration with
LGC
Teddington, Middlesex,
TW11 OLY
UK

February 2004

UNIVERSITY OF PLYMOUTH	
Item No.	900605 8448
Date	23 JUN 2004
Class No.	THESIS 574.586TUR
Cont. No.	
PLYMOUTH LIBRARY	

ABSTRACT

The Interference Free Determination of Selenium in Environmental and Clinical Samples by ICP-MS

Justine Clare Turner

The determination of selenium in environmental and clinical samples by ICP-MS is complicated by both poor sensitivity and severe interferences resulting from both the sample matrix and the argon plasma. The purpose of this study was to investigate ways of overcoming these problems thus enabling Se to be determined both accurately and precisely. A novel procedure for the accurate determination of selenium in serum using electrothermal vaporisation inductively coupled plasma mass spectrometry (ETV-ICP-MS) has been developed. A simple 1:20 dilution of the serum with 1% nitric acid negates the need for a lengthy sample digestion procedure. Several of the interferences normally associated with the analysis of selenium by ICP-MS are successfully eliminated. Analytical method characteristics include; detection limits of approximately 0.1 ng g^{-1} for ^{77}Se and ^{82}Se , short and long term reproducibility between 4.7% and 4.9%, and 3.2% and 3.8% (RSD) for ^{77}Se and ^{82}Se respectively, and accuracy of $\pm 1.81\%$ (^{77}Se) and $\pm 1.10\%$ (^{82}Se) for the certified reference material NIST SRM 1598.

Further development of the procedure involved the application of isotope dilution analysis with the measurement of the $^{82}\text{Se}/^{77}\text{Se}$ isotope ratio, following spiking with selenium enriched in ^{77}Se . Accuracy ($\pm 0.2\%$) and precision ($\pm 1.3\%$) of the method is demonstrated with the analysis of several certified reference materials (TMRAIN-95, LGC 6010, TMDA-54.2 and NIST 1598) where all results fell within the certified limits.

A comparison of the new ETV procedures with established ICP-MS methods involving hydride generation and the use of organic solvents with pneumatic nebulisation was performed. Full uncertainty estimates for each of the procedures investigated were calculated. The uncertainty estimates calculated highlight the improvements in accuracy and precision achievable with isotope dilution analysis, demonstrated by a 2.5 fold improvement in the uncertainty compared with the non-IDMS ETV procedure.

The addition of nitrogen and helium to the different Ar gas streams of the ETV-ICP-MS system was performed. The introduction of both nitrogen and helium to the argon nebuliser and outer gas streams, resulted in a reduction in the interference from argon polyatomic species. Careful optimisation of plasma parameters such as RF power and gas flow rates using a plasma containing 50% helium in the argon outer gas stream, successfully gave rise to a 2-fold improvement in the detection limits for ^{76}Se and ^{78}Se compared with an argon only plasma.

This study has resulted in the successful development of a high accuracy procedure to determine selenium in both environmental and clinical samples. This is of great importance considering the high level of interest regarding selenium and human health matters and the significance of accurate analytical data.

LIST OF CONTENTS

	Page
Copyright Statement	i
Abstract	iii
List of Contents	iv
List of Tables	xi
List of Figures	xiv
Acknowledgements	xix
Authors Declaration	xx
Chapter 1. Introduction	
1. Introduction	1
1.1 Analytical Methods	1
1.2 Inductively Coupled Plasma Mass Spectrometry (ICP-MS)	2
1.2.1 Instrumentation	2
1.2.1.1 Ion source	2
1.2.2 Mass Analyser	3
1.2.2.1 Quadrupole ICP-MS	4
1.3 Interference Problems	5
1.3.1 Polyatomic interferences	5
1.3.2 Isobaric interferences	6
1.3.3 Matrix effects	7
1.3.4 Elemental oxides and doubly charged ions	7
1.4 Solutions to ICP-MS Interference Problems	8
1.4.1 ETV-ICP-MS	8

1.4.2 Hydride generation	9
1.4.3 Mixed gas plasmas	10
1.4.4 Organic solvents	10
1.4.5 High resolution magnetic sector ICP-MS	11
1.4.6 Mathematical correction	12
1.4.7 Dynamic reaction cell/collision cell ICP-MS	13
1.5 The Biological Importance of Selenium	13
1.5.1 Selenium toxicity	14
1.5.2 Selenium deficiency	15
1.5.3 Selenium dietary intake	17
1.5.4 Selenium – isotopes and interferences	17
1.6 A Review of Applications of ICP-MS for the Determination of Selenium in Clinical and Environmental Samples	18
1.6.1 ETV-ICP-MS applications	18
1.6.2 HG-ICP-MS applications	19
1.6.3 Applications using mixed gas plasmas	20
1.6.4 Applications using organic solvents	21
1.7 Aims of the work	22
Chapter 2. Development of an Electrothermal Vaporisation (ETV) ICP-MS Method for the Determination of Selenium in Serum	
2.1 Introduction	24
2.2 Electrothermal Vaporisation	25
2.3 Instrumentation	27
2.3.1 Reagents	28
2.3.2 Sample Preparation	28
2.4 Choice of Matrix Modifier	29

2.5 Optimisation of ETV-ICP-MS Operating Parameters	33
2.5.1 Pyrolysis and Vaporisation	33
2.5.2 Power and Nebuliser Gas	41
2.6 Analytical Performance	43
2.6.1 Linearity	43
2.6.2 Reproducibility	43
2.6.3 Detection Limits	45
2.6.4 Accuracy	45
2.7 Conclusions	49
Chapter 3. Development of an Isotope Dilution Method for the Accurate Determination of Selenium in Serum and Water	
3.1 Introduction	50
3.2 Isotope Dilution Analysis	51
3.2.1 Single IDMS	52
3.2.2 Reverse IDMS	52
3.2.3 Mass Bias	52
3.3 Optimisation of Measurement Parameters	54
3.3.1 Dwell Time	54
3.3.2 Points/Spectral Peak	56
3.3.3 Number of Replicates	56
3.3.4 Peak Measurement Mode	57
3.3.5 Effect of Ca and Zn on $^{82}\text{Se}/^{77}\text{Se}$ Ratio	58
3.4 Accuracy and Precision of Isotope Ratio Measurements	60
3.5 Method Validation	61
3.5.1 Reagents	61
3.5.2 Preparation of IDMS Solutions	63

3.5.2.1 Natural Se Standard	63
3.5.2.2 ⁷⁷ Se Enriched Spike Solution	63
3.5.2.3 Characterisation of the Spike Concentration by Reverse IDMS	63
3.5.3 Preparation of Samples	65
3.6 Analysis of CRMs	65
3.7 Conclusions	67

Chapter 4 . Comparison of Analytical Methods for the Determination of Selenium

4.1 Introduction	68
4.2 Hydride Generation (HG-ICP-MS)	68
4.3 HG-ICP-MS Procedure	69
4.3.1 Instrumentation	69
4.3.2 Reagents	71
4.3.3 Sample Preparation	71
4.3.4 Analytical Performance	72
4.3.4.1 Linearity	72
4.3.4.2 Reproducibility	73
4.3.4.3 Detection Limits	73
4.3.5 Analysis of Certified Reference Materials	73
4.4 Addition of Organic Solvents	76
4.5 PN-ICP-MS Method	77
4.5.1 Instrumentation	77
4.5.2 Reagents	77
4.5.3 Sample Preparation	78
4.5.4 Effect of Butanol on Sensitivity	79
4.5.5 Analytical Performance	81

4.5.5.1 Linearity	81
4.5.5.2 Reproducibility	82
4.5.5.3 Detection Limits	82
4.5.6 Analysis of Certified Reference Materials	83
4.6 Method Comparison	85
4.6.1 Interference Elimination	85
4.6.2 Speed of Analysis	86
4.6.3 Analytical Performance	89
4.6.4 Accuracy and Precision	89
4.7 Conclusions	94
Chapter 5. Uncertainty Estimates for the Determination of Selenium by ICP-MS	
5.1 Introduction	95
5.2 Measurement Uncertainty – Conventional Calibration ICP-MS	96
5.2.1 Recovery, R	98
5.2.2 Dilution Factor, D	98
5.2.3 Precision, P	99
5.2.4 Concentration, C	99
5.3 Preparation of Uncertainty Solutions	100
5.4 Estimation of Uncertainty Contributions	101
5.4.1 Method Recovery, R _m	101
5.4.1.1 Method 1 – HG-ICP-MS	105
5.4.1.2 Method 2 – PN-ICP-MS	106
5.4.1.3 Method 3 – ETV-ICP-MS	106
5.4.2 Dilution factor, D	106
5.4.2.1 Method 1 – HG-ICP-MS	107

5.4.2.2 Method 2 – PN-ICP-MS	107
5.4.2.3 Method 3 – ETV-ICP-MS	107
5.4.3 Precision, P	107
5.4.3.1 Method 1 – HG-ICP-MS	108
5.4.3.2 Method 2 – PN-ICP-MS	108
5.4.3.3 Method 3 – ETV-ICP-MS	108
5.4.4 Concentration of the dilute working standard, $C_{dil}(w/w)$	109
5.4.5 Instrument drift	110
5.5 Calculation of Combined Standard Uncertainty – Conventional Calibration	111
5.6 Estimation of Uncertainty – ETV-ID-ICP-MS Procedure	112
5.6.1 Uncertainty of the masses; m_{zc} , m_{yc} , m_x , and m_y	112
5.6.2 Uncertainty of the mass fractions of the primary natural standard and the spike solution; c_z and c_y	112
5.6.3 Uncertainty of the isotope ratios of the primary natural standard and the spike material; R_z and R_y	114
5.6.4 Uncertainty of the measured isotope ratio of the sample and mass bias blends; R'_B and R'_{Bc}	115
5.6.5 Uncertainty of the prepared isotope ratio of the mass bias blend; R_{Bc}	116
5.7 Comparison of Combined Uncertainty Estimates	117
5.8 Conclusions	122
Chapter 6. Mixed Gas Plasmas	
6.1 Introduction	123
6.2 Instrumentation	124
6.3 Reagents	125
6.4 Nitrogen Addition	126

6.4.1 Nitrogen addition to Ar nebuliser gas – post ETV	126
6.4.1.1 Variation of RF Power	127
6.4.1.2 Variation of Ar flow-rate	130
6.4.2 Nitrogen addition to Ar nebuliser gas – pre ETV	130
6.4.3 Nitrogen addition to Ar outer gas	132
6.4.3.1 Variation of RF power	132
6.4.4 Nitrogen addition as ETV alternative gas	134
6.4.4.1 Variation of RF power	135
6.5 Helium Addition	135
6.5.1 Helium addition to Ar nebuliser gas	136
6.5.2 Helium addition to Ar outer gas	137
6.5.2.1 Optimisation of RF power	138
6.5.2.2 Optimisation of the AR nebuliser gas flow rate	140
6.5.2.3 Optimisation of the outer gas flow rate	140
6.5.3 Comparison of detection limits (He vs Ar)	142
6.6 Trifluoromethane Addition	143
6.6.1 CHF ₃ addition to the Ar nebuliser gas	143
6.7 Conclusions	144
Chapter 7. Conclusions and Future Work	
7.1 Conclusions	146
7.2 Future Work	148
Appendices	150
References	154
Publications	160

LIST OF TABLES

	Page
Chapter 1	
Table 1.1 Isobaric interferences on the cadmium isotopes	6
Table 1.2 Interference from TiO on the major Zn isotopes	8
Table 1.3 Functions of some of the selenoproteins	16
Table 1.4 Polyatomic interferences affecting the selenium isotopes	17
Chapter 2	
Table 2.1 ICP-MS Operating Conditions	27
Table 2.2 ETV Temperature Program	28
Table 2.3 Analytical performance characteristics for the determination of Se in serum by ETV-ICP-MS	44
Table 2.4 Accuracy data from the analysis of internal quality control samples and NIST SRM 1598. Values are expressed as the mean and standard deviations of 3 measurements	46
Chapter 3	
Table 3.1 Effect of signal profile processing on $^{82}\text{Se}/^{77}\text{Se}$ isotope ratio and %rsd data (n=9)	57
Table 3.2 Ratio and significance data obtained from spiking a 10ng g^{-1} Se standard with increasing amounts of Ca and Zn. (n=10)	59
Table 3.3 ICP-MS operating conditions	62
Table 3.4 Isotopic abundance of the spike and natural selenium standards	62
Table 3.5 Accurate weights taken for the preparation of the natural and spike Se standards	63
Table 3.6 Characterisation of the spike for IDMS analysis	64

Table 3.7 Results for the analysis of certified reference materials TMRAIN-95 (spiked rainwater), TMDA-54.2 (spiked soft water), LGC 6010 (hard drinking water) and NIST 1598 (bovine serum) using ETV-ICP-MS and ETV-ID-ICP-MS (n=3)	66
---	----

Chapter 4

Table 4.1 HG-ICP-MS Operating Conditions	70
Table 4.2 Microwave Temperature Program for the digestion of serum samples	70
Table 4.3 Analytical performance characteristics for the determination of Se by HG-ICP-MS	73
Table 4.4 Accuracy data from the analysis of certified reference materials and spiked serum samples by HG-ICP-MS. Values are expressed as the mean and standard deviations of 3 measurements	74
Table 4.5 Recovery results calculated from the analysis of in-house spiked serum samples analysed by HG-ICP-MS	75
Table 4.6 PN-ICP-MS operating conditions	78
Table 4.7 Analytical performance characteristics for the determination of Se by PN-ICP-MS	82
Table 4.8 Accuracy data from the analysis of certified reference materials and spiked serum samples by PN-ICP-MS. Values are expressed as the mean and standard deviations of 3 measurements	84
Table 4.9 Recovery results calculated from the analysis of in-house spiked serum samples analysed by PN-ICP-MS	84
Table 4.10 Interferents and corresponding isotopes alleviated by each of the procedures	85
Table 4.11 Comparison of performance characteristics for each of the methods investigated. (HG-ICP-MS and ETV-ICP-MS = ^{77}Se ,	

Table 4.12 Comparison of data from the analysis of four certified reference materials obtained by the 4 different methods. (HG-ICP-MS and ETV-ICP-MS = ^{77}Se , PN-ICP-MS = ^{78}Se , and ETV-ID-ICP-MS = $^{82}\text{Se}/^{77}\text{Se}$ ratio) 90

Chapter 5

Table 5.1 Preparation of uncertainty solutions by serial dilution of NIST 3149 Se standard 101

Table 5.2 Repeatability data for the analysis of uncertainty solution two 102

Table 5.3 Reproducibility data for the analysis of uncertainty solutions one, two and three 109

Table 5.4 Uncertainty budget for the determination of Se by HG-ICP-MS, PN-ICP-MS and ETV-ICP-MS 111

Table 5.5 Data used to calculate the uncertainty associated with the preparation of the natural Se standard, c_z 113

Table 5.6 Abundance and uncertainty data for the natural primary standard and the enriched spike solution taken from the IUPAC isotopic composition table and the manufacturers certificate respectively 115

Table 5.7 Summary of individual uncertainty terms and combined standard uncertainty for the ETV-ID-ICP-MS methods 117

Table 5.8 Standard and expanded uncertainty estimates for methods 1-4 118

Chapter 6

Table 6.1 Effect of RF power on the signals (I , in counts/s) of a 1% HNO_3 blank, a 10ng g^{-1} Se standard and the S/B ratio, for 2% N_2 in the Ar outer gas 134

Table 6.2 Comparison of detection limits for ^{76}Se and ^{78}Se determined using a 100% Ar plasma and a 50% He plasma 142

LIST OF FIGURES

	Page
Chapter 1	
Figure 1.1 A typical quadrupole ICP-MS instrument	5
Chapter 2	
Figure 2.1 A typical ETV furnace unit showing internal and external gas flow during (a) pyrolysis and (b) vaporisation	26
Figure 2.2 Optimisation of Pd(NO ₃) ₂ matrix modifier	30
Figure 2.3 Effect of pyrolysis temperature on the signal of a 10ng g ⁻¹ Se standard with (a) a standard pyrolytically coated graphite tube, and (b) a L'vov platform pyrolytically coated graphite tube	32
Figure 2.4 Pyrolysis/vaporisation curves for ⁷⁴ Se, ⁷⁷ Se, ⁷⁸ Se and ⁸² Se. 10µl injection of a 10ng g ⁻¹ standard with 10µl of 500µg g ⁻¹ Pd(NO ₃) ₂ modifier	34
Figure 2.5 Pyrolysis curve for ⁷⁷ Se, ⁸² Se and ¹²⁸ Te, 10µl injection of a serum sample (with an approximate Se concentration of 5ng g ⁻¹) Using 10µl of a 500µg g ⁻¹ Pd(NO ₃) ₂ modifier	34
Figure 2.6 The effect of pyrolysis temperature with respect to elimination of Na interference; 10µl injection of a serum sample in 1% HNO ₃ , approximate concentration 5 ng g ⁻¹ . (a) ⁷⁷ Se and ²³ Na signal profiles- pyrolysis temperature 800°C; (b) ⁷⁷ Se and ²³ Na signal profiles – pyrolysis temperature 1200°C	36
Figure 2.7 The effect of pyrolysis temperature with respect to elimination of Cl interference; 10µl injection of a serum sample in 1% HNO ₃ , approximate concentration 5 ng g ⁻¹ . (a) ⁷⁷ Se and ³⁵ Cl signal profiles – pyrolysis temperature 800°C, (b) ⁷⁷ Se and ³⁵ Cl signal profiles - pyrolysis	

temperature 1200°C 37

Figure 2.8 The effect of pyrolysis temperature with respect to elimination of Br interference; 10µl injection of a serum sample in 1% HNO₃, approximate concentration 5 ng g⁻¹.(a) ⁸²Se and ⁷⁹Br signal profiles - pyrolysis temperature 800°C, (b) ⁸²Se and ⁷⁹Br signal profiles - pyrolysis temperature 1200°C 39

Figure 2.9 The effect of vaporisation temperature on ⁷⁷Se signal profile. 10µl injection of a serum sample in 1% HNO₃ - approximate concentration 5ng g⁻¹.(a) Vaporisation temperature of 2300°C; (b) vaporisation temperature of 2600°C 40

Figure 2.10 Effect of RF power on Se signal: 10µl injection of a 10ng g⁻¹ Se standard prepared in 1% HNO₃ 42

Figure 2.11 Effect of argon nebuliser gas flow rate on Se signal; 10µl injection of a 10ng g⁻¹ Se standard prepared in 1% HNO₃ 42

Figure 2.12 Typical signal profiles for a 10µl injection with 10µl 500µg g⁻¹ Pd(NO₃)₂ modifier. (a) 5ng g⁻¹ Se standard in 1% HNO₃; (b) Diluted serum sample - approximate concentration 5ng g⁻¹ 44

Figure 2.13 Results obtained for the analysis of two serum samples, (a) IQC level 1 and (b) IQC level 2. Error bars represent the standard deviations for 3 replicate analyses 47

Figure 2.14 Results obtained for the analysis of two serum samples, (a) IQC level 3 and (b) NIST SRM 1598. Error bars represent the standard deviations for 3 replicate analyses 48

Chapter 3

Figure 3.1 Optimisation of dwell time with respect to ⁸²Se/⁷⁷Se ratio %rsd values (n=5), 10µl injection of a 100ng g⁻¹ Se standard in 1% HNO₃ 55

Figure 3.2 Optimisation of points per spectral peak with respect to $^{82}\text{Se}/^{77}\text{Se}$ ratio %rsd values (n=5), 10 μl injection of a 100ng g $^{-1}$ Se standard in 1% HNO $_3$	55
Figure 3.3 Nine consecutive injections of a serum sample diluted in 1% HNO $_3$, 10 μl injection and approximate concentration of 10ng g $^{-1}$	60
 Chapter 4	
Figure 4.1 Plot of Se concentration vs integrated signal for the 77 and 82 isotopes	72
Figure 4.2 Plots of concentration vs integrated signal for standards prepared in 1% HNO $_3$ and modifier B (containing 1% butanol); (a) ^{77}Se , (b) ^{78}Se and (c) ^{82}Se	80
Figure 4.3 Plots of concentration vs integrated signal for the ^{77}Se , ^{78}Se and ^{82}Se isotopes; calibration standards prepared in modifier B	81
Figure 4.4 Comparison of the time required for sample preparation and analysis of 1 aqueous sample by each of the 4 methods examined	88
Figure 4.5 Comparison of the time required for sample preparation and analysis of 10 aqueous samples by each of the 4 methods examined	88
Figure 4.6 Summary of results obtained by each of the methods investigated; (a) spiked rain water TMRain-95 and (b) spiked soft water TMDA-54.2. The error bars represent the standard deviation from triplicate analyses. The certified level and permitted range of each of the CRMs are represented by the solid and dashed black lines respectively	92
Figure 4.7 Summary of results obtained by each of the methods investigated; (a) hard drinking water LGC 6010 and (b) bovine serum NIST 1598. The error bars represent the standard deviation from triplicate analyses. The certified level and permitted range of each of the CRMs are represented by the solid and dashed black lines respectively	93

Chapter 5

Figure 5.1 Cause and Effect diagram for the determination of Se by ICP-MS with conventional calibration	97
Figure 5.2 Contribution of the different variables to the uncertainty budget; (a) HG-ICP-MS procedure and (b) PN-ICP-MS procedure	119
Figure 5.3 Contribution of the different variables to the uncertainty budget; (a) ETV-ICP-MS procedure and (b) ETV-ID-ICP-MS procedure	120
Figure 5.4 Plot of the results obtained for uncertainty solution two by each of the methods	121

Chapter 6

Figure 6.1 The effect of nitrogen addition to the argon nebuliser gas on the S/B ratio of the 76, 77, 78, 80 and 82 selenium isotopes	128
Figure 6.2 The effect of nitrogen addition to the argon nebuliser gas on 76 and 78 selenium isotopes at (a) 975W RF power and (b) 1075W RF power	129
Figure 6.3 The effect of Ar nebuliser gas flow rate on 76 and 78 selenium isotopes, with the nitrogen flow rate set at 0.041 min^{-1}	131
Figure 6.4 The effect of nitrogen addition to Ar outer gas on S/B ratio for the 76 and 78 Se isotopes with an outer gas flow rate of 0.801 min^{-1}	133
Figure 6.5 The effect of nitrogen addition as ETV alternative gas on the S/B ratio of the 76, 77, 78, 80 and 82 selenium isotopes	135
Figure 6.6 The effect of helium addition to the argon nebuliser gas on the S/B ratio of the 76, 77, 78, 80 and 82 selenium isotopes	136
Figure 6.7 The effect of helium addition to Ar outer gas on S/B ratio of the 76, 77, 78, 80 and 82 Se isotopes	137
Figure 6.8 The effect of RF power on the S/B ratio for ^{76}Se with (a)100% He plasma, (b)50% He plasma and (c)100% Ar plasma	139

Figure 6.9 The effect of RF power on the S/B ratio for ^{78}Se with (a)100% He plasma, (b)50% He plasma and (c)100% Ar plasma	139
Figure 6.10 Effect of Ar nebuliser gas flow rate on S/B ratio of ^{76}Se and ^{78}Se with a 100% He plasma	141
Figure 6.11 Effect of outer gas flow rate on S/B ratio ^{76}Se and ^{78}Se with a 50% He plasma	141

ACKNOWLEDGEMENTS

I would like to thank the following people for their help, support and encouragement throughout the time it has taken me to complete this thesis. Without them I doubt I would ever have got this finished!

Firstly I would like to thank Prof. Steve Hill for his guidance throughout, particularly for his comments and advice on each of the chapters and the time and effort this has taken. I am also grateful to Dr. Hywel Evans for his support in being my second supervisor.

For financial support I would like to acknowledge LGC for funding this work under the DTI National Measurement System Valid Analytical Measurement Programme.

Many thanks go to my colleagues at LGC whom have been a constant source of encouragement, especially Dr. Tim Catterick for his continued support and understanding. In particular I would like to thank Dr. Ben Fairman for his constant nagging (sorry, constructive criticism!) and encouragement over the last six years. His help in enabling me to enrol for the Ph.D. and his continued assistance throughout is very much appreciated.

I would also like to extend my thanks to my friends and family for their help and support, in particular Mum, Dad, Margaret, Derek, Donna and Rob for their frequent offers to babysit Abby whilst I struggled to write up.

Finally I would like to thank Steve for always encouraging and supporting me, and for occupying Abby on Sunday afternoons - McDonalds is appreciative of your financial support!

AUTHOR'S DECLARATION

At no time during the registration for the degree of Doctor of Philosophy has the author been registered for any other University award.

This study was financed by the Department of Trade and Industry as part of the National Measurement System Valid Analytical Measurement Programme in collaboration with LGC Ltd.

Relevant scientific seminars and conferences were regularly attended at which work was often presented; external institutions were visited for consultation purposes and several papers prepared for publication.

Publications

1. "The Use of ETV-ICP-MS for the Determination of Selenium in Serum." Justine Turner, Steve J. Hill, E. Hywel Evans and Ben Fairman. *Journal of Analytical Atomic Spectrometry*.1999, **14**, 121-126.
2. "The Accurate Analysis of Trace Metals in Clinical Samples Using Inductively Coupled Plasma Mass Spectrometry (ICP-MS)." Justine Turner, Ben Fairman and Chris Harrington. *VAM Bulletin*, 1999, **20**, 12-16.
3. "Accurate Analysis of Selenium in Water and Serum Using ETV-ICP-MS with Isotope Dilution." Justine Turner, Steve J. Hill, E. Hywel Evans, Ben Fairman and Celine S. J. Wolff Briche. *Journal of Analytical Atomic Spectrometry*.2000, **15**, 743-736.

Presentations and Conferences Attended

1. "The Use of ETV-ICP-MS for the Determination of Selenium in Serum." Justine Turner, Steve J. Hill, E. Hywel Evans and Ben Fairman. Paper presented at the Clinical Trace Metal Measurement Meeting, 1st July 1998, LGC Ltd, Teddington, UK.

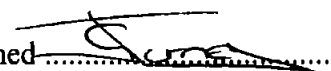
2. "The Use of ETV-ICP-MS for the Determination of Se in Serum." Justine Turner, Steve J. Hill, E. Hywel Evans and Ben Fairman. Paper presented at the Ninth Biennial Atomic Spectroscopy Symposium (BNASS), 8th–10th July 1998, Bath, UK.
3. "The Determination of Selenium in Serum using ETV-ICP-MS." Justine Turner, Steve J. Hill, E. Hywel Evans and Ben Fairman. Paper presented at the University of Plymouth Environmental Sciences Inter-Departmental Meeting, December 1998, Plymouth, UK.
4. "The Determination of Selenium in Serum using ETV-ICP-ID-MS." Justine Turner, Steve J. Hill, E. Hywel Evans and Ben Fairman. Poster presented at the European Winter Conference on Plasma Spectrochemistry, 10th-15th January 1999, Pau, France.
5. "Comparison of ICP-MS Methodologies for the Determination of Selenium in Environmental and Clinical Samples." Justine Turner, Steve J. Hill, E. Hywel Evans and Ben Fairman. Poster presented at the 36th Research and Development Topics in Analytical Chemistry, 12th-14th April 1999, Greenwich, UK.
6. "Selenium and Human Health : High Accuracy Analysis using ETV-ID-ICP-MS." Justine Turner, Steve J. Hill, E. Hywel Evans and Ben Fairman. Poster presented at the Frontiers of Science and Technology Conference, June 1999, NPL, Teddington, UK.
7. "Elimination of Interferences for the Determination of Selenium using ICP-MS." Justine Turner, Steve J. Hill, E. Hywel Evans and Ben Fairman. Paper presented at the University of Plymouth, Environmental Sciences Inter-Departmental Meeting, March 2000, Plymouth, UK.
8. "Estimation of Uncertainties : Determination of Selenium by ICP-MS." Justine Turner, Steve J. Hill, E. Hywel Evans, Ben Fairman and Celine S. J. Wolff Briche. Poster presented at the Tenth Biennial Atomic Spectroscopy Symposium (BNASS), 17th-20th July 2000, Sheffield, UK.
9. "Determination of Selenium by Isotope Dilution ICP-MS: Interlaboratory Comparison with Other Techniques." Justine Turner, Steve J. Hill, E. Hywel Evans and Ben Fairman. Poster presented at the European Winter Conference on Plasma Spectrochemistry, 4th-8th February 2001, Hafjell, Norway.

Awards

1. Best Poster Prize - Isotopic Measurements Session, European Winter Conference on Plasma Spectrochemistry, 10th-15th January 1999, Pau, France.

External Contacts

1. Dr H. Trevor Delves, Southampton General Hospital, Southampton, UK.
2. Dr Margaret Rayman, University of Surrey, Guildford, Surrey, UK.
3. Dr Jennifer Cook, British Geological Survey, Keyworth, Nottingham, UK.

Signed 

Date 16th June 2004

CHAPTER 1

Introduction

1. Introduction

Elemental analysis of clinical and environmental samples has for a long time been considered an important part of biological monitoring. Metal ions play an important role in the well being of humans with different elements exhibiting various different effects. Several elements are essential for life, others are relatively inert, i.e. show little effect unless present in extreme high or low levels, while some exhibit a high toxicity even in low concentrations. In addition to the well-recognised toxic metals such as Al, As, Cd, Hg, Se and Pb, other elements have become a focus of attention. For example, elements used in implants in joint-replacement surgery such as Cr, Co, Ni, and Mo¹, precious metals such as Pt and Rh² present in catalytic converters, and actinides including U, Th and Pu,³ present in the environment from nuclear fuel processing. Recognising the significance of trace elements in human health and the narrow divide between the concentration at which the element is considered deficient, optimal or toxic, it is essential that sensitive, precise and accurate analytical methods are available.

1.1 Analytical Methods

There are numerous analytical procedures available for the analysis of trace elements, with the method of choice dependant on the element to be determined, the matrix and the level at which the element is present. Traditionally atomic absorption spectrometry (AAS) has been used, both flame and furnace methods. Whilst this technique offers adequate detection limits for many applications, in the main it is limited to single element determinations. The growing demand for multi-element analysis has resulted in the comprehensive method development of inductively coupled plasma (ICP) techniques whose main advantage over the AAS procedures is its multi-element capability. ICP together with atomic emission spectrometry (ICP-AES) is readily used for the analysis of clinical samples⁴ but its use is often restricted to the analysis of elements such as sodium,

potassium and calcium, which are present in the body at relatively high levels – there is an average of 94.0mmol l^{-1} Na in whole blood and approximately 1Kg of Ca present in the human body⁵. The analysis of trace levels of metals is better performed using the more sensitive technique of inductively coupled plasma mass spectrometry (ICP-MS).

1.2 Inductively Coupled Plasma Mass Spectrometry (ICP-MS)

Inductively coupled plasma mass spectrometry (ICP-MS) was first developed by the groups of Gray⁶ and Fassel⁷ who successfully combined the highly efficient ion source of an ICP with the great sensitivity of mass spectrometry. The advantages of this technique over other atomic spectrometry procedures such as atomic absorption or atomic emission, are low detection limits, greater sensitivity, a multi-element capability, large linear response range and the ability to measure different isotopes of the same element.

On its introduction to the commercial market approximately 20 years ago, ICP-MS was considered to be an interference free technique. However as the use of the instrumentation developed, it was discovered that like most other analytical techniques, ICP-MS was by no means perfect and several problems soon became apparent. In particular issues surrounding sensitivity and interference were identified which would require alternative analytical approaches to eliminate.

1.2.1 Instrumentation

An ICP-MS consists of two fundamental sections – the ion source and the mass analyser.

1.2.1.1 Ion source

The ion source, the inductively coupled plasma (ICP), is formed from a stream of argon gas flowing through a collection of three concentric quartz tubes called a torch. The

top of the torch is surrounded by a copper coil which is connected to a radio frequency (rf) generator. When an rf current passes through the coil a magnetic field is generated which induces a current in the stream of argon. The argon gas is seeded with electrons which accelerate in the magnetic field causing numerous collisions with the gaseous argon atoms. This results in the ionisation of the argon atoms, which then collide with other atoms thus continuing the ionisation process, and results in a self-sustaining plasma. Sample introduction to the plasma takes place via the central channel of the torch, and is most commonly in the form of an aerosol generated by a pneumatic nebuliser.^{8,9} The aerosol passes into a spray chamber where it is partitioned so that only the smallest droplets progress further into the injector tube and the plasma, with the remaining droplets passing to waste. This removes approximately 98% of the sample. The sample aerosol is carried in a stream of Ar gas into the centre of the plasma where the processes of desolvation, vaporisation, atomisation, excitation and ionisation take place. Once ionisation of the sample has occurred the ions are extracted from the plasma and transferred to the mass spectrometer (MS) for measurement. Due to the pressure difference between the ICP and the MS – the ICP operates at atmospheric pressure and the MS require a vacuum of at least 10^{-9} atm - the ions pass through a sampling interface comprising of pumped vacuum chambers (Figure 1.1). Firstly the ions travel through a sampling cone with an orifice of 1mm in diameter, into an expansion stage with a pressure of approximately 2×10^{-3} atm. Some of the ions then pass through a second cone, the skimmer into a vacuum chamber at less than 10^{-7} atm – the intermediate stage. A set of ion lenses then deflect the resulting ion beam towards the mass analyser, where the ions are separated according to their mass to charge ratio (m/z).¹⁰

1.2.2 Mass analyser

There are various different ICP-MS instruments available on the market utilising a variety of mass analysers. The most frequently used are the quadrupole and the magnetic

sector although there are alternatives currently available such as the time of flight and ion trap.

1.2.2.1 Quadrupole ICP-MS

The quadrupole mass analyser is made up of four parallel electrically conducting metal rods arranged in square geometry, with each pair held at equal but opposite charge. A variable rf/dc ratio is applied to each pair of rods, creating an electric field within the inner region. As ions pass through the rods they experience oscillations, causing them to either collide with the rods or travel through and reach the detector. By adjusting the (rf) voltage applied on the rods it is possible to control which ions will pass through and which will collide. Hence it is possible to scan a mass range simply by altering the (rf) voltage to allow ions of an increasing m/z to pass through. The voltage can also be altered to allow ions of a specific m/z to pass through, rather than performing a sequential scan. This is called peak hopping and permits the analysis of ions with different masses to be measured, thereby only collecting data for the peaks of interest. Figure 1.1 shows a schematic diagram of a typical quadrupole ICP-MS. Advantages of the quadrupole mass analyser include low cost of manufacture, reliability and ease of use. However it can only be operated in sequential mode and is limited to single mass resolution.

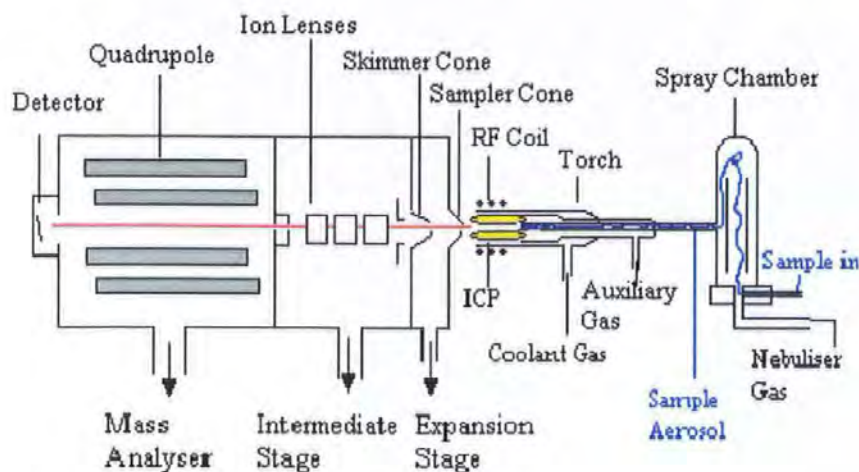


Figure 1.1 A typical quadrupole ICP-MS instrument

1.3 Interference Problems

ICP-MS is the obvious method of choice for trace metal determinations due to its excellent sensitivity, low detection capability (2-3 orders of magnitude greater than ICP-AES), and speed of analysis. However the technique suffers from several types of interference which lessen the accuracy and precision of its measurements. This may simply be a lack of sensitivity and ultimately poor precision due to a build-up of salt deposits on components such as the torch and cones, however more fundamental interference problems centre around the presence of ions with the same nominal m/z ratio as the isotope of interest. These interferences can be divided into four different areas: polyatomic, isobaric, matrix effects and the formation of oxides and doubly charged ions.

1.3.1 Polyatomic interferences

Polyatomic species form after ionisation of the sample has occurred and arise from the plasma gases, atmospheric gases, water, dissolution reagents and components of the

sample matrix. This kind of interference produces a positive bias on the isotope being measured. Examples include $^{40}\text{Ar}^{35}\text{Cl}^+$ on ^{75}As , $^{40}\text{Ar}^{16}\text{O}^+$ on ^{56}Fe , $^{40}\text{Ar}^{12}\text{C}^+$ on ^{52}Cr , $^{40}\text{Ar}^{40}\text{Ar}^+$ on ^{80}Se , $^{16}\text{O}^{35}\text{Cl}^+$ on ^{51}V and $^{32}\text{S}^{16}\text{O}^{16}\text{O}^+$ on ^{64}Zn . Polyatomic interferences are mainly encountered between the mass range 12-120, with the most concentrated between 40-80.^{11,12} All aspects of sample preparation, ie. use of mineral acids or organic solvents, need to be carefully evaluated in order to minimise the interference problems.

1.3.2 Isobaric interferences

Isobaric interference occurs when there is a direct isobaric overlap between isotopes of different elements. This can be quite a common occurrence as demonstrated with the example of Cd, detailed in Table 1.1. Even with 7 available isotopes only ^{111}Cd is free from any kind of isobaric interference. Fortunately, it is extremely rare for an isotope with a high abundance to have a severe isotopic overlap, the worst case being ^{40}Ar (99.6% abundance) on ^{40}Ca (96.94% abundance).

Cd Isotope	% Abundance	Interference	% Abundance
106	1.25	Pd	27.33
108	0.89	Pd	26.46
110	12.49	Pd	11.72
111	12.8	-	-
112	24.13	Sn	0.97
113	12.22	In	4.3
114	28.73	Sn	0.65

Table 1.1 Isobaric interferences on the cadmium isotopes.

1.3.3 Matrix effects

Matrix effects manifest themselves in two main forms. Firstly, high concentrations of matrix components in the sample can interfere with the plasma thereby affecting the ionisation efficiency of the analytes. This will cause a discrepancy in the signals obtained for the standards and samples. The most well known example of this type of effect is the introduction of high concentrations of easily ionisable elements (EIE) such as Na, Ca and K. The introduction of high concentrations of these elements can “cool” the plasma causing a reduction in the excitation temperature, thus less energy is available for the production of ions and a suppression in the signal of the sample containing the matrix is observed. Ramsey and Thompson¹⁰⁶ studied the effect of calcium on the sensitivity of various analytes including Li and Cu using ICP-AES, and observed a decrease in the excitation temperature of approximately 100K in the presence of a 1% Ca matrix. The authors also noted a decrease in excitation temperature of approximately 20K with as little as $100\mu\text{g ml}^{-1}$ Ca present in the matrix.

The mass transport efficiency of the analyte (amount of analyte that reaches the plasma) can also be effected by EIEs. This effect has been seen with the analysis of Mn in the presence of several EIEs¹³. The authors have reported a decrease in the mass transport efficiency of a $100\mu\text{g ml}^{-1}$ Mn only solution by 15% and 40% in the presence of equimolar concentrations (0.05M) of Na and K respectively. This is attributed to an increase in the overall mass loading of the solution having an effect on amongst other factors the density of the solution.

1.3.4 Elemental oxides and doubly charged ions

This type of interference occurs when there are significant amounts of another analyte present in the sample and either its oxide (mass +16) or doubly charged ions (mass/2) cause a spectral overlap on the analyte isotope of interest. Oxide formation is particularly troublesome when trying to determine trace amounts of zinc in the presence of titanium. As shown in Table 1.2 the major Zn isotope suffers from a significant interference from

TiO. The other Zn isotopes are also hampered by interference from TiO but to a lesser extent. The formation of doubly charged ions is characteristic of elements which have a low second ionisation potential for example Ba ($E_{II} = 10.00\text{eV}$) and Sr ($E_{II} = 11.03\text{eV}$)¹⁴.

Zn Isotope	% Abundance	TiO Interference % Abundance
64	48.6	73.62
66	27.9	5.39
67	4.1	0.01
68	18.8	0.01

Table 1.2 Interference from TiO on the major Zn isotopes.

1.4 Solutions to ICP-MS Interference Problems

There are numerous different ways of overcoming the interferences described above. These include optimisation of the sample matrix, (i.e. choice of digestion/dilution acid), alteration of the plasma gas, alternative sample introduction techniques and mathematical corrections.

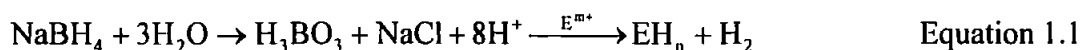
1.4.1 ETV-ICP-MS

The use of electrothermal vaporisation to convert a sample to the vapour state has been in use for a long time in atomic spectrometry in the form of graphite furnace atomic absorption (GFAAS).¹⁵⁻²⁰ The ETV unit used with an ICP-MS is very similar to that normally used on an atomic absorption instrument. The electrothermal vaporisation process involves the programmed heating of a graphite tube held between two graphite contacts. With careful optimisation of the heating program, the sample, which is deposited onto the tube, is dried, ashed and then vaporised. A stream of argon carries the vapour to the plasma where atomisation and ionisation take place. This method of sample

introduction can, with the correct combination of matrix modifier, eliminate many major polyatomic interferences. For example, the significant interference from $^{40}\text{Ar}^{16}\text{O}$ on ^{56}Fe is reduced due to the elimination of all of the moisture from the system. As the Fe is vaporised and swept into the plasma, no ArO polyatomics are formed due to the lack of O_2 .²¹ Chemical modifiers are often used with electrothermal techniques to thermally stabilise the analyte. This allows higher ash temperatures to be used which aids the removal of the matrix. Hence with the appropriate chemical modifier the ETV can be used to selectively vaporise certain analytes before others. In the case of ^{75}As which suffers from the $^{40}\text{Ar}^{35}\text{Cl}^+$ interference, and ^{77}Se which is hampered by interference from the $^{40}\text{Ar}^{37}\text{Cl}^+$ species, the use of an optimised temperature programme together with a $\text{Pd}(\text{NO}_3)_2:\text{Ni}(\text{NO}_3)_2$ modifier, successfully separated the interfering Cl^- species from the analytes of interest.²²

1.4.2 Hydride generation

This form of sample introduction makes use of the fact that elements such as As, Sb, Te, Ge and Se form covalent gaseous hydrides on reaction with a strong reducing agent.⁸ The sample, often prepared in hydrochloric acid, mixes with a sodium borohydride solution in a mixing chamber and the gaseous hydrides are formed. (Equation 1.1)



A gas/liquid separator is used to separate the volatile hydrides from the reagents, which are then swept into the plasma by a stream of argon. This process separates the analyte from the sample matrix, thereby reducing potential sources of polyatomic molecules and increasing the sample transport efficiency. Hydride generation techniques are widely reported in the literature²³⁻³⁰ and are often used for the determination of As in seawater³¹ since As determination by conventional nebulisation is hampered by the formation of

$^{40}\text{As}^{35}\text{Cl}^+$. However with hydride generation, once the hydride (AsH_3) is produced it is separated from the reaction reagents and transported to the plasma. Despite the high concentration of HCl in the sample matrix, the Cl is not in a volatile form, and so not transported past the gas/liquid separator and hence preventing the formation of $^{40}\text{Ar}^{35}\text{Cl}^+$.

1.4.3 Mixed gas plasmas

The introduction of an additional gas to either the outer, intermediate or injector gas flow of the plasma has been shown by numerous workers to reduce spectroscopic and non-spectroscopic interferences.³²⁻³⁸ Mixed gas plasmas have a greater thermal conductivity compared to a conventional Ar ICP due to the higher thermal conductivities of the individual gases (Ar has a thermal conductivity of $0.0162\text{JK}^{-1}\text{m}^{-1}\text{s}^{-1}$ and He has a thermal conductivity of $0.141\text{JK}^{-1}\text{m}^{-1}\text{s}^{-1}$) and hence can improve the degree of ionisation for high ionisation energy elements. As well as an enhanced sensitivity, polyatomic levels, in particular oxides, are reduced. The most common gases used are N_2 , He , and O_2 although Xe ,³⁹ CH_4 , C_2H_4 ⁴⁰ and CHF_3 ⁴¹ have also been used. The ratio of several polyatomic ions ($^{40}\text{Ar}^{35}\text{Cl}^+$, $^{40}\text{Ar}^{36}\text{Ar}^+$, $^{40}\text{Ar}^{37}\text{Cl}^+$ and $^{40}\text{Ar}^{38}\text{Ar}^+$) to an In internal standard was shown by Evans and Ebdon³⁷ to decrease when N_2 was introduced to the carrier gas. Similar observations have been reported by Hill *et al.*⁴², who added methane to the nebuliser gas and noted a reduction in the levels of ArCl^+ , ArO^+ , ClO^+ and MO^+ . Despite the advantages achieved with mixed gas plasmas such as He and Xe they are seldom used routinely due to their high cost, and the considerably cheaper gases such as H_2 , N_2 and O_2 have practical issues to consider such as the need for higher gas flows and forward powers in order to sustain a stable plasma.

1.4.4 Organic solvents

The use of organic solvents for signal enhancement is documented by various authors.⁴³⁻⁴⁶ The addition of small amounts of solvent can alter the physicochemical

properties of the sample solution, decreasing the viscosity and contributing to a smaller droplet size. This in turn aids the efficiency of nebulisation and improves desolvation in the plasma, resulting in an improved signal. However a more likely explanation for signal enhancement is due to an electron transfer mechanism.²⁸ The introduction of an organic solvent leads to a higher population of carbon ions in the expansion chamber. The degree of ionisation of an analyte is improved by transfer of an electron to a carbon ion from an element with an ionisation energy lower than carbon (IE 11.26eV). This mechanism is supported by Larsen and Sturup⁴⁷ who report a 3.5-4.5 fold enhancement in signal for As (IE 9.82eV) and Se (IE 9.75eV) in the presence of 3% methanol.

1.4.5 High resolution magnetic sector ICP-MS

Magnetic sector instruments are more frequently being used to measure elements that are difficult to analyse using a quadrupole instrument.⁴⁸⁻⁵¹ As with the quadrupole instruments described in section 1.2, ions that have been skimmed from the plasma pass through a mass analyser before reaching a detector. However, unlike the quadrupole mass analyser the magnetic sector instruments use a magnet to separate the ions. Ions exiting from the skimmer cone are accelerated through an electric sector which acts as an energy filter. The ions then pass through a magnetic field where they are deflected, with heavier ions being deflected to a greater extent. This arrangement of the electric and magnetic sectors is classed as normal geometry, however the opposite arrangement with the electric sector being placed after the magnetic sector also exists and is termed reverse geometry. The ion beam is then directed through a narrow slit and onto the detector. The narrowness of this slit means that a much smaller ion beam is directed to the detector compared with that produced by a quadrupole instrument. This results in a much greater achievable resolution but also leads to a loss in sensitivity due to less of the ions passing through the slit and onto the detector. Resolution is calculated according to equation 1.2.

$$R = \frac{M}{\Delta M} \quad \text{Equation 1.2}$$

where R is resolution, M is mass (m/z) and ΔM is peak width at 5% peak height. Quadrupoles typically operate at a resolution between 12 and 350, whereas magnetic sectors can run at resolutions greater than 10000. At resolutions of up to 3500 the majority of the common polyatomic interferences for the transition elements (masses 40-80) can be overcome. For example Moens et al.⁴⁸ demonstrated that at resolutions of approximately 2500, the interference from $^{35}\text{Cl}^{16}\text{O}^+$ on $^{51}\text{V}^+$, $^{40}\text{Ar}^{12}\text{C}^+$ on $^{52}\text{Cr}^+$ and $^{40}\text{Ar}^{16}\text{O}^+$ on ^{56}Fe could be negated.

1.4.6 Mathematical correction

This type of correction involves the measurement of a second isotope of the interfering species and then applying a correction factor to the analytical isotope signal taking into account the abundances of the species involved. The advantage of this approach is that on some instruments this type of correction is completely automated and fully controlled by the instrument software. One example of this type of correction is given below in Equation 1.2 which corrects the ^{94}Zr isotope for isobaric interference from ^{94}Mo by monitoring the ^{95}Mo isotope intensity.⁵²

$$i(^{94}\text{Zr}) = i(^{94}) - (i(^{95}) \times (a(^{94}\text{Mo}) / a(^{95}\text{Mo}))) \quad \text{Equation 1.2}$$

where i = intensity at the specified mass, and a = abundance of the isotope.

By monitoring the intensity of the non-interfering isotope ^{95}Mo , and knowing the ratio of naturally occurring $^{94}\text{Mo} : ^{95}\text{Mo}$, it is possible to subtract the intensity of the interfering isotope from the total intensity. However this form of correction is mainly applicable when the intensity of the interfering species is considerably smaller than that of the analyte isotope of interest.

1.4.7 Dynamic reaction cell/ collision cell ICP-MS

Dynamic reaction cell (DRC) or collision cell (CC) instruments involve passing the ion beam, through a cell pressurised with a gas or mixture of gases. The interfering species are then removed by collisional dissociation and/or gas phase chemical reactions. The DRC employs the principle of reacting the interfering species with a gas such as NH_3 ,⁵³ O_2 ⁵⁴ or CH_4 ,⁵⁵ to convert it into a new species with a m/z ratio different from the analyte of interest. This approach has been used by Simpson et al,⁵⁴ who successfully used oxygen as a reaction gas to remove the oxide based interferences hampering the determination of the noble metals. Collision cell instruments exploit the fact that polyatomic interferences have a larger cross-sectional area than the mono-atomic analyte of interest and as such will undergo a greater number of interactions with the reaction gas, thus losing more kinetic energy. The difference in energy between the analyte and interference can then be used to separate them via an energy filter. Reyes⁵⁶ and co-workers have successfully measured Se in biological materials by measuring the $^{78}\text{Se}/^{77}\text{Se}$ and $^{80}\text{Se}/^{77}\text{Se}$ isotope ratios, when using H_2 as the collision cell gas.

1.5 The Biological Importance of Selenium

Selenium is an essential trace element with a natural abundance of approx. 0.09ppm in the earth's crust, and can be found in rocks, minerals, fossil deposits and volcanic material.⁵ Selenium levels in soil vary widely with average levels ranging from 0.1-2.0ppm. Its chemical speciation and total concentration largely determine its availability to plants and thus entry into the food chain. It is present as a water soluble selenate in alkali soil and as such is available to plants, but as an insoluble ferric selenite in acidic soil and therefore unavailable.

The public perception of selenium has gone through several changes during the last 50 years. In the 1930s it was classed as a toxic element, then as a carcinogen in the 1940s, an

essential element in the 1950s and then an anti-carcinogen in the 1960s and 1970s. As such this illustrates the marginal difference between essentiality and toxicity and explains the great interest in Se and its role in biochemistry, particularly as both an excessive and insufficient intake of selenium can have serious health implications.

1.5.1 Selenium toxicity

Selenium toxicity in its most acute form has been found to be fatal to both animals and humans. Several cases of “blind staggers” - lameness, damaged hooves and emaciation - have been reported in farm animals that have consumed highly seleniferous plants. Similar symptoms such as hair and nail loss, tooth decay, skin lesions and, in severe cases, abnormalities of the nervous system have been reported in humans. An example of selenium toxicity was reported in the early 1960s, when inhabitants of a remote mountainous area in the mid-west of China suffered severe hair and nail loss, mottled teeth, and peripheral anaesthesia (pins and needles) and pain in the extremities.⁵⁷ It was discovered that vegetables and grain consumed by the affected villagers contained extremely high concentrations of selenium compared to similar foods grown in non-seleniferous regions. Cereals were found to contain approximately 200 times more selenium than some grown in a normal soil region and a difference of greater than 45000-fold was observed between the selenium levels of green turnips grown in the area compared with turnips from a selenium deficient region. The diet of the local inhabitants was restricted mainly to plant products grown locally, which meant that the average daily intake of selenium was exceptionally high. This was evident in the case of one resident whose blood selenium level was recorded to be $7.5\mu\text{g ml}^{-1}$, approximately 1000 times greater than the average level recorded for residents in a neighbouring area. The source of the high selenium level of the crops was found to be due to a high level of biologically

available selenium in the soil - $354\mu\text{g Kg}^{-1}$ of water soluble selenium in soil from the affected area compared to $2.8\mu\text{g Kg}^{-1}$ in soil from a non-seleniferous area.

1.5.2 Selenium deficiency

Selenium as the amino acid selenocysteine, is a component of various selenoproteins that have important enzymic functions (Table 1.3). Recognising the role of these selenoproteins helps to explain why selenium deficiency is linked with so many diseases and health conditions such as white muscle disease (WMD), a nutritional muscular dystrophy primarily affecting lambs and calves, which if the limbs of the animal are affected can cause stiffness and difficulty in walking, or if the heart muscles are affected can result in heart failure and death. A survey carried out in 1961 concluded that in New Zealand 20-30% of the total sheep stock at that time were at risk of developing selenium deficient conditions, including WMD.⁵⁷ Conditions observed in humans include Keshan Disease – an often fatal cardiomyopathy - and Kaschin-Beck Disease – a type of osteoarthritis, both reported in a region of China where the soil was extremely low in selenium.⁵⁷ Other health issues include a compromised immune system, rheumatoid arthritis and cirrhosis of the liver⁵ and more recently selenium deficiency has been associated with cancer. Selenium deficiency has also been linked with people relying on Total Parenteral Nutrition (TPN) as their main source of nutrition. TPN is a method of feeding nutrients through an intravenous line to patients whose digestive systems do not function. Severe gastrointestinal problems such as Crohn's disease can impair selenium absorption resulting in selenium deficiency, hence it is important that TPN solutions contain selenium. Due to the links between selenium and cancer, numerous workers have investigated the effect of selenium supplementation at supra-nutritional levels ($>200\mu\text{g}$ per day compared with "adequate" levels of $60-75\mu\text{g}$ per day) and whether this would afford greater protection. A study carried out at the New York Dental Hospital showed that

supplementation with Se could result in an increased production of cytotoxic T-lymphocytes and natural killer cells, which are able to destroy tumour cells. Several other studies have been performed where by blood or tissue samples have been taken from a group of healthy individuals who are then monitored to see if they develop cancer. Such studies have revealed that the effectiveness of Se for cancer reduction is strongest in men and in relation to prostate, lung and liver cancers. A Nutritional Prevention of Cancer (NPC) trial carried out in the USA, investigated if selenium supplementation could in fact reduce the risk of cancer. 1312 individuals with a history of non-melanoma skin cancer were given either placebo or 200µg Se per day. The findings indicated that those participants receiving selenium showed 50% lower total cancer mortality and 37% lower total cancer incidence, with the strongest benefit observed in those individuals with the lowest Se status at the beginning of the trial .⁵⁸

Selenoprotein	Function
Glutathione peroxidase	Maintains cell membrane integrity by removing hydrogen peroxide and lipid and phospholipid hydroperoxides
Iodothyronine deiodinase	Produces and controls the level of active thyroid hormone
Selenoprotein P	Has antioxidant and transport functions. Protects cells lining blood vessels
Selenoprotein W	Involved in skeletal and cardiac muscle metabolism
Selenoprotein N	Linked to congenital muscular dystrophy
18 kDa selenoprotein	Found in kidney and other organs

Table 1.3 Functions of some of the selenoproteins.⁵⁹

1.5.3 Selenium dietary intake

The UK recommended daily intakes of selenium are 75µg and 60µg for males and females respectively. The current UK average level is between 34µg and 39µg, considerably lower than the levels reported in 1974 of between 60µg and 63µg.⁵⁹ Food sources rich in selenium are brazil nuts, kidney, liver, crab and shellfish, however the reported reduction in UK daily intakes is mainly attributed to the reduced importation of North American selenium rich wheat. This was previously favoured for bread making due to its high protein content which aids the baking process. Currently European varieties of wheat are generally used, which contain much lower amounts of selenium.

1.5.4 Selenium – isotopes and interferences

The determination of selenium by ICP-MS is complicated for two main reasons. Firstly the ionisation energy is high, resulting in only 30% ionisation in the plasma and hence poor sensitivity.⁶⁰ Secondly all of the six naturally occurring isotopes suffer from interferences (see Table 1.4). Both of these factors can contribute towards high background levels, poor detection limits and ultimately biased analytical results. Consideration of the health implications overviewed earlier highlights the significance of selenium in environmental and clinical studies, and thus how important it is that sensitive, precise and accurate analytical methods are available.

Se Isotope	% Abundance	Interfering Species
⁷⁴ Se	0.89	⁴⁰ Ar ³⁴ S ⁺ , ³⁷ Cl ₂ ⁺
⁷⁶ Se	9.36	³⁶ Ar ⁴⁰ Ar ⁺ , ³⁸ Ar ³⁸ Ar ⁺ ,
⁷⁷ Se	7.63	⁴⁰ Ar ³⁷ Cl ⁺ , ⁴⁰ Ar ³⁶ Ar ¹ H ⁺
⁷⁸ Se	23.78	³⁸ Ar ⁴⁰ Ar ⁺
⁸⁰ Se	49.61	⁴⁰ Ar ⁴⁰ Ar ⁺
⁸² Se	8.73	¹ H ⁸¹ Br ⁺ , ⁸² Kr ⁺

Table 1.4 Polyatomic interferences affecting the selenium isotopes.

1.6 A Review of Applications of ICP-MS for the Determination of Selenium in Clinical and Environmental Samples

ICP-MS with pneumatic nebulisation has been used for the determination of selenium in serum.⁴³ The procedure employed dilution of serum with a mixture of reagents required to prevent blockage of the nebuliser. Standards containing 'blank' bovine serum and with butanol added were used in order to eliminate any matrix differences. A detection limit of $1.5\mu\text{g l}^{-1}$ was achieved. Several authors have documented ICP-MS detection with pre-concentration using ion-exchange resins. Jiang and co-workers⁶¹ used Dowex 1-X8 resin for the analysis of water samples but found the best results were obtained when using a standard addition procedure. Ebdon *et al.*⁶² developed a similar for the determination of selenium in biological samples following microwave digestion. A flow-injection system was utilised for the on-line elution of analytes from an alumina column. 1.0ng ml^{-1} detection limits were observed.

1.6.1 ETV-ICP-MS applications

The use of ETV-ICP-MS for the determination of As, Sb and Se in aqueous matrices is addressed by Fairman and Catterick.²² Complex interactions between the analyte and modifier are discussed, with details of the optimisation process and the resulting compromise conditions required for a simultaneous analysis. The procedure overcomes negative interferences on Se in the presence of high concentrations of HCl. Good results for several reference materials are documented with detection limits of $\leq 0.08\text{ng g}^{-1}$. Ir coated graphite tubes were investigated by Pozebon and co-workers.⁶⁵ Reduction of the blank signal and an increased sample throughput owing to the pre-treated tubes are discussed. An ETV-ICP-MS procedure using polyhydroxy compounds to enhance sensitivity is reported.⁶⁶ The authors report a detection limit of 0.01ng ml^{-1} for Se with mannitol as the matrix modifier compared with a detection limit of 0.50ng ml^{-1} in the

absence of a modifier. Ultrasonic slurry sampling (USS) coupled with ETV-ICP-MS for the determination of Se in fish samples is discussed.⁶⁷ Good agreement between results obtained using a standard additions procedure and the certified values for two reference materials are shown.

1.6.2 HG-ICP-MS applications

Due to the enhanced sensitivity achieved with hydride generation, numerous procedures have been published based on this technique. Rayman *et al.*²³ used an adapted ICP torch for the introduction of hydrides to the plasma. A lengthy sample preparation procedure was used for the digestion of serum samples followed by generation of the hydrides. The influence of Cu and Fe on the Se signal was investigated but the authors found that no adverse effects were observed at the levels of Cu and Fe likely to be present in serum. A negative bias on the materials analysed was reported. The performance of HG-ICP-MS was compared with GFAAS by M. Haldimann *et al.*⁶³ Both methods gave good agreement with acceptable results for the reference materials analysed. Quijano and co-workers²⁴ reported a detection limit of 35ng l⁻¹ when using a flow injection-HG system. Off-line conversion of Se^{VI} to Se^{IV} is required prior to hydride formation. The linear range of the method was limited to 30µg l⁻¹. An isotope dilution method based on HG-ICP-MS has been documented by Ting and co-workers.²⁵ Hydrides are formed on-line with measurement of the ⁸²Se/⁷⁷Se and ⁷⁴Se/⁷⁷Se ratios. Absolute detection limits of 0.2-0.9ng Se are reported. The analysis of several CRMs indicated a negative bias in most cases. Mestek *et al.*²⁶ compared the techniques of ICP-MS, HGAAS, ETAAS and ICP-OES for the analysis of whole blood. The authors concluded that ICP-OES was unsuitable for blood analysis due to poor sensitivity, and ETAAS was difficult to optimise with acceptable results only achieved when using a standard additions procedure. The ICP-MS and HGAAS procedures showed good agreement with the ICP-MS method being favoured due

to greater automation and speed of analysis. A detection limit of 0.10ng g^{-1} for Se in water is reported by Bowman *et al.*²⁷ The procedure involves off-line conversion of Se^{VI} to Se^{IV} and on-line formation of the hydrides using a flow injection system. The effect of the transition metals on the hydride generation system is investigated. Approximately 50% reduction of the Se signal was observed in the presence of $100\mu\text{g g}^{-1}$ Cu. Hall and Pelchart³⁰ developed a HG-ICP-MS procedure for the analysis of geological samples, and have detailed the effect of interfering analytes such as Bi, Fe, and La on the signal. The spray chamber of an ICP-MS was successfully used as a gas/liquid separator by Zhang and co-workers.²⁹ A limit of determination of $0.01\mu\text{g l}^{-1}$ and recovery values in the region of 85% for SRM 1643c (Water) are reported. A continuous flow HG system was used by Santosa *et al.*³¹ for the determination of Se in sea water. A detection limit of 0.5ng l^{-1} is reported. Enhancement of the Se signal in the presence of methanol was also observed. Moor⁶⁴ and colleagues used a modified spray chamber as a gas/liquid separator for the determination of Se in biological samples. Results for the analysis of two biological reference materials agreed well with the certified values when using both external calibration and isotope dilution methodologies.

1.6.3 Applications using mixed gas plasmas

Evans and Ebdon³⁷ investigated the addition of N_2 to the Ar carrier gas and illustrated that the ratio of several polyatomic ions ($^{40}\text{Ar}^{35}\text{Cl}^+$, $^{40}\text{Ar}^{36}\text{Ar}^+$, $^{40}\text{Ar}^{37}\text{Cl}^+$ and $^{40}\text{Ar}^{38}\text{Ar}^+$) to In internal standard decreased with N_2 introduction. Two mechanisms for this effect are suggested by the authors - a reduction in the ionisation temperature of the plasma with a simultaneous increase in the kinetic energy, may result in a suppression of the ionisation of some polyatomic species and increase their breakdown, or that a competitive formation of ArC^+ , ArO^+ and ArN^+ occurs in the expansion chamber which would lead to a decrease in the formation of the interfering ions detailed above. Laborda *et al.*³⁵ introduced N_2 to the

aerosol carrier gas and observed that the intensities of the polyatomic species ArAr^+ , ArCl^+ and ClO^+ decreased with both an increase in the N_2 concentration of the carrier gas, and an increase in the total carrier gas flow rate. However the intensities of the analytes decreased in a similar manner. The authors also investigated the effect of spray chamber temperature and found that an increase in the ArAr^+ signal was associated with an increase in temperature. This observation supports the theory of several workers who suggest that a low spray chamber temperature (which results in a reduced aerosol water content) may significantly reduce oxide and doubly charged ion formation. A slight worsening of the detection limits for Se in food digests is reported when using a N_2 -Ar plasma compared with an Ar only plasma. A similar procedure was adopted by van der Velde-Koerts and de Boer³⁶ with the multi-element analysis of environmental samples. An optimum N_2 carrier gas flow of $4\text{-}6\text{ ml min}^{-1}$ was established with higher gas flows giving rise to greater background signals and increased levels of doubly charged ions. A reduction in the levels of polyatomic interferences by a factor of 1.5 to 3 is reported.

The use of a helium ICP-MS for the determination of As and Se in urine has also been addressed.⁶⁸ Advantages over an Ar plasma include elimination of mass spectral interferences arising from Ar or species containing Ar, and more easily ionised elements due to the higher energy of He plasma species. The absence of spectral features above mass 40 mean that the determination of ^{80}Se is possible. Analysis of NIST SRM 2670 (urine) gave 85% recovery when using a standard addition method with internal standardisation.

1.6.4 Applications using organic solvents

The use of organic solvents for signal enhancement and interference elimination is widely documented. Larsen and Sturup⁴⁷ report a 3.5-4.5 fold enhancement in signal for As and Se in the presence of 3% methanol, but observed a similar increase in the signal-to-

noise ratio. Krushevskaja and co-workers⁶⁷ have addressed the application of water soluble tertiary amines on As and Se signals. An enhancement in the signals together with a reduction in the ArCl interference was observed. The advantage of amines over additives such as Triton X-100, ethanol and glycerol are owed to their neutralisation and complexing properties. A lower dilution factor is needed and problems of corrosive attack of the ICP-MS cones can be ruled out. The addition of 4% ethanol to diluted serum and urine samples is reported by Goossens and colleagues.⁴⁴ The authors show that As and Se can be accurately measured in a chlorine matrix with a combination of ethanol addition and nebuliser gas flow-rate optimisation. Olivas *et al.*²⁸ studied the effect of several organic solvents on the Se signal, using both pneumatic nebulisation and HG sample introduction modes. Results show that several polyatomic interferences can be reduced with addition of alcohol to the system and that a 10-fold enhancement of the Se signal can also be achieved.

1.7 Aims of the work

Although ICP-MS has fast become one of the mainstay analytical techniques in many areas of inorganic analytical chemistry, many problems still exist for a wide variety of analytes and matrices. Despite the introduction of 3rd and 4th generation quadrupole and high resolution magnetic sector ICP-MS instrumentation many important analyses are still hampered by unresolved interferences or lack of sensitivity.

The aim of this study was to evaluate the analysis of both environmental and clinical samples using ICP-MS instrumentation, with the focus being the inherent difficulties of determining total Se in serum. A variety of sample introduction techniques such as ETV-ICP-MS, HG-ICP-MS, PN-ICP-MS with the addition of organic solvents and the use of mixed gas plasmas have been investigated, for their ability to overcome spectroscopic and non-spectroscopic interferences. The analysis of certified reference

materials and 'real' samples was performed with the aim of evaluating and comparing the analytical performance of each procedure. Finally isotope dilution analysis was investigated in order to achieve the highest accuracy and precision, along with experiments to establish a full uncertainty estimate to underpin the data obtained.

CHAPTER 2

Development of an Electrothermal Vaporisation (ETV) ICP-MS

Method for the Determination of Selenium in Serum

2. Development of an Electrothermal Vaporisation (ETV) ICP-MS Method for the Determination of Selenium in Serum

2.1 Introduction

The determination of selenium in serum by ICP-MS is hampered by several problems. The first ionisation energy of selenium is high, resulting in an ionisation efficiency of only 30% in the plasma which leads to low signals and poor sensitivity. The majority of the selenium isotopes also suffer from spectroscopic interferences and matrix effects, which often result in signal suppression.

Hydride generation (HG-ICP-MS) techniques have been used to overcome some of these problems. Greater sensitivity is attainable owing to the improved sample delivery rate and reduction of interferences is achieved due to analyte removal from the matrix. However, lengthy sample preparation procedures are generally required to convert the non-hydride forming organic selenium compounds present in the sample to Se (IV), so that the volatile hydrogen selenide can be formed.

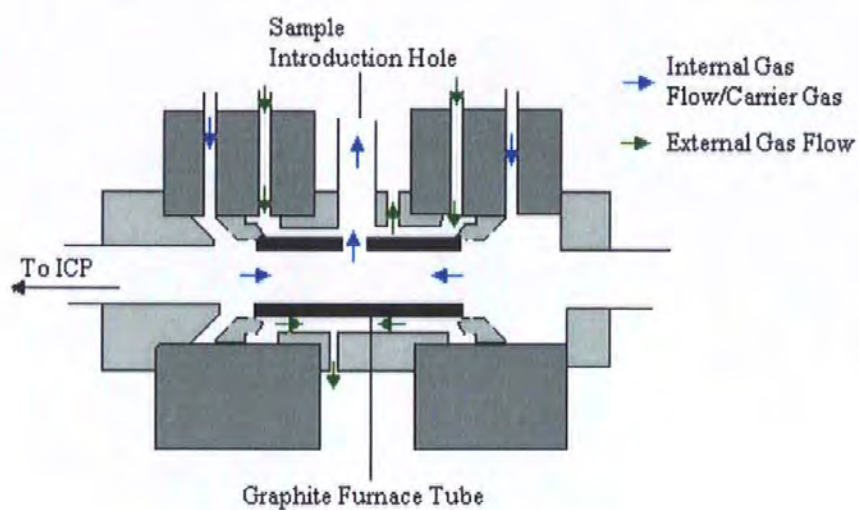
An alternative and more direct method is electrothermal vaporization (ETV) coupled with ICP-MS detection. This technique has the advantage of using very small sample sizes (typically 5-50 μ l), an important consideration when dealing with clinical samples which may be of limited size, and unlike hydride generation does not require lengthy sample preparation procedures. Elimination of interferences is also feasible with this method. With careful optimisation of the temperature program it is possible to control the vaporization of interfering elements so that they do not arrive at the plasma at the same time as the analyte under investigation.

This chapter describes the development of an ETV-ICP-MS procedure for the analysis of Se in serum. Optimisation of the ETV temperature program including the successful elimination of several interferences, together with evaluation of the procedure using spiked sera and a certified reference material is described in detail.

2.2 Electrothermal Vaporisation

When using electrothermal vaporisation the sample is deposited into a small graphite tube which is electrically heated in a programmed fashion. The graphite tube is held between two graphite contact cylinders. On initiation of a temperature program, a current up to approximately 500 amps is applied to the tube. As the temperature of the tube increases, the processes of drying, matrix pre-treatment and thermal dissociation into free atoms can be separated and optimised in turn.⁶⁹ During the process the interior and exterior of the tube are purged with argon to prevent combustion at high temperatures. The external gas stream flows through the contact cylinders, and around the graphite tube, exiting via the sample introduction hole. The internal gas stream passes through the graphite tube and also exits via the sample introduction hole. The external gas stream flows constantly, but the internal gas stream only flows during the program cycle. This flow of inert gases cools the tube and removes solvent and matrix vapours. During the vaporisation stage the sample introduction hole is sealed so that all of the gaseous sample is transferred to the plasma and none is able to escape. Figure 2.1(a) and (b) shows a typical unit with representation of the gas flows during pyrolysis and vaporisation.

(a)



(b)

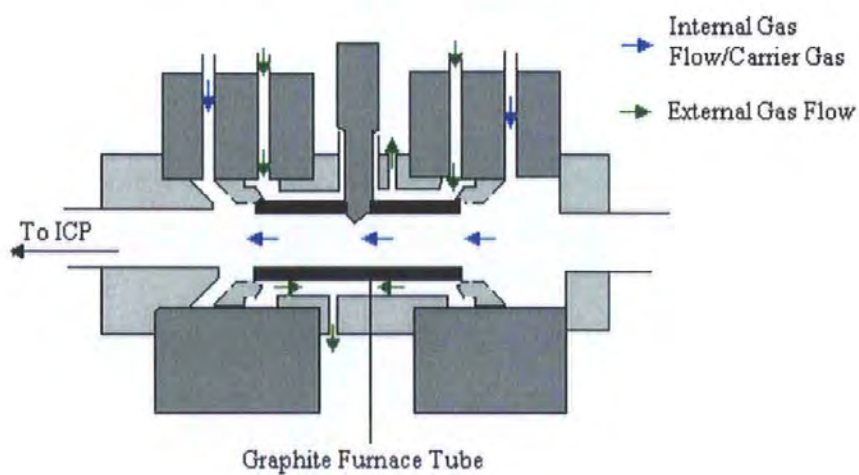


Figure 2.1 A typical ETV furnace unit showing internal and external gas flows during (a) pyrolysis and (b) vaporisation.⁶⁹

2.3 Instrumentation

An ELAN 5000A ICP-MS instrument coupled to an HGA 600MS ETV unit with an AS60 autosampler attachment (Perkin Elmer, Beaconsfield, UK) were used throughout this work. A 140cm long PTFE tubing (0.6cm id) was used to connect the furnace to the ICP-MS. The optimised operating conditions for the ICP-MS instrument and the ETV temperature program are given in Table 2.1 and Table 2.2 respectively. Optimisation of the ICP-MS instrument (i.e. lens settings, resolution, oxide and doubly charged ion formation) was performed using conventional nebulisation prior to coupling the instrument to the ETV unit.

ICP-	
Power	1150W
Plasma Gas	15.0 l min ⁻¹
Auxiliary Gas	0.80 l min ⁻¹
Nebuliser Gas	0.95 l min ⁻¹
Cones	Pt
Lenses P	48
B	43
S	45
E	25
Parameter File -	
Dwell Time	15ms
Sweeps/Reading	3
Readings/Replicate	60
Points Across Peak	1
Resolution	Normal
Masses	⁷⁴ Se
	⁷⁷ Se
	⁷⁸ Se
	⁸² Se

Table 2.1 ICP-MS Operating Conditions

Sample Volume 10 μ l Modifier Volume 10 μ l		Injection Speed 60% Read Delay 2.5sec				
Step	Temperature / $^{\circ}$ C	Ramp /s	Hold /s	Gas l min $^{-1}$		Read
				Internal	External	
Dry 1	110	10	15	0.3		
Dry 2	120	10	45	0.3		
Pyrolysis	1100	10	45	0.3		
Vaporisation	2600	0.5	1	0.3	0.95	Yes
Clean	2700	0.0	1		0.95	
Cool	20	15	1		0.95	

Table 2.2 ETV Temperature Program

2.3.1 Reagents

All solutions were prepared using high purity deionised water (18M Ω , Elga, High Wycombe, Buckinghamshire, UK). Stock solutions (1000 μ g ml $^{-1}$) of Se and Te (internal standard) (Alfa, Johnson Matthey, Royston, UK) were used. Working standards were prepared daily by dilution in 1% m/m HNO $_3$, ultrapure Ultrex II grade acid (JT Baker(UK), Milton Keynes, Buckinghamshire, UK). Palladium(II)nitrate (Sigma, Poole, Dorset, UK) was used to prepare the chemical modifier solution.

2.3.2 Sample Preparation

Initial work centred on the analysis of Se standards prepared in 1% HNO $_3$. Due to the viscous nature and limited quantity of the serum samples, it was necessary to identify a suitable diluent to dilute the samples. Several workers^{70,90} have opted for diluents containing EDTA, mainly for the analysis of whole blood where it is required to prevent coagulation. Five different diluents were examined based on these previous publications, these were; i) 1% HNO $_3$ acid; ii) 1% NH $_3$; iii) 0.2% NH $_3$: 0.1% Triton-X 100; iv) 0.0002M ammoniumEDTA reagent (containing 0.2% NH $_3$ and 0.1% Triton-X 100) and v) 0.002M

sodiumEDTA reagent (containing 0.2% NH₃ and 0.1% Triton-X 100). A 1+19 dilution of the serum was utilised with each of the diluents. A series of 10ng g⁻¹ Se standards were prepared in each of the diluents and the intensity of the signal for each measured. Examination of the Se signal from pyrolysis to vaporisation showed that the Se intensity was significantly reduced in the presence of both of the EDTA reagents, and to a lesser extent in the presence of 1% NH₃ or the NH₃: Triton-X-100 solution. This may be due to the complex make-up of the reagents 'swamping' the Se signal and resulting in signal suppression. The best signal was obtained for the standard prepared in 1% HNO₃ and this was therefore used as the diluent in future work.

2.4 Choice of Matrix Modifier

The use of matrix modifiers with electrothermal techniques is well established. In ETV-ICP-MS an enhancement in signal on addition of a chemical modifier is attributed to a more efficient transport of the vaporised analyte to the plasma.⁷¹ Matrix modification is also important to avoid losses of volatile analytes during the ashing stage via the formation of more stable analyte species.⁷² It has become clear that the choice of matrix modifier is dependant on both the analyte under investigation and the surrounding matrix. In this study numerous chemical modifiers were examined including, Pd(NO₃)₂, Pd(NO₃)₂:Ni(NO₃)₂, Pd(NO₃)₂:Mg(NO₃)₂, ascorbic acid and Pd(NO₃)₂:Mg(NO₃)₂:ascorbic acid. Ascorbic acid proved to be the most unsuccessful modifier examined as it resulted in total signal suppression. Initial work with a modifier made up of Mg(NO₃)₂ and Pd(NO₃)₂ both present at 10µg g⁻¹, was encouraging with a significant increase in the signal obtained for a 10ng g⁻¹ Se standard compared to that obtained with either no modifier or when using ascorbic acid. The concentration of both the Mg(NO₃)₂ and Pd(NO₃)₂ in the combined modifier were both increased with little effect. On examination of each of the solutions separately it was observed that Mg(NO₃)₂ alone produced very little signal where as a

solution of $\text{Pd}(\text{NO}_3)_2$ gave rise to a signal comparable to that obtained with the combined modifier but with improved peak shapes. An experiment was then undertaken to establish the optimum concentration of this modifier. This was carried out by examination of the changes in signal of a 10ng g^{-1} Se standard in 1% HNO_3 with increasing $\text{Pd}(\text{NO}_3)_2$ concentration (see Figure 2.2). Findings indicated that $10\mu\text{l}$ of a $100\mu\text{g g}^{-1}$ $\text{Pd}(\text{NO}_3)_2$ solution was consistent with a maximum signal, i.e. approximately 4000cps for ^{78}Se , approximately 2000cps for ^{82}Se and approximately 1100cps for ^{77}Se (blank subtracted).

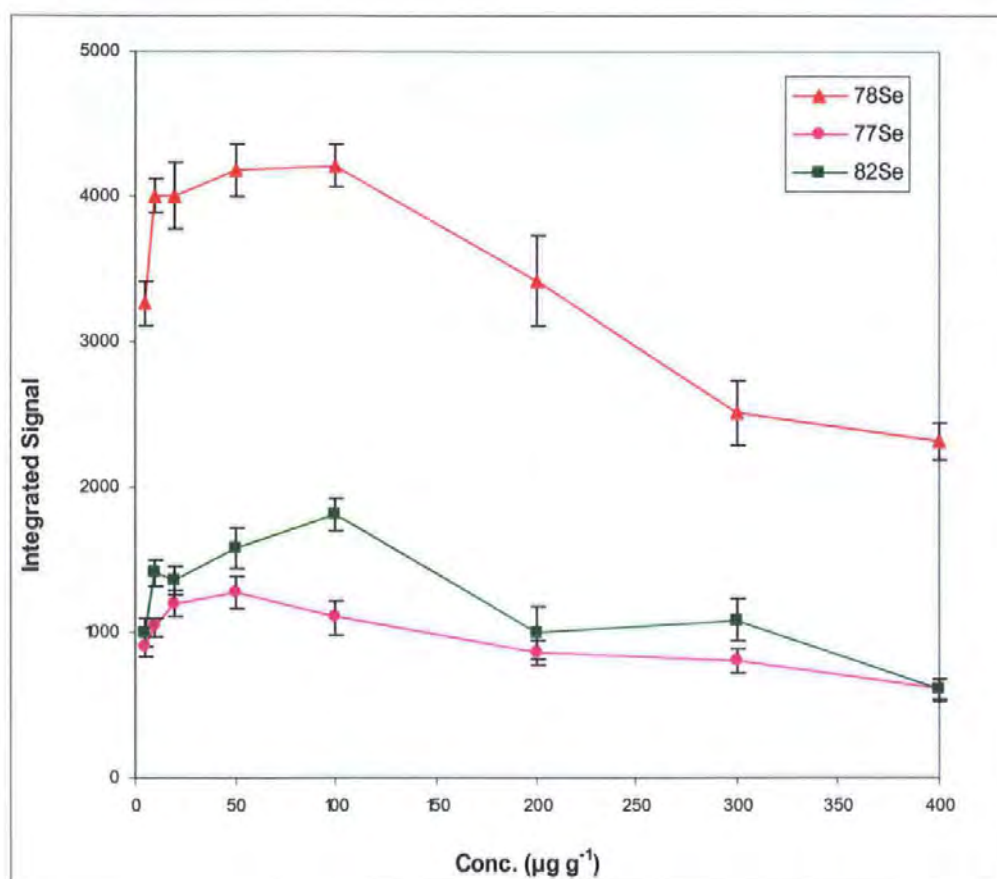


Figure 2.2 Optimisation of $\text{Pd}(\text{NO}_3)_2$ matrix modifier.

This initial work with matrix modifiers was performed using standard pyrolytically coated graphite furnace tubes, however these were found to be unreliable with large changes in both signal intensity and peak shape from day to day. A L'vov platform pyrolytically coated graphite tube was therefore used for all further work. The advantages of this type of tube have been documented by several authors^{73,74} who describe the platform furnace tube at a stabilised "steady state" temperature. A comparison was made between the two types of graphite tube with the analysis of a 10ng g⁻¹ Se standard at increasing pyrolysis temperatures. Data showed that despite an eventual decrease in signal with an increase in pyrolysis temperature, a more consistent signal was obtained with the L'Vov tube than with a non-platform graphite tube, as illustrated in Figure 2.3(a) and (b). This supports the work of Slavin *et al.*⁷² who demonstrated the differences between analyte atomisation from the furnace wall and the platform.

On analysing a serum CRM (NIST 1598 bovine serum), low results were initially obtained when using a 100µg g⁻¹ Pd(NO₃)₂ modifier and pyrolysis temperatures in excess of 1000°C. On monitoring the Se signal through both the pyrolysis and vaporisation stages, it was noted that in addition to the Se peak observed at approximately 60sec (i.e. during vaporisation) a smaller Se peak was seen at approximately 10sec corresponding to the pyrolysis stage. This suggests that a more volatile Se species was forming in the serum matrix that wasn't present in the Se standard. Numerous experiments were performed with different modifiers to try and overcome this problem. Ni(NO₃)₂ was investigated but was unsuccessful as the initial peak was still evident. The gaseous modifier trifluoromethane (CHF₃) was examined as it had been reported⁷⁵ that this gave rise to a considerable increase in sensitivity for the analysis of uranium and thorium by ETV-ICP-MS. Unfortunately no improvements in signal were noted, only a considerable build of carbon on the furnace tube and ETV contact cylinders. Eventually it was discovered that using the Pd(NO₃)₂ modifier as discussed earlier, but at a higher concentration of 500µg g⁻¹, successfully overcame this problem with little effect on overall sensitivity.

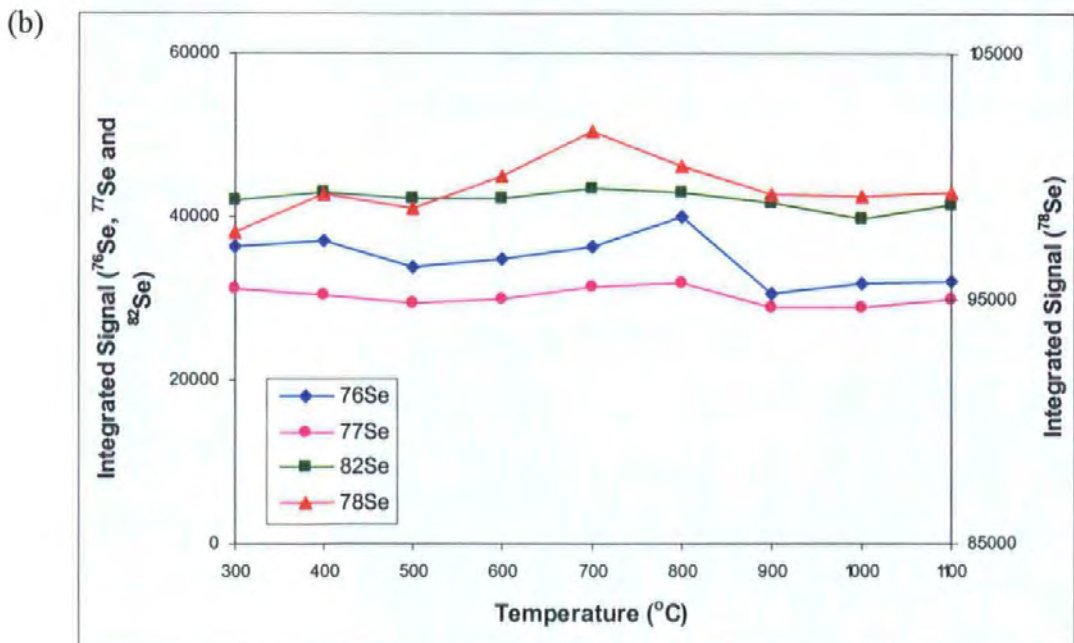
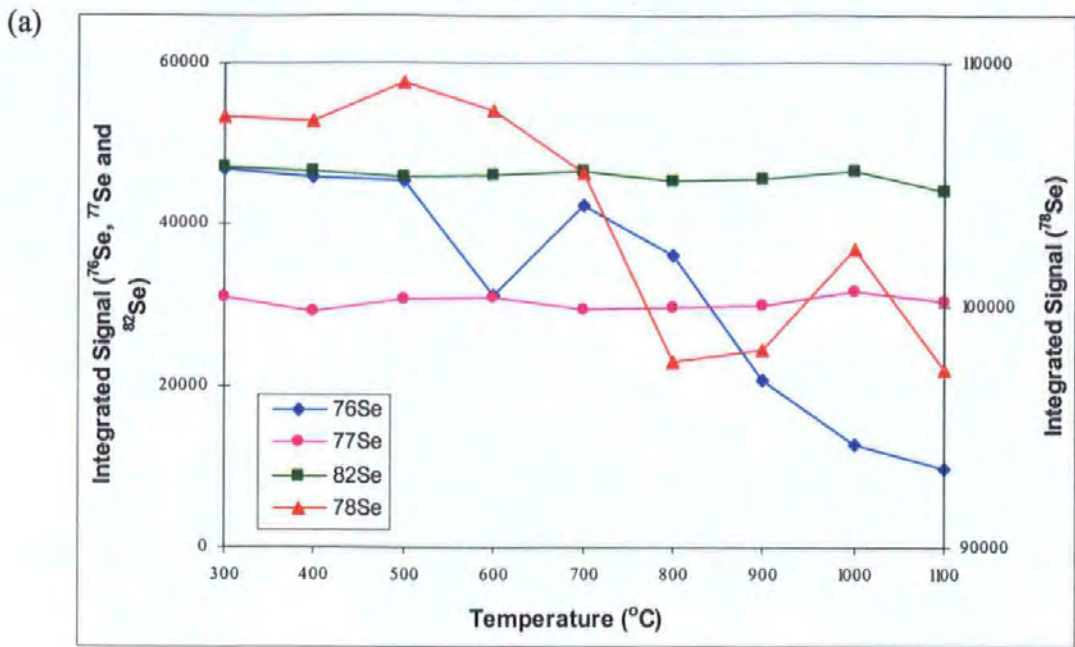


Figure 2.3 Effect of pyrolysis temperature on the signal of a 10ng g^{-1} Se standard with (a) a standard pyrolytically coated graphite tube, and (b) a L'vov platform pyrolytically coated graphite tube.

2.5 Optimisation of ETV-ICP-MS Operating Parameters

2.5.1 Pyrolysis and Vaporisation

The main stages of any electrothermal vaporisation program are the pyrolysis (matrix removal) and vaporisation (dissociation of atoms) processes. Parameters at each of these stages, i.e. ramp rate, temperature and hold time, were evaluated to establish the optimum conditions. Pyrolysis and vaporisation temperatures were optimised by the repeated analysis of a 10ng g^{-1} Se standard at increasing temperature settings. Temperature curves constructed with the data from these experiments can be seen in Figure 2.4. For the optimisation of the pyrolysis temperature the vaporisation temperature was set at 2600°C , and for the vaporisation temperature experiment, the pyrolysis temperature was set at 1100°C . These are typical temperature settings used in many ETV programs.

The pyrolysis curves in Figure 2.4 show a stable signal between 500°C and 1300°C , and a decrease in signal at temperatures above this, suggesting that a pyrolysis temperature within the range mentioned would be suitable. Due to the fact that the graphite tube degrades with the number of firings, it was decided that a pyrolysis temperature midway in the range rather than at the higher end would be chosen, to minimise the detrimental affect on the lifetime of the tube. A temperature of 800°C was selected and a repeat experiment using a serum sample performed. Figure 2.5 shows the response of the ^{77}Se , ^{82}Se and ^{128}Te (internal standard) signals with an increase in temperature in the presence of the serum matrix. Suppression of the Te signal and to a lesser extent the selenium signal, can be seen at lower temperatures, indicating that a higher temperature is required to ensure complete removal of the serum matrix.

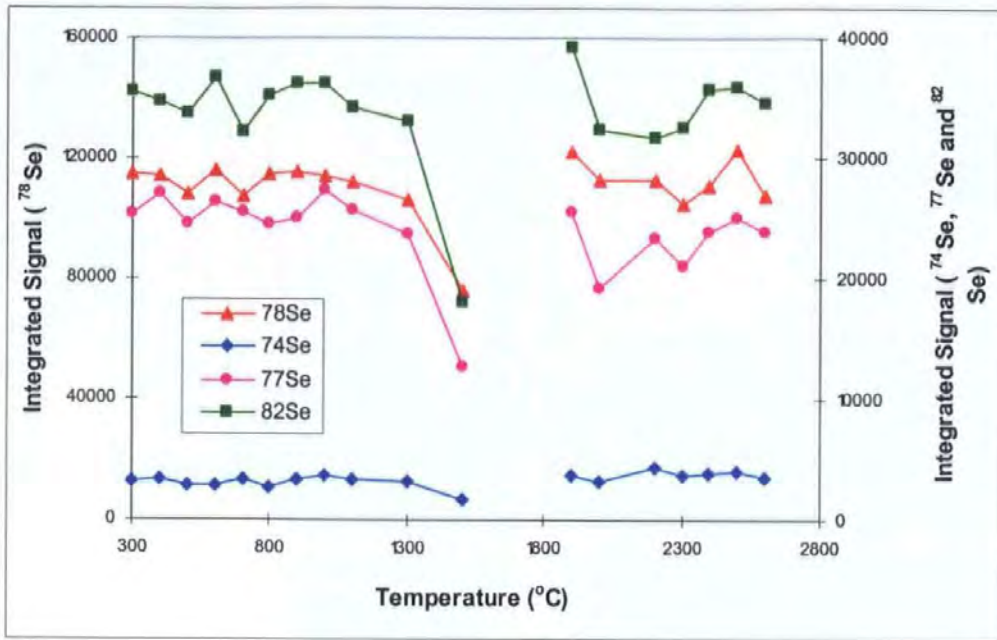


Figure 2.4 Pyrolysis/vaporisation curves for ^{74}Se , ^{77}Se , ^{78}Se and ^{82}Se . 10 μl injection of a 10ng g $^{-1}$ standard with 10 μl of 500 $\mu\text{g g}^{-1}$ Pd(NO $_3$) $_2$ modifier.

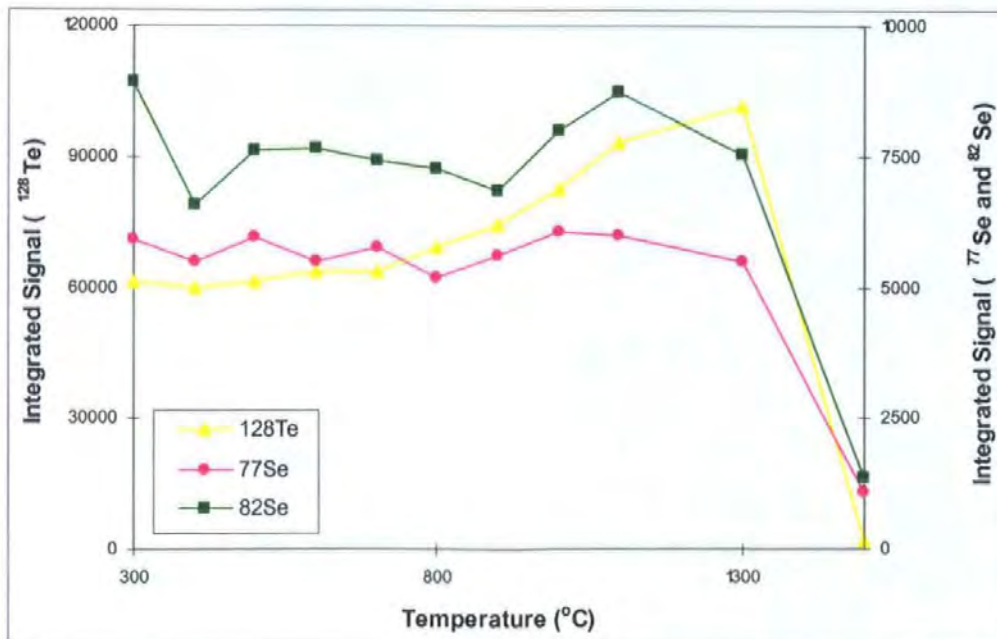


Figure 2.5 Pyrolysis curve for ^{77}Se , ^{82}Se and ^{128}Te . 10 μl injection of a serum sample (with an approximate Se concentration of 5ng g $^{-1}$). Using 10 μl of a 500 $\mu\text{g g}^{-1}$ Pd(NO $_3$) $_2$ modifier.

Serum contains high concentrations of components such as sodium, chlorine and bromine. Examination of these analytes alongside Se in the proposed system, gave clear evidence of their role as potential interferents. Na is an easily ionised element (EIE) which can effect the mass transport efficiency of analytes - the amount of analyte that reaches the plasma and ultimately the signal intensity. O'Hanlon *et al.*¹³ investigated the effect of several EIEs with a plasma emission system, demonstrating a reduction in the transport efficiency of Mn in the presence of Na. Figure 2.6(a) shows the signal profiles of ⁷⁷Se and ²³Na at a pyrolysis temperature of 800°C. The detector was desensitised at m/z 23 using the Omnirange option in the ELAN software used for this study. This enabled the Na signal to be plotted on the same axis as the Se in order to gain a direct comparison between the two signals. As can be seen the Na signal coincides directly with the Se signal, resulting in large amounts of Na ions in the ETV transfer line and plasma at the same time as the analyte of interest. This could potentially effect the transport and ionisation efficiency of Se, thus causing a suppression of the signal. An increase in the pyrolysis temperature to 1200°C, has successfully separated the two signals, with the Na vaporising earlier (Figure 2.6(b)).

Similar responses were observed with Cl and Br signals. Figure 2.7 illustrates the problems presented by Cl on ⁷⁷Se. The formation of ⁴⁰Ar³⁷Cl⁺ ions in the plasma would enhance the signal at m/z 77, coinciding with the ⁷⁷Se isotope, leading to high background signals, poor detection limits and biased analytical results. From Figure 2.7(a) and (b) it can be seen that at 800°C the Cl signal profile is overlapping with the Se signal. However an elevated pyrolysis temperature of 1200°C has separated the Cl from the Se resulting in the interference free analysis of ⁷⁷Se.

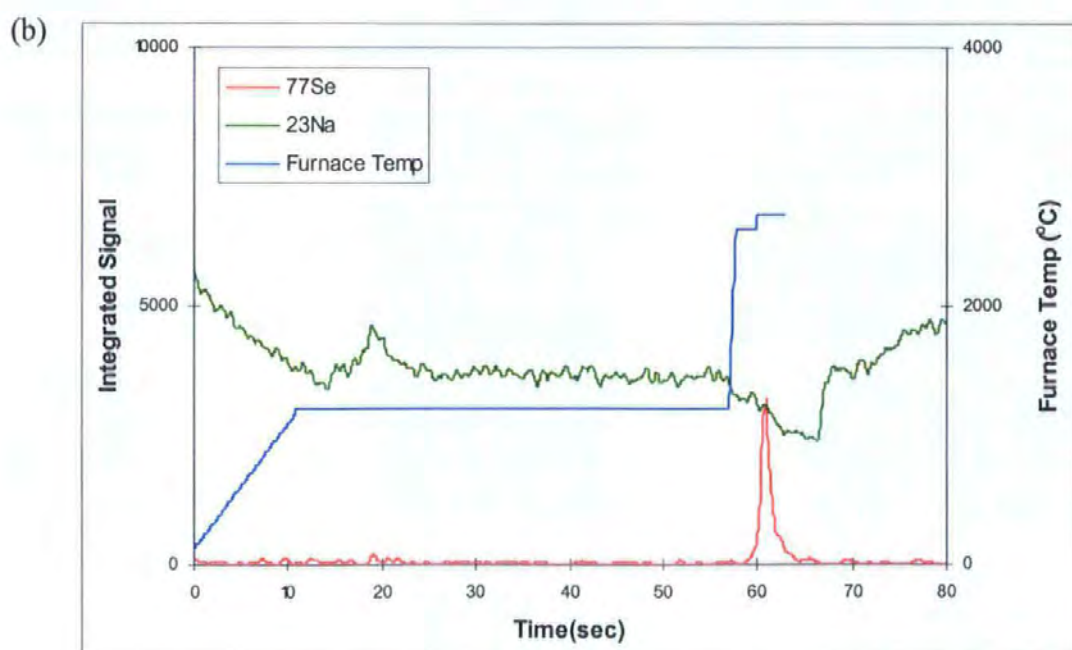
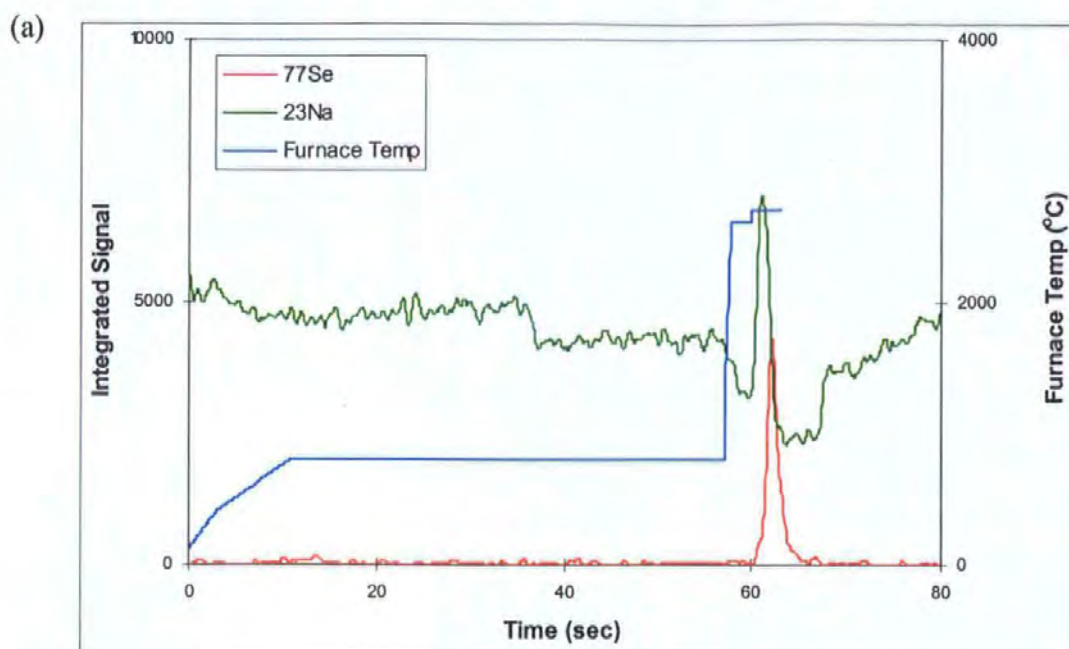


Figure 2.6 The effect of pyrolysis temperature with respect to elimination of Na interference; 10 μl injection of a serum sample in 1% HNO_3 , approximate concentration 5 ng g^{-1} . (a) ^{77}Se and ^{23}Na signal profiles, pyrolysis temperature 800 $^{\circ}\text{C}$, and (b) ^{77}Se and ^{23}Na signal profiles, pyrolysis temperature 1200 $^{\circ}\text{C}$.

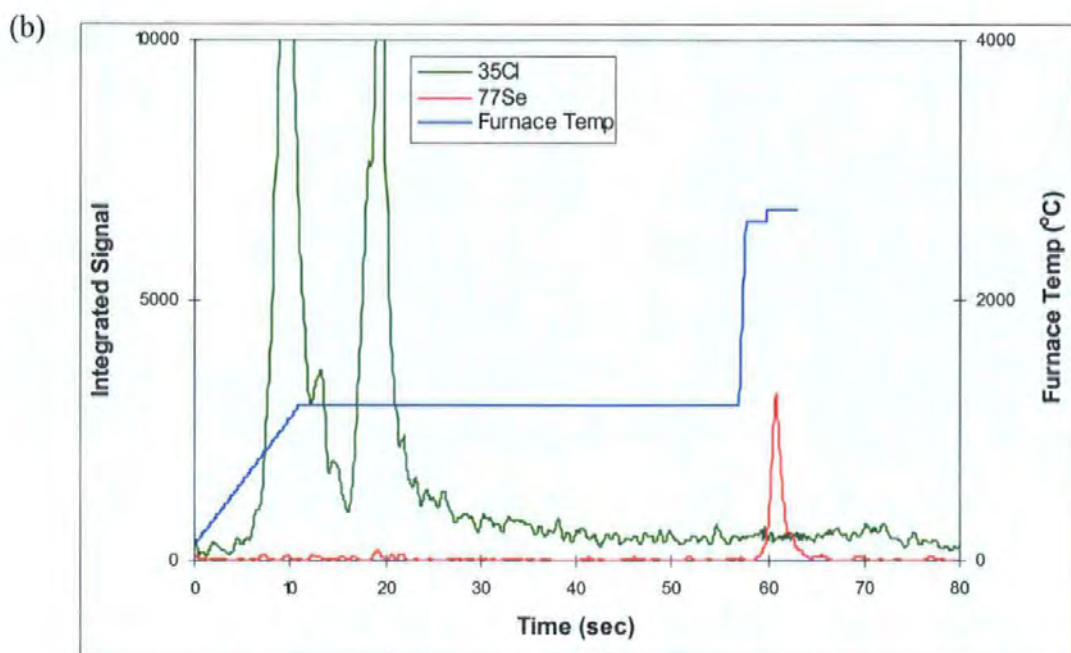
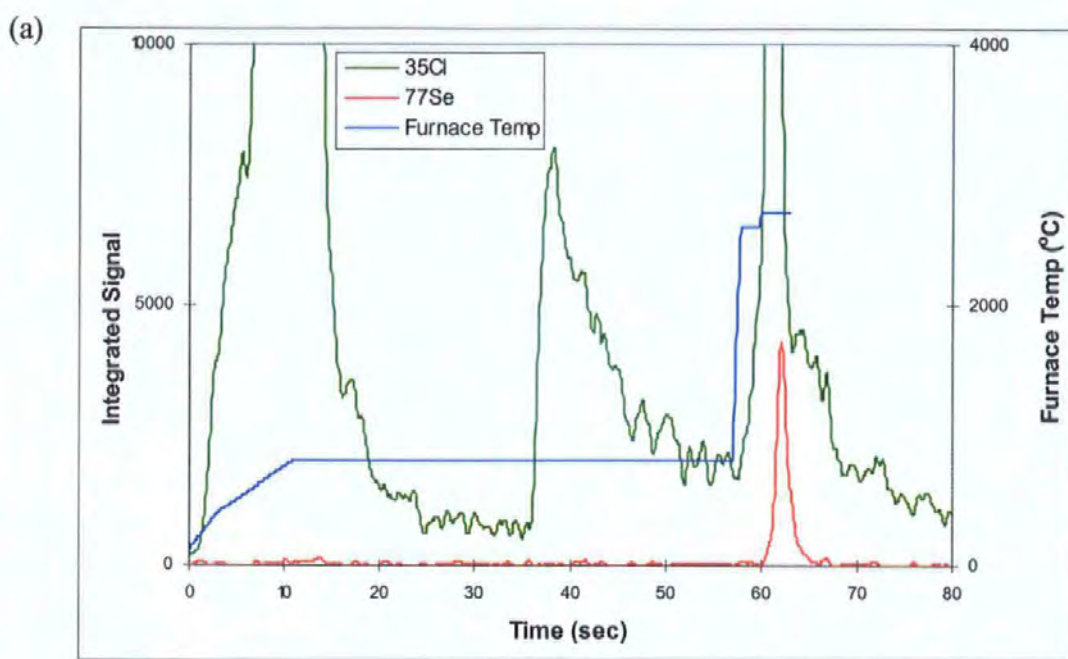


Figure 2.7 The effect of pyrolysis temperature with respect to elimination of Cl interference; 10 μl injection of a serum sample in 1% HNO_3 , approximate concentration 5 ng g^{-1} . (a) ^{77}Se and ^{35}Cl signal profiles, pyrolysis temperature 800 $^{\circ}\text{C}$, and (b) ^{77}Se and ^{35}Cl signal profiles, pyrolysis temperature 1200 $^{\circ}\text{C}$.

Bovine serum (used to prepare the Internal Quality Control (IQC) samples donated by Dr T. Delves, Southampton University and NIST 1598 discussed later in section 2.6.4) contain high levels of bromine. The combination of ^{81}Br with hydrogen produces HBr with a m/z of 82, coinciding with the ^{82}Se isotope. Again at 800°C the Br signal overlaps with the Se signal (Figure 2.8(a)), but is successfully removed at the higher temperature of 1200°C (Figure 2.8(b)). The degree of interference from HBr is further reduced by the elimination of water vapour. With conventional nebulisation the sample is introduced as an aqueous solution, resulting in a considerable amount of hydrogen and oxygen ions in the plasma. With the ETV the sample is introduced as a gas, hence the level of hydrogen and oxygen are greatly reduced. The advantage of hydrogen and oxygen reduction with ETV sample introduction has also been discussed by Marshall and Franks.⁷⁶

As shown in Figure 2.4, the Se signal remained fairly constant throughout the vaporisation temperature range examined. Using 2300°C as the vaporisation temperature, Figure 2.9(a) shows the signal profile for a serum sample diluted in 1% HNO_3 . A large analyte peak is observed at approximately 60s, but a second much smaller peak is seen slightly later at approximately 70s. During the temperature program (Table 2.2) the graphite tube is rapidly heated to 2700°C after the vaporisation stage to remove any residual matrix components and the overall gas flow rate drops due to a cease in the internal gas flow. The second peak observed approximately 10secs later is probably Se vaporising as the furnace temperature increases but is seen slightly later than expected from the timings listed in the ETV temperature program (Table 2.2) due to the decrease in the overall gas flow rate. The evidence of this later peak suggests that the temperature of 2300°C is insufficient for complete vaporisation. This is verified in Figure 2.9(b) where the vaporisation temperature has been increased to 2600°C . Only one peak is now observed indicating that all of the Se has been vaporised and transferred to the ICP-MS.

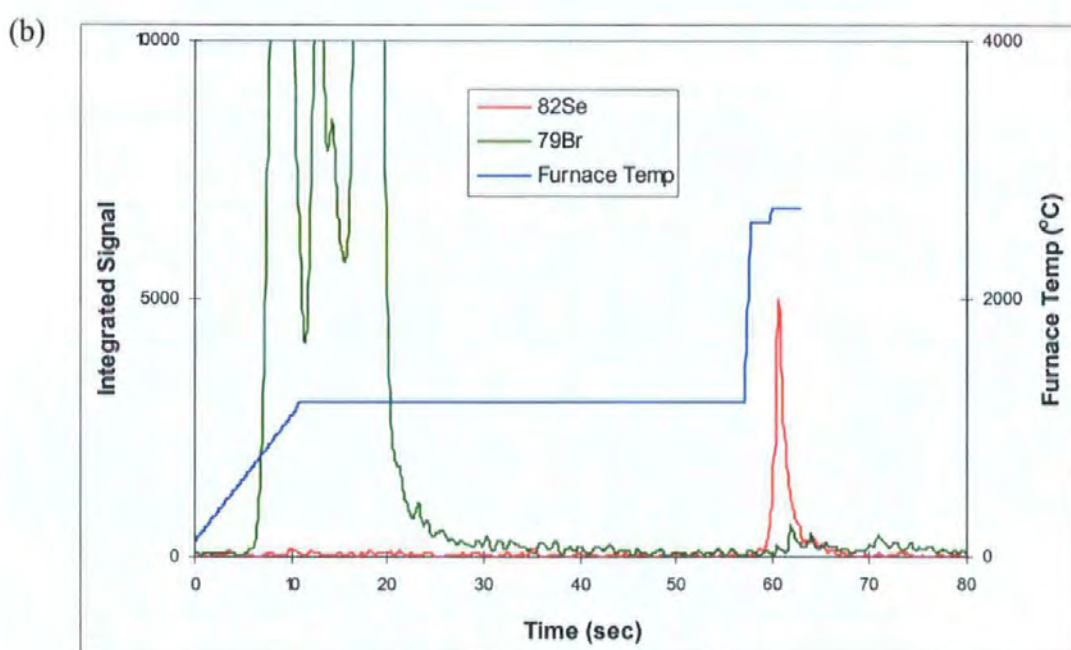
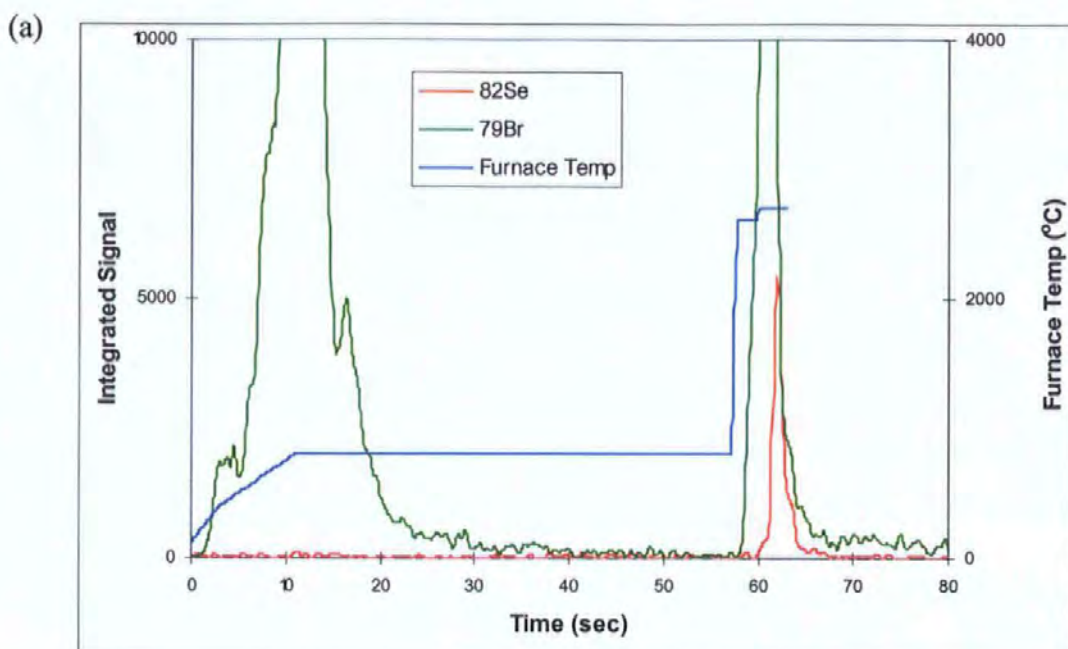


Figure 2.8 The effect of pyrolysis temperature with respect to elimination of Br interference; 10 μl injection of a serum sample in 1% HNO_3 , approximate concentration 5 ng g^{-1} . (a) ^{82}Se and ^{79}Br signal profiles, pyrolysis temperature 800 $^{\circ}\text{C}$, and (b) ^{82}Se and ^{79}Br signal profiles, pyrolysis temperature 1200 $^{\circ}\text{C}$.

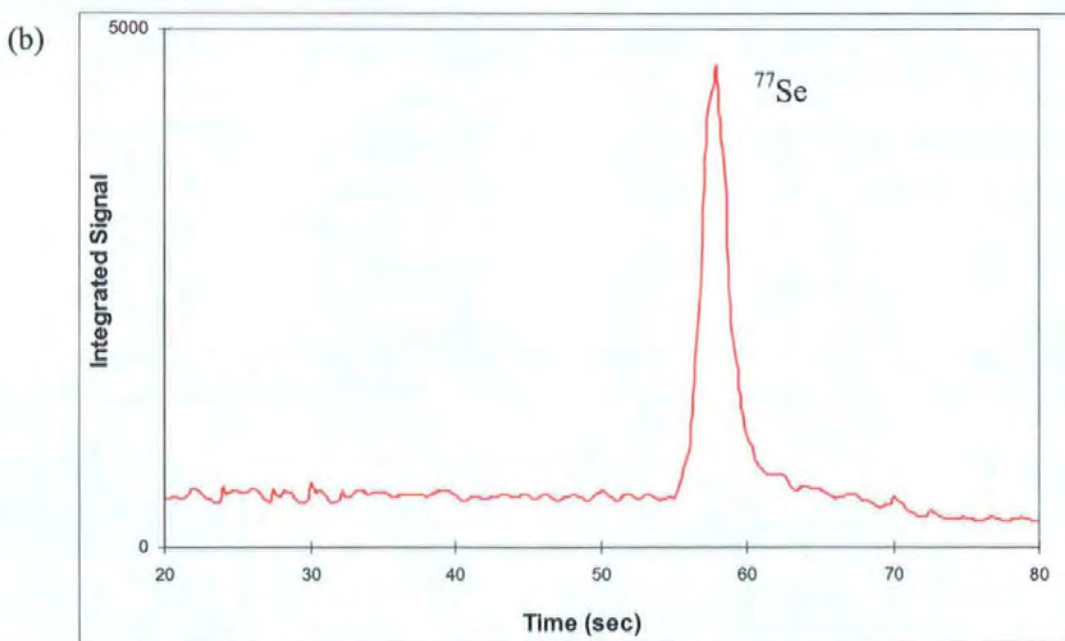
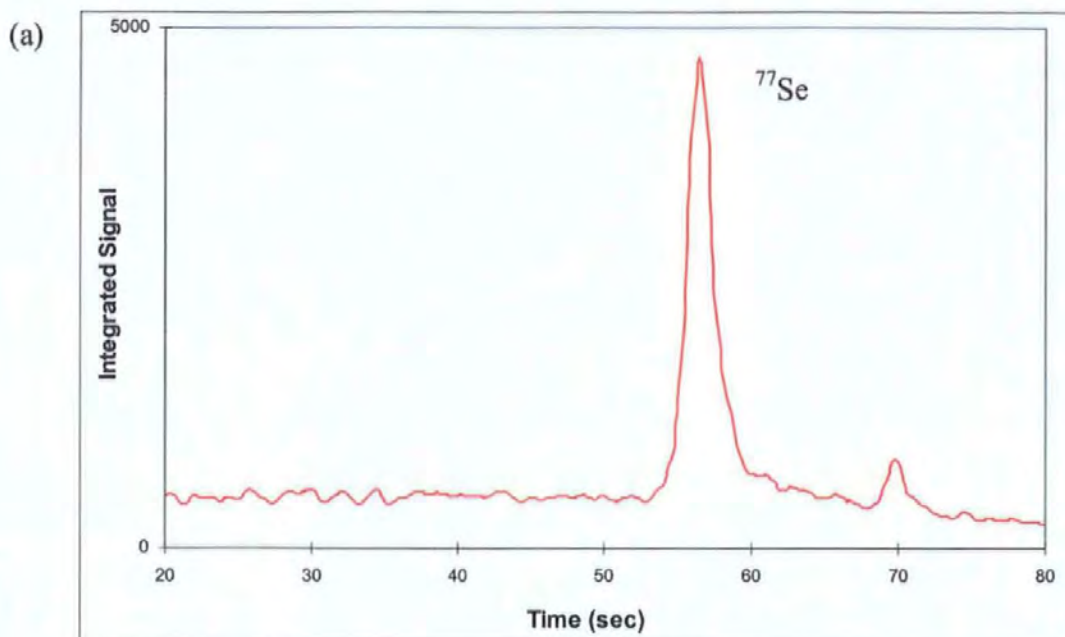


Figure 2.9 The effect of vaporisation temperature on ^{77}Se signal profile. 10 μl injection of a serum sample in 1% HNO_3 - approximate concentration 5ng g^{-1} . (a) Vaporisation temperature of 2300 $^\circ\text{C}$; (b) vaporisation temperature of 2600 $^\circ\text{C}$.

2.5.2 Power and Nebuliser Gas

Operating parameters including plasma power, nebuliser gas flow rate and lens settings were optimised. An increase in signal intensity for all isotopes was observed with an increase in plasma power, upto a maximum of 1150W. Above this the signal begins to decrease as illustrated in Figure 2.10. All further work was performed at 1150W, a higher setting than that favoured by other workers⁴³ when using conventional nebulisation. This can improve the ionisation of Se, and hence the sensitivity, but on the downside also increases the ionisation of polyatomic species. However with the proposed system the interferences on ⁷⁷Se and ⁸²Se are already eliminated during the ETV process, therefore this improvement in ionisation produces a net increase in sensitivity.

The effect of the argon nebuliser gas flow rate was also investigated. The Se signal increased steadily with an increase in gas flow rate from 0.85 l min⁻¹, reaching a maximum at 0.95 l min⁻¹, and decreasing at flow rates above this (Figure 2.11). It should be noted that the internal flow rate of Ar in the furnace is 0.30 l min⁻¹. This combined with the ICP-MS carrier gas optimum flow rate of 0.95 l min⁻¹ leads to a total carrier gas flow rate of 1.25 l min⁻¹, a similar optimum rate as reported previously.²²

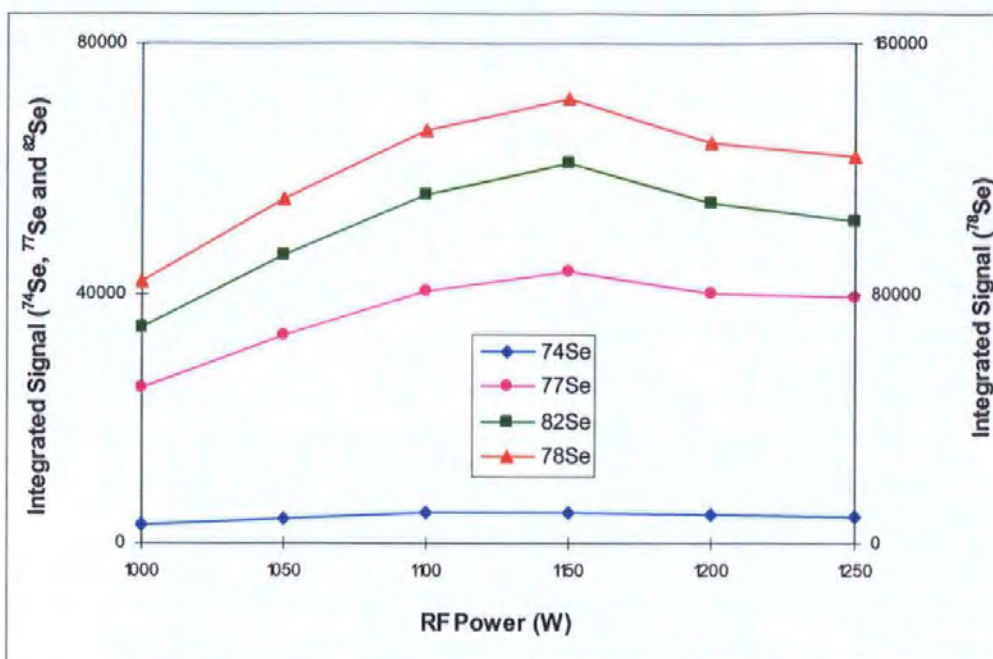


Figure 2.10 Effect of RF power on Se signal; 10 μ l injection of a 10ng g⁻¹ Se standard prepared in 1% HNO₃.

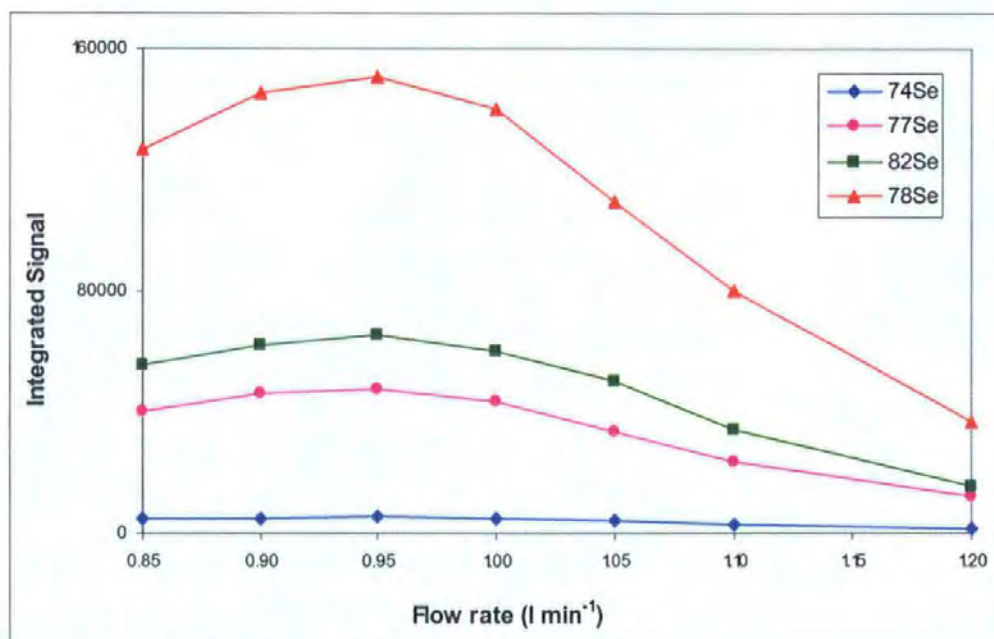


Figure 2.11 Effect of argon nebuliser gas flow rate on Se signal; 10 μ l injection of a 10ng g⁻¹ Se standard prepared in 1% HNO₃.

2.6 Analytical Performance

Typical transient signal profiles for a 5 ng g^{-1} Se standard and a serum sample with an approximate concentration of 5 ng g^{-1} , are shown in Figure 2.12(a) and (b). The sensitivity of the system corresponds to between 200 and 6000 counts per ng g^{-1} of Se depending on the isotopic abundance.

2.6.1 Linearity

The linearity of the proposed system was investigated by analysing standards ranging from 0.10 to 100 ng g^{-1} and plotting concentration vs integrated signal to construct calibration lines for each of the isotopes. The system was found to be linear from 0 - 100 ng g^{-1} for the 77, 78 and 82 isotopes but only linear from 1 - 100 ng g^{-1} for ^{74}Se . This non-linearity below 1 ng g^{-1} for ^{74}Se may be attributed to its low isotopic abundance (0.90%) and hence lack of sensitivity.

2.6.2 Reproducibility

Short term stability data for 10 consecutive analyses (triple firings) of a diluted serum sample, followed by 10 determinations over a 4hr period to give the long term stability of the system, for a typical analytical run are detailed in Table 2.3. Data were obtained with the intensity ratioed to the Te internal standard.

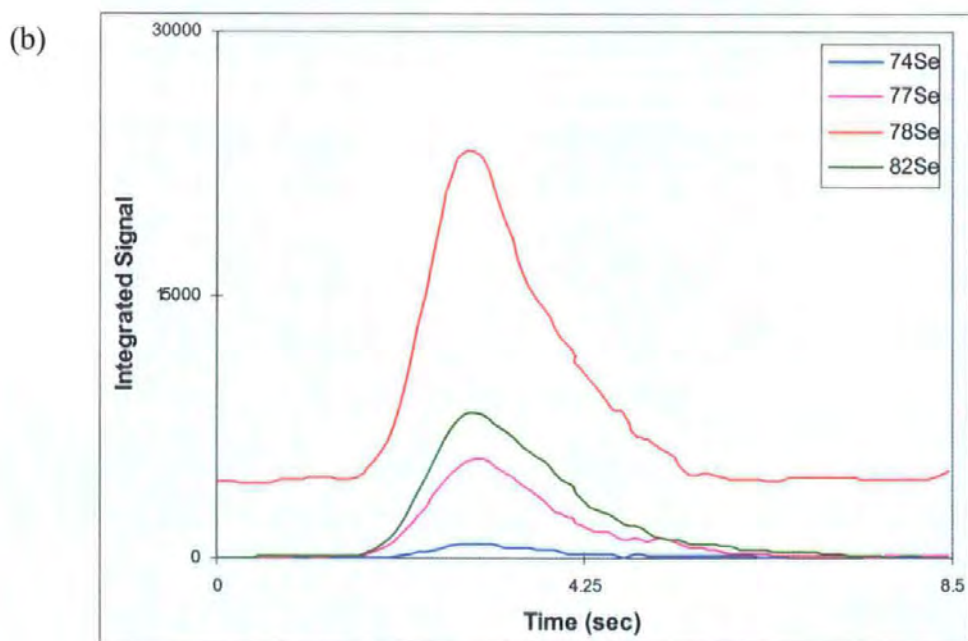
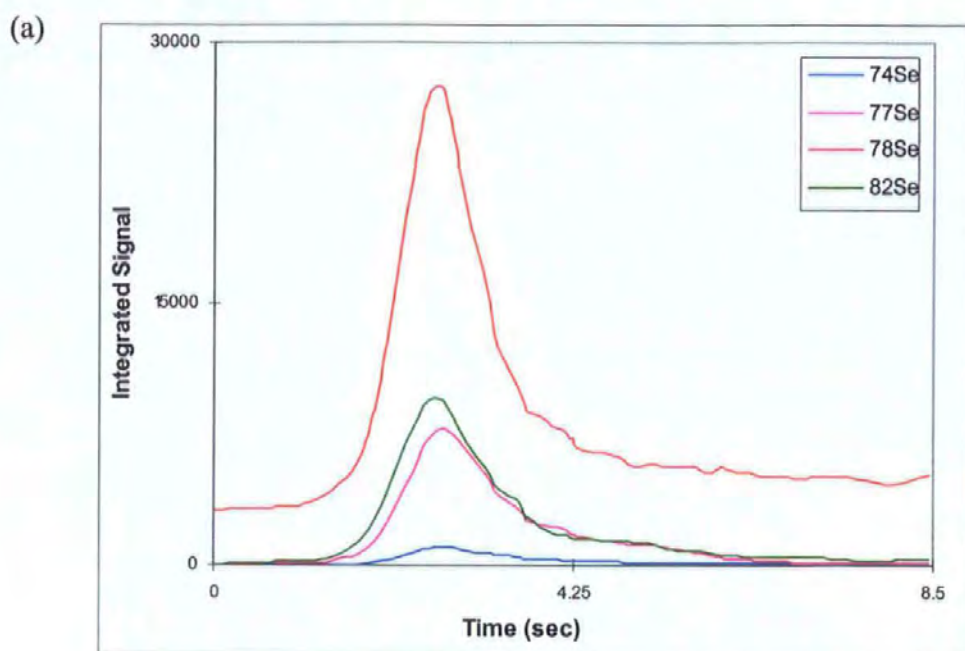


Figure 2.12 Typical transient signal profiles for a $10\mu\text{l}$ injection with $10\mu\text{l}$ $500\mu\text{g g}^{-1}$ $\text{Pd}(\text{NO}_3)_2$ modifier. (a) 5ng g^{-1} Se standard in 1% HNO_3 ; (b) Diluted serum sample - approximate concentration 5ng g^{-1} .

Parameter	⁷⁴ Se	⁷⁷ Se	⁷⁸ Se	⁸² Se
Detection Limit	0.85ng g ⁻¹	0.14ng g ⁻¹	0.58ng g ⁻¹	0.13ng g ⁻¹
Absolute Detection Limit	8.5pg	1.4pg	5.8pg	1.3pg
Short-term stability (n=10)	±15%	±4.9%	±4.6%	±3.2%
Long-term stability (n=10)	±13%	±4.7%	±5.7%	±3.8%
Linearity	1-100ng g ⁻¹	0-100ng g ⁻¹	0-100ng g ⁻¹	0-100ng g ⁻¹

Table 2.3 Analytical performance characteristics for the determination of Se in serum by ETV-ICP-MS.

2.6.3 Detection Limits

Typical limits of detection (calculated as 3σ based on 10 determinations of 1% HNO₃ blank) are also found in Table 2.3. These also take into account the 1+19 dilution factor applied to all of the serum samples. The poor detection limits of ⁷⁴Se and ⁷⁸Se are due to the low abundance and poor sensitivity of ⁷⁴Se, and the substantial interference from argon polyatomics on ⁷⁸Se. Further work to improve the detection limit of ⁷⁸Se will continue, with the addition of nitrogen to the various Ar gas channels. This is discussed in detail later in Chapter 6.

2.6.4 Accuracy

To check on the accuracy of the method a number of IQC sera (prepared by the addition of Se standards to bovine serum, donated by Dr T. Delves, Southampton University) and

NIST SRM 1598 (bovine serum) were diluted 1+19 with 1% HNO₃ and analysed. Results can be found in Table 2.4. A linear calibration was performed utilising the blank correction facility in the ELAN software. Excellent agreement between the results obtained and the target values for ⁷⁴Se, ⁷⁷Se and ⁸²Se are shown. High results were obtained with ⁷⁸Se, but again this is attributed to the large interference from argon adduct ions at mass 78. The RSD's calculated from triplicate analyses of each sample were between 3.1% and 5.7% for ⁷⁷Se and ⁸²Se, and 4.0% and 14.0% for ⁷⁴Se and ⁷⁸Se in the IQC samples, and between 1.1% and 1.8% for NIST SRM 1598 with the exception of ⁷⁴Se which gave an RSD of 14.0%.

	Concentration /ng g ⁻¹			
	IQC 1 (54.5ng g ⁻¹)	IQC 2 (103ng g ⁻¹)	IQC 3 (148ng g ⁻¹)	NIST 1598 (42.4ng g ⁻¹ ±3.5ng g ⁻¹)
⁷⁴ Se	48.9 ±6.9	97.9 ±7.2	146 ±5.8	37.9 ±5.2
⁷⁷ Se	51.1 ±2.9	96.7 ±4.0	142 ±7.0	41.4 ±0.75
⁷⁸ Se	64.1 ±9.3	109 ±7.8	146 ±8.0	55.6 ±0.72
⁸² Se	50.7 ±2.2	94.3 ±4.4	138 ±4.3	40.8 ±0.45

Table 2.4 Accuracy data from the analysis of internal quality control samples and NIST SRM 1598. Values are expressed as the mean and standard deviations of 3 measurements.

These data are further illustrated in Figure 2.13 and Figure 2.14, where the excellent data can be seen more clearly.

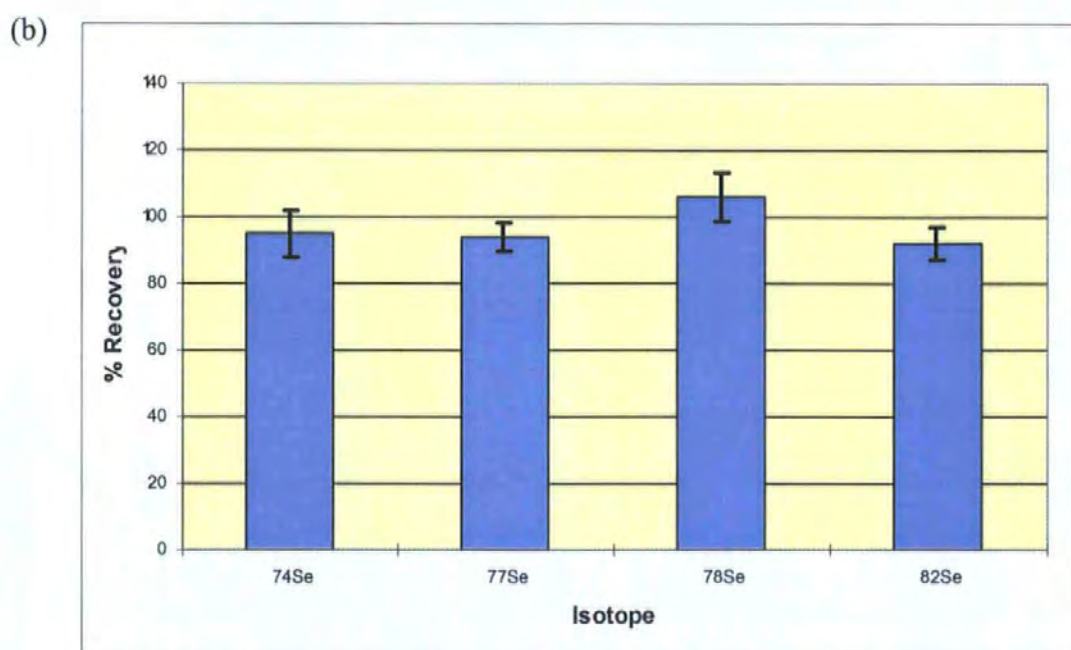
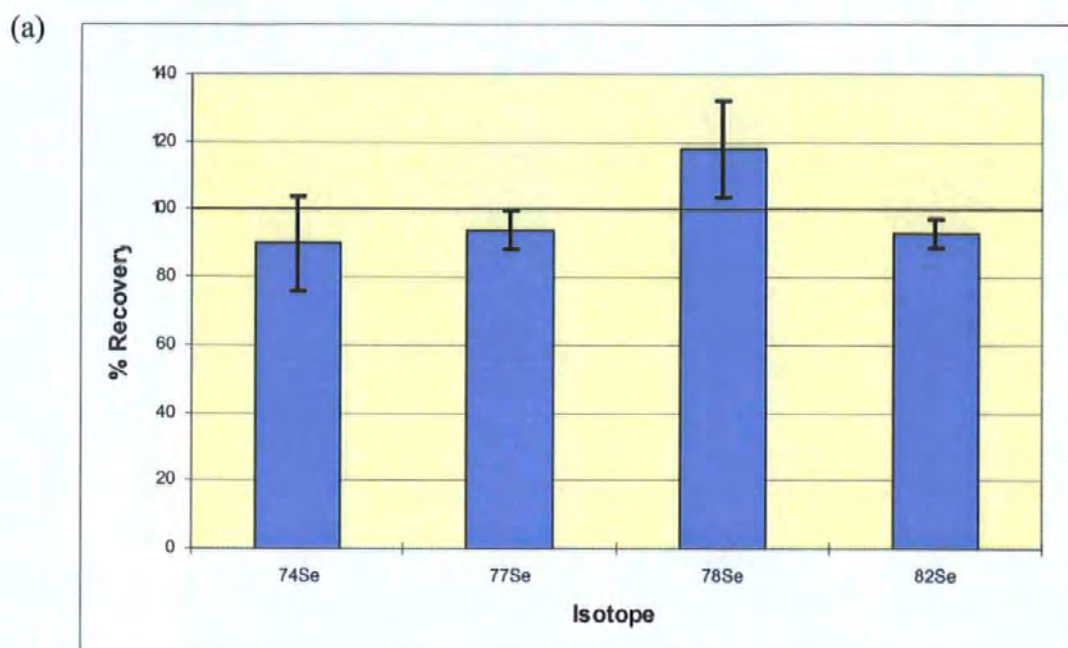


Figure 2.13 Results obtained for the analysis of two serum samples, (a) IQC level 1 and (b) IQC level 2. Error bars represent the standard deviations for 3 replicate analyses.

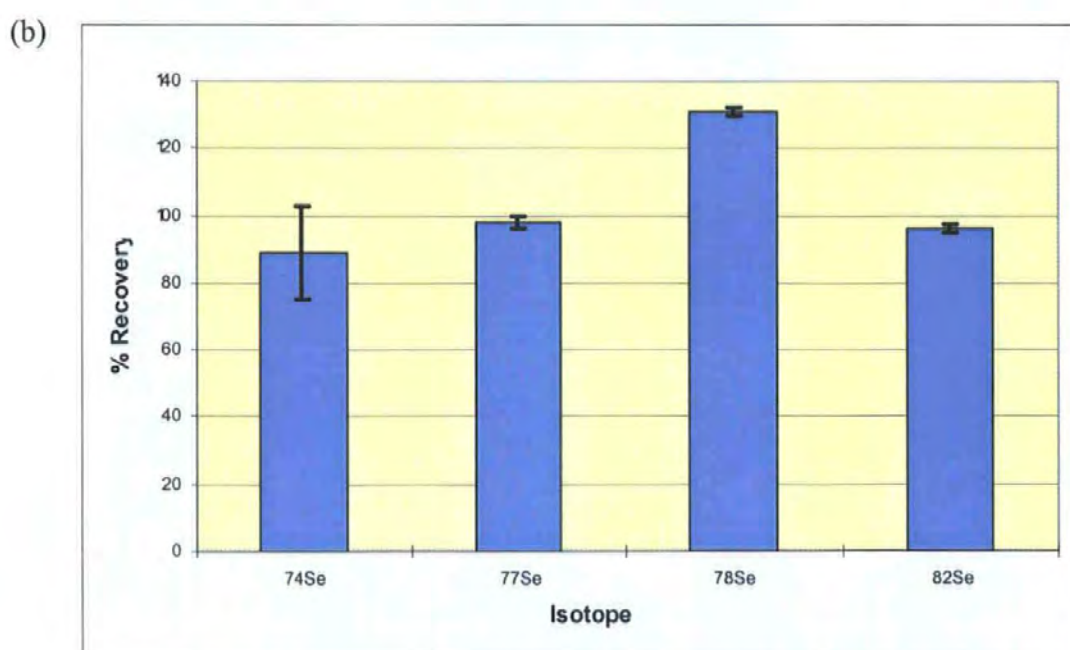
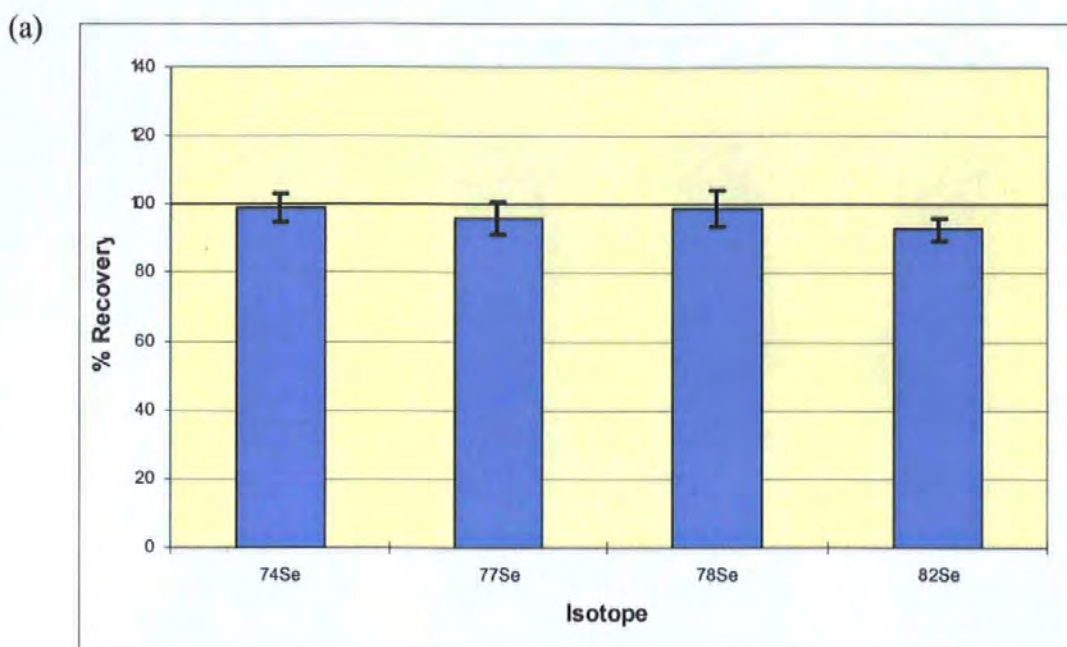


Figure 2.14 Results obtained for the analysis of two serum samples. (a) IQC level 3 and (b) NIST SRM 1598. Error bars represent the standard deviations for 3 replicate analyses.

2.7 Conclusions

Selenium is a complicated element to analyse by ICP-MS, particularly in a biological matrix such as serum. The majority of existing procedures include a sample pre-treatment stage to digest the samples prior to ICP-MS measurement. Others use standard addition procedures to overcome matrix effects. Both of these approaches are lengthy and time consuming for the analyst. This work has centred on the development of an ETV procedure that would be accurate, reliable and efficient. With careful optimisation of all aspects of the method including the choice of matrix modifier, sample diluent and finely tuned temperature program, this has been successfully achieved. The ETV procedure developed allows the interference free analysis of two of the isotopes of selenium - 77 and 82 - resulting in the accurate analysis of Se in serum with minimal sample pre-treatment.

CHAPTER 3

Development of an Isotope Dilution Method for the Accurate Determination of Selenium in Serum and Water

3. Development of an Isotope Dilution Method for the Accurate Determination of Selenium in Serum and Water

3.1 Introduction

Isotope dilution mass spectrometry (IDMS) has been described as a definitive analytical technique that is capable of providing improved accuracy and precision over alternative ICP-MS methods.⁷⁷ Its numerous applications are well documented in the literature⁷⁸⁻⁸² where it has been used to establish a reference value for Cu in sediment,⁸³ and Cu, Mo and Se in biological reference materials.⁸⁴ The technique is based on the addition of an isotopically enriched material, which, when present in an equilibrated form in the sample, acts as the perfect internal standard. Determinations involve the measurement of isotope ratios of the analyte in the sample, and the altered isotope ratio following the addition of the spike. Essential requirements for IDMS are that more than one isotope of the element in question occurs in nature and that the selected isotopes are free from interference. Providing these criteria are met or any interferences are negligible, the accuracy of isotope dilution determinations is dependent on the precision of the isotope ratio measurements.

This chapter describes the development of a high accuracy method for the determination of selenium in both serum and water. By combining the established ETV-ICP-MS procedure detailed in Chapter 2 with the technique of isotope dilution, a highly precise and accurate procedure has been established. Optimisation of the measurement parameters such as dwell time, peak measurement mode and number of replicates are described. The accuracy and precision of the method is demonstrated with the analysis of several certified reference materials.

3.2 Isotope Dilution Analysis

With isotope dilution analysis the sample is spiked with a known amount of an enriched isotopic standard. The resulting isotopic ratio is then measured and from this it is possible to calculate the mass fraction of the element in the sample by using the following double IDMS equation.

$$w_X = w_Z \cdot \frac{m_Y}{m_X} \cdot \frac{m_{Zc}}{m_{Yc}} \cdot \frac{R_Y - R'_B \cdot \frac{R_{Bc}}{R'_{Bc}}}{R'_B \cdot \frac{R_{Bc}}{R'_{Bc}} - R_X} \cdot \frac{R_{Bc} - R_X}{R_Y - R_{Bc}} \quad \text{Equation 3.1}$$

where w_X is the mass fraction of the element in the sample X, w_Z is the mass fraction of the element in the primary standard solution Z, m_Y is the mass of spike Y added to the sample X to prepare the blend B (=X+Y), m_X is the mass of sample X added to the spike Y to prepare the blend B (=X+Y), m_{Zc} is the mass of primary standard solution Z added to the spike Y to make mass bias blend Bc (=Y+ Z), m_{Yc} is the mass of spike Y added to the primary standard solution Z to make mass bias blend Bc (=Y+ Z), R'_B is the measured isotope amount ratio of sample blend (X+Y), R'_{Bc} is the measured isotope amount ratio of mass bias blend (Bc=Z+Y), R_{Bc} is the gravimetric value of the isotope amount ratio of mass bias blend (Bc=Z+Y), R_X is the isotope amount ratio of sample X (IUPAC value), R_Y is the isotope amount ratio of spike Y (certified value).

Equation 3.1 encompasses the 3 main aspects of any IDMS analysis, namely i) the calculation of the mass fraction of the sample (single IDMS), ii) the calculation of the mass fraction of the spike (reverse IDMS) and iii) correction for instrumental biases. By taking each of these areas in turn it is easier to see how the double IDMS equation is derived.

3.2.1 Single IDMS

Once the sample has been spiked by the addition of a known amount of the enriched standard, and the modified isotope ratio determined, it is possible to calculate the mass fraction of the element in the sample providing the amount of enriched isotope added to the sample is known. This is calculated according to the following equation:-

$$w_x = w_y \cdot \frac{m_y}{m_x} \cdot \frac{R_y - R_B}{R_B - R_x} \cdot \frac{\sum_i R_{ix}}{\sum_i R_{iy}} \quad \text{Equation 3.2}$$

where R_B is the isotope amount ratio of sample blend B (=X+Y).

3.2.2 Reverse IDMS

In order to obtain the mass fraction of the spike a reverse IDMS procedure is carried out. This involves combining the enriched solution with a primary standard (usually gravimetrically prepared from the pure metal) which has a natural isotopic composition as defined by IUPAC.⁸⁷ The mass fraction is then determined according to Equation 3.3:-

$$w_y = w_z \cdot \frac{m_{zc}}{m_{yc}} \cdot \frac{R_z - R_{bc}}{R_{bc} - R_y} \cdot \frac{\sum_i R_{iy}}{\sum_i R_{iz}} \quad \text{Equation 3.3}$$

Equation 3.2 and 3.3 can then be combined to minimise the affect of the spike mass fraction on the final result,

$$w_x = w_z \cdot \frac{m_y}{m_x} \cdot \frac{m_{zc}}{m_{yc}} \cdot \frac{R_y - R_B}{R_B - R_z} \cdot \frac{R_{bc} - R_z}{R_y - R_{bc}} \quad \text{Equation 3.4}$$

3.2.3 Mass Bias

Isotope ratio measurements are affected by a number of instrumental biases that need to be accounted for in order for the isotope ratio experiment to be carried out correctly. The main factor to be considered is that of mass bias, so called because of the variable

transmission of ions of different masses through the quadrupole, resulting in discrepancies between the observed and expected isotope ratios.⁸⁵ Isotopes at the low mass range are affected to the greatest degree and those at the mid-mass range to the least. Detector dead time is another important factor that needs to be taken into consideration. This describes the period of time when the detector is unable to detect any ions, and occurs after each pulse. Typically this lasts between 20 and 100ns and must be accounted for to prevent inaccuracies in the isotope ratio measurement. To be able to compensate for these biases, a calibration solution is prepared to characterise the instrumental response. This solution is a blend of the enriched isotopic spike and the gravimetrically prepared standard solution. By measuring the isotope amount ratio it is possible to calculate a correction factor, K , which compensates for the difference between the observed and expected isotope amount ratios. This factor is expressed by the following equation:-

$$K = \frac{R_{true}}{R'_{measured}} = \frac{R_{Bc}}{R'_{Bc}} \quad \text{Equation 3.5}$$

It therefore follows that the sample isotope amount ratio R_B can be determined from the measured isotope amount ratio of the sample blend R'_B , the gravimetric value R_{Bc} and the measured isotope amount ratio of the calibration blend Bc in accordance with Equation 3.6 :-

$$R_B = \frac{R_{Bc}}{R'_{Bc}} \cdot R'_B \quad \text{Equation 3.6}$$

By combining Equations 3.4 and 3.6 the full double IDMS equation detailed in equation 3.1 is derived.

3.3 Optimisation of Measurement Parameters

Selenium has six naturally occurring isotopes, all of which suffer from polyatomic interferences (Table 1.4). When using isotope dilution analysis it is critical that all possible interferences, matrix, polyatomic or isobaric, are eliminated. For this work the ^{77}Se and ^{82}Se isotopes were used. These are not the most abundant of the isotopes but were selected over the others as the interfering polyatomic species ($^{40}\text{Ar}^{37}\text{Cl}^+$ and $^{81}\text{Br}^1\text{H}^+$) could be eliminated using the ETV temperature program developed previously (see Chapter 2).

Optimisation of the scan parameters is of paramount importance to minimise errors in the isotope ratio measurement and achieve the highest accuracy and precision possible. Electrothermal vaporisers generate transient signals of short life spans, typically between 3 and 6 seconds. It is important for the processing with this type of signal to collect enough readings to accurately define the signal profile. Influencing factors such as dwell time, points per spectral peak, peak measurement mode and number of replicates were evaluated and the optimum settings established, for the measurement of the $^{82}\text{Se}/^{77}\text{Se}$ isotope ratio.

3.3.1 Dwell Time

This defines the amount of time spent measuring each mass during a sweep. The ratio for a 100ng g^{-1} Se standard was measured repeatedly at a range of dwell times, five injections were performed at each setting (Figure 3.1). From the data obtained it can be seen that short dwell times, between 3ms and 5ms, give rise to high % rsd values. An improvement in precision, demonstrated with a decrease in the % rsd values of the $^{82}\text{Se}/^{77}\text{Se}$ isotope ratio, is observed with dwell times in excess of 10ms. The optimum dwell time corresponding to the lowest % rsd is 15ms, which was consequently used throughout the work.

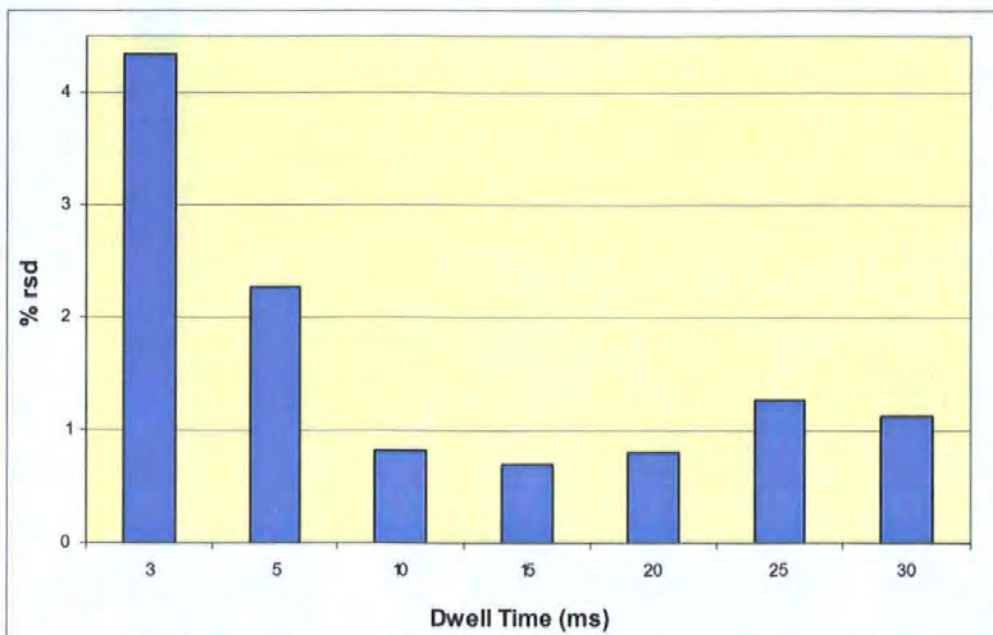


Figure 3.1 Optimisation of dwell time with respect to $^{82}\text{Se}/^{77}\text{Se}$ ratio % rsd values ($n = 5$), $10\mu\text{l}$ injection of a 100ng g^{-1} Se standard in 1% HNO_3 .

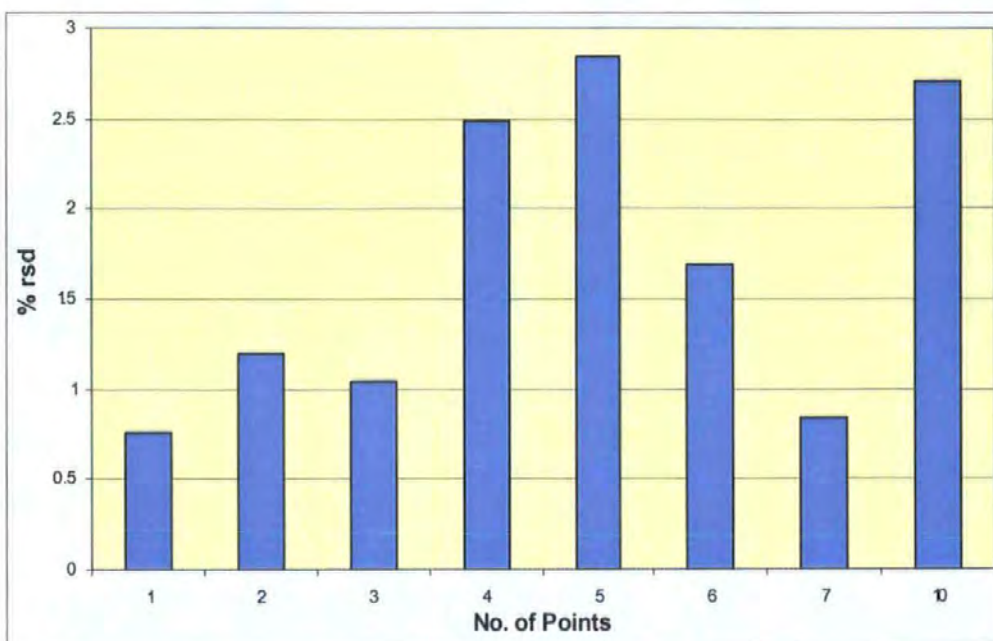


Figure 3.2 Optimisation of points per spectral peak with respect to the $^{82}\text{Se}/^{77}\text{Se}$ ratio % rsd values ($n=5$), $10\mu\text{l}$ injection of a 100ng g^{-1} Se standard in 1% HNO_3 .

3.3.2 Points/Spectral Peak

This parameter determines how many mass spectral data points the instrument collects as it scans each isotope. As with the dwell time experiment the ratio for a 100ng g⁻¹ Se standard was analysed repeatedly over a range of points, 1 -10. Again five replicates were performed for each setting. (Figure 3.2). The results obtained from this experiment are quite varied, however the general trend suggests that lower % rsd values are obtained with fewer points per mass spectral peak. Increasing the number of points has the disadvantage of increasing the analysis time and may also result in a loss of signal if the average taken across a number of points is less than the signal maximum. One point per mass spectral peak was used for all further work.

3.3.3 Number of Replicates

The aim of this work was to develop a procedure that was both highly accurate and precise but also practical in its use. To improve the precision of the ratio measurement a number of replicate injections were performed for each solution, to provide an averaged value for the isotope ratio. The number of replicates used had to strike a balance between total analysis time, avoiding long term drift and producing the desired improvements in the precision of the final result. The outcome of too few replicates may be a loss of precision, whereas too many may be construed an unnecessary consumption of time. This is a particularly important consideration with ETV sample introduction as the number of firings (which is determined by the number of replicate injections performed) has a direct effect on the lifetime of the graphite tube. Experiments carried out using a 100ng g⁻¹ Se standard indicated that nine replicates for each solution provided an optimum compromise. The % rsd for the nine replicates was 0.72%. This equates to a relative standard deviation of the mean⁸⁶ (sometimes referred to as standard error) for 9 such replicates of 0.24% relative.

3.3.4 Peak Measurement Mode

Each signal profile is made up of a series of intensity data points that are processed to generate an intensity value that can be used in quantitative calculations. There are four options for signal processing available within the ELAN software used in this study, each of which were evaluated. *Signal profile averaged* calculates the average intensity of the points which comprise each peak; *signal profile integrated* calculates the integrated intensity of the area under the signal; *signal profile counted* sums the total counts for all readings; and *signal profile maximum* identifies the reading with the largest intensity. To evaluate each of the processing options solutions at two different concentrations (2ng g⁻¹ and 10ng g⁻¹) in two different matrices (1% nitric acid and serum) were analysed. The data, expressed as the ⁸²Se/⁷⁷Se isotope ratio, are detailed in Table 3.1 with corresponding % rsd values for the nine replicate injections performed.

Solution	Averaged	Integrated	Maximum	Counted
2ng g ⁻¹ Se (1% HNO ₃)	1.4054 rsd = 2.29%	1.4060 rsd = 2.31%	1.3013 rsd = 2.15%	1.4061 rsd = 2.32%
2ng g ⁻¹ (serum)	1.4550 rsd = 2.14%	1.4553 rsd = 2.12%	1.3942 rsd = 2.96%	1.3858 rsd = 2.66%
10ng g ⁻¹ Se (1% HNO ₃)	1.3624 rsd = 0.21%	1.3666 rsd = 0.22%	1.3537 rsd = 1.08%	1.3621 rsd = 0.23%
10ng g ⁻¹ Se (serum)	1.3676 rsd = 0.87%	1.3677 rsd = 0.87%	1.3462 rsd = 2.46%	1.3680 rsd = 0.87%

Table 3.1 Effect of signal profile processing on ⁸²Se/⁷⁷Se isotope ratio and % rsd data (n =9).

From Table 3.1 it can be seen that similar % rsd values were achieved with the signal profile averaged, signal profile counted and signal profile integrated options. The signal profile maximum mode gave rise to the greatest % rsd values, which were higher than those obtained by any of the other procedures. Slightly higher % rsd values were also observed for the 2ng g⁻¹ Se standard and serum sample compared with the 10ng g⁻¹ solutions. This may be due to counting statistics. Signal profile integrated was selected for the work as this processing mode is the preferred option in many analytical laboratories due to the higher number of counts this measurement mode produces which may result in improved measurement statistics.

3.3.5 Effect of Ca and Zn on ⁸²Se/⁷⁷Se Ratio

Serum has a complex matrix consisting of organic matter, and high levels of inorganic components such as Na, Ca and Zn. The effect of Na on the Se signal has already been investigated and overcome with the optimised ETV temperature program (Chapter 2, Section 2.5.1). The potential interference from Ca and Zn in the form of polyatomic species such as ⁴⁰Ca³⁷Cl⁺ and ⁶⁶Zn¹⁶O⁺ on the ⁸²Se/⁷⁷Se, was evaluated. A series of 10ng g⁻¹ Se standards were spiked with increasing amounts of Ca and Zn. 10 replicate injections of each solution were performed and the ⁸²Se/⁷⁷Se isotope ratios examined. Significance tests, namely F-tests and t-tests, were carried out on the data. The results from this experiment can be seen in Table 3.2 and the F-test and t-test equations used to calculate the significance values are shown in Equations 3.7 and 3.8.

	$^{82}\text{Se}/^{77}\text{Se}$	sd	%rsd	S^2	F-test	t-test
10ng g ⁻¹ Se	1.369	0.032	2.37	0.0010	-	-
10ng g ⁻¹ Se/5ng g ⁻¹ Zn	1.373	0.029	2.10	0.0008	0.13	0.29
10ng g ⁻¹ Se/20ng g ⁻¹ Zn	1.370	0.044	3.21	0.0019	0.53	0.06
10ng g ⁻¹ Se/100ng g ⁻¹ Zn	1.391	0.029	2.05	0.0008	0.13	1.60
10ng g ⁻¹ Se/5μg g ⁻¹ Ca	1.381	0.041	2.97	0.0017	0.59	0.72
10ng g ⁻¹ Se/20μg g ⁻¹ Ca	1.384	0.024	1.74	0.0006	0.17	1.15
10ng g ⁻¹ Se/100μg g ⁻¹ Ca	1.388	0.042	3.02	0.0018	0.56	1.11

Table 3.2 Ratio and significance data obtained from spiking a 10ng g⁻¹ Se standard with increasing amounts of Ca and Zn. (n=10)

$$F = \frac{S_a^2}{S_b^2} \quad \text{Equation 3.7}$$

Where S_a and S_b represent the standard deviations of the two sets of data being compared.

$$t = \frac{(x_1 - x_2)}{\sqrt{\left(\frac{1}{n_1} + \frac{1}{n_2}\right) \times \left(\frac{s_1^2(n_1 - 1) + s_2^2(n_2 - 1)}{(n_1 + n_2 - 2)}\right)}} \quad \text{Equation 3.8}$$

Where x_1 and x_2 represent the mean $^{82}\text{Se}/^{77}\text{Se}$ ratio of the two variances being compared, s_1 and s_2 are the standard deviations of the two sets of data, and n is the number of replicates.

Each of the F and t significance values were compared to the F_{critical} and t_{critical} values of 3.23 and 2.10 respectively at the 95% confidence level. All of the values calculated are below these values, indicating that there is no significant difference between the $^{82}\text{Se}/^{77}\text{Se}$ ratio for the unspiked standard compared to the standards with added Ca or Zn.

3.4 Accuracy and Precision of Isotope Ratio Measurements

A typical signal profile for nine consecutive replicate injections of a serum sample with an approximate concentration of 10ng g^{-1} Se diluted 1+19 in 1% HNO_3 (initial concentration 200ng g^{-1}) is shown in Figure 3.3. Although the % rsd values obtained, based on the ^{77}Se and ^{82}Se isotope intensities were 6.69% and 5.84% respectively, this compares with 0.80%, for the $^{82}\text{Se}/^{77}\text{Se}$ isotope ratio obtained for the same nine injections. This illustrates that the measurement procedure has been optimised correctly and that there is sufficient correlation with the two signals for the precision advantages of ratio measurements to be realised.

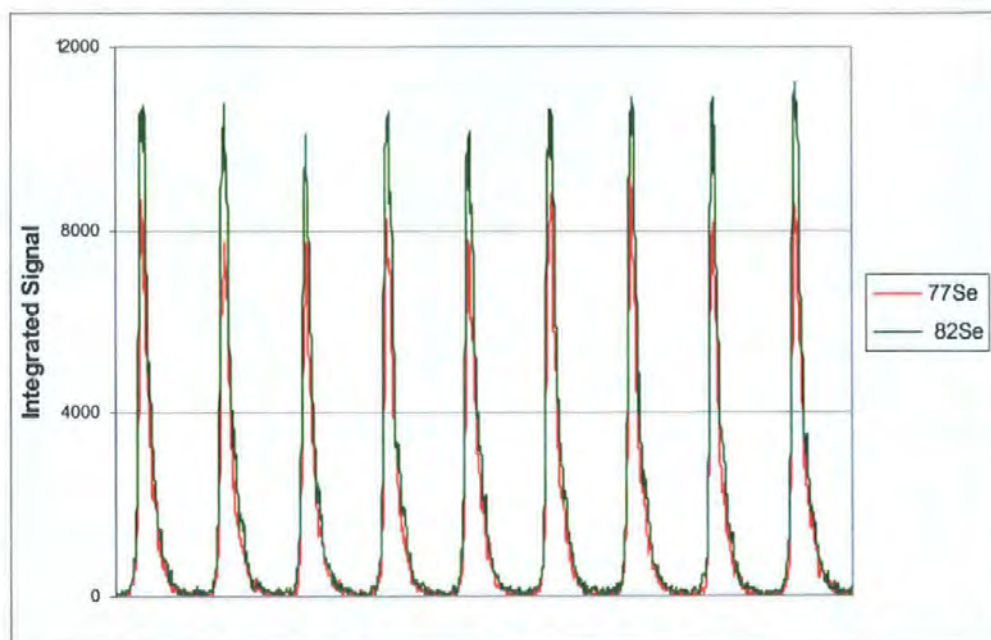


Figure 3.3 Nine consecutive injections of a serum sample diluted in 1% HNO_3 , $10\mu\text{l}$ injection, and approximate concentration of 10ng g^{-1} .

The natural theoretical $^{82}\text{Se}/^{77}\text{Se}$ isotope ratio is 1.1442 based on IUPAC⁸⁷ defined abundances of 8.73% and 7.63% for ^{82}Se and ^{77}Se respectively. From Table 3.1 it can be seen that the experimental $^{82}\text{Se}/^{77}\text{Se}$ isotope ratios for the solutions analysed differ considerably from this theoretical value (by approximately 20%). However, it should be noted that no difference in the $^{82}\text{Se}/^{77}\text{Se}$ isotope ratio is observed between the standard solution in 1% HNO_3 and the serum samples of similar concentrations. This suggests that the difference is due to instrumental mass discrimination and not matrix effects. A more marked difference is however observed between the ratios obtained for the higher concentration solutions than the lower concentration solutions irrespective of matrix. By exactly matching the mass bias solution to the sample solution with respect to concentration and matrix, any discrepancies will be compensated for and this problem negated.

3.5 Method Validation

The ETV temperature program used throughout this work was the same as that detailed in Table 2.2, Chapter 2. The ICP-MS parameter file was slightly different from that used to develop the non-IDMS ETV procedure and can be seen in Table 3.3.

3.5.1 Reagents

All solutions were prepared using high purity distilled deionised water (18M Ω , Elga, High Wycombe, Buckinghamshire, UK). The enriched standard solution (spike) was purchased from AEA Technology, (Didcot, Oxfordshire, UK) and the natural Se solution was prepared from >99.999% Se pellets (Aldrich, Poole, Dorset, UK). The isotopic composition of both standards is detailed in Table 3.4. Stock solutions of the two standards were prepared by dissolving accurately weighed quantities of the materials in concentrated nitric acid, Ultrex II ultra pure nitric acid (JT Baker, Milton Keynes, Buckinghamshire, UK) with final dilution to 100ml with deionised water. Gentle heating was required to aid

dissolution. The concentration of the ^{77}Se enriched solution was determined by performing a reverse isotope dilution procedure (see 3.5.2). The chemical modifier solution was prepared from palladium (II) nitrate (Sigma, Poole, Dorset, UK).

ICP-	
Power	1150W
Plasma Gas	15.0 l min ⁻¹
Auxiliary Gas	0.80 l min ⁻¹
Nebuliser Gas	0.95 l min ⁻¹
Cones	Pt
Lenses P	48
B	43
S	45
E	25
Parameter File -	
Dwell Time	15ms
Sweeps/Reading	1
Readings/Replicate	130
Number of Replicates	9
Points Across Peak	1
Resolution	Normal
Masses	^{77}Se ^{82}Se

Table 3.3 ICP-MS operating conditions.

	^{74}Se	^{76}Se	^{77}Se	^{78}Se	^{80}Se	^{82}Se	Atomic Weight.
Accurate Mass	73.9225	75.9192	76.9199	77.9173	79.9165	81.9167	
Natural Abundance ⁸⁷	0.89	9.40	7.63	23.77	49.61	8.73	78.960
Spike Abundance	0.27	2.60	68.69	17.51	9.28	1.65	77.421

Table 3.4 Isotopic abundance of the spike and natural selenium standards.

3.5.2 Preparation of IDMS Solutions

3.5.2.1 Natural Se Standard

A quantity of 99.999% pure Se pellets were accurately weighed out and dissolved in 5g of concentrated nitric acid (15.9M). Once dissolved the solution was diluted to 100g with distilled de-ionised water. The actual weights taken and resulting concentration of the natural Se standard are detailed in Table 3.5.

3.5.2.2 ⁷⁷Se Enriched Spike Solution

The enriched spike material was accurately weighed out and again dissolved in 5g of concentrated nitric acid (15.9M). It was also diluted to 100g with distilled de-ionised water. Table 3.5 details the accurate weights taken.

Solution	Wt of Material /g	Wt of Material + Acid /g	Concentration /$\mu\text{g g}^{-1}$
Natural Se	0.61959	92.42918	6703.4025
Spike Se	0.00911	100.5557	90.5966

Table 3.5 Accurate weights taken for the preparation of the natural and spike Se standards.

3.5.2.3 Characterisation of the Spike Concentration by Reverse IDMS

The natural Se standard solution was diluted accurately with 1% HNO₃ to give a solution with a concentration of approximately 100 $\mu\text{g g}^{-1}$. The spike was mixed with the natural standard to give an isotope amount ratio of 1:3 (⁸²Se:⁷⁷Se). This ratio is not the best theoretical ratio required to minimise error propagation, as calculated by Equation 3.9, but was the optimum compromise for this work considering the amount of sample and spike

available and the ultimate dilution of serum required to take full advantage of the optimised ETV temperature program.

$$\begin{aligned} & \sqrt{\left(\left(\frac{\text{Main spike abundance}}{\text{Minor spike abundance}} \right) \times \left(\frac{\text{Minor sample abundance}}{\text{Main sample abundance}} \right) \right)} && \text{Equation 3.9} \\ & = \sqrt{\left(\left(\frac{68.69}{1.65} \right) \times \left(\frac{7.63}{8.73} \right) \right)} \\ & = 6.03 \end{aligned}$$

A reverse isotope dilution procedure was then performed to establish the exact concentration of the spike. This was achieved by measuring the ratio of the blend, and substituting it into Equation 3.3. The measurement process was repeated several times, using the previous mass fraction value to prepare the mass bias blend for the next measurement, following the iterative procedure detailed by Henrion.⁸⁸ The mass fraction values for the spike solution obtained from each iteration are shown in Table 3.6.

Measurement No.	Mass fraction $\mu\text{g g}^{-1}$	% Difference
Gravimetric estimate	90.5966	-
1 st iteration	69.2530	23.6
2 nd iteration	71.7793	3.65
3 rd iteration	71.7660	0.02

Table 3.6 Characterisation of the spike for IDMS analysis.

3.5.3 Preparation of Samples

All samples were spiked gravimetrically with the enriched solution to give a final isotopic ratio of 1:3 ($^{82}\text{Se}:$ ^{77}Se). Typically, 1g of the enriched solution was used to spike between 1g and 2g of each sample. The serum samples were diluted 1 + 19 with 1% m/m nitric acid following spiking, but no dilution was necessary with the water samples. A mass bias solution was prepared by spiking a natural selenium standard to match the ratio in the sample. For the measurement sequence a blank was analysed first, followed by the mass bias solution, the sample blend and then the mass bias solution again, so that each sample blend was bracketed by the mass bias solution. This follows the matching procedure detailed by Catterick *et al.*⁸⁹

3.6 Analysis of CRM's

Several certified reference materials, TMRAIN-95 (spiked rainwater), TMDA-54.2 (spiked soft water), LGC 6010 (hard drinking water) and NIST 1598 (bovine serum) were analysed using both the IDMS and non-IDMS procedures. The results, which were all within the certified limits, can be seen in Table 3.7. The method precision, represented by the % rsd values obtained for triplicate analyses of each reference material, and the deviation from the certified level, represented by the % recovery values, are lower with the IDMS method than with the non-IDMS method. The result obtained for NIST 1598 bovine serum by the IDMS procedure was within $\pm 4\%$ of the certified amount.

CRM	Certified Level /ng g ⁻¹	ETV-ICP-MS				ETV-ID-ICP-MS			
		Mean	% Rec	sd	%rsd	Mean	% Rec	sd	%rsd
TMRAIN-95 Spiked rainwater	0.74 ±0.29	0.68	92%	0.04	5.50	0.750	101%	0.006	0.80
LGC 6010 Hard drinking water	9.30 ±1.60	10.9	117%	0.13	1.15	9.57	103%	0.05	0.48
TMDA-54.2 Spiked soft water	15.0 ±3.0	15.5	103 %	0.43	2.79	15.06	100%	0.01	0.07
NIST 1598 Bovine serum	42.4 ±3.5	40.8	96%	0.37	0.92	40.89	96%	0.02	0.06

Table 3.7 Results for the analysis of certified reference materials TMRAIN-95 (spiked rainwater), TMDA-54.2 (spiked soft water), LGC 6010 (hard drinking water) and NIST 1598 (bovine serum) using ETV-ICP-MS and ETV-ID-ICP-MS (n=3).

3.7 Conclusions

This chapter describes the further development of the ETV-ICP-MS procedure detailed in Chapter 2 to encompass the technique of isotope dilution. The rigorous optimisation of this procedure in order to obtain results of optimum accuracy and precision has been described in detail. Parameters such as peak measurement mode, dwell time, points per spectral peak and number of replicates were evaluated. Each of these factors was found to contribute some way to the accuracy of the isotope ratio measurement. Several certified reference materials have been analysed and this analysis has successfully demonstrated the improvements in precision achievable with the IDMS procedure compared with the non-IDMS procedure.

CHAPTER 4

Comparison of Analytical Methods for the Determination of Selenium

4. Comparison of Analytical Methods for the Determination of Selenium

4.1 Introduction

As mentioned previously in Chapters 1 and 2 the determination of selenium by ICP-MS is hampered by several factors such as poor sensitivity and severe interferences caused by the formation of argon polyatomic species (Table 1.4). Despite these problems there are numerous publications in the literature concerning the determination of Se, reporting the adoption of various techniques to overcome these issues. Approaches such as hydride generation, addition of an organic solvent to the sample solution and electrothermal vaporisation have been used.

This chapter investigates two further methods for the determination of Se and compares them with the ETV-ICP-MS procedure already discussed. The comparison is based on factors such as i) sample pre-treatment requirements; ii) interference removal; iii) analytical performance characteristics and iv) accuracy and precision through the analysis of certified reference materials.

4.2 Hydride Generation (HG-ICP-MS)

Hydride generation (HG) coupled with either atomic absorption, atomic fluorescence or ICP-MS for the determination of selenium has been widely used.²³⁻³¹ The technique involves generation of Se hydride through reaction with a strong reducing agent such as sodium borohydride. Once the hydride has been generated it is separated from the liquid reagents in a gas-liquid separator before being swept into the ICP by the argon carrier. This form of sample introduction gives rise to greater sensitivity due to the complete introduction of the gaseous analyte to the plasma⁴⁴ and reduction of spectroscopic and non-

spectroscopic interferences is achieved due to analyte removal from the matrix. The efficiency of the hydride generation step is dependent upon the experimental conditions and in particular the oxidation state of the analytes. Se^{VI} is unable to form a hydride and therefore must be reduced to Se^{IV} prior to hydride generation. This pre-reduction is often achieved by heating the sample with hydrochloric acid^{24,27}. Careful optimisation of the reagent concentration and the reaction times employed is required to ensure optimum response and minimal interference effects.

4.3 HG-ICP-MS Procedure

4.3.1 Instrumentation

All determinations were carried out using a Perkin Elmer ELAN 5000A ICP-MS (Perkin Elmer, Beaconsfield, UK). The on-line reduction of Se^{VI} to Se^{IV} was performed using a continuous a hydride generation system with a Perkin Elmer gas/liquid separator and two peristaltic pumps. One peristaltic pump was used to deliver the sample solution and reductant (NaBH_4) to the gas/liquid separator and the other peristaltic pump was required to divert waste away from it. The operating conditions for the ICP-MS are given in Table 4.1.

Digestion of the serum samples was carried out using a Paar Physica multiwave microwave sample preparation system (Anton Paar GmbH, Graz, Austria) using the temperature program detailed in Table 4.2. A Tecam water bath fitted with a Techne TE-8A thermoregulator (Techne (Cambridge) Ltd, Duxford, UK) was used for the pre-reduction stage. Sample preparation and pre-reduction was performed using 25 ml sterilin tubes (Bibby Sterilin LTD, Staffordshire, UK).

ICP-	
Power	1080W
Plasma Gas	15.0 l min ⁻¹
Auxillary Gas	0.80 l min ⁻¹
Nebuliser Gas	1.015 l min ⁻¹
Cones	Pt
Lenses P	48
B	40
S	43
E	27
Parameter File -	
Dwell Time	60ms
Sweeps/Reading	100
Readings/Replicate	1
Replicates	6
Points Across Peak	1
Resolution	Normal
Masses	⁷⁷ Se ⁸² Se

Table 4.1 HG-ICP-MS Operating Conditions.

Power /W	Time /min	Power /W	Fan
0	5.0	500	1
500	20	500	1
0	15	0	3

Table 4.2 Microwave Temperature Program for the Digestion of Serum Samples.

4.3.2 Reagents

All solutions were prepared using high purity deionised water (18M Ω , Elga, High Wycombe, Buckinghamshire, UK). Working standards were prepared daily by dilution of a 1000 $\mu\text{g ml}^{-1}$ Se stock solution (Alfa, Johnson Matthey, Royston, UK) in 1% m/m HNO₃, ultrapure Ultrex II grade acid (JT Baker(UK), Milton Keynes, Buckinghamshire, UK). Digestion of the serum samples was carried out with concentrated nitric acid (JT Baker, UK) and hydrogen peroxide (Romil, Cambridge, UK) and concentrated hydrochloric acid (JT Baker ultra pure) was used to acidify the samples/standards for the pre-reduction step. Sodium borohydride 1.5% (>99.99%, Aldrich, Poole, Dorset, UK) prepared in 0.1M NaOH (AR grade, BDH, Leicestershire, UK) was used for the hydride generation reaction.

4.3.3 Sample Preparation

0.2g of sample (serum samples only) was mixed with 2ml HNO₃ and 1ml H₂O₂, and heated in accordance with the microwave program detailed in Table 4.2. Once cooled the digests were transferred into 25ml sterilin tubes and diluted to approximately 10ml with ultra pure water. A series of calibration standards over the concentration range 0.5–5.0 ng g⁻¹ were prepared. All samples/standards were then diluted with concentrated HCl in the ratio 12.5g:10g (sample:HCl) giving an acid concentration of 5M, and placed in a water-bath set at 80–85°C for 90min. This was to convert any Se^{VI} to Se^{IV} prior to hydride generation. Once cooled the samples/standards were transferred to the hydride generation system for reaction with the NaBH₄ solution and the subsequent formation of gaseous selenium hydride.

4.3.4 Analytical Performance

Performance characteristics such as linearity, stability and limit of detection were evaluated.

4.3.4.1 Linearity

In order to establish the linearity of the HG-ICP-MS system a number of standards ranging from 0.10 to 50 ng g⁻¹ were analysed and plots of concentration vs integrated signal were constructed. The system was found to be linear from 0 to 50 ng g⁻¹ for both ⁷⁷Se and ⁸²Se, with correlation coefficients of 0.9992 for both isotopes as can be seen in Figure 4.1.

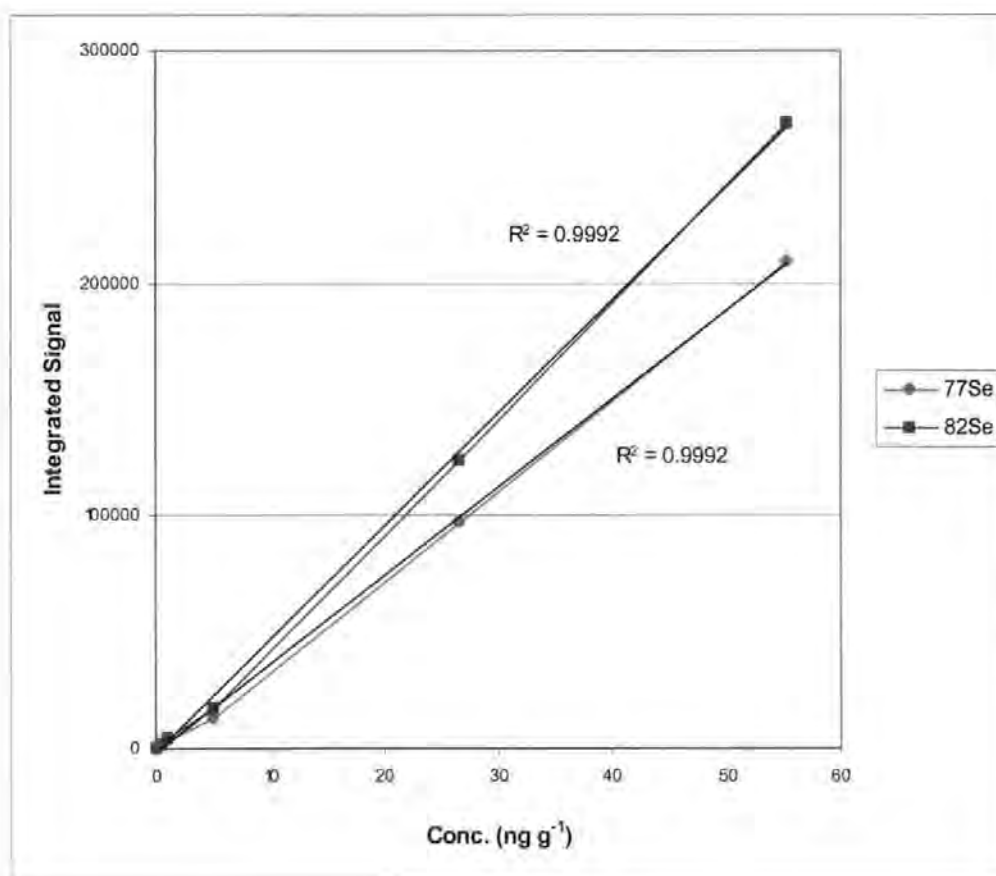


Figure 4.1 Plot of Se concentration vs integrated signal for the ⁷⁷Se and ⁸²Se isotopes.

4.3.4.2 Reproducibility

The reproducibility of the system was established from the continued analysis of a 5ng g^{-1} Se standard prepared in 1% HNO_3 acid. The short-term stability of the system was based on 10 consecutive measurements, and the long-term stability was established from 10 analyses performed over a 4hr period. The data from both of these experiments can be seen in Table 4.3.

	^{77}Se	^{82}Se
Short-term Stability (n=10)	$\pm 4.60\%$	$\pm 4.76\%$
Long-term Stability (n=10)	$\pm 5.55\%$	$\pm 5.64\%$
Detection Limit (3σ)	0.06ng g^{-1}	0.07ng g^{-1}

Table 4.3 Analytical performance characteristics for the determination of Se by HG-ICP-MS.

4.3.4.3 Detection Limits

Table 4.3 details the limits of detection achievable with this system. The values are calculated as 3σ of 10 determinations of a 1% HNO_3 acid blank.

4.3.5 Analysis of Certified Reference Materials

Four certified reference materials and three spiked serum samples (prepared in-house by adding accurate amounts of inorganic selenium standard to bovine serum) were analysed to evaluate the accuracy of the procedure. Each of the serum samples (NIST 1598 bovine serum certified reference material, and spiked serum samples LGC-S1, LGC-S2 and LGC-

S3) were digested following the microwave digestion procedure detailed in section 4.3.3. These and the aqueous certified reference materials (TMRAIN-95 spiked rainwater, TMDA-54.2 spiked soft water and LGC 6010 hard drinking water) were then mixed with concentrated HCl acid in the ratio 12.5g:10g (sample:HCl) and heated for 90mins in a water bath prior to measurement by HG-ICP-MS. The results obtained are shown in Table 4.4. A linear calibration was performed utilising the blank correction facility in the ELAN software.

Sample	Concentration/ng g ⁻¹		
	Expected	⁷⁷ Se	⁸² Se
TMRAIN-95			
Spiked rainwater	0.74 ±0.29	0.61 ±0.03	0.62 ±0.03
TMDA-54.2			
Spiked soft water	15.0 ±3.0	14.3 ±0.11	14.3 ±0.14
LGC 6010			
Hard drinking water	9.30 ±1.9	9.18 ±0.16	9.18 ±0.15
NIST 1598			
Bovine serum	42.4 ±3.5	37.9±10.3	37.5 ±11.0
LGC-S1			
Spiked bovine serum	-	17.5 ±1.5	15.4 ±1.6
LGC-S2			
Spiked bovine serum	-	55.2 ±2.3	52.7 ±2.0
LGC-S3			
Spiked bovine serum	-	112 ±6.6	110 ±5.9

Table 4.4 Accuracy data from the analysis of certified reference materials and spiked serum samples by HG-ICP-MS. Values are expressed as the mean and standard deviations of three measurements.

From Table 4.4 it can be seen that good agreement has been achieved between the expected values and the results obtained for the majority of the CRMs. All of the results for the aqueous reference materials are within the certified limits for both of the isotopes and the results for NIST 1598 (serum) fall just outside the stated range. The in-house spiked serum samples (LGC-S1, LGC-S2 and LGC-S3) were prepared by adding known quantities of a selenium standard to accurately weighed portions of bovine serum. LGC-S1 contains no added selenium, and therefore represents the level of Se present in the bulk serum. In order to make a comparison between the results obtained for LGC-S2 and LGC-S3 which did contain added Se, the level of Se found in LGC-S1 was subtracted from the values obtained for LGC-S2 and LGC-S3 and recovery results calculated. These recovery results can be seen in Table 4.5.

Sample	Conc./ng g ⁻¹	Conc.– blk/ng g ⁻¹	Se added/ng g ⁻¹	% Recovery
⁷⁷Se				
LGC-S1	17.5	-	-	-
LGC-S2	55.2	37.7	29.2	129%
LGC-S3	112	94.5	88.4	107%
⁷⁸Se				
LGC-S1	15.4	-	-	-
LGC-S2	52.7	37.3	29.2	128%
LGC-S3	110	94.6	88.4	107%

Table 4.5 Recovery results calculated from the analysis of in-house spiked serum samples analysed by HG-ICP-MS.

The results and hence recovery values calculated for each of the isotopes are in good agreement with one another, however the recovery values for LGC-S2 are considerably higher than those for LGC-S3. This may be attributed to an incorrectly determined value for the unspiked sample (LGC-S1). The possible error in the measurement of the low level of Se present in the unspiked sample is considerably higher than with the two spiked samples, hence if this value was determined incorrectly and then subtracted from the values obtained for the spiked samples this could result in high recovery values, which would be more significant for LGC-S2 than LGC-S3.

4.4 Addition of Organic Solvents

The role of organic solvents when used with ICP-MS to achieve enhanced sensitivity has been well documented and theorised.^{28,37,43-47} Improvements in analyte signal have been explained in a number of ways; - firstly that the presence of the organic solvent could affect the droplet formation giving rise to a finer aerosol, and ultimately leading to a greater nebulisation efficiency and improved desolvation in the plasma prior to ionisation. This phenomena is supported by Olivas *et al.*²⁸ who investigated the effect of several organic solvents (methanol, ethanol, propanol, acetone and acetonitrile) on the signal for a Se standard, using both pneumatic nebulisation and hydride generation sample introduction approaches. A second theory is suggested by Evans and workers³⁷ who studied the effect of propanol on the reduction of the polyatomic interferences affecting ⁷⁵As, ⁷⁷Se and ⁸²Se. The authors found that the intensity of the ArCl⁺ and ArAr⁺ species were greatly reduced when the sample solutions were spiked with propanol, and suggest that this is due to the competitive formation of polyatomic species such as ArC⁺ in the expansion chamber reducing the level of argon related interferents at the m/z of interest. One further explanation deals with changes in the ionisation potential of the analyte. The introduction of an organic solvent leads to an increase in C⁺ and carbon containing polyatomic ions

(CO⁺ and COH⁺) in the plasma. The degree of ionisation of analytes is improved through the transfer of an electron from the analyte to the C⁺ ions. This mechanism is possible with analytes that have a lower ionisation potential than carbon, i.e. selenium (9.8eV) compared with carbon (11.26eV) and is supported by Llorente *et al.*⁴⁵ who evaluated the effect of several organic compounds on the Se/ArCl signal ratio. The authors found that improvements in sensitivity and detection limits could be achieved with both the addition of an organic compound and careful optimisation of the operating parameters such as RF power and nebuliser gas flow-rate.

The following section covers the determination of selenium by pneumatic nebulisation PN-ICP-MS, and investigates the effect of butanol addition on signal enhancement.

4.5 PN-ICP-MS Method

4.5.1 Instrumentation

An ELAN 5000 ICP-MS instrument (Perkin Elmer Ltd, Beaconsfield, Bucks., UK) connected to an AS90 autosampler was used. The standards and samples were introduced into a standard cross-flow nebuliser (gem tip) into a 'Ryton' double-pass spray chamber (Perkin Elmer Ltd, Beaconsfield, Bucks., UK) via a peristaltic pump at a flow-rate of 1.0ml min⁻¹. ICP-MS operating conditions are detailed in Table 4.6.

4.5.2 Reagents

Ethylenediaminetetraacetic acid diammonium salt, (NH₄)₂EDTA, dihydrogen ammonium phosphate, NH₄H₂PO₄, and ammonia solution (all AR grade, Aldrich, Poole, Dorset, UK), butanol (HPLC grade, BDH, UK) and Triton-X-100 (Scintran grade, BDH, Leicestershire, UK) were used to prepare a modifier solution for the dilution of samples and standards. Stock solutions (1000µg ml⁻¹) of Se and In (internal standard) (Alfa,

Johnson Matthey, Royston, UK) were used to prepare the working standards by daily dilution in 1% m/m nitric acid, ultrapure Ultrex II grade acid (JT Baker(UK), Milton Keynes, Buckinghamshire, UK). Bovine serum (Selbourne Biological Services, Alton, Hampshire, UK) was used to prepare matrix matched calibration standards.

ICP-	
Power	1025W
Plasma gas	15.0 l min ⁻¹
Auxillary gas	0.80 l min ⁻¹
Nebuliser gas	0.90 l min ⁻¹
Cones	Ni
Lenses P	47
B	42
S	44
E	27
Parameter File -	
Dwell Time	80ms
Sweeps/Reading	75
Readings/Replicate	1
Replicates	4
Points across peak	1
Resolution	Normal
Masses	⁷⁷ Se ⁷⁸ Se ⁸² Se ¹¹⁵ In

Table 4.6 PN-ICP-MS Operating Conditions.

4.5.3 Sample Preparation

The procedure used for sample preparation in this work was based on a method published by Delves *et al.*⁴³ and involves dilution of the sample/standard with a mixture of reagents including butanol, Triton-X 100, ammonia, ammonium EDTA and ammonium dihydrogen phosphate. The authors have reported enhanced sensitivity with the addition of butanol, and report the need of the other reagents to prevent blockage of the nebuliser and injector. A solution (called Modifier A) was prepared in the following way;- 0.65g of (NH₄)₂EDTA and 1.6g of NH₄H₂PO₄ were dissolved in approximately 100ml of water.

5.6ml of Triton-X-100 and 5.6ml of NH_3 were then added and the solution diluted to 500ml with water. Modifier A was then diluted 10-fold with a 1.8% solution of butanol to give Modifier B which was used to dilute the samples and standards. Once diluted (1 + 14 with modifier B) the samples/standards were pumped through red/red tubing (internal diameter 1.14mm) into a mixing coil where they were combined on-line with In internal standard, 5ng g^{-1} which was pumped through blk/blk tubing (0.76mm internal diameter). This resulted in a further 1.5 fold dilution of the samples/standards and produced a solution with a final butanol concentration of 1%, the optimum concentration required for maximum signal as reported by Sieniawska and workers.⁹⁰

4.5.4 Effect of Butanol on Sensitivity

To evaluate the effect of butanol on the sensitivity of the system two sets of calibration standards were prepared. One set were prepared in 1% nitric acid and the other in the modifier B solution described earlier (section 4.6.3). Both sets of standards were measured using the conditions presented in Table 4.6 and plots of concentration vs integrated signal constructed (Figure 4.2). From Figure 4.2 it can be seen that by using the modifier containing 1% butanol the sensitivity of the system has increased considerably. A 2-fold increase in signal has been achieved for the ^{77}Se isotope, a 3-fold increase in signal for the ^{82}Se isotope and a 4-fold increase in signal for the ^{78}Se isotope.

This increase in sensitivity may be attributed to the competitive formation of ArN^+ , ArO^+ and ArC^+ through electron transfer mechanisms⁴⁷, resulting in the mass of the interfering polyatomic species being altered and therefore different to the mass of the isotopes of interest. The ^{78}Se isotope suffers from the greatest interference from argon adducts, therefore reduction of these species through the addition of butanol will have the most significant effect on the signal, as observed in Figure 4.2(b).

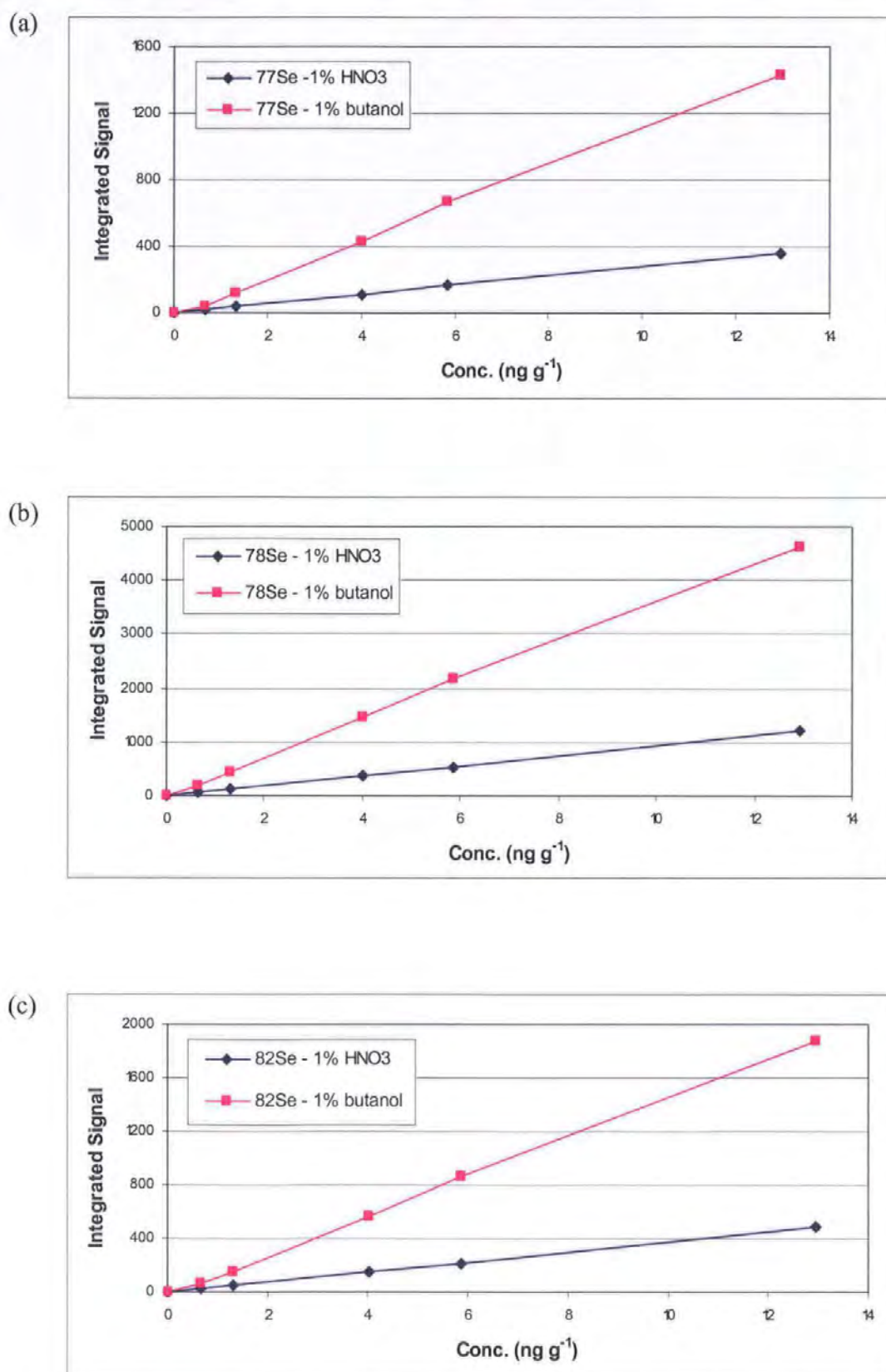


Figure 4.2 Plots of concentration vs integrated signal for standards prepared in 1% HNO₃ and Modifier B (containing 1% butanol); (a) ⁷⁷Se, (b) ⁷⁸Se and (c) ⁸²Se.

4.5.5 Analytical Performance

4.5.5.1 Linearity

A series of calibration standards ranging from 1.0 – 500ng g⁻¹ were prepared in 1% HNO₃. These were then diluted 1+ 14 with modifier B solution, resulting in standards ranging from approximately 0.10 – 40.0 ng g⁻¹. The linearity of the PN-ICP-MS system was evaluated through the analysis of these standards. Plots of concentration vs integrated signal were constructed and the linearity derived. The system was found to be linear over the range investigated for each of the isotopes, with correlation coefficients of 0.9999, 0.9998 and 0.9998 for the ⁷⁷Se, ⁷⁸Se and ⁸²Se isotopes respectively (Figure 4.3).

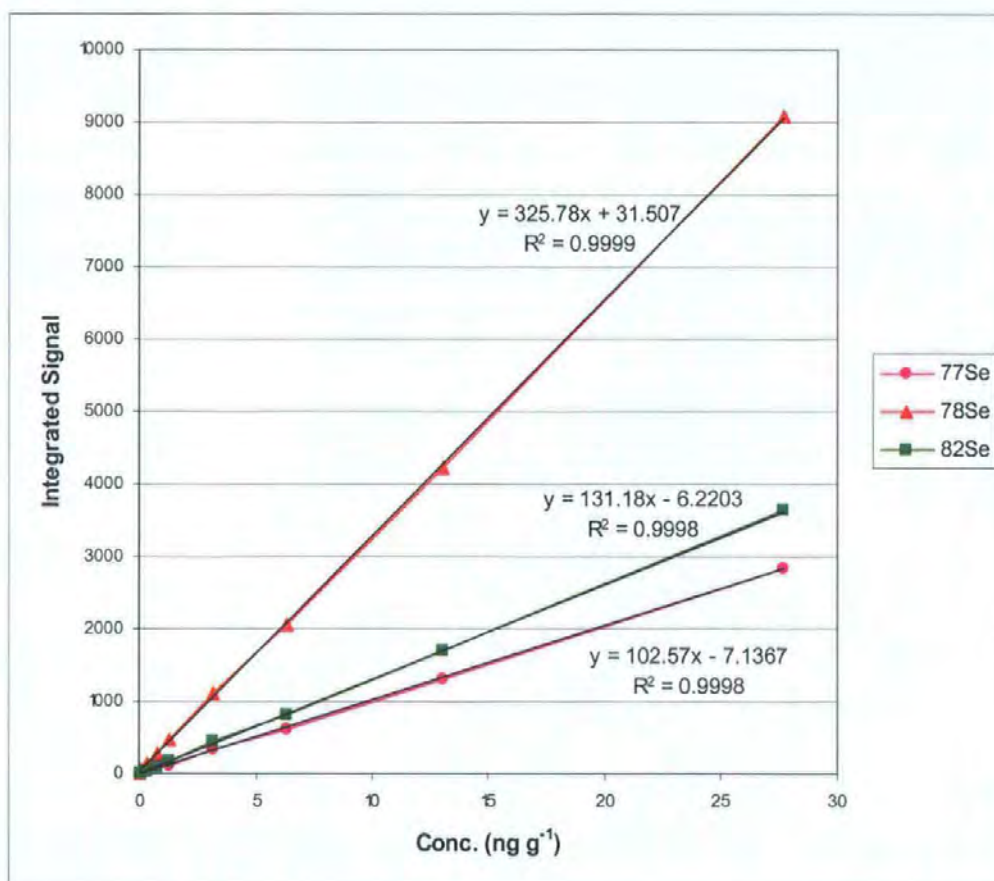


Figure 4.3 Plots of concentration vs integrated signal for the ⁷⁷Se, ⁷⁸Se and ⁸²Se isotopes; calibration standards prepared in modifier B.

4.5.5.2 Reproducibility

A 25 ng g⁻¹ Se standard prepared in 1% HNO₃ and then diluted 1 + 14 with modifier B, was repeatedly analysed to establish the reproducibility of the system. The short-term stability of the system was based on 10 consecutive measurements performed over 1 hour, and the long-term stability was calculated from 10 analyses performed over a 4 hr period. The data from both of these experiments can be seen in Table 4.7.

	⁷⁷ Se	⁷⁸ Se	⁸² Se
Short-term Stability (n=10)	±1.22%	±2.03%	±2.68%
Long-term Stability (n=10)	±4.11%	±6.15%	±4.71%
Detection Limit (3σ)	0.11 ng g ⁻¹	0.33 ng g ⁻¹	0.09 ng g ⁻¹

Table 4.7 Analytical performance characteristics for the determination of Se by PN-ICP-MS.

4.5.5.3 Detection Limits

As with the HG-ICP-MS, the detection limits of the method were calculated from the repeated analysis of a 1% HNO₃ acid blank. The values, quoted as 3σ of 10 determinations can be seen in Table 4.7.

4.5.6 Analysis of Certified Reference Materials

Several certified reference materials and in-house spiked serum samples were analysed to evaluate the accuracy of the procedure. All of the CRMs were analysed following a 15 fold dilution with modifier B. The aqueous CRMs (TMDA 54.2 and LGC 6010) were analysed against a calibration line constructed from standards prepared in 1% HNO₃ and then diluted with modifier B, and the serum CRM (NIST 1598) and spiked serum samples (LGC-S1, LGC-S2 and LGC-S3) were analysed using matrix matched standards. This involved mixing 500µl of each standard (including the standard blank) with 500µl of blank bovine serum prior to final dilution with modifier B. This follows the procedure used by Delves and workers⁴³. The results obtained are shown in Table 4.8.

All of the results obtained by this method are in good agreement with the expected values, with the exception of NIST 1598 where the result for the ⁷⁸Se isotope is just outside the certified limits. The results obtained for the ⁷⁷Se and ⁸²Se isotopes are unsatisfactory and do not fall within the stated range. Recovery values for the analysis of NIST 1598 for each of the isotopes measured (77, 78 and 82) are 128%, 111% and 121% respectively. This compares with recovery values for TMDA-54.2 of 103%, 100% and 120%, and LGC 6010 of 103% , 106% and 115% for the 77, 78 and 82 isotopes. The serum samples LGC-S1, LGC-S2 and LGC-S3 were prepared by spiking bulk serum with a known quantity of selenium. LGC-S1 represents the level of selenium in the bulk serum, i.e. with no added selenium. LGC-S2 and LGC-S3 contain enhanced levels of selenium in excess of that present in the bulk serum. Recovery values have been calculated for LGC-S2 and LGC-S3 after subtraction of the amount of Se found in LGC-S1, and are detailed in Table 4.9.

CRM	Concentration /ng g ⁻¹			
	Expected	⁷⁷ Se	⁷⁸ Se	⁸² Se
TMDA-54.2 Spiked soft water	15.0 ±3.0	15.5 ±0.36	15.0 ±0.40	18.0 ±0.51
LGC 6010 Hard drinking water	9.30 ±1.9	9.56 ±0.62	9.86 ±0.65	10.7 ±0.78
NIST 1598 Bovine serum	42.4 ±3.5	54.2 ±0.07	47.1 ±1.56	51.3 ±1.27
LGC-S1 Spiked bovine serum	-	37.6 ±6.8	29.7 ±5.7	43.9 ±9.7
LGC-S2 Spiked bovine serum	-	63.0 ±2.6	54.4 ±1.7	68.4 ±2.1
LGC-S3 Spiked bovine serum	-	121 ±1.0	112 ±0.6	125 ±0.9

Table 4.8 Accuracy data from the analysis of certified reference materials and spiked serum samples by PN-ICP-MS. Values are expressed as the mean and standard deviations of 3 measurements.

Sample	Conc. /ng g ⁻¹	Conc.– blk /ng g ⁻¹	Se added / ng g ⁻¹	% Recovery
⁷⁷Se				
LGC-S1	37.6	-	-	-
LGC-S2	63.0	25.4	29.2	87%
LGC-S3	121	83.4	88.4	94%
⁷⁸Se				
LGC-S1	29.7	-	-	-
LGC-S2	54.4	24.7	29.2	85%
LGC-S3	112	82.3	88.4	93%
⁸²Se				
LGC-S1	43.9	-	-	-
LGC-S2	68.4	24.5	29.2	84%
LGC-S3	125	81.1	88.4	92%

Table 4.9 Recovery results calculated from the analysis of in-house spiked serum samples analysed by PN-ICP-MS.

Acceptable recovery results (within $\pm 16\%$ of the expected amount) have been achieved with all of the isotopes for each of the spiked samples. The recovery values obtained for LGC-S3 are better than those achieved for LGC-S2. This may be due to counting statistics due to the higher level of selenium present in LGC-S3 compared with LGC-S2.

4.6 Method Comparison

All aspects of the two analytical methods discussed in this chapter have been compared with the procedures covered in Chapters 2 and 3 (ETV-ICP-MS and ETV-ID-ICP-MS). A comparison has been made between factors such as interference elimination, sample pre-treatment, analytical time, performance statistics and accuracy and precision.

4.6.1 Interference Elimination

Each of the procedures examined used different approaches to interference elimination, targeting different isotopes. The main interference effects which are alleviated by each of the methods examined are detailed in Table 4.10.

Procedure	Interference	Isotope
Hydride Generation	$^{40}\text{Ar}^{37}\text{Cl}^+$	^{77}Se
Organic Solvent	$^{36}\text{Ar}^{40}\text{Ar}^+$, $^{38}\text{Ar}^{38}\text{Ar}^+$, $^{38}\text{Ar}^{40}\text{Ar}^+$	^{76}Se and ^{78}Se
Electrothermal Vaporisation	$^{40}\text{Ar}^{37}\text{Cl}^+$, $^1\text{H}^{81}\text{Br}^+$	^{82}Se

Table 4.10 Interferents and corresponding isotopes alleviated by each of the procedures.

The hydride generation method involves formation of SeH through a reaction between NaBH₄ and HCl. Despite the high population of Cl present in the reagents, the gas/liquid separator ensures that only the SeH passes into the plasma, hence decreasing the affect of ⁴⁰Ar³⁷Cl⁺ on ⁷⁷Se. This process also means that the analyte is effectively removed from the original sample matrix thereby reducing the level of interference from other matrix components. The addition of an organic solvent to the sample matrix reduces the formation of ArAr⁺ adducts, due amongst other reasons to the competitive formation of species such as ArC⁺ and ArN⁺, resulting in a shift in the m/z ratio of the interfering species away from that of the analyte, ie ⁷⁶Se and ⁷⁸Se. Electrothermal vaporisation uses a different approach to interference reduction. This method eliminates the interferences on ⁷⁷Se and ⁸²Se through careful optimisation of the temperature program. At a temperature of 1200°C it possible to separate the signals of Cl and Br from that of Se, thereby eliminating any interference from ⁴⁰Ar³⁷Cl⁺ on ⁷⁷Se and ¹H⁸¹Br⁺ on ⁸²Se. The thermal process can also be tailored to vaporise matrix components such as Na which could affect the transport efficiency of Se.

4.6.2 Speed of Analysis

The time required for analysis is an important factor for any commercial laboratory. All aspects of sample preparation, instrumental analysis time, data processing and operator time need to be considered when comparing different procedures for criteria such as speed of analysis and efficiency. Figure 4.4 illustrates the time required for both sample preparation and analysis for each of the procedures examined, for the analysis of a single aqueous sample. From the graph it can be seen that the ETV procedures, both IDMS and non-IDMS, have the shortest sample preparation time. This is because a simple 1 + 19 dilution with 1% HNO₃ acid is all that is required for both aqueous and clinical samples.

The measurement time is considerably longer. With the non-IDMS ETV method each cycle of the temperature program takes approximately 2.5mins. A total of 3 replicates of each sample (and standard) is required for each solution, therefore the total analysis time for a single sample including 4 calibration standards is 37.5mins. With the ETV IDMS procedure the sample preparation time is very similar – again the samples are diluted 1 + 19 with 1% HNO₃ acid after spiking with the enriched material. The analytical time however is approximately double. This is due to the need to perform 9 replicate injections instead of the 3 performed with the conventional ETV method, in order to obtain sufficient data to realise the potential of increased accuracy and precision that this method offers. The sample preparation time required for the PN-ICP-MS method is slightly longer than that for the conventional ETV method. Both procedures require the preparation of a series of calibration standards, however a further dilution of standards and samples with a modifier solution prepared from (NH₄)₂EDTA, NH₄H₂PO₄, Triton-X-100, NH₃ and butanol, which in turn is quite time consuming to prepare, is required. The analysis time however is faster than the conventional ETV procedure. The total time required for the analysis of 4 calibration standards and a single sample is 25mins, including a 2min read delay to allow the sample to reach the plasma and a 1min wash between samples. The final method under investigation, the HG-ICP-MS procedure, has the longest sample preparation time. With this procedure each solution is acidified with conc. HCl acid prior to placement in a water bath for 90mins. This pre-reduction stage is essential to convert all Se^{VI} to Se^{IV} before reaction with NaBH₄ to produce the hydride. Once this pre-reduction has been completed the actual analysis time is quite short – total analysis time for a series of calibration standards and 1 sample is 15mins. As the number of samples to be analysed increases to 10, the sample preparation time will have less of an impact on the overall time required, as can be seen in Figure 4.5.

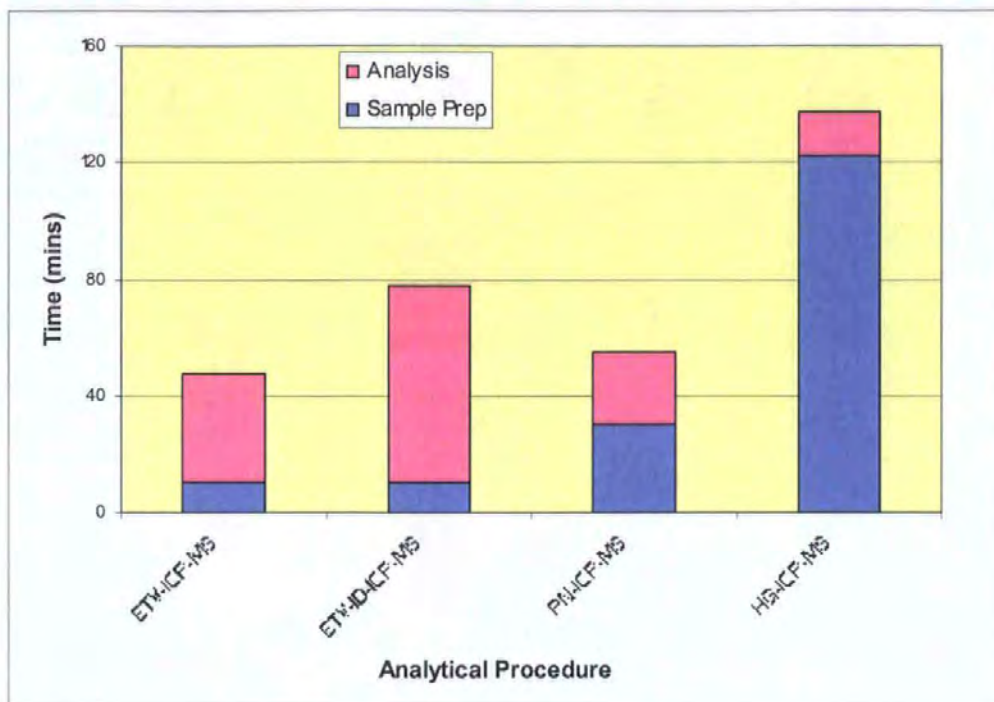


Figure 4.4 Comparison of the time required for sample preparation and analysis of 1 aqueous sample by each of the 4 methods examined.

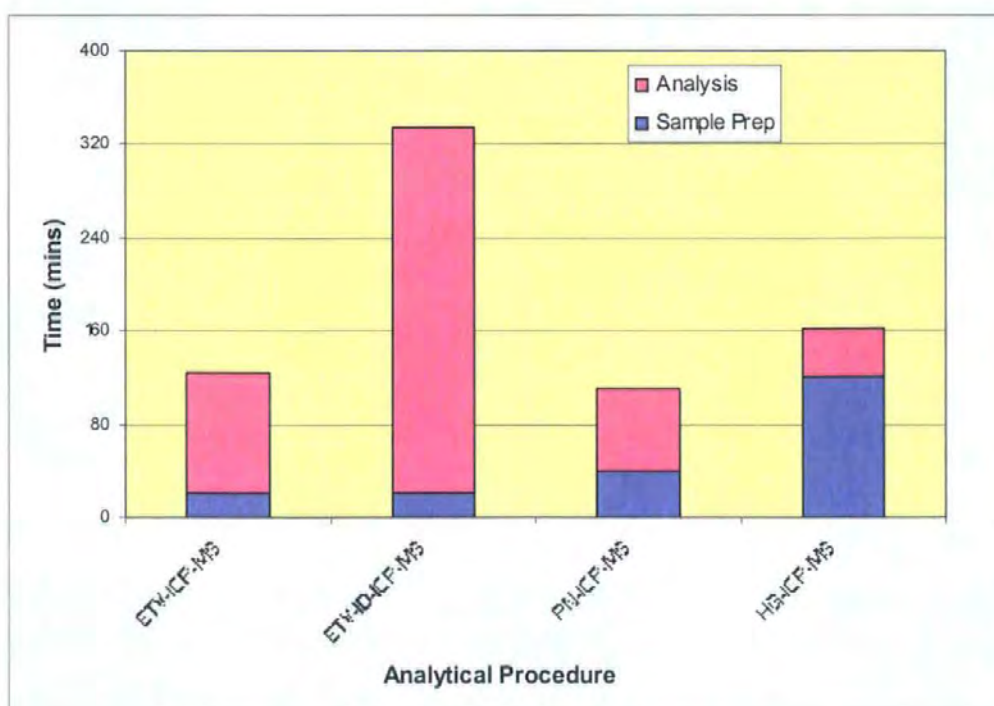


Figure 4.5 Comparison of the time required for sample preparation and analysis of 10 aqueous sample by each of the 4 methods examined.

4.6.3 Analytical Performance

Performance characteristics for each of the methods incorporating the different sample introduction techniques, have been evaluated and are compared in Table 4.11. The short-term stability of the PN-ICP-MS method is better than that of the other two methods, however the long-term stability is very similar for all of the procedures. Over the concentration range investigated, the linearity of each of the systems for the isotopes measured is again very consistent, with both the HG and PN procedures with linear ranges from 0-50ng g⁻¹ and the ETV procedure linearity from 0-100 ng g⁻¹.

	Method		
	HG-ICP-MS	PN-ICP-MS	ETV-ICP-MS
Short-term Stability (n=10)	±4.60%	±2.03%	±4.90%
Long-term Stability (n=10)	±5.55%	±6.15%	±4.70%
Linearity	0-50	0-50	0-100
Detection Limit	0.06ng g ⁻¹	0.33ng g ⁻¹	0.14ng g ⁻¹

Table 4.11 Comparison of performance characteristics for each of the methods investigated. (HG-ICP-MS and ETV-ICP-MS = ⁷⁷Se, PN-ICP-MS = ⁷⁸Se).

4.6.4 Accuracy and Precision

The accuracy and precision of the four methods was evaluated using a range of certified reference materials. The results from the analysis of these CRMs can be seen in Table 4.12. It can be seen that good recovery values have been obtained for each of the CRMs tested by each of the procedures. The poorest results, ie lowest recovery values, were achieved for the analysis of the spiked rainwater (TMRAIN-95). This CRM has a certified level of 0.74 ng g⁻¹ which is close to the detection limit of all of the methods. It was not possible to obtain a result for this CRM using the PN-ICP-MS method as once the sample had been

diluted in accordance with the method, the concentration of Se present was below the method detection limit of 0.33 ng g^{-1} . Excellent results were obtained for the remaining aqueous CRM's for all of the procedures, with all results falling within the certified limits and producing recovery values from 95% to 117%. Slightly worse recovery values were acquired for the analysis of the bovine serum CRM, NIST 1598 by the HG-ICP-MS procedure. This may be due to the more complex matrix of this CRM and the need to carry out a microwave digestion of the sample prior to measurement.

CRM	Certified Level ng g^{-1}	Method	Result ng g^{-1}	% Recovery
TMRAIN-95 spiked rain water	0.74 ± 0.29	HG-ICP-MS	0.61 ± 0.03	82%
		PN-ICP-MS	< DL	-
		ETV-ICP-MS	0.64 ± 0.04	86%
		ETV-ID-ICP-MS	0.750 ± 0.006	101%
TMDA-54.2 Spiked soft water	15.0 ± 3.0	HG-ICP-MS	14.3 ± 0.11	95%
		PN-ICP-MS	15.0 ± 0.40	100%
		ETV-ICP-MS	15.5 ± 0.43	103%
		ETV-ID-ICP-MS	15.06 ± 0.01	100%
LGC 6010 Hard drinking water	9.30 ± 1.9	HG-ICP-MS	9.18 ± 0.16	99%
		PN-ICP-MS	9.86 ± 0.65	106%
		ETV-ICP-MS	10.9 ± 0.13	117%
		ETV-ID-ICP-MS	9.57 ± 0.05	103%
NIST 1598 Spiked bovine serum	42.4 ± 3.5	HG-ICP-MS	37.9 ± 10.3	89%
		PN-ICP-MS	47.1 ± 1.56	111%
		ETV-ICP-MS	40.8 ± 0.37	96%
		ETV-ID-ICP-MS	40.89 ± 0.02	96%

Table 4.12 Comparison of data from the analysis of four certified reference materials obtained by 4 different methods. (HG-ICP-MS and ETV-ICP-MS = ^{77}Se , PN-ICP-MS = ^{78}Se and ETV-ID-ICP-MS = $^{82}\text{Se}/^{77}\text{Se}$ ratio).

The results obtained for each of the CRMs have been plotted in Figure 4.5 and Figure 4.6 together with their corresponding error bars to illustrate more clearly the accuracy and precision of each of the methods. From these graphs it can be seen that with the exception of NIST 1598 by the HG-ICP-MS procedure, all of the results fall well within the certified limits for all of the CRMs. The HG-ICP-MS method involves an initial microwave digestion stage. The large spread of results may be an indication that this step has not been fully optimised, and further development is required. It can also be seen from these plots that the results acquired by the ETV-ID-ICP-MS procedure have the smallest error bars ($n = 3$) for all of the CRMs. In most cases the precision on the measurement with this method is at least an order of magnitude better than with the other procedures.

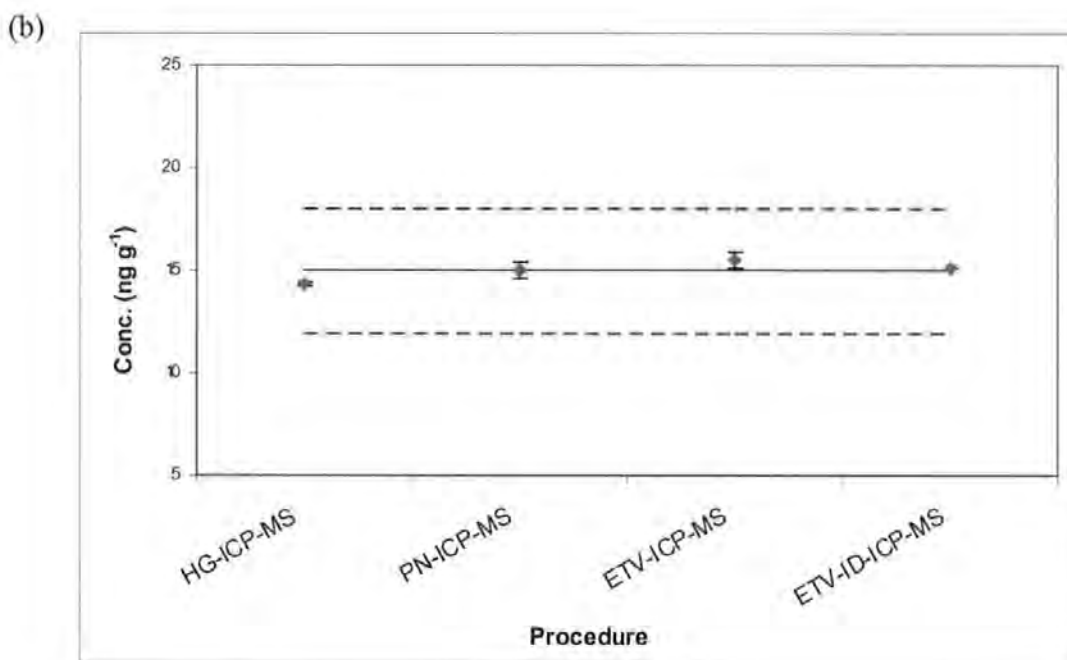
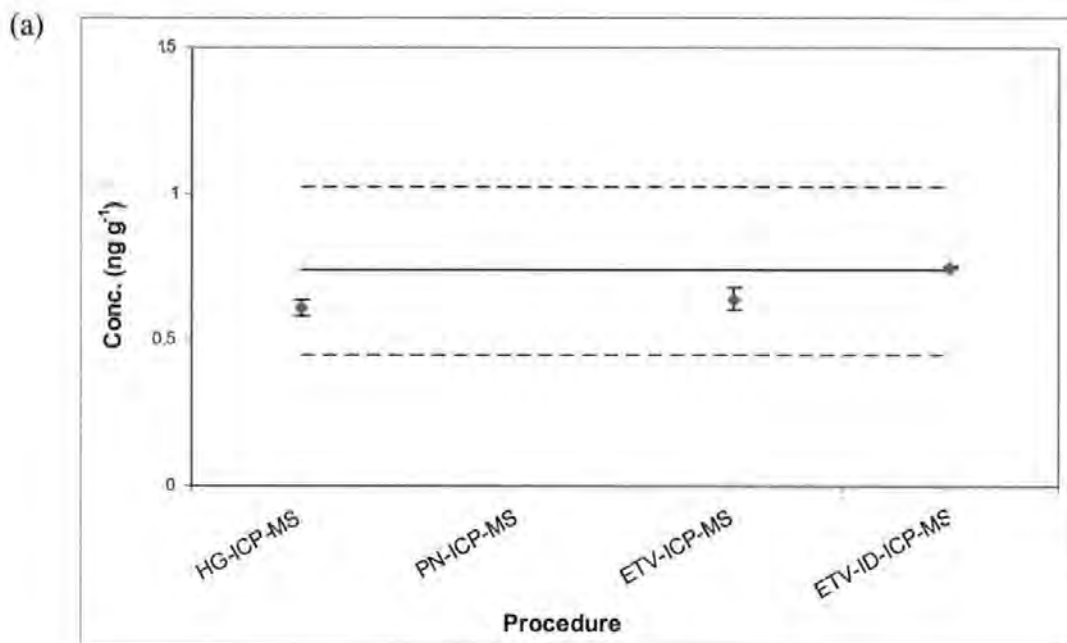


Figure 4.6 Summary of results obtained by each of the methods investigated: (a) Spiked rain water TMRAIN-95 and (b) spiked soft water TMDA-54.2. The error bars represent the standard deviation from triplicate analyses. The certified level and permitted range of each CRM are represented by the solid and dashed black lines respectively.

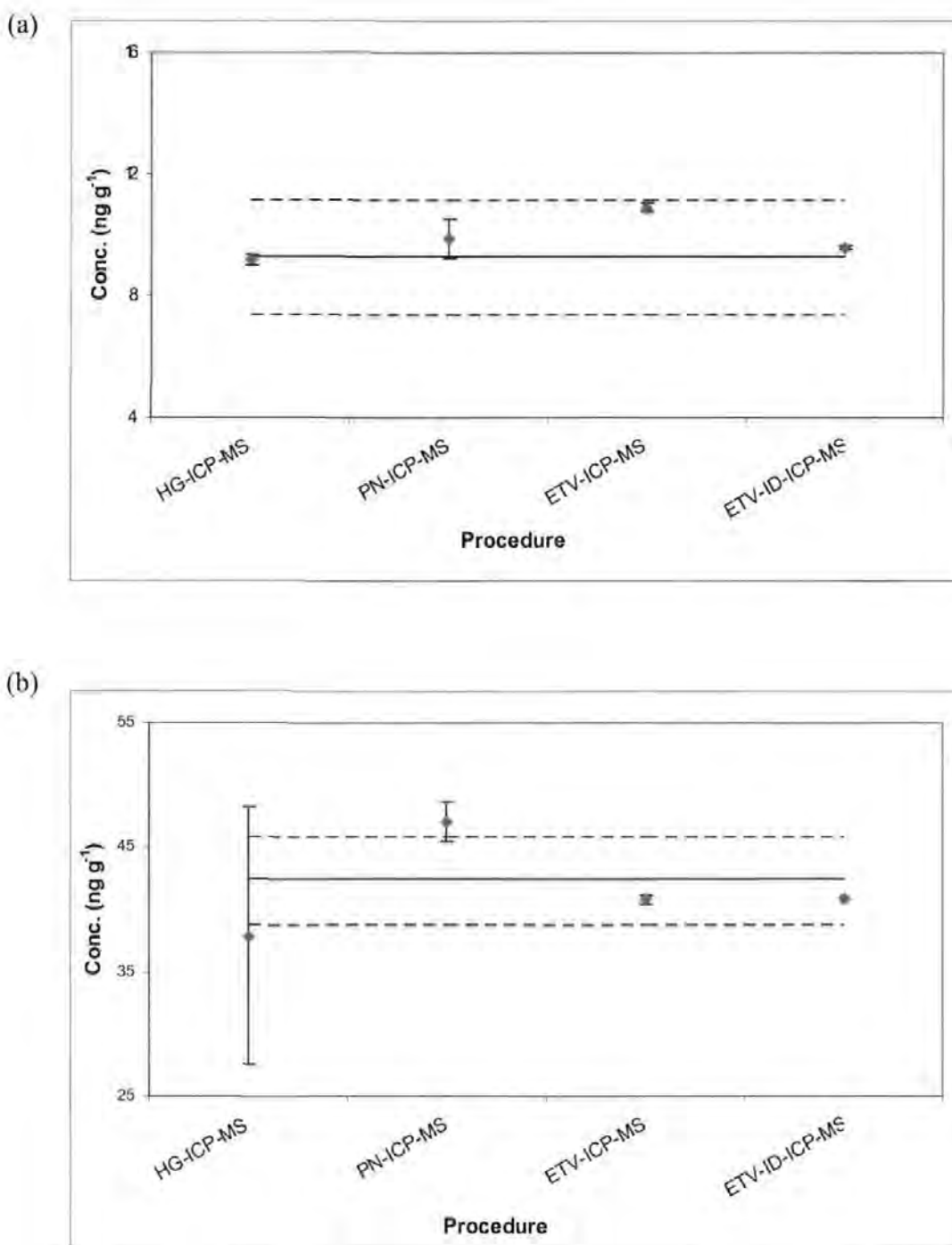


Figure 4.7 Summary of results obtained by each of the methods investigated; (a) hard drinking water LGC 6010 and (b) spiked bovine serum NIST 1598. The error bars represent the standard deviation from triplicate analyses. The certified level and permitted range of each CRM are represented by the solid and dashed black lines respectively.

4.7 Conclusions

This chapter has covered two further methods for the determination of selenium, utilising different sample introduction techniques (hydride generation and pneumatic nebulisation) and alternative ways to overcome the interferences associated with this element. The two methods have been compared with the ETV procedure (both conventional and IDMS) developed earlier (Chapters 2 and 3) and a comparison of all aspects of the procedures has been made. Similar performance characteristics such as stability, linearity and detection limits are achievable with each of the methods, however there are differences with the sample preparation and analysis time. The ETV procedure has the simplest preparation stage and the fastest overall analysis time, whereas the HG-ICP-MS is by far the most complicated and time consuming. A final comparison of the accuracy and precision of each of the methods was made, using four certified reference materials. All of the methods produced accurate results, however the ETV-ID-ICP-MS procedure gave the best precision.

CHAPTER 5

Uncertainty Estimates for the Determination of Selenium by ICP-MS

5. Uncertainty Estimates for the Determination of Selenium by ICP-MS

5.1 Introduction

The evaluation of the uncertainty associated with a result is often deemed an essential part of any quantitative analysis⁹¹ indeed an analytical result is thought incomplete without an indication of the uncertainty associated with it. The importance of measurement uncertainty is rapidly increasing in many different areas of analytical chemistry, and it is a requirement that analytical laboratories accredited in accordance with ISO Guide 25⁹² have an estimate of the associated measurement uncertainty. This will ultimately lead to improved intercomparability of analytical results. The knowledge of measurement uncertainty in the analytical community is often quite limited, therefore there is a need for the education of both analysts and customers, in the understanding of the measurement uncertainty of a particular result. An approach to the estimation of measurement uncertainty has been described in the International Standards Organisation (ISO) "*Guide to Expression of Uncertainty in Measurement*"⁹³ (GUM) and the Eurachem interpretation for analytical chemistry.⁹⁴ The principles of the GUM approach are that all sources of uncertainty, both random and systematic, are identified. For example, uncertainty contributions may result from the observations of repeated analysis, or from published data such as uncertainties for reference materials. Ultimately these individual contributions then give standard and expanded uncertainties. This approach differs from many methods currently used in analytical chemistry, which tend to use "whole method" performance parameters as a guide to the uncertainty of the procedure. Some applications of this approach to analytical chemistry have been published^{95,96} however, only a few uncertainty budgets have been reported.^{97,98}

This chapter discusses the estimation of the uncertainty of the four procedures for the determination of selenium by ICP-MS compared in Chapter 4, i.e.;

1. Hydride generation - HG-ICP-MS
2. Pneumatic nebulisation with butanol addition – PN-ICP-MS
3. Electrothermal vaporisation – ETV-ICP-MS
4. Electrothermal vaporisation with isotope dilution – ETV-ID-ICP-MS

The data required for the uncertainty estimates were obtained from specially designed experiments to include contributions from all aspects of the procedures.

5.2 Measurement Uncertainty – Conventional Calibration ICP-MS

The ISO definition of measurement uncertainty is:- “A parameter, associated with the result of a measurement, that characterises the dispersion of the values that could reasonably be attributed to the measurand.”⁹³ The first step in establishing the uncertainty of a method is to identify the sources of uncertainty through the construction of a cause and effect diagram.^{99,100} (Figure 5.1). The main horizontal line represents the “effect” which is the result of the analysis, i.e. concentration of Se in ng g⁻¹. Factors that control the result are represented by the lines protruding from this effect line and are known as the “cause” branches.

The starting point in the construction of a cause and effect diagram is to write out the complete equation for the result (Equation 5.1) Methods 1,2,and 3 each involve the determination of Se concentration by direct comparison to a calibration curve, therefore all of these method are represented by this equation.

$$C_{\text{Se}} = C \times D \times \frac{1}{R} \quad \text{Equation 5.1}$$

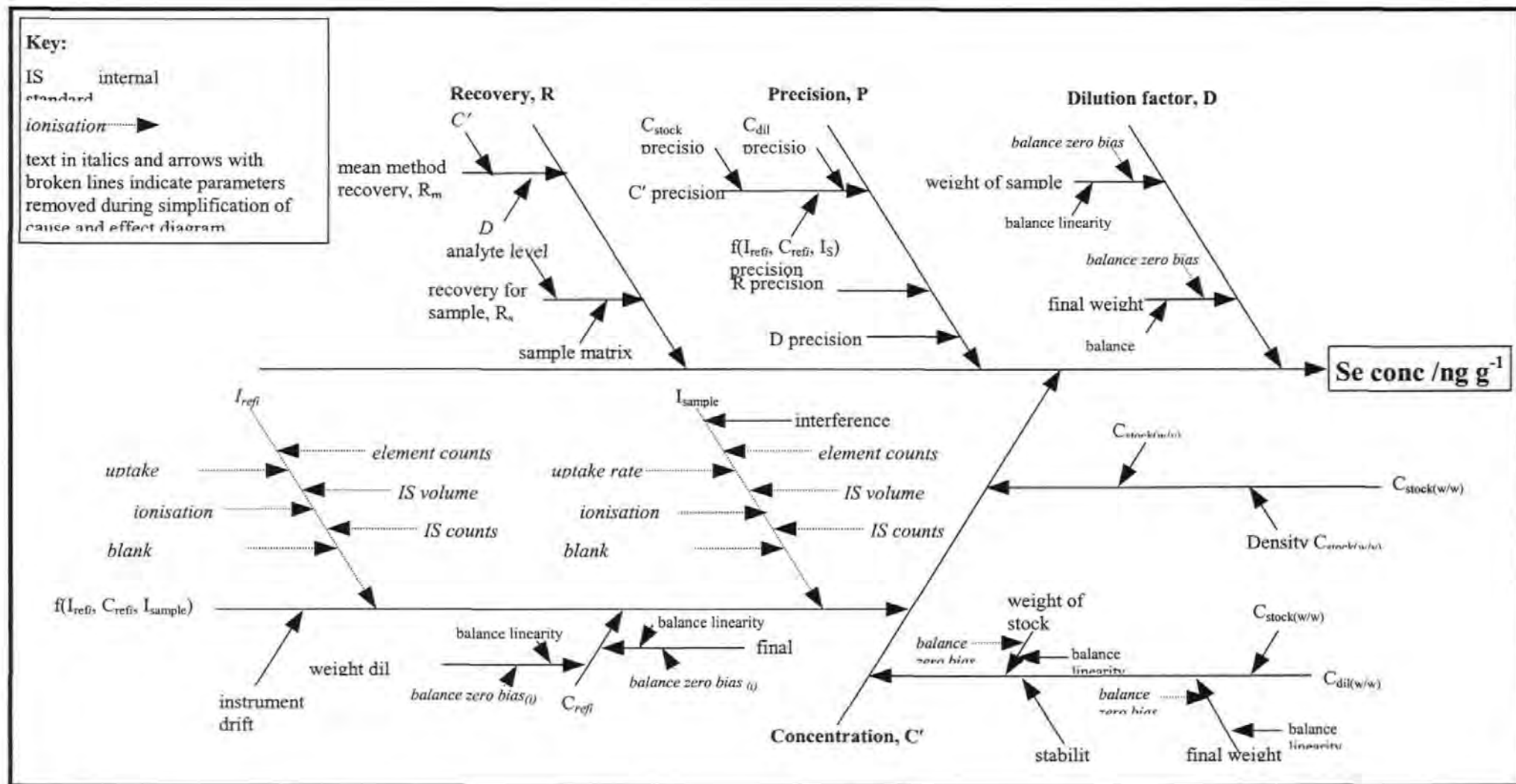


Figure 5.1 Cause and Effect Diagram for the Determination of Se by ICP-MS with Conventional Calibration

Here C' is the concentration of the sample solution as read from the calibration curve, D is the dilution factor applied to the sample and R is the mean recovery. The parameters present in the equation make up the main cause branches of the diagram. Once these main cause branches are identified, any additional contributing factors to the uncertainty need to be recognised and added to the diagram working outwards from the main branches until the effects on the end result become negligible. The diagram can then be simplified and factors which are duplicated on different branches can be removed. Each of the main cause branches is discussed in detail below.

5.2.1 Recovery, R

The overall recovery R for a particular sample is made up of two components, R_m and R_s , where $R = R_m \times R_s$, where R_m is an estimate of the recovery for the entire procedure, including preparation of calibration standards and any dilution of the sample. R_m is ideally measured on a suitable reference material, or as a mean recovery over several materials. Both the reference value used and the measurement of the recovery on that material, will have uncertainties associated with them. As well as determining the variation between R_m and the reference value, it is important to consider differences between R_m and the recovery for “real” samples. R_s represents this difference between the reference and a particular sample. Ideally there would be no difference and R_s would therefore be equal to 1.0. However different materials may have a different effect and this appears as an uncertainty in R_s . Thus $u(R_s)$ describes the variation in recovery between the different sample matrices and different analyte levels. Hence the uncertainty associated with R , $u(R)$, has contributions from $u(R_m)$ and $u(R_s)$.

5.2.2 Dilution Factor, D

With each of the methods investigated, the samples are diluted prior to analysis. For example – with the ETV method all samples are diluted 1 + 19 with 1% HNO_3 , and with

the HG method all standards and samples are diluted in the ratio 1.25:1 during the pre-reduction stage. There are two contributions to the uncertainty associated with this dilution factor, namely;

1. the uncertainty about the weight of the sample taken
2. the uncertainty about the final weight of the solution after dilution

As both of these measurements are weights by difference, with the tare and gross weights performed on the same balance within a short period of time, any balance “zero bias” cancels.

5.2.3 Precision, P

The precision covers terms which contribute to the random variability of the entire method. Repeatability data and QC data are excellent sources of information for estimates of precision. In general, if an operation was repeated during the period in which the precision data were obtained, the run-to-run variability associated with that operation will be included in the overall precision estimate and a separate estimate is not required.

5.2.4 Concentration, C'

The uncertainty associated with the concentration of the analyte, C', has contributions from three major areas;

1. $f(I_{refi}, C_{refi}, I_{sample})$ – calibration function, where C_{refi} represents a series of calibration standards and observed intensities I_{refi} , to the observed sample intensity, I_{sample} , to obtain the interpolated concentration value for the solution.
2. $C_{stock(w/w)}$ – concentration of the Se stock solution.
3. $C_{dil(w/w)}$ – concentration of the diluted Se working solution.

For this work, the concentration of the $1000 \mu\text{g ml}^{-1}$ Se stock solution has to be calculated in terms of weight by weight. This is achieved using the density data provided by the

supplier of the stock solution. The second source of uncertainty that contributes to the uncertainty in C' is the concentration of the dilute working standard, C_{dil} , from which the calibration solutions are prepared. This solution is prepared by diluting the stock solution on a weight by weight basis. Any uncertainties associated with the concentration of the dilute working standard (apart from run-to-run variations in preparing the standard) which need to be considered are the uncertainties about C_{stock} (w/w) and associated balance linearity terms.

The uncertainty associated with the calibration function $f(I_{refi}, C_{refi}, I_{sample})$ needs to be considered. The counts for the standards and sample (I_{refi} and I_{sample} respectively) will be affected by the instrument performance. A fresh set of calibration standards is used to calibrate the instrument at the beginning of each run, thus any errors linked to the instrument performance will be the same for both the calibration standards and the sample solutions, and should cancel out. Throughout a run of samples, the instrumental drift is monitored by the periodical analysis of one of the calibration standards. If a drift of greater than 10% is observed then the instrument is recalibrated and the samples reanalysed. A term representing the uncertainty due to this maximum permitted drift also needs to be included in the budget. The contribution to the overall uncertainty from the run-to-run variability of the instrument performance should be included in an estimate of the overall precision of the method. It is not therefore necessary to obtain individual uncertainty estimates for the components feeding into both the I_{refi} and I_{sample} branches.

5.3 Preparation of Uncertainty Solutions

In order to evaluate the uncertainties of each of the methods, a series of experiments were performed involving the analysis of a range of 'uncertainty solutions'. The aim of this study was to minimise the effect of each procedure by using the same solutions throughout the work. The solutions were prepared by serial dilution of NIST

3149 (Se standard) with 1% nitric acid on a w/w basis - details of these dilutions can be seen in Table 5.1. The data obtained from the analysis of these solutions were used to calculate the uncertainty budget of each method. The experiments involved the repeated analysis of the uncertainty solutions (during individual analytical runs and over a series of analytical runs, to generate both repeatability and reproducibility data) along with recovery information, for use in the uncertainty budgets. The instrumentation, operating conditions, reagents, sample preparation and standard preparation used for each of the methods are the same as those listed in previous chapters. Details of the ETV-ICP-MS procedure can be found in Chapter 2, section 2.3, the ETV-ID-ICP-MS procedure is given in Chapter 3, section 3.5, and details of the HG-ICP-MS and PN-ICP-MS procedures can be found in Chapter 4, sections 4.3 and 4.5 respectively.

NIST 3149 = 9.1130 mg g⁻¹ Se			
Dilution	Wt of Std (g)	Wt of Std + 1% HNO₃ (g)	Se Conc. (ng g⁻¹)
1	1.1091	100.5297	100,540
2	0.9760	100.9873	971.67
2a (uncertainty soln 1)	0.1994	101.2213	1.9141
2b (uncertainty soln 2)	0.4980	100.2226	4.8280
2c (uncertainty soln 3)	1.8206	97.7369	18.0998

Table 5.1 Preparation of 'uncertainty solutions' by serial dilution of NIST 3149 Se standard.

5.4 Estimation of Uncertainty Contributions

5.4.1 Method Recovery, R_m

The method recovery is calculated from repeatability data (Table 5.2) - i.e. data obtained during one analytical run using the same calibration data.

Method	1 HG-ICP-MS	2 PN-ICP-MS	3 ETV-ICP-MS
	5.08	4.71	4.39
	5.17	4.62	4.31
	5.20	5.10	4.36
	5.22	4.78	4.27
	-	5.01	4.31
	-	5.03	4.33
Mean (C_{OBS})	5.168	4.875	4.328
Std. Dev. (S_{OBS})	0.062	0.197	0.042
Relative s.d.	0.012	0.040	0.009
n	4	6	6

Table 5.2 Repeatability data for the analysis of uncertainty solution two.

This was obtained from the analysis of uncertainty solution two, prepared by serial dilution of NIST SRM 3149, with 1% nitric acid. The uncertainty associated with R_m , $u(R_m)$, is a combination of the uncertainty associated with concentration of the solution $u(C_{RM})$, and the uncertainty in the mean of the observations. (Equations 5.2 and 5.3).

$$u(R_m) = R_m \times \sqrt{\left(\frac{u(C_{RM})}{C_{RM}}\right)^2 + \frac{s_{obs}^2}{n \times c_{obs}^2}} \quad \text{Equation 5.2}$$

Where:-

$$R_m = \frac{c_{obs}}{C_{RM}} \quad \text{Equation 5.3}$$

Firstly the uncertainty associated with the concentration of the NIST SRM 3149 stock solution used to prepare solution two, needs to be determined. The concentration is certified as $9.97 \text{ mg ml}^{-1} \pm 0.06$. The density of the solution is quoted as $1.094 \text{ g ml}^{-1} \pm 0.002$. The first step is to convert the concentration of the stock solution from mg ml^{-1} to mg g^{-1} .

$$C_{(w/w)} = C_{(w/v)} / \text{density} = 9.97 / 1.094 = 9.113 \text{ mg g}^{-1} \quad \text{Equation 5.4}$$

The uncertainty of the concentration on a w/w basis is calculated from the uncertainty of the concentration on a w/v basis and the uncertainty associated with the density value used for the conversion. The uncertainty in the concentration of the solution is calculated by the supplier from the equation;

$$U = (2U_c + 0.001Y + B) \quad \text{Equation 5.5}$$

A coverage factor of 2 is assumed (using 95% confidence interval), therefore the uncertainty value (0.06) can be divided by 2, giving a value of 0.03 to be used in the calculations. The uncertainty associated with the density value is given by the supplier as 0.002 and is assumed to be a rectangular distribution, i.e. the true density value could fall equally anywhere between the stated range of 1.092g ml⁻¹ and 1.096g ml⁻¹. To convert this to a standard uncertainty the value of 0.002 can be divided by the square root of 3.

These two components are combined in the following equation to give the uncertainty of the concentration of the stock solution(w/w).

$$\frac{u(C_{\text{STOCK}(w/w)})}{C_{\text{STOCK}(w/w)}} = \sqrt{\left(\frac{u(C_{\text{STOCK}(w/v)})}{C_{\text{STOCK}(w/v)}}\right)^2 + \left(\frac{u(\text{STOCK}_{\text{density}})}{\text{STOCK}_{\text{density}}}\right)^2} \quad \text{Equation 5.6}$$

Therefore:-

$$u(C_{\text{STOCK}(w/w)}) = 9.113 \times \sqrt{\left(\frac{0.03}{9.97}\right)^2 + \left(\frac{0.00115}{1.094}\right)^2} = 0.029 \quad \text{Equation 5.7}$$

And hence :- $C_{\text{STOCK}(w/w)} = 9.113 \text{ mg g}^{-1} \pm 0.029 \text{ mg g}^{-1}$

Each of the uncertainty solutions were prepared by serial dilution of the NIST 3149 stock solution. The dilution factor is defined as:-

$$C_{DIL} = \frac{C_{STOCK(w/w)} \times W_{STOCK}}{W_{FINAL}} \quad \text{Equation 5.8}$$

where W_{STOCK} is the weight of the stock solution taken and W_{FINAL} is the final weight of the dilute working standard. The precisions associated with W_{STOCK} and W_{FINAL} need to be included in the uncertainty budget. Replicate weighings of 1g and 100g calibrated weights gave standard deviations of 0.00006 g and 0.00024 g respectively. Combining these values with the uncertainty calculated for the concentration of the stock solution gives the following equation to calculate the uncertainty of the dilute solution, $u(C_{DIL})$:-

$$u(C_{DIL}) = C_{DIL} \times \sqrt{\left(\frac{u(C_{STOCK(w/v)})}{C_{STOCK(w/v)}}\right)^2 + \left(\frac{u(W_{STOCK})}{W_{STOCK}}\right)^2 + \left(\frac{u(W_{FINAL})}{W_{FINAL}}\right)^2} \quad \text{Equation 5.9}$$

From Table 5.1 it can be seen that two serial dilutions (dilution 1 and dilution 2) of the stock solution were prepared initially. Dilution 2 was further diluted to prepare the three uncertainty solutions – noted as dilutions 2a, 2b and 2c in Table 5.1. The uncertainty associated with each of these dilutions is calculated in turn.

Dilution 1 - 1.1091g of $C_{STOCK(w/w)}$ was diluted to 100.5297g with 1% HNO_3 .

$$u(C_{DIL1}) = 100540 \times \sqrt{\left(\frac{0.029}{9.113}\right)^2 + \left(\frac{0.0006}{1.1091}\right)^2 + \left(\frac{0.00024}{100.5297}\right)^2} \quad \text{Equation 5.10}$$

Therefore:- $u(C_{DIL1}) = 319.96$

Dilution 2 - 0.9760g of DIL 1 was diluted to 100.9873g with 1% HNO₃.

$$u(C_{DIL2}) = 971.67 \times \sqrt{\left(\frac{319.96}{100540}\right)^2 + \left(\frac{0.0006}{0.9760}\right)^2 + \left(\frac{0.00024}{100.9873}\right)^2} \quad \text{Equation 5.11}$$

Therefore:- $u(C_{DIL2}) = 3.0926$

Dilution 2a - 0.1994g of DIL 2 was diluted to 101.2213g with 1% HNO₃.

$$u(C_{DIL2a}) = 1.9141 \times \sqrt{\left(\frac{3.0926}{971.67}\right)^2 + \left(\frac{0.0006}{0.1994}\right)^2 + \left(\frac{0.00024}{101.2213}\right)^2} \quad \text{Equation 5.12}$$

Therefore:- $u(C_{DIL2a}) = 0.0061$

Dilution 2b - 0.4980g of DIL 2 was diluted to 100.2226g with 1% HNO₃.

$$u(C_{DIL2b}) = 4.8280 \times \sqrt{\left(\frac{3.0926}{971.67}\right)^2 + \left(\frac{0.0006}{0.4980}\right)^2 + \left(\frac{0.00024}{100.2226}\right)^2} \quad \text{Equation 5.13}$$

Therefore:- $u(C_{DIL2b}) = 0.0154$

Dilution 2c - 1.8206 g of DIL 2 was diluted to 97.7369g with 1% HNO₃.

$$u(C_{DIL2c}) = 18.0998 \times \sqrt{\left(\frac{3.0926}{971.67}\right)^2 + \left(\frac{0.0006}{1.8206}\right)^2 + \left(\frac{0.00024}{97.7369}\right)^2} \quad \text{Equation 5.14}$$

Therefore:- $u(C_{DIL2c}) = 0.0576$

As mentioned previously, the data acquired to calculate the method recovery was obtained through the repeated analysis of uncertainty solution two. Therefore the uncertainty associated with the concentration of this solution, $u(C_{RM})$, is actually $u(C_{DIL2b})$ and has a value of 0.0154. This and the concentration of the solution, C_{RM} which is 4.8280 ng g^{-1} , are the same for all methods, but the values for C_{OBS} , S_{OBS} and n will vary. These are detailed in Table 5.2. This data is used to determine the method recovery for each procedure in accordance with equations 5.2 and 5.3 in the following way:-

5.4.1.1 Method 1 - HG-ICP-MS

$$R_m = \frac{5.168}{4.828} = 1.0704 \quad \text{Equation 5.15}$$

$$u(R_m) = 1.0704 \times \sqrt{\left(\frac{0.0154}{4.828}\right)^2 + \frac{0.062^2}{4 \times 5.168^2}} \quad \text{Equation 5.16}$$

Therefore :- $u(R_m) = 0.00730$

5.4.1.2 Method 2 - PN-ICP-MS

$$R_m = \frac{4.875}{4.828} = 1.0097 \quad \text{Equation 5.17}$$

$$u(R_m) = 1.0097 \times \sqrt{\left(\frac{0.0154}{4.828}\right)^2 + \frac{0.197^2}{6 \times 4.875^2}} \quad \text{Equation 5.18}$$

Therefore:- $u(R_M) = 0.01697$

5.4.1.3 Method 3 - ETV-ICP-MS

$$R_m = \frac{4.328}{4.828} = 0.8965 \quad \text{Equation 5.19}$$

$$u(R_m) = 0.8965 \times \sqrt{\left(\frac{0.0154}{4.828}\right)^2 + \frac{0.042^2}{6 \times 4.328^2}} \quad \text{Equation 5.20}$$

Therefore:- $u(R_M) = 0.00456$

5.4.2 Dilution Factor, D

With each of the methods considered, the samples are diluted prior to analysis. The dilution factor is given by:-

$$D = \frac{W_f}{W_s} \quad \text{Equation 5.21}$$

where W_s is the weight of sample taken and W_f is the final weight after dilution. As mentioned in section 5.3.1 replicate weighings of 1g and 10g weights gave standard deviations of 0.000060g and 0.00024g respectively. These values can be used as estimates of the uncertainty of the balance used to carry out the dilutions. As different dilutions were

required for each of the procedures, the uncertainty estimate associated with the dilution factor will be calculated for each method separately.

5.4.2.1 Method 1 – HG-ICP-MS

12.5g of sample is mixed with 10g of concentrated HCl acid.

$$u(D) = 4.828 \times \sqrt{\left(\frac{0.00024}{12.5}\right)^2 + \left(\frac{0.00024}{22.5}\right)^2} \quad \text{Equation 5.22}$$

Therefore:- $u(D) = 0.00011$

5.4.2.2 Method 2 – PN-ICP-MS

1g of sample is diluted to 15g with modifier B.

$$u(D) = 4.828 \times \sqrt{\left(\frac{0.00006}{1}\right)^2 + \left(\frac{0.00024}{15}\right)^2} \quad \text{Equation 5.23}$$

Therefore:- $u(D) = 0.00026$

5.4.2.3 Method 3 – ETV-ICP-MS

0.2g of sample is diluted to 2.0g with 1% HNO₃.

$$u(D) = 4.828 \times \sqrt{\left(\frac{0.00006}{0.2}\right)^2 + \left(\frac{0.00006}{2}\right)^2} \quad \text{Equation 5.24}$$

Therefore:- $u(D) = 0.00145$

5.4.3 Precision, P

This is calculated from reproducibility data, i.e. data obtained over several runs - and compares the relative standard deviations of the results obtained. The reproducibility data obtained for the three solutions can be seen in Table 5.3. To calculate the precision of the methods over a concentration range from approx. 2-20ng g⁻¹ the relative standard

deviations of the data obtained at each concentration are pooled using the following equation:-

$$RSD_{(POOL)} = \sqrt{\frac{(n_1 - 1) \times RSD_1^2 + (n_2 - 1) \times RSD_2^2 + (n_3 - 1) \times RSD_3^2}{(n_1 - 1) + (n_2 - 1) + (n_3 - 1)}} \quad \text{Equation 5.25}$$

Where n represents the number of replicate measurements made at each concentration. The reproducibility data obtained by each of the methods investigated (Table 5.3) will be evaluated in turn.

5.4.3.1 Method 1 - HG-ICP-MS

$$RSD_{(POOL)} = \sqrt{\frac{2 \times 0.057^2 + 2 \times 0.005^2 + 2 \times 0.169^2}{2 + 2 + 2}} \quad \text{Equation 5.26}$$

Therefore:- **RSD_(POOL) = 0.0989**

5.4.3.2 Method 2 - PN-ICP-MS

$$RSD_{(POOL)} = \sqrt{\frac{2 \times 0.130^2 + 2 \times 0.031^2 + 2 \times 0.022^2}{2 + 2 + 2}} \quad \text{Equation 5.27}$$

Therefore:- **RSD_(POOL) = 0.0790**

5.4.3.3 Method 3 - ETV-ICP-MS

$$RSD_{(POOL)} = \sqrt{\frac{5 \times 0.071^2 + 5 \times 0.040^2 + 5 \times 0.016^2}{5 + 5 + 5}} \quad \text{Equation 5.28}$$

Therefore:- **RSD_(POOL) = 0.0510**

METHOD	1 HG-ICP-MS	2 PN-ICP-MS	3 ETV-ICP-MS
Soln. 1 (1.910 ng g ⁻¹)	2.11	1.34	1.76
	2.03	1.74	1.76
	2.00	1.55	1.48
	-	-	1.80
	-	-	1.75
	-	-	1.80
Mean	2.05	1.543	1.73
Std. Dev.	0.057	0.200	0.122
Relative S.D.	0.028	0.130	0.071
Soln. 2 (4.828 ng g ⁻¹)	5.20	4.53	4.30
	5.22	4.28	4.51
	5.17	4.32	4.83
	-	-	4.55
	-	-	4.59
	-	-	4.41
Mean	5.20	4.38	4.53
Std. Dev.	0.025	0.134	0.180
Relative S.D.	0.005	0.031	0.040
Soln. 3 (18.10 ng g ⁻¹)	14.9	17.7	16.7
	12.0	17.1	16.6
	16.9	17.0	16.5
	-	-	17.1
	-	-	17.0
	-	-	17.1
Mean	14.6	17.3	16.8
Std. Dev.	2.464	0.379	0.266
Relative S.D.	0.169	0.022	0.016

Table 5.3 Reproducibility data for the analysis of uncertainty solutions one, two and three.

5.4.4 Concentration of the dilute working standard, Cdil(w/w)

Each method requires the preparation of a series of calibration standards. A dilute working standard with a concentration of 10 $\mu\text{g g}^{-1}$ was prepared from a 1000 $\mu\text{g g}^{-1}$ stock solution. The uncertainty associated with the concentration of this dilute standard needs to be determined. This is accomplished in the same way as the uncertainty associated with the concentration of NIST SRM 3149 in section 5.3.1. The certificate for the stock solution used for this work quoted a concentration of 1004 $\mu\text{g ml}^{-1}$ with an uncertainty of $\pm 0.5\%$, which is equal to 5.02 $\mu\text{g ml}^{-1}$. The certificate also gave a density for the solution of 1.0113 at 23.3°C, therefore the concentration of the stock on a w/w basis is 992.8 $\mu\text{g g}^{-1}$. As with

the concentration of NIST SRM 3149 in section 5.3.1, the uncertainty of the concentration on a w/w basis is calculated from the uncertainty associated with the density value used for the conversion. As before the uncertainty in the concentration of the solution as specified by the supplier is assumed to be a rectangular distribution, the standard uncertainty is therefore obtained by dividing the stated uncertainty by the square root of 3 which gives $2.898 \mu\text{g ml}^{-1}$. No uncertainty statement for the density was given by the supplier, therefore it is estimated as $\pm 0.0001 \text{ g cm}^{-3}$ (i.e., the uncertainty in the last decimal place). Again a rectangular distribution is assumed, so this is divided by the square root of 3 giving an uncertainty associated with the density of $0.000058 \text{ g cm}^{-3}$.

The uncertainty associated with the stock solution is obtained by combining these 2 components according to equation 5.6 above giving:-

$$u(C_{\text{STOCK}(w/w)}) = 992.8 \times \sqrt{\left(\frac{2.898}{1004}\right)^2 + \left(\frac{0.000058}{1.0113}\right)^2} = 2.866 \quad \text{Equation 5.29}$$

Hence:- $C_{\text{STOCK}(w/w)} = 992.8 \mu\text{g g}^{-1} \pm 2.866 \mu\text{g g}^{-1}$

This stock solution was diluted with 1% HNO₃ to give the dilute working standard that was used to prepare the calibration standards for each method. As with NIST SRM 3149 in section 5.3.1, the uncertainties associated with this dilution are accounted for using equation 5.9. This gives:-

Working Std Prep = 1.0108g of stock diluted to 102.0025g with 1% HNO₃.

$$u(C_{\text{DIL}}) = 9.84 \times \sqrt{\left(\frac{2.866}{992.8}\right)^2 + \left(\frac{0.0006}{1.0108}\right)^2 + \left(\frac{0.00024}{102.0025}\right)^2} \quad \text{Equation 5.30}$$

Therefore:- $u(C_{\text{DIL}}) = 0.0284$

5.4.5 Instrument Drift

As mentioned previously in section 5.1.5, since fresh calibration standards were prepared daily, any variation in day to day performance of the instrument will be the same

for standards and samples and will therefore cancel out. Hence only the variation of the instrument performance within a batch of samples needs to be considered. With each of the procedures one of the calibration standards is re-analysed at intervals throughout the run. A drift of $\pm 10\%$ is permitted before action is taken, i.e. instrument re-calibrated. The maximum permitted drift is therefore $\pm 10\%$. Since there is no evidence of lower probability towards the extremes of the range this can be treated as a rectangular distribution and divided by the square root of 3 to obtain the standard uncertainty associated with instrument drift, ($u(\text{drift})$), which is equal to 0.0577 (as a relative standard deviation).

5.5 Calculation of Combined Standard Uncertainty – Conventional Calibration

To obtain an uncertainty estimate for each method, the individual uncertainty terms are combined as relative standard deviations. (The uncertainty contributions and combined standard uncertainty are listed in Table 5.4) The combined standard uncertainty is calculated from the square root of the sum of the squares of the individual components.

PARAMETER		1	2	3
		HG-ICP-MS	PN-ICP-MS	ETV-ICP-MS
Method Recovery	$u(R_m)$	0.0073	0.0170	0.0046
Dilution Factor	$u(D)$	0.00011	0.00026	0.00145
Conc. Of Dil Solution	$u(C_{DIL})$	0.0029	0.0029	0.0029
Precision	$u(P)$	0.0989	0.0790	0.0510
Instrument Drift	$u(\text{drift})$	0.0577	0.0577	0.0577
Combined Standard Uncertainty	$U(C_{Se})$	0.554ng g^{-1}	0.480ng g^{-1}	0.373ng g^{-1}

Table 5.4 Uncertainty budget for the determination of Se by HG-ICP-MS, PN-ICP-MS and ETV-ICP-MS.

5.6 Estimation of Uncertainty – ETV-ID-ICP-MS Procedure

The uncertainty of the ETV-ID-ICP-MS procedure is calculated differently from the other methods already covered. The combined uncertainty is calculated in accordance with the uncertainty propagation law as detailed in the Eurachem guide.⁹⁴ The following equation is used (see Table 5.7 for notation definitions):-

$$c_X = c_Z \cdot \frac{m_Y}{m_X} \cdot \frac{m_{Zc}}{m_{Yc}} \cdot \frac{R_Y - R'_B \cdot \frac{R_{Bc}}{R'_{Bc}}}{R'_B \cdot \frac{R_{Bc}}{R'_{Bc}} - R_X} \cdot \frac{R_{Bc} - R_X}{R_Y - R_{Bc}} \quad \text{Equation 5.31}$$

This equation combines factors such as the ratios of the spiked sample and mass bias solutions, the standard deviation of repeated ratio measurements and the instrument drift. An explanation of how the uncertainty associated with each of the variables present in equation 5.31 is calculated, is given below.

5.6.1 Uncertainty of the masses; m_{Zc} , m_{Yc} , m_X , m_Y

As with the determination of the uncertainty associated with the concentration of the dilute stock standard in section 5.3.1, the standard uncertainty of replicate weighings of a 1g calibrated weight was previously calculated to be 0.00006g. All of the weights used in this work were in the range of 1g, therefore their standard uncertainty is equal to 0.00006g.

5.6.2 Uncertainty of the mass fractions of the primary natural standard and the spike solution; c_Z and c_Y

High purity Se pellets were used to prepare the primary natural standard solution used for this work. The pellets were dissolved in conc. HNO_3 and then diluted with water to give a solution with a concentration of $6703.4 \mu\text{g g}^{-1}$. This was further diluted to give a

final solution with a mass fraction of 3.9343ng g⁻¹. The mass fraction c_z was calculated according to:

$$c_z = p \cdot \frac{m_{Se\ metal}}{m(S_1)} \cdot \frac{m_1}{m(S_2)} \cdot \frac{m_2}{m(S_3)} \cdot \frac{m_3}{m(S_4)} \quad \text{Equation 5.32}$$

where p is the purity of the selenium dissolved, $m_{Se\ metal}$ the mass of metallic Se dissolved into $m(S_1)$ mass of acid solution, m_1 , m_2 and m_3 are the masses of the solutions S_1 , S_2 and S_3 further diluted to the masses $m(S_2)$, $m(S_3)$ and $m(S_4)$ to get solutions S_2 , S_3 and S_4 . The Se metal had a stated purity of 0.99999, but no uncertainty estimate for this purity was given. The standard uncertainty was therefore estimated at 0.00010. Details of the weights taken and their corresponding uncertainties are given in Table 5.5. The data was used to calculate the combined uncertainty of c_z , from the square root of the sum of the squares of the variables identified in equation 5.32. This gives a combined standard uncertainty of 0.00080ng g⁻¹.

Component	Value	Uncertainty	Concentration	Uncertainty
P	0.99999	0.00010	-	-
$m_{Se\ metal}$	0.61959g	0.00006g	-	-
$m(S_1)$	92.4292g	0.00024g	-	-
m_1	1.4959g	0.00006g	-	-
$m(S_2)$	100.5854g	0.00024g	-	-
m_2	1.0024g	0.00006g	-	-
$m(S_3)$	101.9919g	0.00024g	-	-
m_3	0.4038g	0.00006g	-	-
$m(S_4)$	100.5619g	0.00024g	-	-
S_1	-	-	6703µg g ⁻¹	0.9240µg g ⁻¹
S_2	-	-	99.69µg g ⁻¹	0.0141µg g ⁻¹
S_3	-	-	979.8ng g ⁻¹	0.1486ng g ⁻¹
$S_4 (= c_z)$	-	-	3.9343ng g ⁻¹	0.0008ng g ⁻¹

Table 5.5 Data used to calculate the uncertainty associated with the preparation of the natural Se standard, c_z

Reverse isotope dilution mass spectrometry analysis was used to determine the mass fraction of the spike. This has already been discussed in Chapter 3, section 3.2.2, and is calculated according to the following equation:-

$$w_Y = w_Z \cdot \frac{m_{Zc}}{m_{Yc}} \cdot \frac{R_Z - R_{Bc}}{R_{Bc} - R_Y} \cdot \frac{\sum_i R_{iY}}{\sum_i R_{iZ}} \quad \text{Equation 5.33}$$

The combined standard uncertainty associated with the spike was calculated in the same way as the uncertainty associated with the sample, i.e involved the combination of the standard uncertainties of the individual quantities present in equation 5.33.

5.6.3 Uncertainty of the isotope ratios of the primary natural standard and the spike material; R_Z and R_Y

The IUPAC isotopic composition table⁸⁷ gives the relative abundance of each isotope with their corresponding uncertainties. The isotope ratios were calculated from these abundances by dividing the abundance of each isotope by the abundance of the ^{77}Se isotope. The IUPAC uncertainties were assumed to have a rectangular distribution and were therefore divided by the square root of 3 to give the standard uncertainty of each abundance.(Table 5.7). The uncertainty associated with the isotope ratios were determined by combining the relative uncertainties of both isotopic abundances present in the ratio according to the following equation:-

$$u_c(R_{iZ}) = R_{iZ} \times \sqrt{\left(\frac{u(f({}^i\text{Se}))}{f({}^i\text{Se})}\right)^2 + \left(\frac{u(f({}^{77}\text{Se}))}{f({}^{77}\text{Se})}\right)^2} \quad \text{Equation 5.34}$$

The isotope ratio of the spike R_Y , was calculated from the isotopic composition stated on its certificate. The uncertainties associated with these abundances were combined

in the same way as for the primary standard, to give the uncertainty associated with the isotope ratio of the spike. These can also be seen in Table 5.6.

Isotope	Abundance	Uncertainty	Isotope amount ratio	$u(R_i)$
<i>Natural Primary Standard</i>				
74Se	0.89	0.04	0.1166	0.0033
76Se	9.37	0.29	1.228	0.0265
77Se	7.63	0.10	1	0
78Se	23.77	0.28	3.115	0.0432
80Se	49.61	0.41	6.502	0.0845
82Se	8.73	0.22	1.144	0.0216
<i>Enriched Spike Solution</i>				
74Se	0.27	0.04	0.0039	0.00058
76Se	2.60	0.30	0.0379	0.0045
77Se	68.69	0.40	1	0
78Se	17.51	0.30	0.2549	0.0051
80Se	9.28	0.30	0.1351	0.0048
82Se	1.65	0.20	0.0240	0.0030

Table 5.6 Abundance and uncertainty data for the natural primary standard and the enriched spike solution taken from the IUPAC isotopic composition table⁸⁷ and the manufacturers certificate respectively.

5.6.4 Uncertainty of the measured isotope ratio of the sample and mass bias blends, R'_B and R'_{Bc}

As discussed in Chapter 3, nine replicate measurements were performed for each solution, and each sample was analysed with a corresponding mass bias solution following

the bracketing method detailed by Catterick and workers.⁸⁹ The standard deviation of these nine replicate measurements was used to calculate the uncertainty associated with the measurement of the isotope ratio of the sample blend. This involved dividing the standard deviation by the square root of the number of replicates, i.e. the square root of nine.

The uncertainty associated with the mass bias blend is calculated from the standard deviation of the nine replicate measurements and the difference between the 2 bracketing mass bias blend isotope ratio measurements to compensate for drift.

5.6.5 Uncertainty of the prepared isotope ratio of the mass bias blend, R_{Bc}

The prepared isotope ratio of the gravimetrically prepared mass bias blend is calculated from data for the natural primary standard and the enriched spike solution namely; the isotope ratios and the mass fractions of both solutions. The standard uncertainties associated with each of these components are then combined to give the standard uncertainty associated with the preparation of the mass bias solution, R_{Bc} , which is equal to 0.00659.

Due to the extent and complexity of the calculations involved in establishing the uncertainty of this IDMS procedure, a spreadsheet has been constructed to assist with the calculations. This is presented in Appendix 1. Four individual blends of uncertainty solution two were prepared. The example given in Appendix A contains data from the analysis of one of these blends, however the average concentration and combined uncertainty for all four blends is given as the ultimate result and final uncertainty estimate for the method. Data from this spreadsheet is also presented in Table 5.7, showing the magnitude of each variable contributing to the combined uncertainty and illustrating which factors had the greatest influence on the final uncertainty value.

Parameter		Value	Standard Uncertainty	Relative Uncertainty
Mass fraction of Se in the natural primary standard	c_z	3.9343ng g ⁻¹	2.20x10 ⁻³ ng g ⁻¹	5.59x10 ⁻⁴
Mass of sample (sample blend)	m_x	1.8807g	6.00x10 ⁻⁵ g	3.19 x10 ⁻⁵
Mass of spike (sample blend)	m_y	1.0012g	6.00x10 ⁻⁵ g	5.99x10 ⁻⁵
Mass of natural primary standard (mass bias blend)	m_{zc}	2.3075g	6.00x10 ⁻⁵ g	2.60x10 ⁻⁵
Mass of spike (mass bias blend)	m_{yc}	1.0094g	6.00x10 ⁻⁵ g	5.94x10 ⁻⁵
Isotope amount ratio of the spike	R_y	0.0240	3.00x10 ⁻³	0.1250
Isotope amount ratio of the natural primary standard	R_z	1.1442	0.0220	0.0192
Prepared isotope amount ratio of the mass bias blend	R_{Bc}	0.3312	6.59x10 ⁻³	0.0199
Measured isotope amount ratio of the sample blend	R'_B	0.3795	2.81x10 ⁻³	7.40x10 ⁻³
Measured isotope amount ratio of the mass bias blend	R'_{Bc}	0.3750	5.05x10 ⁻³	0.0135
Mass fraction of Se in the sample (blend 1)	C_x	4.8751ng g ⁻¹	0.112ng g ⁻¹	2.29%
Average mass fraction of Se in uncertainty Solⁿ. two	$\overline{c'_x}$	4.8633ng g⁻¹	0.1418ng g⁻¹	2.92%

Table 5.7 Summary of individual uncertainty terms and combined standard uncertainty values for the ETV-ID-ICP-MS methods.

5.7 Comparison of Combined Uncertainty Estimates

Table 5.8 shows the combined uncertainty estimates for each of the four methods investigated. The standard and relative uncertainties (expressed as a percentage of the analyte concentration) of each procedure are given. The expanded uncertainty estimate is also shown, which is calculated by applying a coverage factor, k , of 2 which represents a 95% confidence level.

METHOD	1 HG-ICP-MS	2 PN-ICP-MS	3 ETV-ICP-MS	4 ETV-ID-ICP-MS
Standard $u_c(\text{Se})$	0.55ng g ⁻¹	0.48ng g ⁻¹	0.37ng g ⁻¹	0.1418ng g ⁻¹
Relative $u_c(\text{Se})$	11.0%	9.60%	7.40%	2.92%
Expanded $U(C_{\text{Se}})^1$	22.0%	19.2%	14.8%	5.83%

Table 5.8 Standard and expanded uncertainty estimates for methods 1 - 4.

¹ using the coverage factor $K=2$.

From the data in Table 5.8 it can be seen that for the conventional calibration methods the HG-ICP-MS procedure has the largest uncertainty estimate and the ETV-ICP-MS procedure the smallest. By incorporating the technique of isotope dilution analysis a 2.5 fold improvement in the uncertainty of the ETV procedure has been achieved. The main contributors to the uncertainty budget are precision and instrument drift for methods 1, 2, and 3 and the measured isotope amount ratio of the sample and mass bias blends with the ETV-ID-ICP-MS method. Figure 5.2 and Figure 5.3 better illustrates these parameters with a graphical representation of the contributing factors expressed as a percentage of the total uncertainty budget.

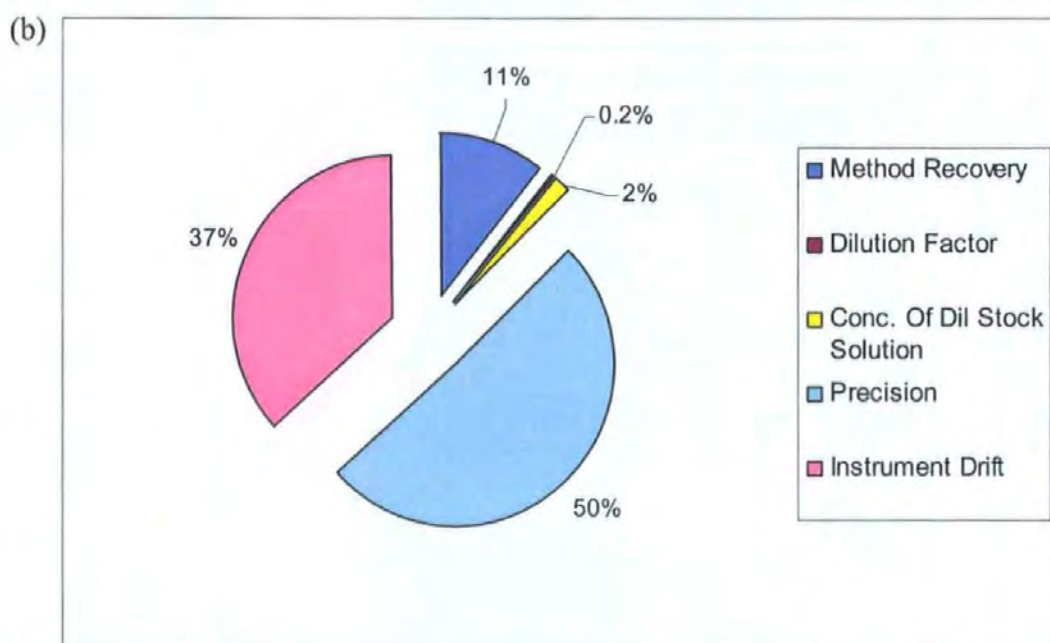
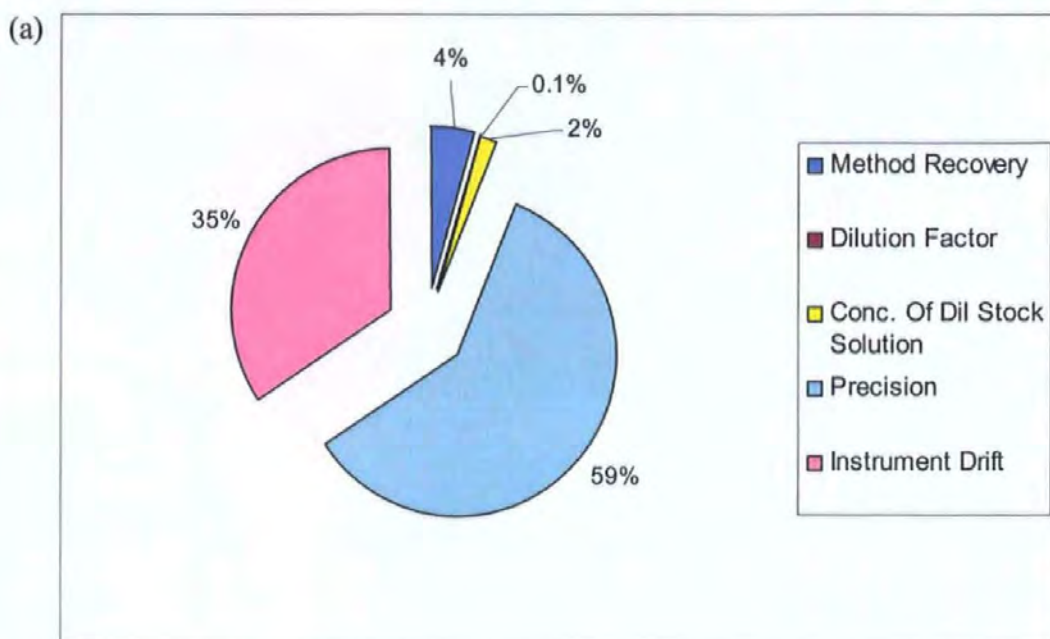


Figure 5.2 Contribution of the different variables to the uncertainty budget; (a) HG-ICP-MS procedure and (b) PN-ICP-MS procedure.

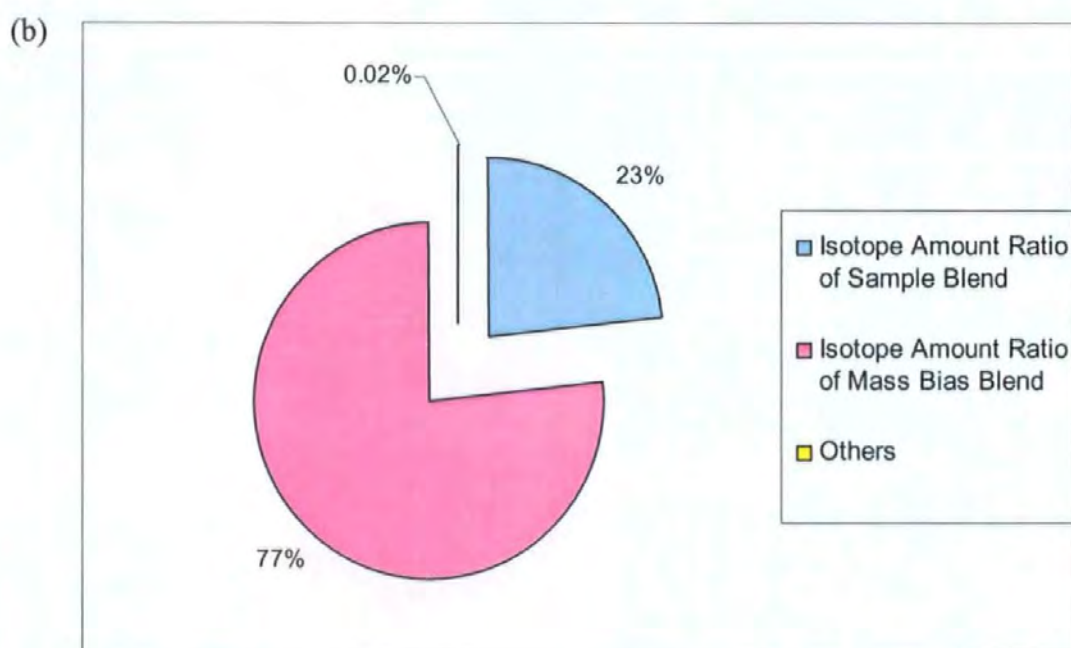
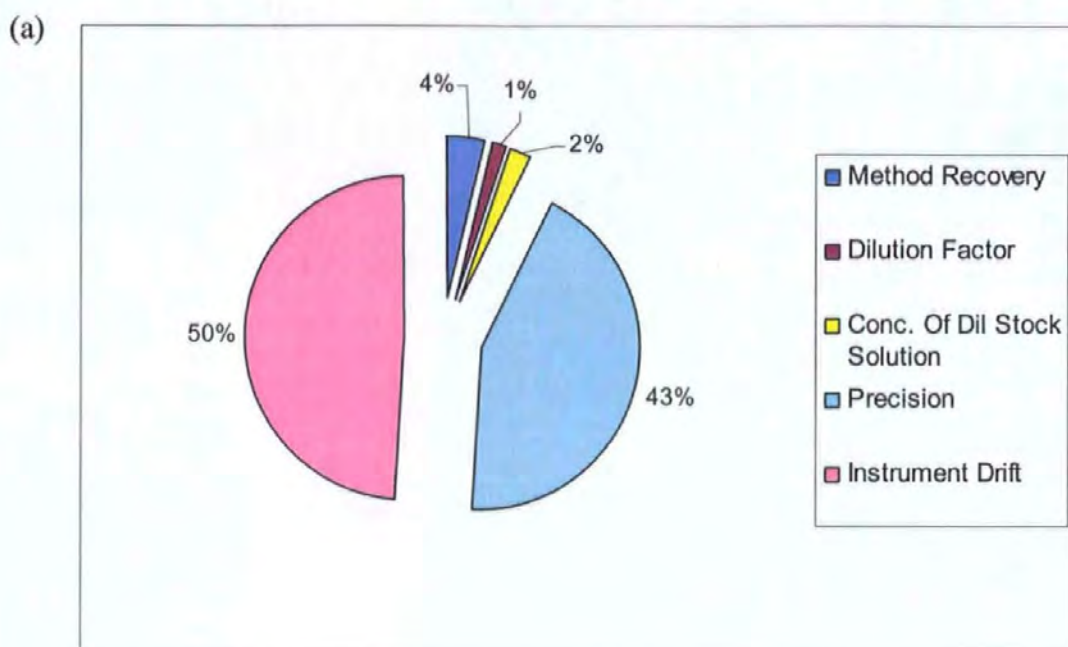


Figure 5.3 Contribution of the different variables to the uncertainty budget; (a) ETV-ICP-MS procedure and (b) ETV-ID-ICP-MS procedure.

A further comparison of the uncertainty estimates of each method is given in Figure 5.4, where the average concentration of uncertainty solution two as determined by each method, is plotted against the expected value of 4.828 ng g^{-1} . The expanded uncertainty for each method is represented by the error bars. The values used for the conventional calibration methods are the mean results from the reproducibility data detailed in Table 5.3, and the value used for the IDMS procedure is the average of the four blends as detailed in Table 5.7.

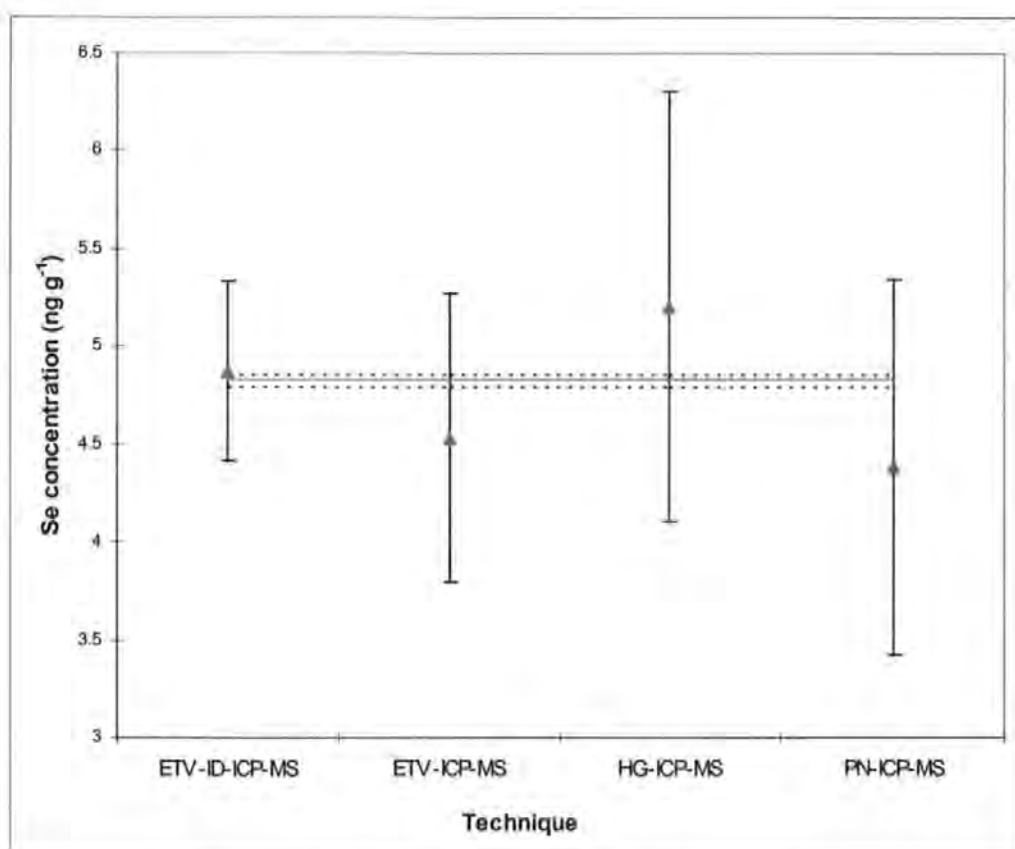


Figure 5.4 Plot of the results obtained for uncertainty solution two by each of the methods.

5.8 Conclusions

The standard uncertainties of four methods for the determination of Se have been evaluated, using data obtained from specially designed experiments. The resulting values indicate that for the conventional calibration methods the ETV-ICP-MS procedure has the smallest uncertainty. This is most probably due to the minimal sample pre-treatment required for this procedure - both the hydride generation and the conventional nebulisation sample introduction procedures involve additional sample preparation stages. These uncertainty values were based on data obtained for an in-house uncertainty solution prepared in 1% nitric acid. The uncertainty is likely to increase with the analysis of more complex matrices such as sediment, blood or serum.

Chapter 3 discussed the extension of the developed ETV-ICP-MS procedure to incorporate the technique of isotope dilution analysis, and data from the analysis of several certified reference materials highlighted the improvements in accuracy and precision achievable with this method. This enhancement is further emphasised here, with a 2.5 fold improvement in the uncertainty estimate for the ETV-ID-ICP-MS method compared with the conventional calibration ETV-ICP-MS procedure.

CHAPTER 6

Mixed Gas Plasmas

6. Mixed Gas Plasmas

6.1 Introduction

ICP-MS is a powerful analytical tool which can be used to determine a large number of trace elements in a wide variety of matrices (i.e environmental, clinical and foodstuffs) both accurately and precisely. However the technique suffers from several inherent disadvantages, one of which is the formation of polyatomic interferences particularly below m/z 80.^{11,12} This is especially problematic for the determination of Se whose first five isotopes with m/z below 80, all suffer from interference from polyatomic species. One way of reducing these interferences is via the addition of a molecular gas to one of the three channels of the ICP. Evans and Ebdon^{37,38} successfully reduced the interference from CCl^+ , OCl^+ , ArC^+ , ArO^+ , $ArCl^+$, and $ArAr^+$, at m/z 47, 51, 52, 56, 75, 76, 77 and 78 with the introduction of N_2 to nebuliser gas. The suggested mechanism for this reduction is either the competitive formation of carbides, nitrides and oxides with Ar and Cl, or that greater decomposition of the polyatomic species occurs due to an increase in the kinetic energy as a direct result of the introduction of the molecular gas. Laborda et al³⁵ also investigated the effect of an argon-nitrogen mixed gas plasma, and reported improvements in the measurement of ^{77}Se amongst other analytes, in five different reference materials using the addition of 8% N_2 to the nebuliser gas. The incorporation of nitrogen has not been restricted solely to introduction via the nebuliser gas. Lam and Horlick¹⁰¹ introduced nitrogen to the outer gas flow of the plasma and reported a 5-fold improvement in the background equivalent concentration for ^{80}Se . Other workers³²⁻³⁴ have studied the effect of adding N_2 to the outer gas, and have shown significant increases in signal to noise (S/N) and signal to blank ratios (S/B) for Se and other analytes in the presence of between 2% and 10% N_2 .

The use of helium-argon mixed gas plasmas is also well documented in the literature.¹⁰²⁻¹⁰³ He has a higher ionisation energy than Ar, and as such is able to enhance the degree of ionisation of difficult to ionise elements. Also, He is monoisotopic, therefore the amount of high mass polyatomics experienced with Ar ICPs is automatically significantly reduced.

This chapter covers an investigation taking these experiments one stage further by the addition of molecular gases (nitrogen, helium and trifluoromethane) to an Ar ETV-ICP-MS instrument, and the effect this has on the signal to blank ratio (S/B) of several of the selenium isotopes.

6.2 Instrumentation

The ELAN 5000 ICP-MS and HGA 600 ETV unit detailed in Chapter 2, section 2.3, along with the operating conditions listed in Chapter 2, Tables 2.1 and 2.2, were used throughout this study unless stated otherwise. A gas blender (series 850, Signal, Camberley, Surrey, UK) was used to introduce the different gases. Operation of the gas blender involves setting a control dial to deliver the required blend of gases. The dial settings are obtained from a calibration graph supplied with the equipment (see Appendix 2). When blending gases with different specific gravities the dial settings obtained from the graph will not be correct. The following equation is therefore used to allow for these differences in specific gravity.

$$P_n = \frac{R_n}{100.C_n} \sum_{n=1}^{n=S+1} R_n.C_n \quad \text{Equation 6.1}$$

where:- R_n = required % of stream n gas, C_n = correction factor for n gas, S = number of controlled streams, $S+1$ = Diluent stream and P_n = Percentage to be set for stream n to achieve R_n .

During this work nitrogen and helium were each blended with argon. The corresponding dial settings needed to deliver the required mixtures of each of these gases have been calculated in accordance with Equation 6.1 and can be found in Appendices 3 and 4.

6.3 Reagents

All solutions were prepared using high purity deionised water (18M Ω , Elga, High Wycombe, Buckinghamshire, UK). A stock solution (1000 $\mu\text{g ml}^{-1}$) of Se (Alfa, Johnson Matthey, Royston, UK) was used, diluted with 1% m/m HNO₃, ultrapure Ultrex II grade acid (JT Baker(UK), Milton Keynes, Buckinghamshire, UK) to give a 10ng g⁻¹ working standard. Palladium(II)nitrate (Sigma, Poole, Dorset, UK) was used to prepare the chemical modifier solution.

During each experiment the signal intensities of a 10ng g⁻¹ Se standard and a 1% HNO₃ acid blank solution were monitored. The signal to blank ratio (S/B) could then be calculated at each stage of the experiment and plotted against the parameter being varied (i.e. N₂ content, He content, gas flow rate etc). The signal intensities of the 76, 77, 78, 80 and 82 selenium isotopes were monitored and the S/B calculated using the following equation:-

$$S/B = \frac{I_{(std)} - I_{(blk)}}{I_{(blk)}} \quad \text{Equation 6.2}$$

where:-

$I_{(std)}$ = intensity of 10ng g⁻¹ Se standard

$I_{(blk)}$ = intensity of 1% HNO₃ blk

6.4 Nitrogen Addition

An evaluation of the effect of nitrogen addition on the ETV-ICP-MS system was performed via several different experiments. These included; i) N₂ addition to nebuliser gas – post ETV, ii) N₂ addition to nebuliser gas – pre ETV, iii) N₂ addition to auxillary (outer) gas, and iv) N₂ addition as ETV alternative gas. The findings from each of these experiments are discussed below.

6.4.1 Nitrogen addition to Ar nebuliser gas – post ETV

Nitrogen was connected to the ICP-MS via the oxygen inlet tube and the nitrogen level regulated using the oxygen mass/flow controller. A T-piece fitted in the PTFE transfer tube allowed the nitrogen to mix with the argon nebuliser gas before arriving at the plasma, i.e. after it had passed through the ETV unit. The N₂ content was increased from 0-10% in 1% increments, with the nebuliser gas flow rate maintained at 1.0 l min⁻¹ throughout, and the RF power set at 975W. This power setting is lower than the optimum level established during the development of the ETV procedure (see Chapter 2, section 2.5.2), but was chosen in an attempt to limit the formation of ³⁸Ar³⁸Ar⁺, ³⁸Ar⁴⁰Ar⁺ and ⁴⁰Ar⁴⁰Ar⁺ polyatomics due to the reduced ionisation of Ar gas at the lower power setting. The formation of these Ar polyatomic species was less important during the work detailed in Chapter 2 as the main isotopes of interest. ⁷⁷Se and ⁸²Se, are not affected by these interferences unlike the isotopes under investigation here. As the N₂ content increased, the signal for the 1% HNO₃ blank solution decreased for the 76, 78 and 80 selenium isotopes, but increased slightly for the 77 and 82 isotopes. However the signal for the 10ng g⁻¹ selenium standard decreased for all isotopes. It was therefore more informative to examine the signal to blank ratio (S/B) in order to establish the full effect of the nitrogen. Figure 6.1 illustrates the variation in the S/B ratio as the nitrogen content increases, for the five

isotopes monitored. It can be seen that an increase in the S/B ratio for the 76 and 78 isotopes is observed as the nitrogen content is increased initially, which then decreases as the nitrogen exceeds 5%. The optimum S/B is observed at 4% nitrogen. The plots for the 77 and 82 isotopes show a large decrease of the S/B ratio with an increase in nitrogen content, and little variation in the S/B ratio of the ^{80}Se isotope. This response is generally as expected, with the 76 and 78 isotopes showing the greatest beneficial effect due to the reduction of the Ar polyatomic interferences on these two isotopes. Despite the increase in the S/B ratio of the 76 and 78 isotopes with the introduction of 4% nitrogen to the nebuliser gas, the overall sensitivity of the system was greatly reduced – by approximately 50%. A series of experiments were therefore performed to try and increase the sensitivity whilst maintaining the improved S/B ratio.

6.4.1.1 Variation of RF Power

The initial experiment adding nitrogen to the nebuliser gas in the range 0-10%, was repeated at a higher power setting of 1075W. This was to establish i) if the overall sensitivity could be improved at a higher power setting, and ii) if the optimum S/B ratio differed at a higher power setting. Figure 6.2 shows the S/B ratio versus nitrogen content for the 76 and 78 isotopes at both power settings of 975W and 1075W and illustrates that no significant gains in sensitivity were achieved. In fact, the trends plotted are identical to those obtained at the lower power setting, with the optimum S/B ratio again achieved with 4% nitrogen.

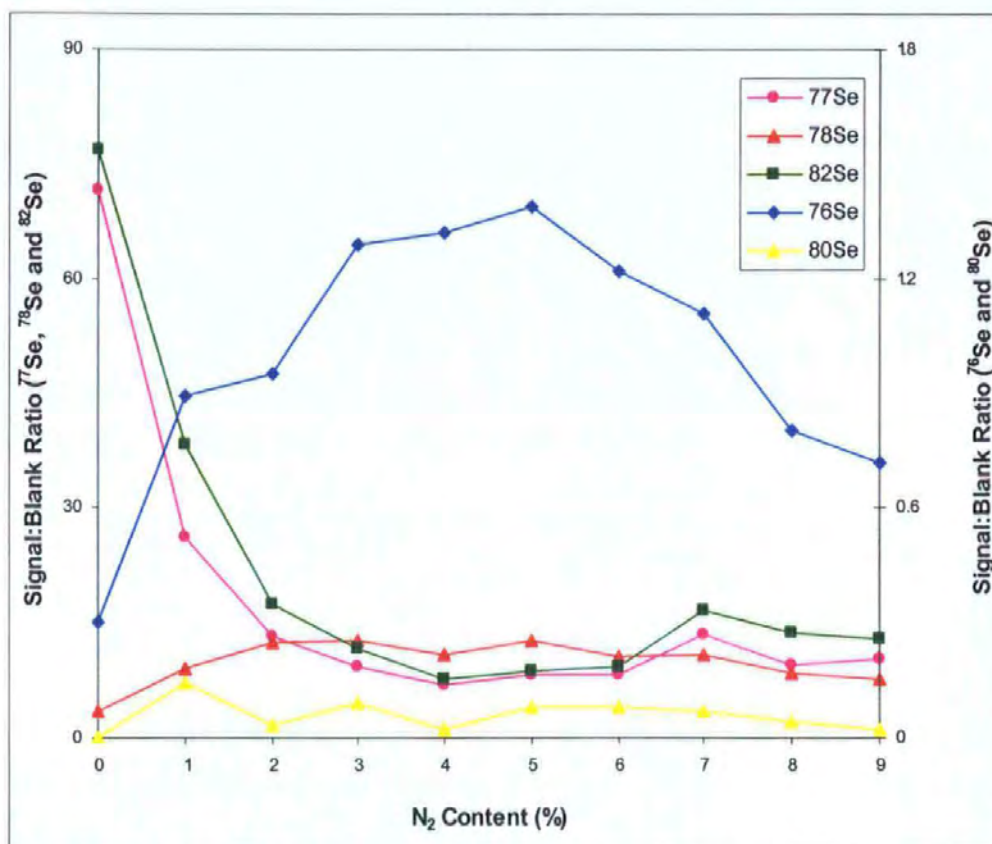


Figure 6.1 The effect of nitrogen addition to the argon nebuliser gas on the S/B ratio of the 76, 77, 78, 80 and 82 selenium isotopes.

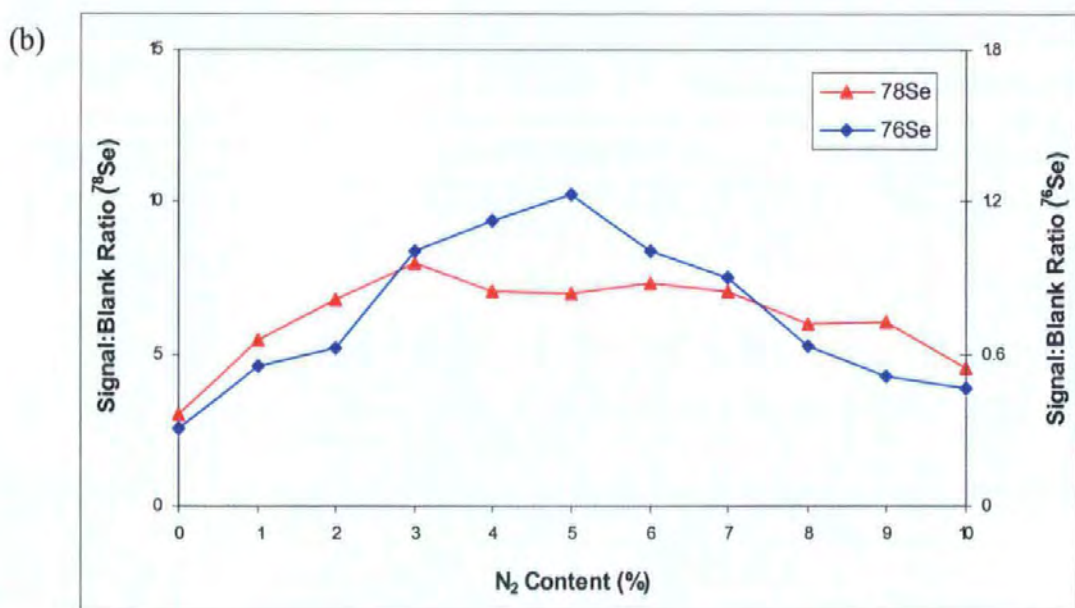
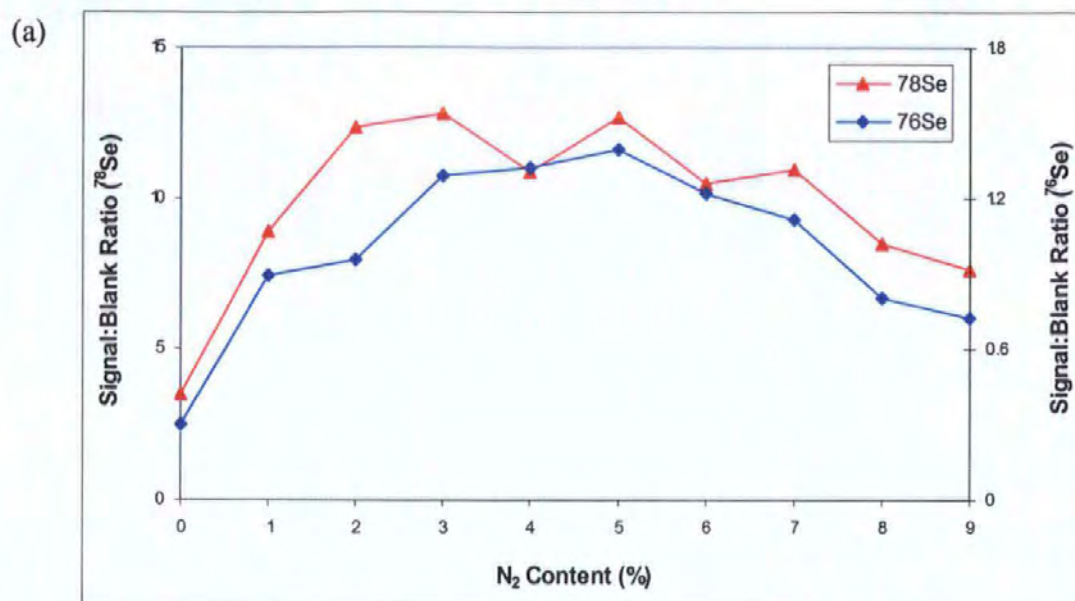


Figure 6.2 The effect of nitrogen addition to argon nebuliser gas on 76 and 78 selenium isotopes at a) 975W RF power and b) 1075W RF power.

6.4.1.2 Variation of Ar flow-rate

In the previous experiment (section 6.4.1.1) the nebuliser gas flow rate was maintained at 1.00 l min^{-1} throughout. The optimum S/B ratio was observed with the introduction of 4% N_2 to the nebuliser gas, i.e. 0.04 l min^{-1} . The nitrogen flow rate was therefore set at 0.04 l min^{-1} and the Ar flow rate was systematically increased from 0.65 l min^{-1} to 1.10 l min^{-1} , thus altering the total nebuliser gas flow rate from 0.69 l min^{-1} to 1.14 l min^{-1} . The effect of this on the S/B ratio of the 76 and 78 isotopes can be seen in Figure 6.3. This graph shows that the S/B ratio for both isotopes increases as the flow rate is increased from 0.65 to 0.86 l min^{-1} , then decreases at flow rates above this. The optimum S/B ratio for ^{76}Se is observed with an Ar flow rate of 0.86 l min^{-1} , and for ^{78}Se at an Ar flow rate of 0.76 l min^{-1} . This equates to a total nebuliser gas flow rate of 0.90 l min^{-1} and 0.80 l min^{-1} for the 76 and 78 isotopes respectively, with nitrogen additions of 4.4% and 5%. These optimum flow rates and nitrogen additions are very similar to those identified during earlier work. However there was no improvement in the overall sensitivity of the system.

6.4.2 Nitrogen addition to Ar nebuliser gas – pre ETV

Nitrogen was connected to the ETV-ICP-MS system via a gas blender, which was in turn connected to the instrument via the nebuliser gas inlet. The gas blender allowed the nitrogen to be mixed with the argon off-line and one stream of mixed gas introduced to the instrument. This was better than the alternative arrangement of adding the two gases separately and mixing them via a t-piece as in the experiment described in section 6.4.1. The amount of nitrogen added to the argon stream was controlled accurately following the procedure for calculating blender settings for different gases as detailed in section 6.2. The nebuliser gas flow rate was set at 1.0 l min^{-1} , and the nitrogen level slowly increased. As

the nitrogen addition reached 1.5% the plasma began to flicker and then went out. The flow rate was therefore lowered to 0.95 l min^{-1} and the experiment repeated, but again the plasma could not be sustained with a nebuliser gas containing more than 1.5% nitrogen. The flow rate was then dropped further, to 0.80 l min^{-1} at which point a stable plasma could be maintained. An attempt was made to establish the background signal of the 76 and 78 isotopes through the analysis of the 1% HNO_3 blank, however the plasma extinguished as the vaporised analyte was swept into it.

Due to the lack of success with this experiment, no further work was performed.

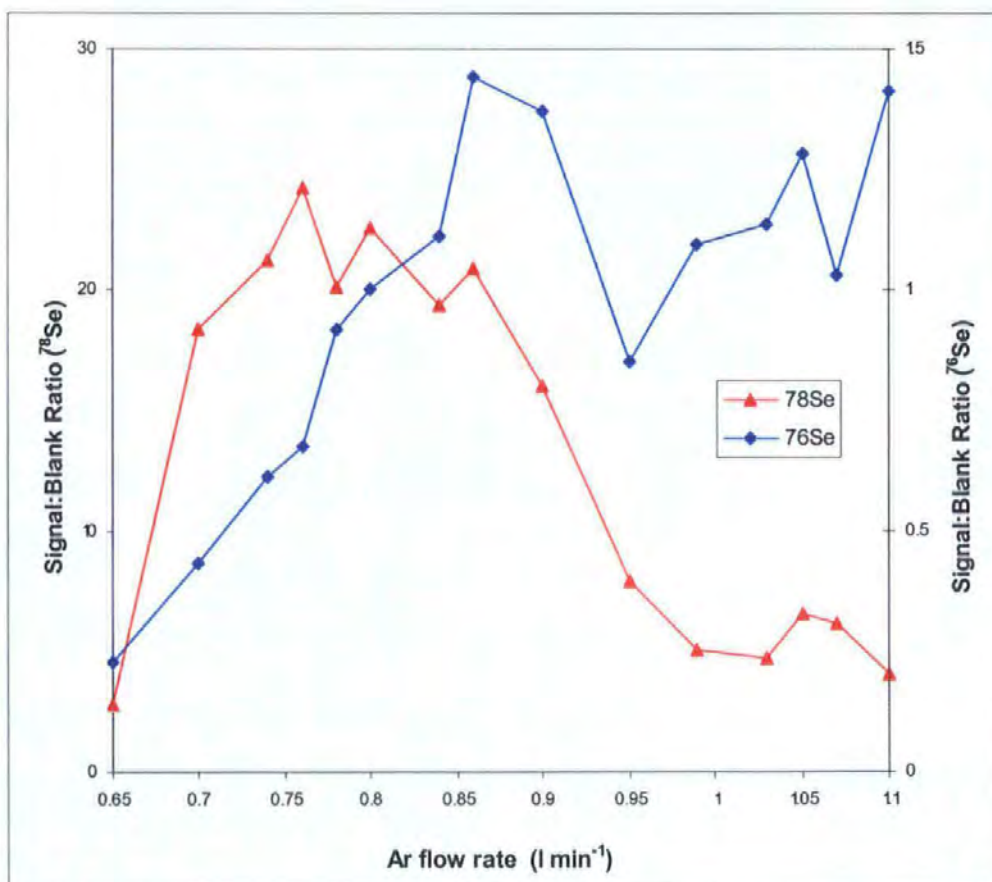


Figure 6.3 The effect of Ar nebuliser gas flow rate on 76 and 78 selenium isotopes, with the nitrogen flow rate set at 0.04 l min^{-1} .

6.4.3 Nitrogen addition to Ar outer gas

As with the experiment detailed in section 6.1.2, the nitrogen was introduced to the ETV-ICP-MS system via a gas blender. This was connected to the instrument via the outer gas inlet. The outer gas flow rate was set at 0.80 l min^{-1} and the RF power at 1150W, the optimum settings established during the development of the ETV-ICP-MS procedure (Chapter 2). The nitrogen content was increased from 0 to 5% at 1% increments (the plasma could not be maintained with a level of greater than 5% nitrogen), and the signal intensity for a 10 ng g^{-1} Se standard and a 1% HNO_3 blank measured. The effect of an increase in nitrogen content on the S/B ratio for the 76 and 78 Se isotopes are shown in Figure 6.4. It can be seen that the S/B ratio for both isotopes increases initially as the nitrogen level increases, reaches an optimum with a nitrogen addition of 2%, and decreases at levels above this. As found previously with the addition of nitrogen to the nebuliser gas, no beneficial effect was seen for the 77, 80 and 82 isotopes and these have therefore not been plotted.

6.4.3.1 Variation of RF power

The previous experiment indicated improvements in the S/B ratio of the 76 and 78 isotopes with the introduction of 2% nitrogen to the Ar outer gas. As found during earlier experiments (section 6.1.1), even though a net increase in the S/B ratio was achieved, the signal of the 10 ng g^{-1} Se standard and the 1% HNO_3 blank was significantly reduced – by approximately 50% for ^{76}Se and approximately 20% for ^{78}Se . A similar response has been reported by Xiao and Beauchemin³³, and is most probably due to a shift in the initial radiation zone (IRZ) away from the sampler cone as a direct result of a decrease in the physical size of the plasma. To evaluate if this loss of sensitivity could be regained, an investigation into the effect of RF power on the signal was performed. The RF power was

increased from 975W to 1150W. A higher signal for both the Se standard and the blank solution were observed at lower RF power settings, however the optimum S/B ratio for both isotopes was observed at the highest power setting of 1150W (See Table 6.1).

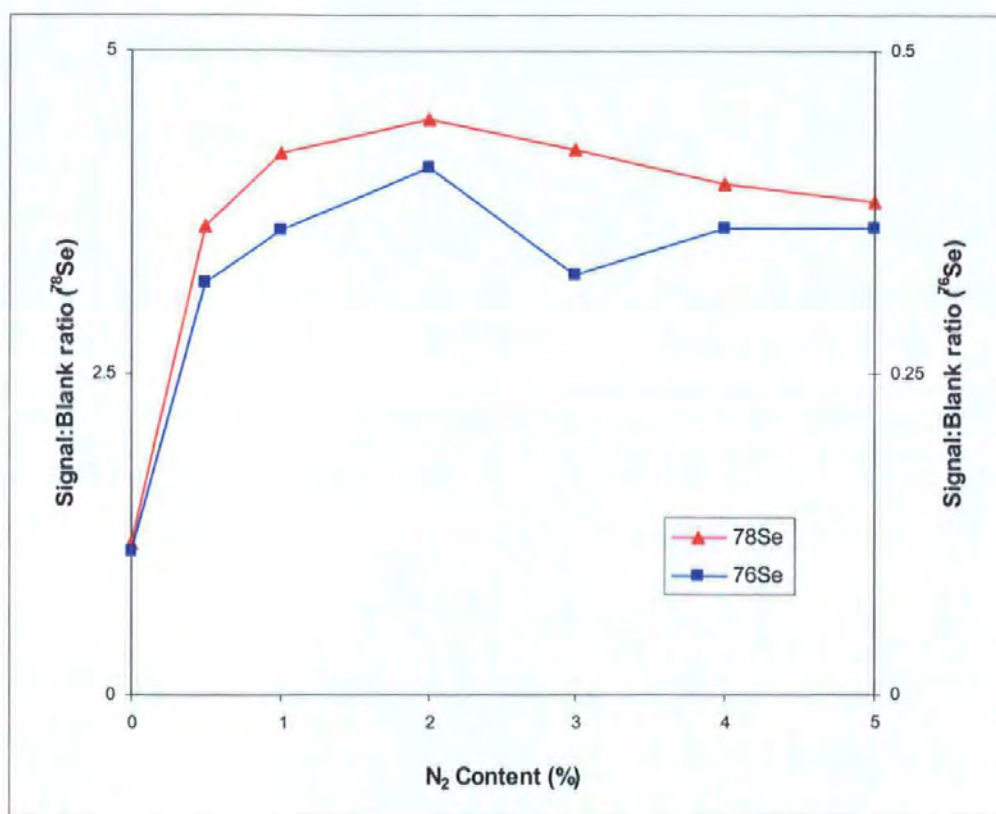


Figure 6.4 The effect of nitrogen addition to Ar outer gas on S/B ratio for the 76 and 78 Se isotopes with an outer gas flow rate of 0.80 l min^{-1} .

RF Power /W	⁷⁶ Se			⁷⁸ Se		
	I _{blk}	I _{std}	S/B	I _{blk}	I _{std}	S/B
975	66480	90380	0.36	15570	77910	4.00
1000	67480	90570	0.34	16440	79780	3.85
1050	59890	80600	0.35	15130	68270	3.51
1100	47570	62460	0.31	13520	56370	3.17
1150	34310	48340	0.41	8174	44710	4.47

Table 6.1 Effect of RF power on the signals (I, in counts/s) of a 1% HNO₃ blank, a 10ng g⁻¹ Se standard and the S/B ratio, for 2% N₂ in the Ar outer gas.

6.4.4 Nitrogen addition as ETV alternative gas

Nitrogen was connected directly to the ETV unit via the alternative gas inlet. Control of the gas flow was then performed using the HGA 600MS software. The flow rate of the nitrogen was steadily increased from 10ml min⁻¹ to a maximum of 200ml min⁻¹. The plasma extinguished at flow rates above 200ml min⁻¹. As with the previous experiments described in sections 6.4.1 to 6.4.3, the S/B ratio of the 76, 77, 78, 80 and 82 selenium isotopes were calculated at each gas flow, from the intensity of a 10ng g⁻¹ Se standard and a 1% HNO₃ blank. All isotopes followed the same trend, a decrease in both the signal of the blank and the 10ng g⁻¹ standard with an increase in nitrogen gas flow rate. This also resulted in a decrease in the S/B ratio of all of the isotopes as the nitrogen content increased (Figure 6.5). The experiment was carried out at a power of 1050W. Previous work detailed in section 6.4.3.1 showed that higher RF powers gave rise to an enhanced S/B ratio for the 76 and 78 isotopes. A further experiment was therefore performed to see if increasing the power with a fixed flow of N₂ alternative gas would result in improvements in the S/B ratio of any of the isotopes measured.

6.4.4.1 Variation of RF power

The flow rate of the N₂ alternative gas was set at 100ml min⁻¹, and the RF power varied from 900W to 1150W. As with the work described in section 6.4.3.1, the signal for both the blank and the 10ng g⁻¹ Se standard decreased with an increase in RF power, with maximum signals obtained at the highest power setting of 1150W. However no significant improvements in the S/B ratios were observed for any of the isotopes.

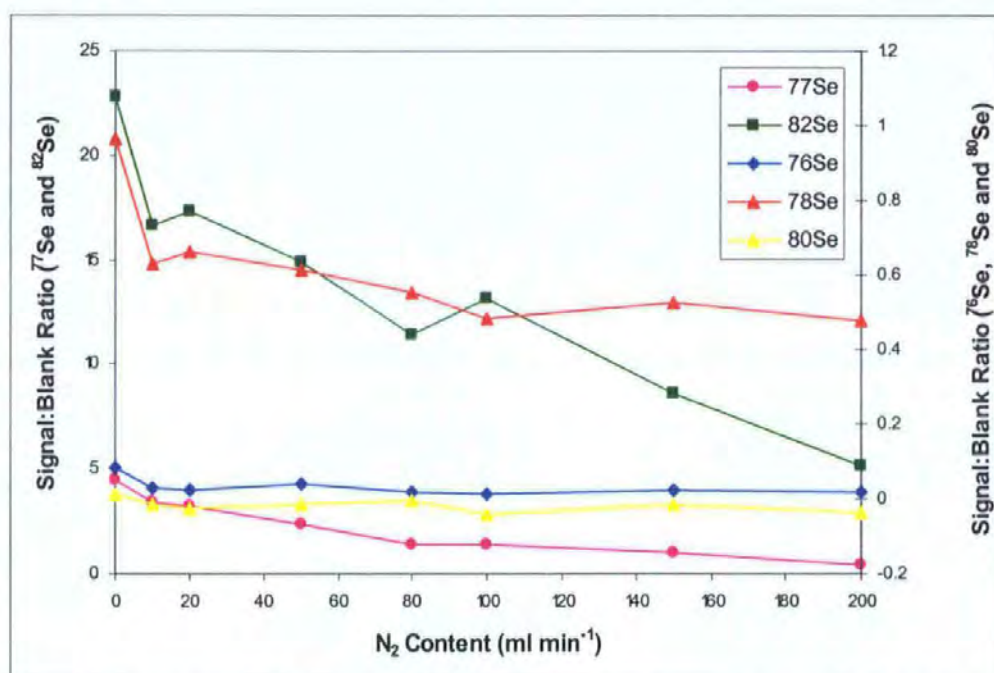


Figure 6.5 The effect of nitrogen addition as ETV alternative gas on the S/B ratio of the 76, 77, 78, 80 and 82 selenium isotopes.

6.5 Helium Addition

As with the investigation into the effect of nitrogen addition in section 6.4, various experiments were performed to evaluate the effect of helium. These centred around the addition of He to both the nebuliser gas and the outer gas. The findings from each of these experiments are discussed below.

6.5.1 Helium addition to Ar nebuliser gas

A gas blender was used to mix the He and Ar, which was connected to the ETV-ICP-MS via the nebuliser gas inlet. The gas was initially set at 100% Ar, at a flow rate of 1.20 l min⁻¹ and an RF power of 1150W. The He was slowly introduced into the Ar stream, from 0.5% to 3.5%, in 0.5% increments. A decrease in the signal of both the standard and the blank were noted, with no improvement in the S/B ratio. The experiment was repeated with a maximum He content of 15% but still no improvement in the S/B ratio of any isotopes was observed. A final experiment was performed with the addition of He from 0% to 100%. As with the initial experiments the signal intensity of both the standard and the blank decreased throughout with no enhancement in the S/B ratio of any of the isotopes – see Figure 6.6. No further work involving the addition of He to the nebuliser gas was performed.

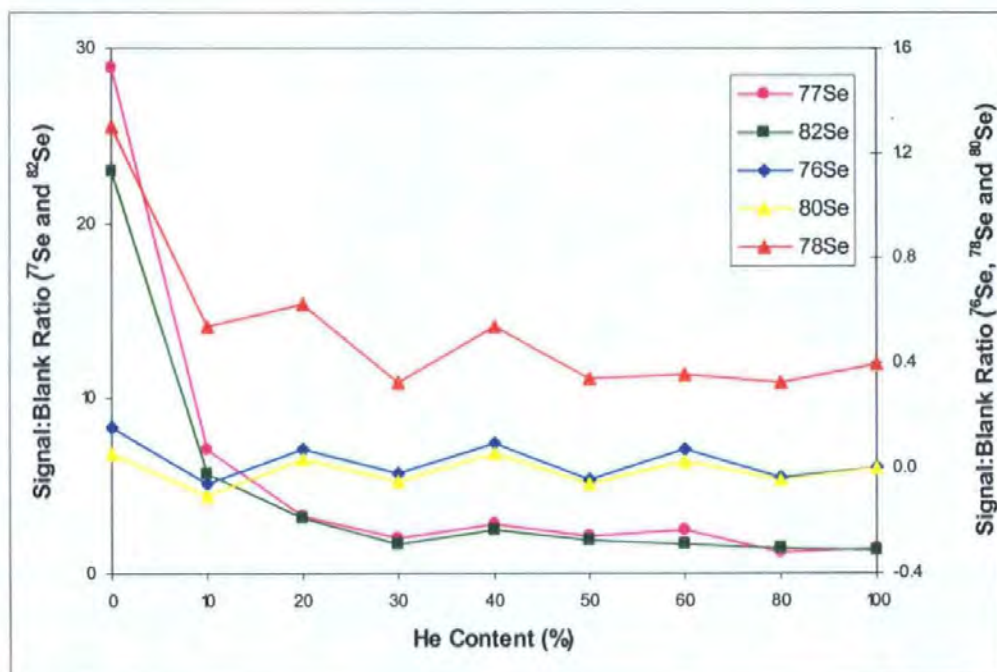


Figure 6.6 The effect of helium addition to the argon nebuliser gas on the S/B ratio of the ⁷⁶Se, ⁷⁷Se, ⁷⁸Se, ⁸⁰Se and ⁸²Se selenium isotopes.

6.5.2 Helium addition to Ar outer gas

As with the experiment detailed in section 6.4.3, the gas blender was connected to the instrument via the outer gas inlet, and He gradually introduced to a maximum of 15%. Despite a slight increase in S/B ratio with the addition of 5% He, no overall improvement was observed with the general trend being that of a gradual decrease in the S/B ratio with an increase in He content (see Figure 6.7).

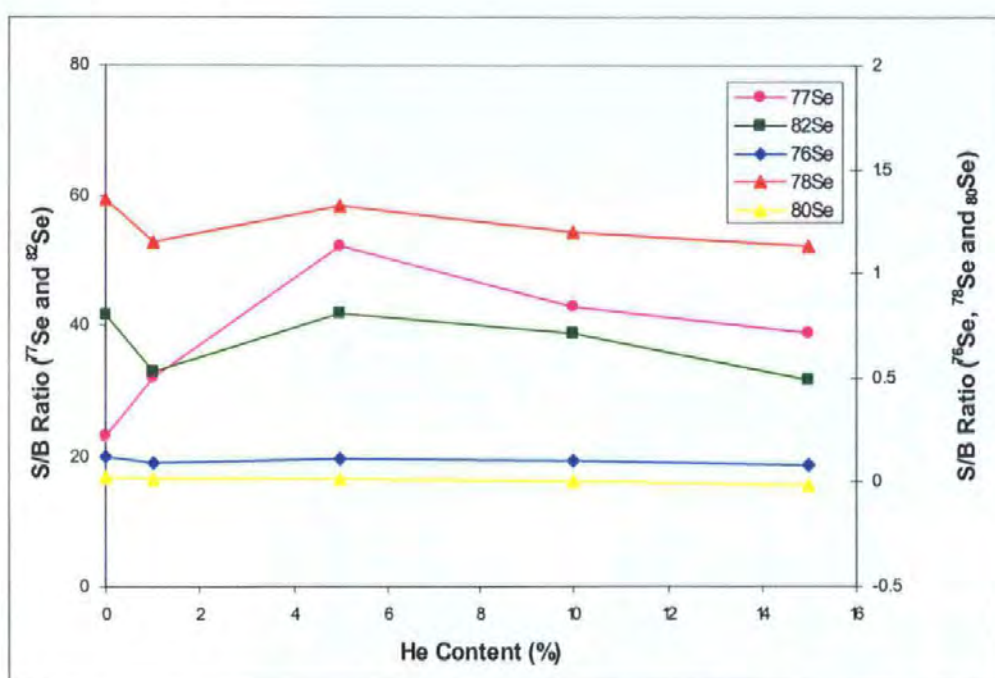


Figure 6.7 The effect of He addition to Ar outer gas on the S/B ratio of the 76, 77, 78, 80 and 82 Se isotopes.

Despite the decrease in the S/B ratio with the introduction of He to the outer gas stream, the experiment was extended to see if the plasma could be maintained with higher levels of He and if optimisation of other parameters could then improve the sensitivity of the system. The He level was gradually increased until the outer gas was made up solely of He

(i.e. 100%). Further experiments were then performed to try and improve the overall sensitivity of the system whilst maintaining any improvements in the S/B ratio. These experiments concentrated on the optimisation of the RF power and the nebuliser and outer gas flow rates.

6.5.2.1 Optimisation of RF power

Three experiments were carried out; firstly with 100% He in the outer gas, secondly using 50% He:50% Ar in the outer gas, and finally with 100% Ar in the outer gas to confirm that any observations seen in the first two experiments were due to changes in the make up of the outer gas. The nebuliser gas flow-rate was set at 1.20 l min^{-1} and the outer gas flow-rate was set at 0.80 l min^{-1} . As shown in Figure 6.8 and 6.9, the sensitivity and hence S/B ratio of the 76 and 78 selenium isotopes responds differently to changes in RF power in the presence of differing amounts of He in the outer gas. For instance, lower power settings of 875W and 950W produced the optimum S/B ratios for ^{78}Se and ^{76}Se respectively with a 100% He plasma, compared with an RF power between 950W and 1050W with a 50% He plasma. And as discussed previously (Chapter 2, section 2.4.2) and again illustrated here, a higher power setting of 1150W is favoured with a 100% Ar plasma.

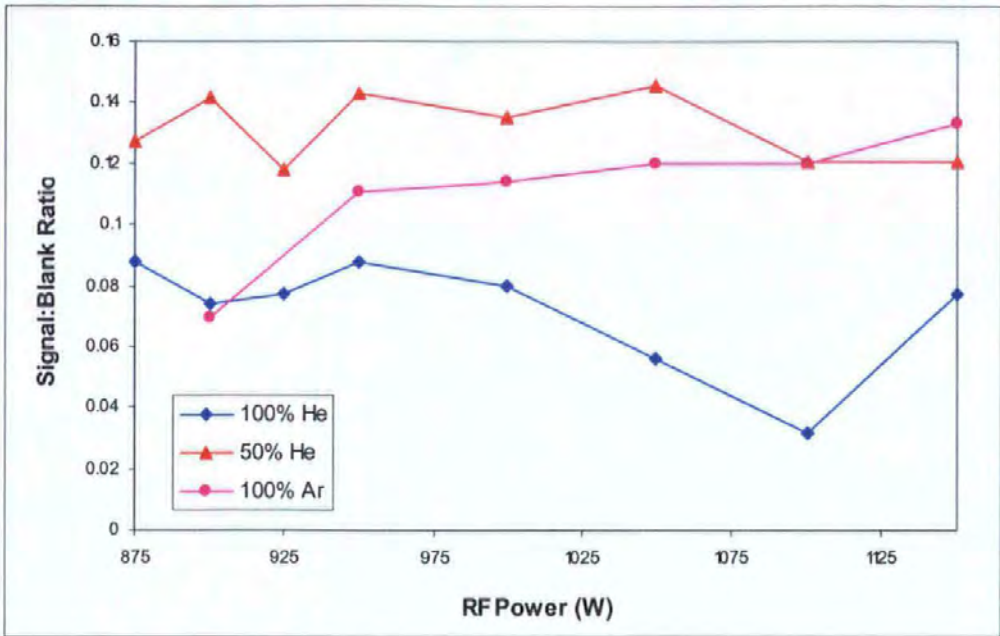


Figure 6.8 The effect of RF power on the S/B ratio for ^{76}Se with a) 100% He plasma, b) 50% He plasma and c) 100% Ar plasma.

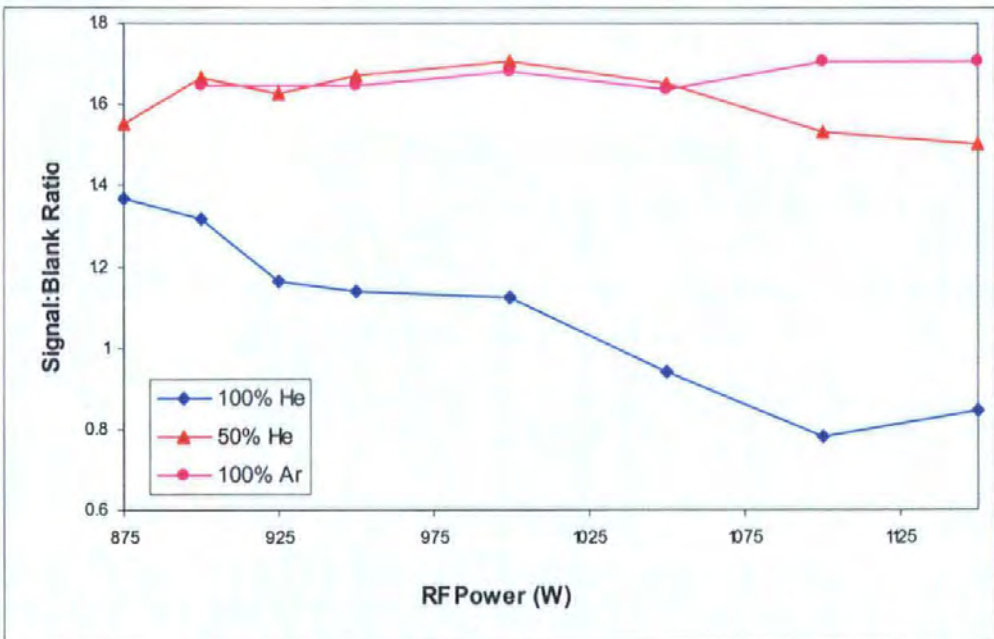


Figure 6.9 The effect of RF power on the S/B ratio of ^{78}Se with a) 100% He plasma, b) 50% He plasma and c) 100% Ar plasma.

6.5.2.2 Optimisation of the Ar nebuliser gas flow rate

The experiment to optimise the RF power detailed in section 6.5.2.1, highlighted that lower RF power settings were required to produce the optimum S/B ratio with He plasmas compared with Ar only plasmas. A second experiment was therefore performed to optimise the nebuliser gas flow-rate. Helium was gradually added to the outer gas until a 100% He plasma could be maintained at a flow-rate of 0.80 l min^{-1} . The RF power was set at 875W, identified as the optimum power setting required to produce the maximum S/B ratio for ^{78}Se with a 100% He plasma (section 6.5.2.1), and the nebuliser gas flow-rate was altered from 0.85 l min^{-1} to 1.30 l min^{-1} . From Figure 6.10 it can be seen that for both isotopes an increase in nebuliser gas flow rate leads to an increase in S/B ratio with the optimum flow rate represented by the maximum S/B ratio falling between 1.20 and 1.25 l min^{-1} . When combined with the ETV internal gas flow rate of 0.30 l min^{-1} , this results in a total nebuliser gas flow rate of between 1.50 and 1.55 l min^{-1} , a considerably higher flow rate to that favoured with an Ar only plasma.

6.5.2.3 Optimisation of the outer gas flow rate

Previous studies indicated that optimum signals for ^{76}Se and ^{78}Se were achieved under quite different operating conditions with He plasmas compared with Ar only plasmas. The flow rate of the Ar/He outer gas itself was therefore optimised. The He content of the outer gas was increased until a 50% He plasma was achieved, the RF power was set at 950W and the nebuliser gas flow rate was set at 1.20 l min^{-1} . The flow rate of the outer gas was steadily increased from 0.30 l min^{-1} to 2.0 l min^{-1} . Figure 6.11 illustrates that an increase in the S/B ratio of the two isotopes studied was obtained with an increase in the flow rate of the outer gas. The optimum flow rate occurred at 1.20 l min^{-1} for ^{76}Se and 1.30 l min^{-1} for ^{78}Se . As with the nebuliser gas flow rate discussed in section 6.5.2.2, these

optimum outer gas flow rates are considerably higher than those favoured with an Ar only plasma.

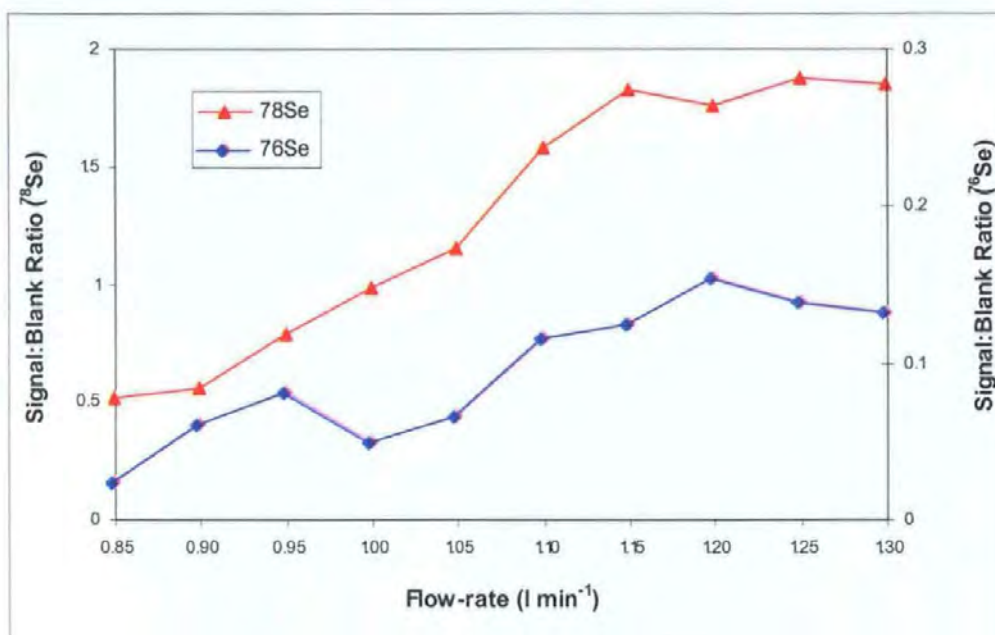


Figure 6.10 Effect of Ar nebuliser gas flow rate on S/B ratio of ⁷⁶Se and ⁷⁸Se with a 100% He plasma.

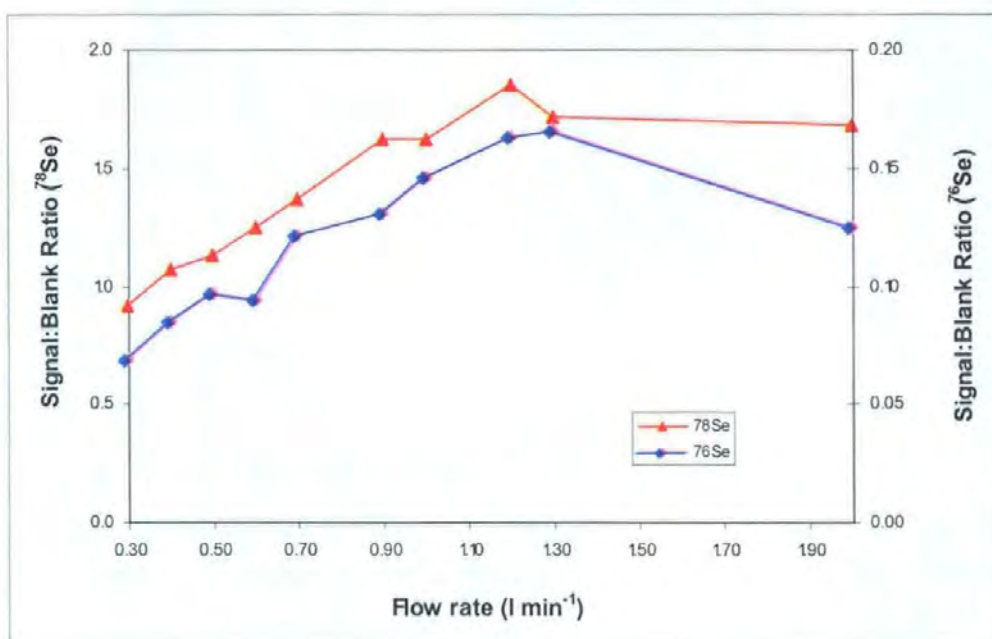


Figure 6.11 Effect of outer gas flow rate on S/B ratio of ⁷⁶Se and ⁷⁸Se with a 50% He plasma.

6.5.3 Comparison of detection limits (He vs Ar)

In order to quantify any gains made due to the addition of 50% He to the Ar outer gas stream, the detection limits for ^{76}Se and ^{78}Se were determined. These were calculated as 3 times the standard deviation of 10 consecutive determinations of a 1% HNO_3 blank solution. Table 6.2 presents the detection limits for an Ar plasma and a 50% He plasma and shows that a 2-fold improvement in the detection limit for ^{78}Se was achieved.

	^{76}Se		^{78}Se	
	100% Ar ¹	50% He	100% Ar	50% He
sd (n = 10)	-	0.85	0.19	0.10
Detection Limit (3σ)	-	2.56	0.58	0.30

Table 6.2 Comparison of detection limits for ^{76}Se and ^{78}Se determined using a 100% Ar plasma and a 50% He plasma.

¹ The detection limits reported using a 100% Ar plasma were determined during the study detailed in Chapter 2. This initial work did not evaluate the ^{76}Se isotope due to the severe interference from Ar polyatomic species, hence a detection limit for ^{76}Se in the presence of 100% Ar is unavailable.

This successful improvement in the detection limits with 50% He:50% Ar in the outer gas stream compared with 100% Ar, is most probably attributed to the fact that He has a larger ionisation potential than Ar which in turn results in a more ionising plasma and an improvement in sensitivity. However He plasmas have a lower gas kinetic temperature than Ar plasmas hence a the combination of both He and Ar in the gas streams is favoured.

6.6 Trifluoromethane Addition

Trifluoromethane (CHF_3) gas has been successfully used as a chemical modifier with ETV-ICP-MS procedures^{104,105} where it has been shown to improve signals, reduce memory effects, and aid the reduction of matrix components. When CHF_3 is heated it forms free fluorine radicals which can combine with the analyte under investigation or other matrix components to form more volatile fluorides. Truscott and co-workers¹⁰⁴ reported 10-fold and 50-fold improvements in the signal intensities of ^{238}U and ^{232}Th respectively, when CHF_3 gas was introduced during the pyrolysis stage of the ETV temperature program. Alvarado and Erickson¹⁰⁵ also used CHF_3 as a modifier for the determination of uranium and thorium and again reported signal enhancements and significant improvements in detection limits.

6.6.1 CHF_3 addition to the Ar nebuliser gas

Initial work using CHF_3 as a gaseous modifier during the development of the ETV procedure (Chapter 2, section 2.3) had been unsuccessful with a large amount of carbon build up on the furnace tube and ETV contact cylinders, with no improvement in signal. The CHF_3 was therefore introduced directly into the nebuliser gas stream. The plasma conditions were initially set up following the optimised conditions detailed in Chapter 2, i.e. RF power 1150W, Ar nebuliser gas at 1.20 l min^{-1} and Ar outer gas at 0.80 l min^{-1} . The CHF_3 was gradually added to the nebuliser gas stream. Initially only 0.1% CHF_3 was added but this resulted in a complete loss of signal. The CHF_3 content was then increased to 1% and a 10 ng g^{-1} Se standard injected, at RF powers of 1150W and 1000W, but this again resulted in a complete loss of signal. As with the work performed earlier, a large amount of carbon was deposited around the end of the injector and on the torch and cones.

This proved difficult to remove. Due to this lack of success no further work was performed.

6.7 Conclusions

The work detailed in this chapter, has looked at the potential role of mixed gas plasmas in the determination of Se, and in particular the effect of combining nitrogen and helium with a conventional Ar plasma. The gases have been introduced via the nebuliser and outer gas streams, and as an alternative gas stream through the ETV instrumentation. The principal aim of this work was to reduce the Ar polyatomic interferences on the 76 and 78 selenium isotopes. Experiments with nitrogen addition via the nebuliser, outer and ETV alternative gas streams were favourable with a significant decrease in the background level of a 1% HNO₃ blank solution. This may be due to the competitive formation of ArN⁺ resulting in a reduction in the formation of ArAr⁺ and hence a decrease in the background levels for the 76 and 78 selenium isotopes. A second explanation may be that a reduction in the ionisation temperature of the plasma on the introduction of nitrogen brings about a reduction in the intensities of the polyatomic species as they require more energy for ionisation than the analytes of interest. However despite the successful reduction of the background signals the overall sensitivity of the system was significantly compromised.

Similar experiments were then performed with the addition of He to both the nebuliser and outer gas streams. The introduction of He to the nebuliser gas stream was unsuccessful with a significant decrease in the signal of both a 1% HNO₃ blank solution and a 10ng g⁻¹ Se standard with no improvements in the S/B ratio of any of the isotopes monitored. Combination of He with the Ar outer gas stream was however more successful. As with the earlier experiments a decrease in both the blank and Se standard signals with

the addition of He was observed, however improvements in the S/B ratios were also noted. Optimisation of the individual plasma parameters then enhanced the S/B ratios further, resulting in a 2-fold improvement in the detection limit of ^{78}Se with 50% He in the Ar outer gas.

This investigation has shown how the introduction of both N_2 and He gas to an Ar ICP can reduce the background levels of ^{76}Se and ^{78}Se due to interference from Ar polyatomic species, and how careful optimisation of the plasma conditions can result in improved detection limits.

CHAPTER 7

Conclusions and Future Work

7. CONCLUSIONS AND FUTURE WORK

7.1 Conclusions

The aim of this study was to evaluate the analysis of both environmental and clinical samples using ICP-MS instrumentation for the determination of total selenium. Selenium is an essential trace element whose presence in the body above or below an optimum level has been linked with numerous health implications such as heart disease, rheumatoid arthritis, cirrhosis of the liver and cancer. Poor sensitivity and severe interferences resulting from both the sample matrix and the argon plasma hamper the measurement of this analyte by ICP-MS making it difficult to achieve precise and accurate results. The purpose of this study was therefore to investigate ways of overcoming these analytical problems with a view to improving the methodology currently available for the determination of Se in both environmental and clinical samples.

During this work a novel method for the interference free determination of selenium by ETV-ICP-MS has been developed. Many of the inherent problems associated with the measurement of this analyte by ICP-MS are eliminated with the application of the carefully optimised ETV temperature program and modifier system. Through the further development of the procedure to encompass the technique of isotope dilution analysis and the rigorous optimisation of each parameter to achieve the optimum isotope ratio measurement, results of the highest accuracy and precision have been achieved. This is demonstrated through the analysis of several certified reference materials where the significant improvements in accuracy and precision achievable with the IDMS procedure compared with the non-IDMS procedure are confirmed.

The significant advantages of the developed ETV procedure have been further illustrated through comparison with two established techniques (hydride generation and the use of organic solvents with pneumatic nebulisation) traditionally employed to overcome the interference issues associated with the determination of selenium. The comparison covered all aspects of the analytical procedures such as interference removal, sample pre-treatment requirements, overall analysis time, analytical performance characteristics and uncertainty. Similar performance characteristics such as stability, linearity and detection limits are achievable with each of the methods. The most significant differences were with the sample pre-treatment requirements and speed of analysis, with the ETV procedure having the simplest preparation stage and the fastest total analysis time. The advantages of this straight forward approach are further reflected in the comparison of the uncertainty estimates where the uncertainty for the ETV procedure is significantly lower than the estimates determined for both the HG and PN sample introduction methods.

The method comparison included an evaluation of the accuracy and precision of each procedure through the analysis of four certified reference materials. Good results were obtained with all of the methods with the majority of the results falling within the certified limits. The best results with the smallest uncertainty were obtained with the ETV-ID-ICP-MS procedure illustrating the improvements in accuracy and precision that can be achieved with this technique.

An investigation into the effect of combining nitrogen and helium with a conventional Ar plasma was also undertaken. The gases were introduced via the nebuliser and outer gas streams, and as an alternative gas stream through the ETV instrumentation. Initial experiments with nitrogen addition via the nebuliser gas were favourable with a significant decrease in the background level of a 1% HNO₃ blank solution with the introduction of 4% N₂. However closer examination of the signal obtained for a 10ng g⁻¹

Se solution indicated that this also decreased in a similar manner. Further work involving N₂ addition to the outer gas and ETV alternative gas streams was equally unsuccessful with a significant decrease in the background levels of the 76 and 78 isotopes, resulting in a significant compromise of the overall sensitivity of the system.

The introduction of He to the nebuliser gas stream was also unsuccessful with no improvements in the S/B ratio of any of the isotopes monitored. Combination of He with the Ar outer gas stream was however more successful with improvements in the S/B ratios of both the 76 and 78 isotopes. Optimisation of the individual plasma parameters enhanced the S/B ratios further resulting in a 2-fold improvement in the detection limit of ⁷⁸Se with 50% He in the Ar outer gas.

Overall this investigation demonstrated how the introduction of both N₂ and He gas to an Ar ICP can significantly reduce the background levels of ⁷⁶Se and ⁷⁸Se due to interference from Ar polyatomic species, and how careful optimisation of the plasma conditions can result in improved detection limits.

7.2 Future Work

The use of mixed gas plasmas for the elimination of argon polyatomic interferences produced some encouraging results with the introduction of nitrogen to the nebuliser gas stream and helium to the outer gas stream. An extension of this work to investigate the effect of adding both of these gases to the individual gas streams simultaneously would be advantageous, i.e adding 4% nitrogen to the argon nebuliser gas and 50% helium to the outer gas. This could build on the improved detection limits already achieved with 50% helium in the outer gas by further reducing the intensities of the polyatomic species due to the lower ionisation temperature of the plasma in the presence of nitrogen.

An alternative approach to interference elimination would be to use a double-focusing magnetic sector ICP-MS. This technique allows operation in much higher mass resolution modes than conventional quadrupole instruments, and as such permits resolution of the analyte of interest from the interfering species. For the determination of selenium, this would need to be performed in the highest resolution mode possible, as the 76, 77, 78 and 80 isotopes require resolutions between 7000 and 9500 in order to achieve separation from the major argon polyatomic interferents. This could potentially allow for the interference free determination of the more abundant isotopes thus leading to improvements in detection capabilities. However sensitivity problems due to low ion transmittance would have to be addressed.

The advent of the new generation of ICP-MS instruments equipped with either a collision cell or a reaction cell provides an alternative approach to interference elimination that could also be considered. Elimination of the argon polyatomic species may be achieved by gas phase chemical reactions and/or collisional dissociation with the introduction of a gas such as helium, hydrogen or methane. This provides the potential to analyse the most abundant selenium isotope, ^{80}Se , which suffers from major interference from the $^{40}\text{Ar}^{40}\text{Ar}^+$ polyatomic species. The interference free determination of this isotope could lead to dramatic improvements in the detection limits provided by current procedures.

APPENDICES

Appendix 1. Excel spreadsheet for the calculation of the mass fraction of Se in uncertainty solution two and the associated standard uncertainty as determined by method 4 (ETV-ID-ICP-MS.)

Excel Spread Sheet to calculate selenium concentration by Isotope Dilution $^{82}\text{Se}/^{77}\text{Se}$

1. Spreadsheet and Sample Details

Sample ID: QC 2
Date analyst 21/05/1999
Analyst: J. Turner

Data set:
Date processed on spreadsheet:

2. Isotopic composition of the materials

		^{74}Se	^{76}Se	^{77}Se	^{78}Se	^{80}Se	^{82}Se	At. weight	ΣR_{zi}
Accurate mass		73.922477	75.919214	76.918913	77.917310	79.916522	81.916700		
Natural standard		R_{1Z}	R_{2Z}	R_{3Z}	R_{4Z}	R_{5Z}	$R_{6Z}=R_Z$		
IUPAC data	R_{1Z}	0.1166	1.228	1	3.115	6.502	1.144	78.960	13.1056
	standard uncertainty	0.0033	0.027	0	0.043	0.085	0.022	0.017	
Spike		R_{1Y}	R_{2Y}	R_{3Y}	R_{4Y}	R_{5Y}	R_{6Y}		ΣR_{yi}
Se spike	R_{1Y}	0.00393	0.0379	1	0.2549	0.1351	0.0240	77.421	1.4558
	standard uncertainty	0.00058	0.0045	0	0.0051	0.0048	0.0030	0.020	

3. ICP-MS Counts for the Sample and Mass Bias Solution

Isotope	Leading Mass Bias	Sample	Trailing Mass Bias	
^{82}Se	4927	5852	5220	
^{77}Se	13214	15419	13844	
RSD ratio	3.92	2.22	3.67	number of runs
ratio	0.3728621	0.37953175	0.3770587	9
Mass bias	0.8882337		0.878348	
Sample blend ratio	R'_B	0.37953	standard uncertainty	0.0028085
Mass bias blend ratio	R'_{Bc}	0.3749604	standard uncertainty	0.005047
	st. dev. drif	-1.2E-03	RSD. repeatability	3.92

4. Concentrations

Natural standard	c_Z	3.9343 ng/g	Check unit	0.0498265 nmol/g	Check unit used
	standard uncertainty	0.0008		1.476E-05	
Spike	c_Y	2.592 ng/g		0.0334793 nmol/g	
	standard uncertainty	0.0022		2.97E-05	

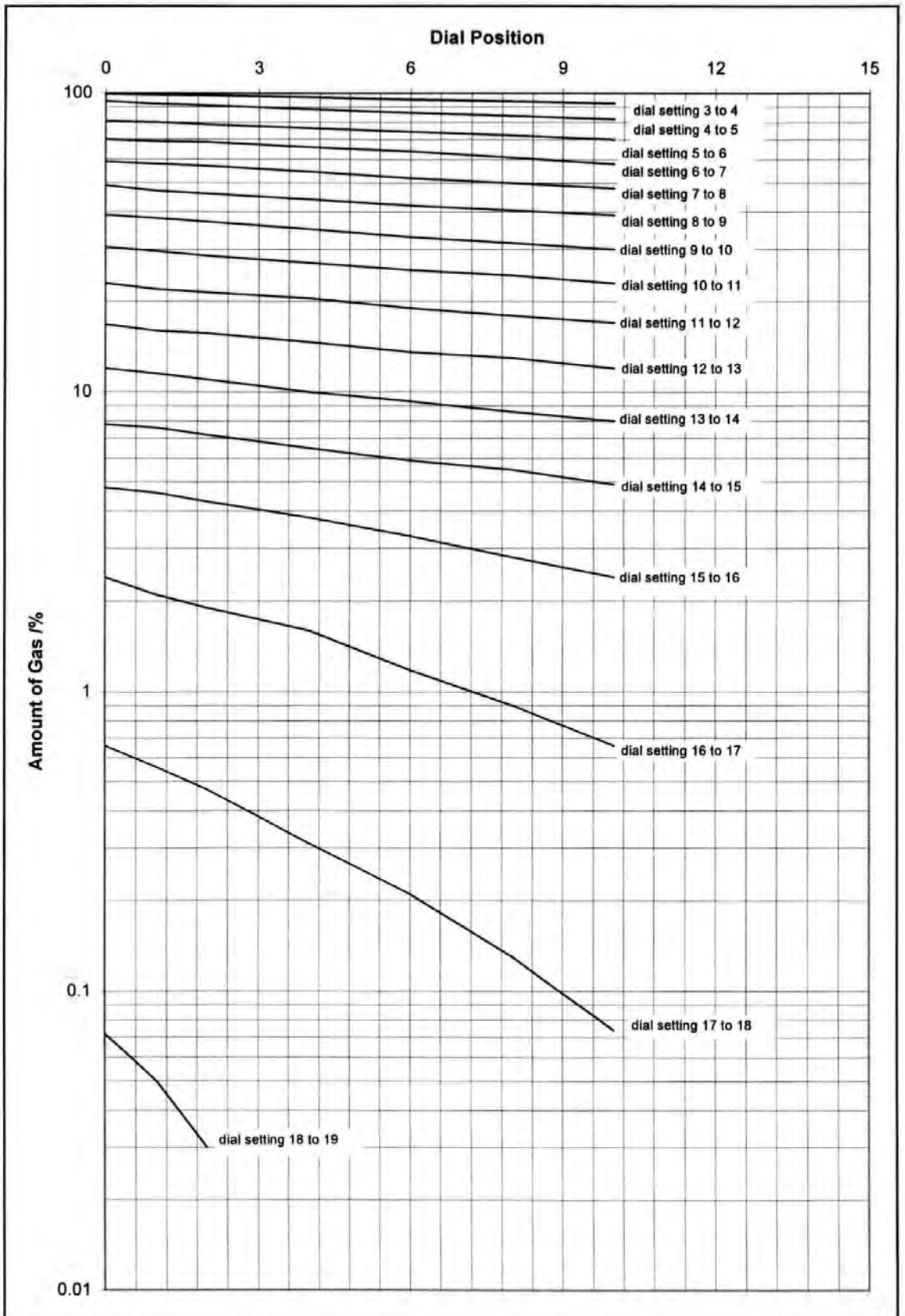
5. Masses used for the blends

		sample blend		mass bias blend
mass sample	m_X	1.8807 g	mass standard	m_{Zc} 2.3075 g
	standard uncertainty	0.00006 g		standard uncertainty 0.00006 g
mass spike	m_Y	1.0012 g	mass spike	m_{Yc} 1.0094 g
	standard uncertainty	0.00006 g		standard uncertainty 0.00006 g
True ratio	R_{Bc}	0.3311887	standard uncertainty	0.0065927

6. Final calculation of elemental Se concentration in the sample

Concentration of Se in sample		4.875074 ng/g	standard uncertainty	0.1117049 ng/g	RSD (%)	2.291				
Variable	c_Z	m_X	m_Y	m_{Yc}	m_{Zc}	R_Y	R_Z	R_{Bc}	R'_B	R'_{Bc}
Budget (%)	0.0079	0.000	0.001	0.001	0.000	0.003	0.003	0.003	23.205	76.776

Appendix 2. Graph to calculate dial settings for the Series 850 Gas Blender.



Appendix 3. Series 850 Gas Blender Settings – Argon:Nitrogen Blends

Rn	Cn	%Ar	CF_{Ar}	Rn.Cn	Pn	Dial setting
0.09	1.032	99.91	0.86	86.02	0.075	17.98
0.10	1.032	99.9	0.86	86.02	0.083	17.95
0.20	1.032	99.8	0.86	86.03	0.167	17.70
0.30	1.032	99.7	0.86	86.05	0.250	17.52
0.40	1.032	99.6	0.86	86.07	0.334	17.37
0.50	1.032	99.5	0.86	86.09	0.417	17.25
0.60	1.032	99.4	0.86	86.10	0.501	17.15
0.70	1.032	99.3	0.86	86.12	0.584	17.07
0.80	1.032	99.2	0.86	86.14	0.668	16.98
0.90	1.032	99.1	0.86	86.15	0.751	16.92
1.00	1.032	99.0	0.86	86.17	0.835	16.85
1.50	1.032	98.5	0.86	86.26	1.254	16.55
2.00	1.032	98.0	0.86	86.34	1.673	16.32
2.50	1.032	97.5	0.86	86.43	2.094	16.10
3.00	1.032	97.0	0.86	86.52	2.515	15.95
3.50	1.032	96.5	0.86	86.60	2.937	15.73
4.00	1.032	96.0	0.86	86.69	3.360	15.57
4.50	1.032	95.5	0.86	86.77	3.784	15.40
5.00	1.032	95.0	0.86	86.86	4.208	15.25
5.50	1.032	94.5	0.86	86.95	4.634	15.10
6.00	1.032	94.0	0.86	87.03	5.060	14.93
6.50	1.032	93.5	0.86	87.12	5.487	14.77
7.00	1.032	93.0	0.86	87.20	5.915	14.60
7.50	1.032	92.5	0.86	87.29	6.344	14.47
8.00	1.032	92.0	0.86	87.38	6.773	14.35
8.50	1.032	91.5	0.86	87.46	7.204	14.20
9.00	1.032	91.0	0.86	87.55	7.635	14.10
9.50	1.032	90.5	0.86	87.63	8.067	13.95
10.00	1.032	90.0	0.86	87.72	8.500	13.87

Rn = required % of stream n gas (N₂)
 Cn = correction factor for stream n gas (N₂)
 Pn = % to be set for stream n to achieve Rn
 CF_{Ar} = correction factor for Argon

Appendix 4. Series 850 Gas Blender Settings – Argon:Helium Blends

Rn	Cn	%Ar	CF _{Ar}	Rn.Cn	Pn	Dial setting
0.10	2.65	99.9	0.86	86.18	0.033	18.20
0.20	2.65	99.8	0.86	86.36	0.065	18.02
0.30	2.65	99.7	0.86	86.54	0.098	17.90
0.40	2.65	99.6	0.86	86.72	0.131	17.80
0.50	2.65	99.5	0.86	86.90	0.164	17.72
0.60	2.65	99.4	0.86	87.07	0.197	17.62
0.70	2.65	99.3	0.86	87.25	0.230	17.55
0.80	2.65	99.2	0.86	87.43	0.264	17.50
0.90	2.65	99.1	0.86	87.61	0.298	17.42
1.00	2.65	99.0	0.86	87.79	0.331	17.37
2.00	2.65	98.0	0.86	89.58	0.676	16.98
3.00	2.65	97.0	0.86	91.37	1.034	16.67
4.00	2.65	96.0	0.86	93.16	1.406	16.50
5.00	2.65	95.0	0.86	94.95	1.792	16.25
6.00	2.65	94.0	0.86	96.74	2.190	16.05
7.00	2.65	93.0	0.86	98.53	2.603	15.90
8.00	2.65	92.0	0.86	100.3	3.029	15.70
9.00	2.65	91.0	0.86	102.1	3.468	15.54
10.0	2.65	90.0	0.86	103.9	3.921	15.35
11.0	2.65	89.0	0.86	105.7	4.387	15.15
12.0	2.65	88.0	0.86	107.5	4.867	15.00
13.0	2.65	87.0	0.86	109.3	5.360	14.80
14.0	2.65	86.0	0.86	111.1	5.867	14.60
15.0	2.65	85.0	0.86	112.9	6.388	14.45
16.0	2.65	84.0	0.86	114.6	6.922	14.37
17.0	2.65	83.0	0.86	116.4	7.469	14.12
18.0	2.65	82.0	0.86	118.2	8.030	13.97
19.0	2.65	81.0	0.86	120.0	8.604	13.80
20.0	2.65	80.0	0.86	121.8	9.192	13.60
21.0	2.65	79.0	0.86	123.6	9.794	13.45
22.0	2.65	78.0	0.86	125.4	10.41	13.33
23.0	2.65	77.0	0.86	127.2	11.04	13.20
24.0	2.65	76.0	0.86	129.0	11.68	13.05
25.0	2.65	75.0	0.86	130.8	12.33	12.90
30.0	2.65	70.0	0.86	139.7	15.82	12.20
35.0	2.65	65.0	0.86	148.7	19.63	11.50
40.0	2.65	60.0	0.86	157.6	23.79	10.90
50.0	2.65	50.0	0.86	175.5	33.11	9.50
60.0	2.65	40.0	0.86	193.4	43.79	8.50
70.0	2.65	30.0	0.86	211.3	55.82	7.30
80.0	2.65	20.0	0.86	229.2	69.19	6.05
90.0	2.65	10.0	0.86	247.1	83.92	4.80
100	2.65	0.0	0.86	265.0	100.00	<3.0

Rn = required % of stream n gas (He)
 Cn = correction factor for stream n gas (He)
 Pn = % to be set for stream n to achieve Rn
 CF_{Ar} = correction factor for Argon

REFERENCES

REFERENCES

1. C. P. Case, L. Ellis, J. C. Turner and B. Fairman, *Clin. Chem.*, 2001, **47**:2, 275.
2. E. S. Beary and P. J. Paulsen, *Anal. Chem.*, 1995, **67**, 3193.
3. J. B. Truscott, P. Jones, B. E. Fairman and E. H. Evans, *Anal. Chim. Acta*, 2001, **433**, 245.
4. A. Krejcová, T. Cernohosky and E. Curdová, *J. Anal. Atom Spectrom*, 2001, **16**, 1002.
5. *Handbook on Metals in Clinical and Analytical Chemistry*. ed H. G. Seiler, A. Sigel and H. Sigel, Marcel Dekker Inc., New York, 1994.
6. A. R. Date and A. L. Gray, *Analyst*, 1981, **106**, 1255.
7. R. S. Houk, V. A. Fassel, G. D. Flesch, H. J. Svec, A. L. Gray and E. Taylor, *Anal. Chem.*, 1980, **52**, 2283.
8. *An Introduction to Analytical Atomic Spectrometry*. ed E. H. Evans, John Wiley and Sons Inc, New York, 1998.
9. E. H. Evans, J. J. Giglio, T. M. Castellano and J. A. Caruso, *Inductively Coupled and Microwave Induced Plasma Sources for Mass Spectrometry*, ed. N. W. Barnett, Royal Society of Chemistry, Cambridge, 1995.
10. A. Montaser, *Inductively Coupled Plasma Mass Spectrometry*, VCH Publishers Inc., New York 1998.
11. M. A. Vaughan and G. Horlick, *Appl. Spectrosc.*, 1986, **4**, 434.
12. S. H. Tan and G. Horlick, *Appl. Spectrosc.*, 1986, **4**, 445.
13. K. O'Hanlon, L. Ebdon and M. Foulkes. *J. Anal. Atom Spectrom*, 1997, **12**, 329.
14. A. A. Pupyshev and E. V. Semenova, *Spectrochim. Acta Part B*, 2001, **56**, 2397.
15. I. Harrison, D. Littlejohn and G. S. Fell, *Analyst*, 1996, **121**, 189.
16. A. Taylor and P. Green, *J. Anal. Atom Spectrom*, 1988, **3**, 115.
17. X-P. Yan, M. Sperling and B. Welz, *Anal. Chem.*, 1999, **71**, 4353.
18. M. Feuerstein and G. Schemmmer, *At. Spectros.*, 1999, **5**, 180.

19. E. N. Drake and T. D. Hain, *Anal. Biochem.*, 1994, **220**, 336.
20. M. A. Z. Arruda, M. Gallego and M. Valcarcel, *J. Anal. At. Spectrom.*, 1994, **9**, 657.
21. D. C. Gregoire, *Can. J. Anal. Sci. and Spectros.*, 1997, **42**, 1.
22. B. Fairman and T. Catterick, *J. Anal. At. Spectrom.*, 1997, **12**, 863.
23. M. Rayman, F. R. Aboushakra and N. I. Ward. *J. Anal. At. Spectrom.*, 1996, **11**, 61.
24. M. A. Quijano, A. M. Gutierrez, M. P. Conde and C. Camara, *J. Anal. At. Spectrom.*, 1995, **10**, 871.
25. B. T. G. Ting, C. S. Mooers and M. Janghorbani. *Analyst*, 1989, **114**, 667.
26. O. Mestek, M. Suchanek, Z. Vodickova, B. Zemanova and T. Zima. *J. Anal. At. Spectrom.*, 1997, **12**, 85.
27. J. Bowman, B. Fairman and T. Catterick. *J. Anal. At. Spectrom.*, 1997, **12**, 313.
28. R. M. Olivas, C. R. Quetel and O. F. X. Donard. *J. Anal. At. Spectrom.*, 1995, **10**, 865.
29. L. S. Zhang and S. M. Combs. *J. Anal. At. Spectrom.*, 1996, **11**, 1043.
30. G. E. M. Hall and J. Pelchart. *J. Anal. At. Spectrom.*, 1997, **12**, 97.
31. S. J. Santosa, H. Mokudai and S. Tanaka, *J. Anal. At. Spectrom.*, 1997, **12**, 409.
32. D. Beauchemin and J. M. Craig, *Spectrochim. Acta*, Part B, 1991, **46**, 603.
33. G. Xiao and D. Beauchemin, *J. Anal. At. Spectrom.*, 1994, **9**, 509.
34. G. Xiao and D. Beauchemin, *Can. J. Anal. Sci. and Spectros.*, 2001, **1**, 28.
35. F. Laborda, M. J. Baxter, H. M. Crews and J. Dennis, *J. Anal. At. Spectrom.*, 1994, **9**, 727.
36. T. van der V.-K. and J. L. M. de Boer, *J. Anal. At. Spectrom.*, 1994, **9**, 1093
37. E. H. Evans and L. Ebdon, *J. Anal. At. Spectrom.*, 1989, **4**, 299.
38. E. H. Evans and L. Ebdon, *J. Anal. At. Spectrom.*, 1990, **5**, 425.
39. F. G. Smith, D. R. Wiederin and R. S. Houk, *Anal. Chem.*, 1991, **14**, 1458.
40. L. Ebdon, M. Ford, R. C. Hutton and S. J. Hill, *Appl. Spectros.*, 1994, **4**, 507.
41. I. Platzner, J. V. Sala, F. Mousty, P. R. Trincherini and A. L. Poletini. *J. Anal. At. Spectrom.*, 1994, **9**, 719.

42. S. J. Hill, M. Ford and L. Ebdon, *J. Anal. At. Spectrom.*, 1992, **7**, 1157.
43. H. T. Delves and C. Sieniawska, *J. Anal. At. Spectrom.*, 1997, **12**, 387.
44. J. Goossens, F. Vanhaecke, L. Moens and R. Dams. *Anal. Chim. Acta*, 1993, **280**, 137.
45. I. Llorente, M. Gomez and C. Camara. *Spectrochim. Acta*, 1997, Part B, **52**, 1825.
46. B. Gammelgaard and O. Jons, *J. Anal. At. Spectrom.*, 1999, **14**, 867.
47. E. H. Larsen and S. Sturup. *J. Anal. At. Spectrom.* 1994, **9**, 1099.
48. L. Moens, F. Vanhaecke, J. Riondato and R. Dams, *J. Anal. At. Spectrom.* 1995, **10**, 569.
49. J. Riondato, F. Vanhaecke, L. Moens and R. Dams *J. Anal. At. Spectrom.* 1997, **12**, 933.
50. C. S. Muniz, J. M. Marchante-Gayon, J. I. G. Alonso and A. Sanz-Medel, *J. Anal. At. Spectrom.* 1999, **14**, 193.
51. C. Moor and J. Kobler, *J. Anal. At. Spectrom.* 2001, **16**, 285.
52. Perkin Elmer ELAN 5000 users manual, May 1992, Rev. B.
53. V. I. Baranov and S. D. Tanner, *J. Anal. At. Spectrom.* 1999, **14**, 1133.
54. L. A. Simpson, M. Thomsen, B. J. Alloway and S. Parker, *J. Anal. At. Spectrom.* 2001, **16**, 1375.
55. J. J. Sloth and E. H. Larsen, *J. Anal. At. Spectrom.* 2000, **15**, 669.
56. H. Reyes, J. M. Marchante-Gayon, J. I. G. Alonso and A. Sanz-Medel, *J. Anal. At. Spectrom.* 2003,.
57. *Selenium in Food and Health*. C. Reilly, Blackie Academic and Professional, London, 1996.
58. M. P. Rayman, *Lancet*, 2000, **356**, 233.
59. M. P. Rayman, *Chemistry in Britain*, 2002, **38**, 28.
60. R. S. Houk, *Anal. Chem.*, 1986, **58**, 97A.
61. S. J. Jiang, P. L. Lu and M. F. Huang, *J. Chin. Chem. Soc.*, 1994, **41**, 139.
62. L. Ebdon, A. S. Fisher and P. Worsfold, *J. Anal. At. Spectrom.* 1994, **9**, 611.

63. M. Haldimann, T. Y. Venner and B. Zimmerli, *J. Trace Elem. Med. Biol.*, 1996, **10**, 31.
64. C. Moor, J. W. H. Lam and R. E. Sturgeon, *J. Anal. At. Spectrom.* 2000, **15**, 143.
65. D. Pozebon, V. L. Dressler and A. J. Curtius, *J. Anal. At. Spectrom.* 1998, **13**, 7.
66. W. C. Wei, P. H. Chi and m. H. Yang, *J. Anal. At. Spectrom.* 2000, **15**, 1466.
67. A. Krushevska, M. Kotrebai, A. Lasztity, R. M. Barnes and D. Amarasiriwardena, *Fresenius J Anal Chem*, 1996, **335**, 793.
68. S. H. Nam, W. R. L. Masamba and A. Montaser. *Spectrochim. Acta*, 1994, **49B**,1325.
69. Perkin Elmer HGA-600 operators manual, September 1990.
70. I. L. Shutler and H. T. Delves, *Analyst*, 1986, **111**, 651.
71. D. C. Gregoire, S. Al-Maawali and C. L. Chakrabarti. *Spectrochim. Acta. Part B*, 1992, **47**, 1123.
72. W. Slavin, D. C. Manning, and G. R. Carnick, *At. Spectrosc.*,1981, **2**, 137.
73. G. F. Kirkbright, S. Hsiao-Chuan and R. D. Snook , *At. Spectros.* 1980, **1**, 85.
74. J. M. Ottaway, *At. Spectrosc.* 1982, **3**, 89.
75. J. B . Truscott, L. Bromley, P. Jones, E. H. Evans, J. Turner and B. Fairman, *J. Anal. At. Spectrom.*, 1999, **14**, 627.
- 76 J. Marshall and J. Franks. *At. Spectros.* 1990, **11**, 177.
77. K. G. Heumann, *Fresenius J. Anal. Chem.*, 1986, **325**, 661.
78. T. Catterick, H. Handley and S. Merson, *At. Spectrosc.*1995, **16**, 229.
79. U. Ornemark, P. D. P. Taylor, P. De Bievre, M. Loikkanen, J. C. Libeer, K. Hesling, L. A. Penberthy, T. Tamberg, J. W. H. Lam, L. Van Nevel, P. Robouch, A. Uldall, M. M. Muller, H. Steensland, A. Squirrell, D. Schiel, T. Walczyk, *Accred Qual Assur.*, 1999, **4**, 463.
80. M. Ohata, T. Ichinose, N. Furuta, A. Shinohara and M. Chiba, *Anal. Chem.*, 1998, **70**, 2726.
81. L. S. Zhang and S. M. Combs, *J. AOAC Int*, 1998, **81**, 1060.

82. W. T. Buckley, J. J. Budac, D. V. Godfrey and K. M. Koenig, *Biol Mass Spectrom*, 1992, **21**, 473.
83. I. Papadakis, P. D. P. Taylor and P. De Bièvre, *J. Anal. At. Spectrom*, 1997, **12**, 791.
84. W. T. Buckley and M. Ihnat, *Fresenius J Anal Chem*, 1993, **345**, 217.
85. *Guidelines for Achieving High Accuracy in Isotope Dilution Mass Spectrometry (IDMS)*, ed. M. Sargent, C. Harrington and R. Harte, Royal Society of Chemistry, Cambridge, 2002.
86. *International Vocabulary of Basic and General Terms in Metrology*. Geneva, Switzerland (1993) (ISBN 92-67-01075-1).
87. IUPAC, Atomic Weights of the Elements, *Pure and Appl. Chem.*, 1998, **70**, 217.
88. A. Henrion, *Fresenius J Anal Chem*, 1994, **350**, 657.
89. T. Catterick, B. Fairman and C. F. Harrington, *J. Anal. At. Spectrom.*, 1998, **13**, 1009.
90. C. E. Sieniawska, R. Mensikov and H. T. Delves, *J. Anal. At. Spectrom.*, 1999, **14**, 109.
91. Ellison, S.L.R., Wegscheider, W., Williams, A., *Anal Chem.*, 1997, **69**, 607A.
92. ISO/IEC Guide 25: 3rd edition, *General requirements for the competence of calibration and testing laboratories*, (1990).
93. *Guide to the Expression of Uncertainty in Measurement*. ISO, Geneva, Switzerland (1993).(ISBN 92-67-10188-9).
94. *Eurachem : Quantifying Uncertainty in Analytical Measurement*. Laboratory of the Government Chemist, London, (1995). (ISBN 0-948926-08-2).
95. M. Pueyo, J. Obiols, E. Vilalta, *Anal Commun.*, 1996, **33**,205.
96. A. Williams, *Anal Proc.*, 1993, **30**, 248.
97. V. J. Barwick and S. L. R. Ellison, *Anal Commun.*, 1998, **35**, 377.
98. V. J. Barwick , S. L. R. Ellison and B. Fairman, *Anal. Chim.Acta*, 1999, **394**, 281.
99. S. L. R. Ellison and V. J. Barwick, *Accred. Qual. Assur.*, 3, 1998, 101.
100. S. L. R. Ellison and V. J. Barwick, *Analyst*, 1998, **123**, 1387.
101. J. W. H. Lam and G. Horlick, *Spectrochim Acta*, 1990, **45B**, 1313.

102. B. S. Sheppard, W. L. Shen and J. A. Caruso, *J. Am. Soc. Mass Spectrom.*, 1991, **2**, 355.
103. B. S. Sheppard, W. L. Shen, T. M. Davidson and J. A. Caruso, *J. Anal. At. Spectrom.*, 1990, **5**, 697.
104. J. B. Truscott, L. Bromley, P. Jones, E. H. Evans, J. Turner and B. Fairman, *J. Anal. At. Spectrom.*, 1999, **14**, 627.
105. J. S. Alvarado and M. D. Erickson, *J. Anal. At. Spectrom.*, 1996, **11**, 923.
106. M. H. Ramsey and M. Thompson, *J. Anal. At. Spectrom.*, 1986, **1**, 185.

PUBLICATIONS

The use of ETV-ICP-MS for the determination of selenium in serum†‡

JAS
Journal of
Analytical
Atomic
Spectrometry

Justine Turner,^{*,†} Steve J. Hill,[‡] E. Hywel Evans[‡] and Ben Fairman^{*}

^{*}LGC (Teddington) Ltd., Queens Road, Teddington, Middlesex UK, TW11 0LY

[‡]University of Plymouth, Department of Environmental Sciences, Drake Circus, Plymouth, Devon UK, PL4 8AA

Received 24th August 1998, Accepted 26th October 1998

The development of a novel procedure for the accurate determination of selenium in serum using electrothermal vapourisation inductively coupled plasma mass spectrometry (ETV-ICP-MS) is described. The proposed method eliminates the need for a lengthy sample digestion procedure (a requirement with many methods for the analysis of biological samples), utilising a simple 1 + 19 dilution of the serum with 1% nitric acid. Many of the interferences normally associated with the determination of selenium by ICP-MS are successfully eliminated with careful optimisation of the ETV temperature program and modifier system. Analytical characteristics for ⁷⁶Se, ⁷⁷Se, ⁷⁸Se and ⁸²Se are reported, including detection limits (3 σ blank) of approximately 0.1 ng g⁻¹ for ⁷⁶Se and ⁸²Se. Short- and long-term reproducibility data between 4.7 and 4.9% and 3.2 and 3.8% (RSD) for ⁷⁶Se and ⁸²Se, respectively, are shown. The accuracy of the method, which included Te as an internal standard, was demonstrated with the analysis of three internal quality control samples and the certified reference material NIST SRM 1598 (bovine serum). Results within 10% of the target value were achieved for three of the four isotopes studied, with slightly worse results for ⁷⁸Se owing to the large interference from argon adduct ions on this isotope. Preliminary work involving the addition of nitrogen to the argon aerosol carrier gas was successful in reducing the ArAr interference at *m/z* 78.

Introduction

Selenium is an essential trace element whose involvement in human health and well being has become evident in recent years. Since the 1930s the perception of selenium has gone through a number of changes, namely from being considered a toxic element, to a carcinogen, to an essential element and then in the 1960s and 1970s to being considered an anticarcinogen,¹ thus illustrating the marginal differences between therapeutic and toxic effect. Both an excessive and insufficient intake of selenium can have serious health implications. Selenium toxicity, selenosis, can be fatal, with symptoms such as hair and nail loss, tooth decay, skin lesions and, in severe cases, abnormalities of the nervous system. Deficiencies have been linked with coronary heart disease, acute myocardial infarction, cirrhosis of the liver² and cancer of several major organs including the large intestine, breast, ovary and lungs.

Considering the health implications detailed and the narrow divide between deficiency and toxicity, it is essential that good, accurate and reliable methods of analysis are available.

ICP-MS is widely used in many routine analytical laboratories. Advantages over rival techniques include low detection limits and speed of analysis. However not all determinations are straightforward, in particular, the determination of selenium in serum is complicated by several factors. The sensitivity achieved with conventional ICP-MS is generally poor: owing to the high first ionisation energy of selenium, only 30% ionisation is achieved with an argon plasma;³ spectroscopic interferences caused by the formation of argon polyatomic species, *i.e.*, ⁴⁰Ar³⁵Cl on ⁷⁵Se and ⁴⁰Ar³⁸Ar on ⁷⁸Se, lead to high background levels, poor detection limits and ultimately biased analytical results; and the presence of high

levels of components such as sodium and organic compounds, for instance proteins, can cause signal suppression. Several workers⁴⁻¹⁰ have used hydride generation techniques to overcome some of the problems. Greater sensitivity is attainable owing to an improved sample delivery rate, and reduction of spectroscopic and non-spectroscopic interferences is achieved as a result of analyte removal from the matrix. However lengthy sample preparation procedures are generally required, to breakdown organic selenium in the matrix and for the conversion of Se^{VI} into Se^{IV} prior to generation of the hydride. Another option for the reduction of interferences involves the addition of an organic solvent to the diluent matrix when using conventional nebulisation ICP-MS,¹¹⁻¹³ although problems of nebuliser blockage associated with the viscous serum matrix still need to be addressed. Electrothermal vapourisation (ETV) sample introduction is an alternative approach, with the potential to eliminate some of the polyatomic interferences already mentioned. Other advantages over conventional and hydride generation procedures include small sample sizes (5-50 μ l), minimal sample pre-treatment, improved sensitivity and low absolute detection limits.

This paper describes the development of an ETV-ICP-MS procedure for the determination of Se in serum. Optimisation of the ETV temperature program including the successful elimination of several interferences, together with evaluation of the procedure using a certified reference material, is described in detail. Preliminary work using an N₂-Ar mixed plasma gas to negate ArAr polyatomic interferences is also discussed.

Experimental

Instrumentation

An ELAN 5000A ICP-MS instrument coupled to an HGA 600MS ETV unit with an AS-60 autosampler attachment (Perkin-Elmer, Beaconsfield, UK) was used. A 140 cm long

†Presented at the Ninth Biennial National Atomic Spectroscopy Symposium (BNASS), Bath, UK, July 8-10, 1998.

‡© Copyright LGC (Teddington) Ltd. 1998.

Table 1 ICP-MS operating conditions

ICP	
Power	1150 W
Outer plasma gas	15.0 l min ⁻¹
Intermediate gas	0.80 l min ⁻¹
Aerosol carrier gas	0.95 l min ⁻¹
Cones	P1
Lenses	P
	B
	S
	E
Parameter file	
Dwell time	15 ms
Sweeps/reading	1
Readings/replicate	60
Points across peak	1
Resolution	Normal
Mass	⁷⁴ Se
	⁷⁶ Se
	⁷⁷ Se
	⁷⁸ Se

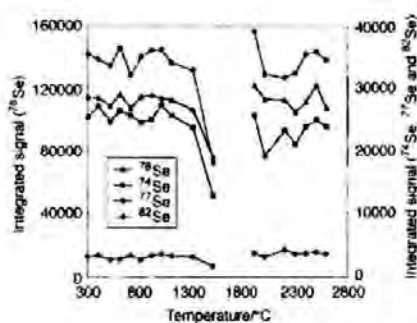


Fig. 1 Pyrolysis vapourisation curves for ⁷⁴Se, ⁷⁶Se, ⁷⁷Se and ⁷⁸Se: 10 μ l injection of a 10 ng g⁻¹ standard with 10 μ l of 500 μ g g⁻¹ Pd(NO₃)₂ modifier.

piece of PTFE tubing (9.6 cm id) was used to connect the furnace to the ICP-MS. Operating conditions for the ICP-MS instrument and the ETV temperature program are given in Tables 1 and 2, respectively. Optimisation of the ICP-MS instrument (*i.e.* lens settings, resolution, oxide and doubly charged ion formation) was performed using conventional nebulization prior to coupling the instrument to the ETV unit.

Reagents

All solutions were prepared using high purity deionised water (18 M Ω , Elga, High Wycombe, Buckinghamshire, UK). Stock solutions (1000 μ g ml⁻¹) of Se and Te (internal standard)

(Alfa Johnson Matthey, Royston, UK) were used. Working standards were prepared daily by dilution in 1% m/m HNO₃, ultrapure Ultrap II grade acid (JT Baker (UK), Milton Keynes, Buckinghamshire, UK). Palladium(II) nitrate (Sigma, Poole, Dorset, UK) was used to prepare the chemical modifier solution.

Preparation of samples and solutions

Chemical modifier. A 500 μ g g⁻¹ solution of Pd(NO₃)₂ containing 5 ng g⁻¹ Te (internal standard) was prepared in the following way: 0.05 g of Pd(NO₃)₂ was dissolved in 50 g of 10% HNO₃; 0.5 g of Te standard (1.0 μ g g⁻¹) was then added and the solution diluted to 100 g with 1% HNO₃.

Samples. All serum samples were diluted (1–19) with 1% HNO₃ (Baker).

Results and discussion

Chemical modifiers

The use of chemical modifiers with electrothermal techniques is well established. In ICP-MS an enhancement in signal on addition of a chemical modifier is attributed to a more efficient transport of the vapourised analyte to the plasma.¹⁴ Chemical modification is also important to avoid losses of volatile analytes during the ashing stage with the formation of more stable analyte species.¹⁵ In this study numerous chemical modifiers were examined including: Pd(NO₃)₂, Pd(NO₃)₂-Ni(NO₃)₂, Pd(NO₃)₂-Mg(NO₃)₂, ascorbic acid and Pd(NO₃)₂-Mg(NO₃)₂+ascorbic acid. The best results were obtained with a Pd(NO₃)₂ only modifier. The optimum concentration was established by examination of the changes in Se signal of a 10 ng g⁻¹ standard in 1% HNO₃ with increasing Pd(NO₃)₂ concentration. Findings indicated that 10 μ l of a 100 μ g g⁻¹ Pd(NO₃)₂ solution were consistent with a maximum signal. However, further work with a serum sample showed evidence of selenium losses during the pyrolysis stage at temperatures above 1000 °C. Increasing the modifier concentration to 500 μ g g⁻¹ successfully overcame this problem with little effect on overall sensitivity.

Optimisation of ETV temperature program

L'vov platform. The work discussed in this study was performed using L'vov platform pyrolytic graphite coated graphite tubes. The advantages of this type of tube have been documented by several workers^{16,17} who have described the platform furnace tube at a stabilised 'steady state' temperature. A comparison was made between this and a non-platform tube with the determination of a 10 ng g⁻¹ Se standard at increasing pyrolysis temperatures. Data showed that despite an eventual decrease in signal with an increase in pyrolysis temperature, a more consistent signal was obtained with the L'vov tube than with a non-platform graphite tube. This supports the work of

Table 2 ETV temperature program

Step	Temperature/°C	Ramp/s	Hold/s	Gas/l min ⁻¹		
				Internal	External	Read
Dry 1	110	10	15	0.3		
Dry 2	120	10	45	0.3		
Pyrolysis	1100	10	45	0.3		
Vapourisation	2600	0.5	(0.3	0.95	Yes
Clean	2700	0.0	(0.95	
Cool	20	15	(0.95	

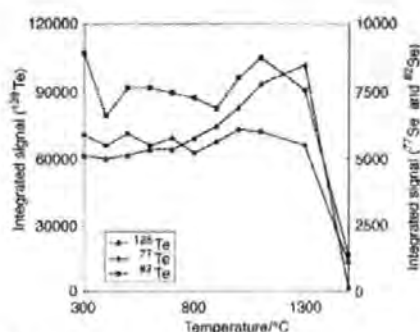


Fig. 2 Pyrolysis curves for ^{125}Te , ^{82}Se and ^{77}Te : 10 μl injection of a serum sample (with an approximate Se concentration of 5 ng g^{-1}); 10 μl of a $500 \mu\text{g g}^{-1}$ $\text{Pd}(\text{NO}_3)_2$ modifier were used.

Slavin *et al.*¹⁵ who demonstrated the differences between analyte atomisation from the furnace wall and the platform.

Pyrolysis and vapourisation. The main stages of any electrothermal vapourisation program are the pyrolysis (matrix

removal) and vapourisation (dissociation of atoms) processes. Parameters at each of these stages, such as ramp rate, temperature and hold time, were evaluated to establish the optimum conditions. Pyrolysis and vapourisation temperatures were optimised by the repeated analysis of a 10 ng g^{-1} Se standard at increasing temperature settings. Temperature curves constructed with the data from these experiments can be seen in Fig. 1. For the optimisation of the pyrolysis temperature the vapourisation temperature was set at 2600 C , and for the vapourisation temperature experiment, the pyrolysis temperature was set at 1100 C . The pyrolysis curve shows a stable signal between 500 and 1300 C , and a decrease in signal at temperatures above this, suggesting that a pyrolysis temperature within the range mentioned would be suitable. Owing to the fact that the graphite tube degrades with the number of firings, it was decided that a pyrolysis temperature midway in the range rather than at the higher end would be chosen, to minimise the detrimental effect on the lifetime of the tube. A temperature of 800 C was selected and a repeat experiment using a serum sample performed. The response of the ^{77}Se , ^{82}Se and ^{125}Te (internal standard) signals with an increase in temperature in the presence of the serum matrix is shown in Fig. 2. Suppression of the Te signal, and to a lesser extent the Se signal, can be seen at lower temperatures. Serum contains high concentrations of components such as sodium, chlorine and bromine. Examination of these analytes alongside Se in

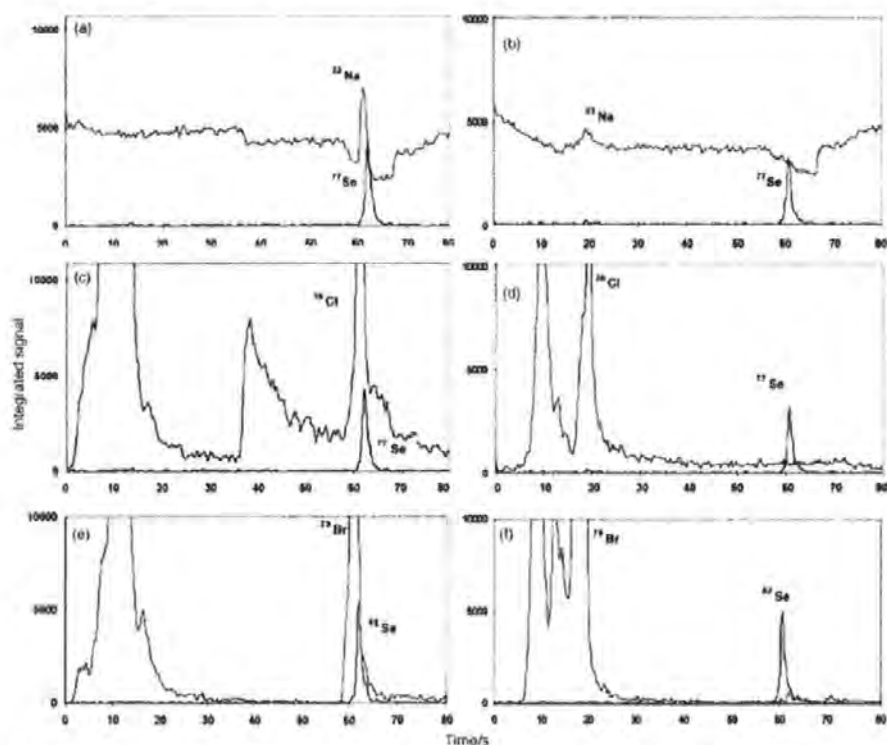


Fig. 3 The effect of pyrolysis temperature with respect to interference elimination, 10 μl injection of a serum sample in $1\% \text{ HNO}_3$, approximate concentration 5 ng g^{-1} . (a) ^{77}Se and ^{23}Na signal profiles, pyrolysis temperature 800 C ; (b) ^{77}Se and ^{23}Na signal profiles, pyrolysis temperature 1200 C ; (c) ^{77}Se and ^{35}Cl signal profiles, pyrolysis temperature 800 C ; (d) ^{77}Se and ^{35}Cl signal profiles, pyrolysis temperature 1200 C ; (e) ^{77}Se and ^{79}Br signal profiles, pyrolysis temperature 800 C ; and (f) ^{77}Se and ^{79}Br signal profiles, pyrolysis temperature 1200 C .

Table 4 Accuracy data from the analysis of internal quality control samples and NIST SRM 1598 (bovine serum). Values are expressed in the mean and standard deviations of three measurements

Isotope	Concentration ng g^{-1}			
	IQC 1 (54.5 ng g^{-1})	IQC 2 (103 ng g^{-1})	IQC 3 (148 ng g^{-1})	NIST SRM 1598 (42.4 \pm 3.5 ng g^{-1})
^{74}Se	48.9 \pm 6.0	97.9 \pm 7.2	146 \pm 5.8	37.9 \pm 5.2
^{76}Se	51.1 \pm 2.9	96.7 \pm 4.0	142 \pm 7.0	41.4 \pm 0.75
^{78}Se	64.1 \pm 9.3	109 \pm 7.8	146 \pm 8.0	55.6 \pm 0.72
^{82}Se	50.7 \pm 2.2	94.3 \pm 4.4	138 \pm 4.3	40.8 \pm 0.45

with an increase in gas flow rate from 0.85 l min^{-1} , reaching a maximum at 0.95 l min^{-1} , and decreased at flow rates above this. It should be noted that the internal flow rate of Ar in the furnace is 0.30 l min^{-1} . This combined with the ICP-MS carrier gas optimum flow rate of 0.95 l min^{-1} leads to a total carrier gas flow rate of 1.25 l min^{-1} , a similar optimum rate to that reported previously.²⁹

Analytical performance

Typical injection profiles for a 5 ng g^{-1} Se standard and a serum sample with an approximate concentration of 5 ng g^{-1} are shown in Fig. 5. The sensitivity of the system corresponds to between 200 and 6000 counts per ng g^{-1} of Se depending on the isotopic abundance.

Linearity. The system was found to be linear from 0 to 100 ng g^{-1} for the 77, 78 and 82 isotopes but only linear from 1 to 100 ng g^{-1} for ^{74}Se . This non-linearity below 1 ng g^{-1} for ^{74}Se may be attributed to its low isotopic abundance (0.90%) and hence the lack of sensitivity.

Reproducibility. Short-term stability data for ten consecutive analyses (triplicate) of a diluted serum sample, followed by ten determinations over a 4 h period to give the long-term stability of the system, are detailed in Table 3. Data were obtained with the intensity ratioed to the Te internal standard.

Detection limits. Typical limits of detection (calculated as 3 σ based on ten determinations of 1% HNO₃ as the blank) are also found in Table 3. The poor detection limits of ^{74}Se and ^{82}Se are due to the low abundance and poor sensitivity of ^{74}Se , and the substantial interference from argon polyatomics on ^{78}Se . Further work to improve the detection limit of ^{78}Se will continue, with the addition of nitrogen to the argon gas.

Accuracy. To check on the accuracy of the method a number of internal quality control (IQC) sera (prepared by the addition of Se standards to bovine serum, donated by H. T. Delves, Southampton University) and NIST SRM 1598 (bovine serum) were analysed. The results can be found in Table 4. A linear calibration was performed utilising the blank correction facility in the ELAN software. Excellent agreement between the results obtained and the target values for ^{74}Se , ^{76}Se and ^{82}Se are shown. High results were obtained with ^{78}Se , but again this is attributed to the large interference from argon adduct ions at m/z 78. The RSDs calculated from triplicate analyses of each sample were between 3.1 and 5.7% for ^{74}Se and ^{76}Se and 4.0 and 14.0% for ^{78}Se and ^{82}Se in the IQC samples, and between 1.1 and 1.8% for NIST SRM 1598, with the exception of ^{74}Se which gave an RSD of 14.0%.

Nitrogen addition

The introduction of nitrogen to argon plasmas and its ability to reduce polyatomic ion formations have been documented by several workers.^{13,20,22} An experiment was performed to

investigate the effect of nitrogen in the proposed system. Nitrogen was connected to the ICP-MS via the oxygen inlet tube and the nitrogen level regulated using the oxygen mass flow controller. A T-piece fitted in the PTFE transfer tube allowed the nitrogen to mix with the argon before arriving at the plasma. A decrease in the blank level of ^{78}Se was observed with an increase in nitrogen content. However the signal intensity of a 10 ng g^{-1} Se standard also decreased in a similar manner. The rate of reduction of the blank and standard signals is illustrated in Fig. 6, along with the variation in the signal to blank ratio as the nitrogen content increases. From the graph it can be seen that aerosol carrier gas containing 4% nitrogen gave rise to the largest decrease in the blank level. This study has shown the ability of nitrogen to reduce the interference at m/z 78, but further work is required to improve the sensitivity of the system. At present the nitrogen is introduced to the aerosol carrier gas after vaporisation of the analyte. An alternative procedure may be to mix the argon and nitrogen prior to the vaporisation stage and use it to carry the analyte from the ETV into the plasma.

Conclusion

The procedure described enables the accurate determination of Se in serum to be performed with minimal sample pretreatment. The main issue addressed in this study was one of interference elimination. The proposed method has successfully achieved this objective, allowing the interference free determination of two of the isotopes of selenium—77 and 82. Further reduction of interference on other selenium isotopes has also been shown to be possible using mixed gas plasmas.

The work carried out in this paper was supported by the Department of Trade and Industry as part of the National Measurement System Valid Analytical Measurement Programme. The authors would also like to thank Dr. Trevor Delves of Southampton University who kindly donated the IQC serum samples used in this work.

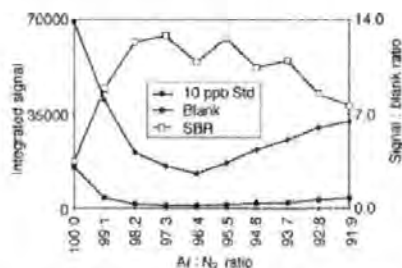


Fig. 6 The effect of nitrogen addition to the argon aerosol carrier gas on the ^{78}Se signal.

References

- 1 *Handbook on Metals in Clinical and Analytical Chemistry*, ed. H. G. Seiler, A. Sigel and H. Sigel, Marcel Dekker, New York, 1994.
- 2 J. Aaseth, J. Alexander, Y. Thomassen, J. P. Bloombhoff and S. Skerde, *Clin. Biochem.*, 1982, **15**, 281.
- 3 R. S. Houk, *Anal. Chem.*, 1986, **58**, 97A.
- 4 M. P. Rayman, F. R. Abou-Shakra and N. J. Ward, *J. Anal. At. Spectrom.*, 1996, **11**, 61.
- 5 M. Haldimann, T. Y. Venner and B. Zimmerli, *J. Trace Elem. Med. Biol.*, 1996, **10**, 31.
- 6 M. A. Quijano, A. M. Gutiérrez, M. Pérez-Corde and C. Cámara, *J. Anal. At. Spectrom.*, 1995, **10**, 871.
- 7 B. T. G. Ting, C. S. Mossers and M. Joughorban, *Analyst*, 1989, **114**, 667.
- 8 O. Mestek, M. Suchánek, Z. Voděčková, B. Zemanová and T. Zima, *J. Anal. At. Spectrom.*, 1997, **12**, 85.
- 9 J. Bowman, B. Fairman and T. Catterick, *J. Anal. At. Spectrom.*, 1997, **12**, 313.
- 10 R. M. Olivus, C. R. Quétel and O. F. X. Donard, *J. Anal. At. Spectrom.*, 1995, **10**, 865.
- 11 H. T. Delves and C. E. Sienkiewicz, *J. Anal. At. Spectrom.*, 1997, **12**, 387.
- 12 J. Goossens, F. Vanhosecke, L. Moens and R. Dams, *Anal. Chim. Acta*, 1993, **280**, 137.
- 13 E. H. Evans and L. Ebdon, *J. Anal. At. Spectrom.*, 1989, **4**, 299.
- 14 D. C. Gregoire, S. Al-Mawadi and C. L. Chakrobarti, *Spectrochim. Acta, Part B*, 1992, **47**, 1123.
- 15 W. Slavin, D. C. Manning and G. R. Carnick, *At. Spectrosc.*, 1981, **2**, 157.
- 16 G. F. Kirkbright, S. Hsiao-Chuan and R. D. Snook, *At. Spectrosc.*, 1980, **1**, 85.
- 17 J. M. Ottaway, *At. Spectrosc.*, 1982, **3**, 89.
- 18 K. O'Hanlon, L. Ebdon and M. Foulkes, *J. Anal. At. Spectrom.*, 1997, **12**, 329.
- 19 J. Marshall and J. Franks, *At. Spectrosc.*, 1990, **11**, 177.
- 20 B. Fairman and T. Catterick, *J. Anal. At. Spectrom.*, 1997, **12**, 863.
- 21 F. Laborda, M. J. Baxter, H. M. Crews and J. Dennis, *J. Anal. At. Spectrom.*, 1994, **9**, 727.
- 22 T. van der Velde-Koeris and J. L. M. de Boer, *J. Anal. At. Spectrom.*, 1984, **9**, 1003.

Paper 8/066381I

Accurate analysis of selenium in water and serum using ETV-ICP-MS with isotope dilution†

JAS

Interlaboratory
Note

Justine Turner,^{a*} Steve J. Hill,^b E. Hywel Evans,^b Ben Fairman^a and Céline S. J. Wolff-Briche^a

^aLGC (Teddington) Ltd., Queens Road, Teddington, Middlesex, TW11 0LY UK

^bUniversity of Plymouth, Department of Environmental Sciences, Drake Circus, Plymouth, Devon, PL4 8AA UK

Received 31st January 2000, Accepted 5th April 2000

Published on the Web 12th May 2000

A procedure for the determination of selenium in water and serum using electrothermal vapourisation isotope dilution inductively coupled plasma mass spectrometry (ETV-ID-ICP-MS) is described. The ^{62}Se : ^{77}Se isotope ratio was measured throughout, following spiking of the samples with a solution containing the enriched ^{77}Se isotope. Elimination of interferences was achieved with an optimised ETV temperature program. Parameters such as peak measurement mode, dwell time, points per spectral peak and number of replicates were evaluated to establish optimum conditions. The accuracy and precision of the method are demonstrated with the analysis of several certified reference materials namely TMRAIN-95 (spiked rainwater), TMDA-54.2 (spiked soft water), LGC 6010 (hard drinking water) and NIST 1598 (bovine serum). Results for all reference materials were within the certified limits. Isotope dilution analysis of TMRAIN-95, TMDA-54.2, LGC 6010 and NIST 1598 gave % RSD values ($n=3$) of 0.80, 0.07, 0.48 and 0.06%, respectively, compared with 5.50, 2.79, 1.15 and 0.92% obtained with the conventional ETV-ICP-MS procedure, thus illustrating improvements in precision with the ETV-ID-ICP-MS method. The uncertainties for the two methods were calculated following ISO guidelines. The uncertainty for the IDMS procedure was 3.4 times smaller than that for the conventional ETV-ICP-MS method (2.26% and 7.73%, respectively).

Introduction

Electrothermal vapourisation (ETV) is an alternative form of sample introduction for use with ICP-MS detection.^{1–3} The technique, which converts the sample to the vapour state, has the ability to reduce oxide formation by the elimination of water vapour, and can reduce the formation of polyatomic ions originating from the sample matrix.⁴ This is particularly advantageous in the determination of selenium, which suffers from poor sensitivity and severe interference from polyatomic species (*i.e.*, interference from $^{40}\text{Ar}^{37}\text{Cl}^+$ on ^{77}Se and $^{81}\text{Br}^{\text{H}^+}$ on ^{62}Se) when determination is performed by conventional nebulisation ICP-MS. In addition, when dealing with clinical samples such as serum, high levels of sodium and organic compounds present in the matrix can cause signal suppression. ETV-ICP-MS has the advantage of using small sample sizes (5–50 μl), greater sensitivity and the capability to eliminate some of the polyatomic interferences already mentioned by thermal pre-treatment of the sample. In a previous publication⁵ we have described the development of an ETV-ICP-MS procedure for the analysis of selenium in serum. The method successfully overcomes spectroscopic interferences with careful optimisation of the temperature program.

Isotope dilution mass spectrometry (IDMS) has been described as a definitive analytical technique that is capable of providing improved accuracy and precision over alternative ICP-MS methods.¹⁰ The technique is based on the addition of an isotopically enriched material, which acts as the perfect internal standard. Detailed explanations and applications of the technique are given in the literature.^{11–15} For example, an ETV-ID-ICP-MS procedure for the determination of selenium in sediments has been described by Lam *et al.*¹⁶ The procedure adopts an alternative approach to interference elimination with the early release of selenium prior to the interfering species.

Essential requirements for IDMS are that more than one isotope of the element in question occurs in nature and that the selected isotopes are free from interference. Once the spike has been equilibrated in the sample, the accuracy and precision of the method are mainly dependent upon the accuracy of the isotope ratio measurement.

This paper describes the development of a high accuracy procedure for the determination of selenium, a complex element whose beneficial and detrimental effects on our health are well documented.^{17,18} Selenium deficiency has been linked closely with heart disease and cancer, and excessive selenium intakes have been associated with hair loss and tooth decay. The difference between toxicity and deficiency is very narrow and thus, together with the health implications referred to, emphasise how important it is that accurate and precise analytical methods are available. By combining the established ETV-ICP-MS procedure with the technique of isotope dilution these criteria can be met. The accuracy and precision of the method is demonstrated with the analysis of several certified reference materials.

It is becoming more frequently recognised that a result obtained from a quantitative analysis is incomplete without a statement of the uncertainty associated with it. In fact, an estimation of the measurement uncertainty is a requirement for analytical methods accredited in accordance with ISO Guide (25).²⁰ An estimate and comparison of the measurement uncertainty associated with both the ETV-ICP-MS and ETV-ID-ICP-MS procedures is reported.

Experimental

Instrumentation

An ELAN 5000A ICP-MS instrument coupled to an HGA 600MS ETV unit with an AS60 autosampler attachment (PerkinElmer, Beaconsfield, Buckinghamshire, UK) were used. A 140 cm long PTFE transfer tube (0.6 cm id) was used to

† Copyright LGC (Teddington) Ltd 2000.

DOI: 10.1039/b000807j

J. Anal. At. Spectrom., 2000, 15, 743–746 743

This journal is © The Royal Society of Chemistry 2000

Table 1 ICP-MS operating conditions

ICP—	
Power	1150 W
Plasma gas	15.0 l min ⁻¹
Auxiliary gas	0.80 l min ⁻¹
Nebuliser gas	0.95 l min ⁻¹
Cones	P
Lenses P	48
B	43
S	45
E	25
Parameter file—	
Dwell time	15 ms
Sweps per reading	J
Readings per replicate	130
Number of replicates	9
Points across peak	J
Resolution	Normal
Masses	⁷⁷ Se ⁸² Se

connect the furnace to the ICP-MS. Pyrolytic graphite coated graphite tubes fitted with L'vov platforms were used throughout the work. Operating conditions for the ETV temperature program are the same as those detailed in an earlier publication.⁹ The ICP-MS operating conditions are detailed in Table 1. Optimisation of the ICP-MS instrument (*i.e.*, lens settings, resolution, oxide and doubly charged ion formation) was performed using conventional nebulisation prior to coupling the instrument to the ETV unit.

Reagents

All solutions were prepared using high purity deionised water (18 M Ω , Elga, High Wycombe, Buckinghamshire, UK). The enriched standard solution (spike) was purchased from AEA Technology (Didcot, Oxfordshire, UK) and the natural Se solution was prepared from >99.999% Se pellets (Aldrich, Poole, Dorset, UK). Stock solutions of the two standards were prepared by dissolving accurately weighed quantities of the materials in concentrated nitric acid (Ultrapure II ultra-pure nitric acid, J.T. Baker, Milton Keynes, Buckinghamshire, UK) with final dilution to 100 g with deionised water. Gentle heating was required to aid dissolution. The concentration of the ⁷⁷Se enriched solution was determined by performing a reverse isotope dilution procedure. The chemical modifier solution was prepared from palladium(n) nitrate (Sigma, Poole, Dorset, UK).

Sample preparation

All samples were spiked gravimetrically with the enriched solution to give a final ratio of 1:3 (⁸²Se:⁷⁷Se). Typically, 1 g of the enriched solution was used to spike each sample. The serum samples were diluted 1+19 with 1% m/m nitric acid following spiking, but no dilution was necessary with the water samples. A mass bias solution was prepared by spiking a natural selenium standard to match the ratio in the sample. This was then analysed before and after the sample following the matching procedure detailed by Catterick *et al.*¹⁴

Results and discussion

Optimisation of measurement parameters

Optimisation of the scan parameters is of paramount importance in minimising errors in the isotope ratio measurement and achieving the highest accuracy and precision possible. Electrothermal vaporisers generate transient signals of short life spans, typically between 3 and 6 s. It is important with this type of signal processing to collect enough readings to accurately define the signal profile. Influencing factors such as dwell time, points per spectral peak, peak measurement mode and number of replicates were evaluated and the optimum settings established, for the measurement of the ⁸²Se:⁷⁷Se isotope ratio. Evaluation of each of the measurement parameters was achieved through the repeated analysis of a 100 ng g⁻¹ Se standard. The optimum settings are detailed in Table 1.

Analytical performance

A typical injection profile for 9 consecutive replicate injections of a serum sample with an approximate concentration of 10 ng g⁻¹ of Se diluted in 1% HNO₃ is shown in Fig. 1. Although the % RSD values obtained, based on the ⁷⁷Se and ⁸²Se isotope intensities, were 6.69% and 5.84%, respectively, this compares with 0.80% for the ⁸²Se:⁷⁷Se isotope ratio obtained for the same 9 injections. This illustrates that the measurement procedure has been optimised so that there is sufficient correlation with the two signals for the precision advantages of ratio measurements to be realised.

Accuracy and precision

The natural theoretical ⁸²Se:⁷⁷Se isotope ratio is 1.1442, based on IUPAC²¹ defined abundances of 8.73 and 7.63% for ⁸²Se and ⁷⁷Se, respectively. From Table 2 it can be seen that the

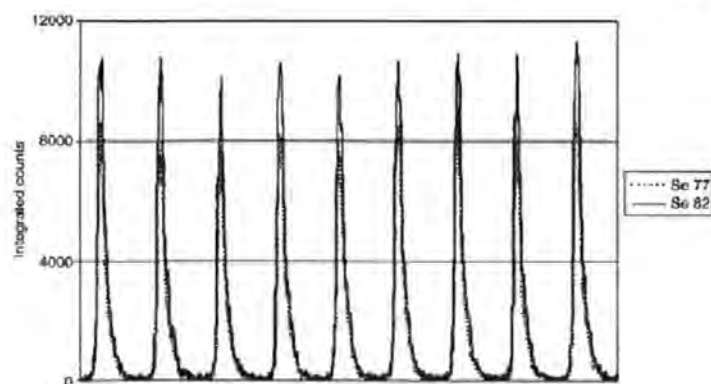


Fig. 1 Nine consecutive injections of a serum sample (diluted in 1% HNO₃), 10 μ l injection, and approximate concentration of 10 ng g⁻¹

Table 1 $^{82}\text{Se}/^{77}\text{Se}$ isotope ratios and corresponding % RSD data obtained for 9 replicate injections of 4 different solutions

Solution	$^{82}\text{Se}/^{77}\text{Se}$ ratio	RSD (%)
1 ng g ⁻¹ Se (1% HNO ₃)	1.4060	2.31
2 ng g ⁻¹ Se (serum)	1.4553	2.12
10 ng g ⁻¹ Se (1% HNO ₃)	1.3666	0.22
10 ng g ⁻¹ Se (serum)	1.3677	0.87

experimental $^{82}\text{Se}/^{77}\text{Se}$ isotope ratios for the solutions analysed differ considerably from this theoretical value (by approximately 20%). However, it should be noted that no difference in the $^{82}\text{Se}/^{77}\text{Se}$ isotope ratio is observed between the standard solution in 1% HNO₃ and the serum samples of similar concentrations. This suggests that the difference is due to instrumental mass discrimination and not matrix effects. A more marked difference is however observed between the ratios obtained for the higher concentration solutions and the lower concentration solutions irrespective of matrix. This may be due to dead time and counting statistics. By exactly matching the mass bias solution to the sample solution with respect to concentration and matrix, any discrepancies will be compensated for and this problem negated.

Several certified reference materials, TMRAIN-95 (spiked rainwater), TMDA-54.2 (spiked soft water), LGC 6010 (hard drinking water) and NIST 1598 (bovine serum) were analysed using both the IDMS and non-IDMS procedures. The results, which were all within the certified limits, are detailed in Table 3. The method precision, represented by the % RSD values obtained for triplicate analyses of each reference material, and the deviation from the certified level, represented by the % recovery values, are significantly lower with the IDMS method than with the non-IDMS method.

Measurement uncertainty

Measurement uncertainty is an important aspect of any analytical method and it is often considered that an analytical result is not complete without an indication of the uncertainty associated with it. The ISO definition of measurement uncertainty is: "A parameter, associated with the result of a measurement, that characterises the dispersion of the values that could reasonably be attributed to the measurand".²² There are many factors that contribute to the overall uncertainty estimate of methods, among which are precision, bias and instrument drift. Some of these parameters greatly affect the final estimate and some are insignificant, but all must be taken into account.

Uncertainty calculation ETV-ICP-MS method. In order to establish an uncertainty estimate, several experiments were performed using solutions prepared by serial dilution of a NIST certified reference solution (SRM 3149) with 1% nitric acid. The data obtained from these experiments were then used

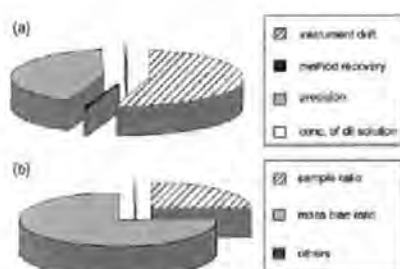


Fig. 2 Contribution of the different variables to the uncertainty budget. (a) ETV-ICP-MS procedure; (b) ETV-ID-ICP-MS procedure.

in the uncertainty calculations following the procedure detailed by Barwick *et al.*,²³ which outlines each of the parameters and explains in detail how they are calculated. The main factors contributing to the uncertainty of this procedure were found to be method recovery, precision, concentration of the dilute standard and instrument drift. The uncertainties associated with the method recovery and the concentration of the dilute standard have been determined from the experimental data obtained and enable both a standard and relative uncertainty to be calculated. The uncertainty associated with precision is calculated from reproducibility data and involves pooling the relative standard deviations of the data obtained; hence only a relative uncertainty is given. The permitted drift of the instrument throughout a run is $\pm 10\%$. Since there is no evidence of lower probability towards the extremes of the range this can be treated as a rectangular distribution and divided by the square root of 3. This calculation gives the uncertainty associated with instrument drift and is estimated as 0.0577 relative uncertainty. All of the individual uncertainty terms are listed in Table 4. The combined standard uncertainty, calculated from the root sum of the squares of the individual components, was calculated to be 0.373 ng g⁻¹.

Uncertainty calculation ETV-ID-ICP-MS method. The combined uncertainty of the ETV-ID-ICP-MS procedure was calculated in accordance with the uncertainty propagation law as detailed in the Eurachem guide.²⁴ The equation used in this calculation [eqn. (1)] is detailed below (see Table 4 for notation definitions). The equation combines factors such as the mass of each solution (spike, natural and sample), the isotope ratios of the spiked sample and mass bias solutions and the isotopic composition of the spike and natural selenium solutions.

$$r_X = c_Z \times \frac{m_Y}{m_X} \times \frac{m_{Zc}}{m_{Yc}} \times \frac{R_Y - R_B \times \frac{R_{Bc}}{R_B}}{R_B \times \frac{R_{Bc}}{R_B} - R_X} \times \frac{R_{Bc} - R_X}{R_Y - R_{Bc}} \quad (1)$$

Table 3 Results for the analysis of certified reference materials TMRAIN-95 (spiked rainwater), TMDA-54.2 (spiked soft water), LGC 6010 (hard drinking water) and NIST 1598 (bovine serum) using ETV-ICP-MS and ETV-ID-ICP-MS ($n=3$)

CRM	Certified level/ng g ⁻¹	ETV-ICP-MS			ETV-ID-ICP-MS		
		Mean/ng g ⁻¹	RSD (%)	Recovery (%)	Mean/ng g ⁻¹	RSD (%)	Recovery (%)
TMRAIN-95							
Spiked rainwater	0.94 ± 0.29	0.68 ± 0.04	5.50	92	0.750 ± 0.006	0.80	101
LGC 6010							
Hard drinking water	9.30 ± 1.00	10.9 ± 0.13	1.15	117	9.57 ± 0.03	0.48	103
TMDA-54.2							
Spiked soft water	15.0 ± 3.0	15.5 ± 0.43	2.79	103	15.06 ± 0.01	0.07	100
NIST 1598							
Bovine serum	42.4 ± 3.5	40.8 ± 0.37	0.92	96	40.89 ± 0.02	0.06	96

Table 4 Summary of individual uncertainty terms and combined standard uncertainty values for both the ETV-ICP-MS and ETV-ID-ICP-MS methods

Parameter		Value	Standard uncertainty	Relative uncertainty
<i>ETV-ICP-MS Method</i>				
Method recovery	R_m	0.8965 ng g ⁻¹	4.56 × 10 ⁻¹ ng g ⁻¹	5.09 × 10 ⁻¹
Precision	P			0.0510
Conc. of dilute solution	C_{dil}	4.8280 ng g ⁻¹	0.0154 ng g ⁻¹	3.19 × 10 ⁻¹
Instrument drift	(Drift)			0.0577
Combined standard uncertainty	$u(C_{Se})$	0.373 ng g ⁻¹		
<i>ETV-ID-ICP-MS Method</i>				
Conc. of natural Se standard	c_s	3.9343 ng g ⁻¹	2.20 × 10 ⁻¹ ng g ⁻¹	5.59 × 10 ⁻²
Mass of sample	m_s	1.8807 g	6.00 × 10 ⁻⁵ g	3.19 × 10 ⁻²
Mass of spike added to sample	m_{sp}	1.0012 g	6.00 × 10 ⁻⁵ g	5.99 × 10 ⁻²
Mass of natural standard	m_{ns}	2.3075 g	6.00 × 10 ⁻⁵ g	2.60 × 10 ⁻²
Mass of spike added to natural standard	m_{sp}	1.0094 g	6.00 × 10 ⁻⁵ g	5.94 × 10 ⁻²
Isotope ratio of the spike	R_s	0.0240	3.00 × 10 ⁻³	0.1250
Isotope ratio of the natural standard	R_n	1.1442	0.0220	0.0192
Prepared isotope ratio of the mass bias blend	R_{pb}	0.3312	6.59 × 10 ⁻³	0.0199
Measured isotope ratio of the sample blend	R'_b	0.3795	2.81 × 10 ⁻³	7.40 × 10 ⁻²
Measured isotope ratio of the mass bias blend	R'_{pb}	0.3750	4.90 × 10 ⁻³	0.0131
Combined standard uncertainty	$u(C_{Se})$	0.109 ng g ⁻¹		

As with the non-IDMS procedure, the combined uncertainty was calculated using data obtained from the analysis of a 5 ng g⁻¹ Se solution, which was prepared by serial dilution of the NIST reference solution SRM 3149 with 1% nitric acid. This was calculated to be 0.109 ng g⁻¹. Table 4 details the individual variables that contribute to the combined uncertainty, the magnitude of each illustrating which factors have the greatest influence on the final uncertainty value.

The main contributors to the uncertainty of the two procedures are precision and instrument drift with the ETV-ICP-MS method, and the measured isotope ratio of the sample and mass bias blends with the ETV-ID-ICP-MS method. Figs. 2(a) and (b) better illustrate these parameters with a graphical representation of the factors expressed as a percentage of the total uncertainty budget as given in Table 4. The standard uncertainties for the ETV-ICP-MS and ETV-ID-ICP-MS methods are 0.373 ng g⁻¹ and 0.109 ng g⁻¹, respectively. These standard uncertainties can also be expressed as a percentage of the analyte concentration, which in the case of the non-IDMS method corresponds to 7.73% and with the IDMS method equates to 2.26%. This represents a 3.4-fold improvement in the uncertainty with the isotope dilution procedure compared with the non-IDMS procedure.

Conclusions

This paper describes the extension and adaptation of an established ETV-ICP-MS procedure to isotope dilution analysis, and the rigorous optimisation of this procedure in order to obtain results of optimum accuracy and precision. Significant improvements in accuracy and precision, demonstrated with the analysis of certified reference materials, were observed with the IDMS procedure compared with the non-IDMS procedure. The uncertainty of the two procedures has been calculated and this further demonstrates the applicability of the ETV-ID-ICP-MS procedure as a definitive method for the analysis of selenium in water and serum matrices.

Acknowledgements

The work described in this paper was supported by the Department of Trade and Industry as part of the National Measurement System Valid Analytical Measurement Programme.

References

1. J. P. Byrne, D. M. Hughes, C. L. Chakrabarti and D. C. Grégoire, *J. Anal. At. Spectrom.*, 1994, **9**, 913.
2. B. Fairman and T. Catterick, *J. Anal. At. Spectrom.*, 1997, **12**, 863.
3. K. Gruenke, H. J. Staerk, R. Wennrich, H. M. Ortner and J. A. C. Broekaert, *Fresenius' J. Anal. Chem.*, 1997, **359**, 465.
4. D. Pozebon, V. L. Dressler and A. J. Curtius, *J. Anal. At. Spectrom.*, 1998, **13**, 7.
5. S. F. Chen and S. J. Jiang, *J. Anal. At. Spectrom.*, 1998, **13**, 673.
6. D. Pozebon, V. L. Dressler and A. J. Curtius, *J. Anal. At. Spectrom.*, 1998, **13**, 1101.
7. J. B. Truscott, L. Bromley, P. Jones, E. H. Evans, J. Turner and B. Fairman, *J. Anal. At. Spectrom.*, 1999, **14**, 627.
8. D. C. Grégoire, *Can. J. Anal. Sci. Spectrosc.*, 1997, **42**, 1.
9. J. Turner, S. J. Hill, E. H. Evans and B. Fairman, *J. Anal. At. Spectrom.*, 1999, **14**, 121.
10. K. G. Heumann, *Fresenius' J. Anal. Chem.*, 1986, **325**, 661.
11. T. Catterick, H. Handley and S. Merson, *At. Spectrosc.*, 1995, **16**, 259.
12. J. Papadakis, P. D. P. Taylor and P. De Bièvre, *J. Anal. At. Spectrom.*, 1997, **12**, 791.
13. M. Ohata, T. Ichinose, N. Furuta, A. Shinohara and M. Chiba, *Anal. Chem.*, 1998, **70**, 2726.
14. T. Catterick, B. Fairman and C. F. Harrington, *J. Anal. At. Spectrom.*, 1998, **13**, 1009.
15. K. Lee, S. Jiang and H. Liu, *J. Anal. At. Spectrom.*, 1998, **13**, 1227.
16. J. W. H. Lam, R. E. Sturgeon and J. W. McLaren, *Spectrochim. Acta, Part B*, 1999, **54B**, 443.
17. *Handbook on Metals in Clinical and Analytical Chemistry*, ed. H. G. Seiler, A. Sigel and H. Sigel, Marcel Dekker, New York, USA, 1994.
18. J. Aaseth, J. Alexander, Y. Thomassen, J. P. Bloenhoff and S. Skerde, *Chin. Biochem.*, 1982, **15**, 281.
19. *Scientist in Food and Health*, C. Rilly, Chapman and Hall, London, UK, 1996.
20. ISO/IEC Guide 25, *General Requirements for the Competence of Calibration and Testing Laboratories*, ISO, Geneva, Switzerland, 3rd edn., 1990.
21. IUPAC, 'Atomic Weights of the Elements', *Pure Appl. Chem.*, 1992, **64**, 1519.
22. *Guide to the Expression of Uncertainty in Measurement*, ISO, Geneva, Switzerland, 1993 (ISBN 92-67-10188-9).
23. V. J. Burwick, S. L. R. Ellison and B. Fairman, *Anal. Chim. Acta*, 1999, **394**, 281.
24. *Furchem. Quantifying Uncertainty in Analytical Measurement*, Laboratory of the Government Chemist, London, 1995 (ISBN 0-948926-08-2).

The accurate analysis of trace metals in clinical samples using ICP-MS

Justine Turner,
Ben Fairman
and Chris
Harrington,
LGC

Introduction

The accurate measurement of trace metals in clinical samples, such as blood, serum and plasma, is vitally important to nutritional and toxicological studies. Metal ions play a key role in the function of many biomolecules, as well as adversely affecting a number of important biological/biochemical processes. It is important that sensitive, precise and accurate analytical methods are available, so that the narrow divide between the concentration at which the metal is considered deficient, optimal or toxic, can be measured with confidence. Development of methods based on isotope dilution mass spectrometry (ID-MS) will help with the certification of reference materials, which are vital for quality control in clinical analysis.

Many trace metals are essential for life, others are inert and some exhibit toxicity at low concentrations. Health implications¹ due to the deficiency or toxicity of various metals are extremely diverse. For example, coronary heart disease, arthritis and certain forms of cancer are linked with selenium deficiency. Lung and nasal cancers have been reported in nickel refinery workers exposed to toxic levels of nickel sulphide ore. In general, occupational exposure to low metal concentrations causes nausea, vomiting, gastrointestinal irritability, headaches and skin allergies. More serious health implications can be caused by the chronic



Element	Daily allowance	Total amount in human body
Cr	0.1 mg	6 mg
Co	3 µg	1 mg
Mn	4 mg	12 mg
Cu	3 mg	72 mg
Se	0.1 mg	5 mg

Table 1: Daily allowance values for several essential trace elements in the human body^{1,2}

toxicity of some elements e.g. haematological disorders resulting from cobalt toxicity, or the high toxicity of others e.g. exposure to lead can result in neurological impairment in children. Owing to the recognition that metal ions and their compounds can induce toxic effects, daily allowances (the dietary intake of a given

element that a human may consume in a day) have been defined. Such levels are detailed in Table 1 for a range of trace metals.

Analytical methods

There are numerous analytical procedures available for the analysis of trace elements in clinical or biomedical samples.

The method of choice will depend on the element to be determined, the sample matrix and the level at which the element is present. Both flame and furnace atomic absorption spectrometry (AAS) have been used, but these methods are limited in most cases to single element determinations. Other methods involve inductively coupled plasmas with detection by atomic emission spectroscopy (ICP-AES) or mass spectrometry (ICP-MS). ICP-AES is used for the analysis of clinical samples, but is often restricted to elements such as sodium, potassium and calcium, which are present in the body at relatively high levels. ICP-MS is the method of choice for trace multi-element analysis and is a necessity if isotope dilution analysis is to be used.

Inductively coupled plasma mass spectrometry (ICP-MS)

The main advantages of this technique are, low detection limits, a multi-element capability and a large linear response range. Unfortunately, there are also a number of problems, which are centred around the presence of ions with the same nominal mass charge (m/z) ratio as the isotope of interest. These can be divided into three different sources: formation of oxides and doubly charged ions e.g. generation of barium oxide; presence of polyatomic ions resulting from reactions between argon, and constituents of the sample matrix e.g. formation of argon oxide; and isobaric overlaps between the isotopes of different elements e.g. overlap of ¹³⁶Cd and ¹³⁶Sn. Table 2 contains examples of several polyatomic ions and the corresponding isotope with which they interfere.



Inductively coupled plasma mass spectrometer

Analyte	Mass	Polyatomic Interference	Mass	Resolution required
⁵¹ Cr	51.94	⁴⁰ Ar ¹² C ⁺ ³⁹ Ar ¹² O ⁺ ³⁹ Ar ¹² N ⁺	51.96	2376
			51.96	2387
			51.97	2054
⁵⁸ Co	58.93	⁴⁰ Ca ¹⁸ O ⁺ ³⁹ Ar ¹⁹ Na ⁺	58.95	2878
			58.96	2444
⁵⁹ Ni	59.93	³⁹ Ar ²⁰ Mg ⁺ ³⁹ Ar ²⁰ Cl ⁺	59.95	2750
			59.96	2410
⁷⁵ Se	75.02	³⁹ Ar ³⁶ Ar ⁺	75.93	7081
⁷⁷ Se	76.92	⁴⁰ Ar ³⁷ Cl ⁺	76.93	9182
⁷⁸ Se	77.92	⁴⁰ Ar ³⁸ Ar ⁺	77.93	9970
⁸⁰ Se	79.92	⁴⁰ Ar ⁴⁰ Ar ⁺	79.92	9688
⁸¹ Se	81.92	⁴⁰ Ar ⁴¹ Ca ⁺	81.92	19069

Table 2: Polyatomic mass spectral interferences affecting the measurement of the trace metal ions of interest¹

This article describes different approaches to the elimination of these problems for two specific applications in clinical analysis. The first method of interference removal is to eliminate the matrix by using electrothermal vaporization, prior to determination by quadrupole ICP-MS. The second example uses an ICP-MS instrument with a sector field mass filter. The greater resolving power of this instrument, facilitates detection of the isotope of interest without interference from other ions.

The analysis of clinical samples present their own particular problems, mainly because of the complex nature of the sample matrix. The presence of sodium, potassium and other easily ionisable elements in the matrix, as well as large biomolecules such as proteins, can cause signal suppression. The direct analysis of blood is particularly difficult because of coagulation effects in the sample introduction system, which lead to blockage of the torch injector and result in a loss of signal.

Conventional multi-element determination of Cr, Co, Ni and Pb in whole blood by sector field ICP-MS

Two approaches have been described for the determination of trace metals in biomedical samples. The first uses mineralisation of the sample with acid, followed by dilution and analysis⁴. The second involves direct analysis and requires sample dilution, usually with ammonia to lyse the red blood cells. EDTA to prevent

loss of the metals by precipitation or adsorption and Triton X-100 to reduce blockage of the torch injector⁵. The direct analysis of whole blood has a number of benefits:

- reduction in the potential for contamination
- reduction in analysis time and therefore cost
- maintenance of low blank concentrations and detection limits.

The present work describes the direct analysis of whole blood for Cr, Co, Ni and Pb, compared to the use of a standard operating procedure involving acid digestion in a microwave oven.

The analysis of chromium is usually carried out by measuring the isotope at mass/charge ratio (m/z) 53, because the more abundant isotope at m/z 52 (83.8%), suffers from interfering polyatomic ions generated from argon adducts of carbon, oxygen or nitrogen (see Table 2). Obviously these other ions are present to a large extent in blood. However, with a double focusing fixed magnetic sector instrument, all of these interferences can be resolved from the m/z of interest. It is not possible to achieve this using quadrupole ICP-MS (Q-ICP-MS), because of the lower mass resolution attainable with these instruments. Figure 1 (a) shows the mass spectrum in the region of m/z 52, for the analysis of chromium in the acid digested blood. It clearly shows the presence of a large interference, which is well resolved from the analyte of interest. Figure 1 (b) shows the same mass range but this time the sample has been diluted down and analysed directly. Again the presence of

a large interference, well resolved from the peak of interest, is clearly shown.

The data for the chromium spike (Table 3) shows quantitative recovery using both sample preparation methods and analysis in medium resolution mode ($R = 3000$). However, analysis of the spiked digestate in low resolution mode resulted in a very large recovery due to the unresolved interference (Figure 1 (a)). This would also be the case if the digest had been analysed using Q-ICP-MS.

The lowest limits of detection for all the metals (3 times the standard deviation of the blank signal, multiplied by the dilution factor), were found with the direct method. Analysis of the reconstituted freeze dried whole blood CRM (AMI B1001, Referensmatræl AB, LGC (Teddington) Ltd, UK) for cobalt and lead using both sample preparation methods, gave good agreement with the certified values using medium resolution mode. However, the value for chromium was higher than the certified figure using both methods. This was also noted by other workers using a similar sector field ICP-MS instrument, for the analysis of human serum⁹. Further work to evaluate the possibility of another interfering ion at m/z 52, using Cr ratio analysis will be carried out.

The only method with a detection limit low enough to determine 5 ng g^{-1} nickel in whole blood, was the direct method in medium resolution mode. Using low resolution mode and sample digestion gave good agreement for cobalt, but both the lead and chromium values were higher than the

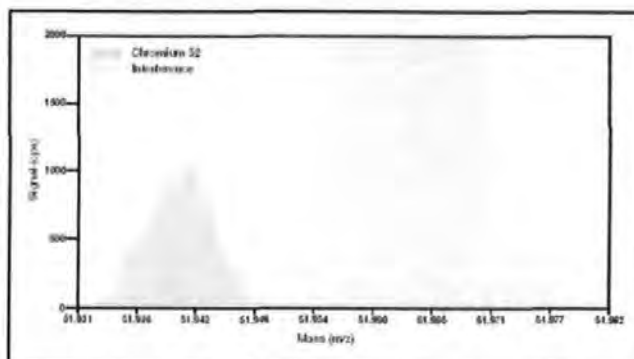


Figure 1 (a): Mass spectrum in the region of chromium m/z 52, showing the interference present in a digested blood sample spiked with 5 ng g^{-1} chromium

certified values. Future work will apply isotope dilution analysis at clinically important concentrations to the analysis of trace metals in whole blood.

High accuracy measurement using isotope dilution analysis (ICP-ID-MS)

The isotope dilution measurement approach has been discussed in previous VAM articles¹⁰. It is based on the addition to the sample of an isotopically enriched material (often referred to as the spike), which acts as an internal standard. Provided the enriched isotope is present in an equivalent state to the natural isotope, it can perform the role of the ideal internal standard

and exactly compensate for errors arising at all stages, from sample preparation through to the final instrument measurement. In order to realize the potential of ID-MS to achieve the highest possible accuracy it is essential to adopt rigorous experimental procedures, such as those developed at LGC¹¹.

Determination of Se in serum by ETV-ICP-ID-MS

The analysis of selenium in serum by ICP-MS is hampered by the problems outlined previously. The first ionisation energy of selenium is high, resulting in only 30% ionisation occurring in the plasma¹², which leads to low signals and poor sensitivity. As illustrated in Table 2, the majority of the

Method	Isotope	Resolution	Calibration			Validation		
			DL ng g ⁻¹	RPL ng g ⁻¹	r ²	Spike ng g ⁻¹	CRM ng g ⁻¹	Value ± SD
Digestion	52 Cr	300	0.9	3	0.9999	649	390	1.98 ± 0.09
	59 Co	300	0.03	0.1	0.9999	5.9	16.3	13.2 ± 0.56
	60 Ni	300	2	5	0.9998	<RPL	<DL	NC ²
	208 Pb	300	0.5	2	0.9998	41.9	45.8	38.3 ± 0.04
Direct	52 Cr	3000	0.1	0.4	0.9986	4.65	3.29	1.96 ± 0.09
	59 Co	3000	0.03	0.1	0.9995	4.78	14.1	13.2 ± 0.56
	60 Ni	3000	1	3	0.9928	4.29	<DL	NC ²
	208 Pb	3000	0.5	2	0.9995	35.0	34.5	38.3 ± 0.04
Digestion	52 Cr	3000	0.3	1	0.9999	4.92	5.02	1.98 ± 0.09
	59 Co	3000	0.08	0.3	1.0000	4.54	13.9	13.2 ± 0.56
	60 Ni	3000	6	20	0.9993	<DL	<DL	NC ²
	208 Pb	3000	0.8	3	0.9986	36.8	36.5	38.3 ± 0.04

¹DL: detection limit, defined as 3 x standard deviation of the reagent blank concentration x dilution factor (10). ²RPL: reporting limit, defined as 10 x standard deviation of the reagent blank concentration x dilution factor (10). NC: not certified. r: correlation coefficient.

Table 3: Summary of results for the analysis of all four metals in spiked whole blood. Sample preparation using two different sample preparation methods, spiking level was 5 ng g^{-1}

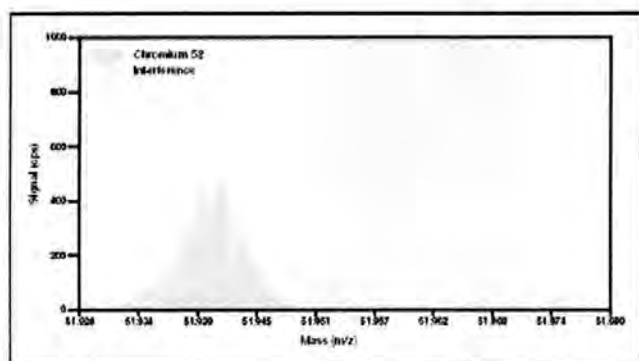


Figure 1 (b): Mass spectrum in the region of chromium m/z 52, showing the interference present in a blood sample spiked with 5 ng g^{-1} chromium and analysed using the direct method

selenium isotopes suffer from spectroscopic interferences, and matrix effects, which often result in signal suppression.

Hydride generation (HG-ICP-MS) techniques have been used to overcome some of these problems¹¹. Greater sensitivity is attainable owing to the improved sample delivery rate and reduction of interferences is achieved due to analyte removal from the matrix. However, lengthy sample preparation procedures are generally required to convert the non-hydride forming organic selenium compounds present in the sample to Se (IV) , so that the volatile hydrogen selenide can be formed.

An alternative and more direct method is electrothermal vaporization (ETV) coupled with ICP-MS detection. This technique has the advantage of using very small sample sizes (typically 5–50 μl), an important consideration when dealing with clinical samples which may be of limited size, and unlike hydride generation does not require lengthy sample preparation procedures. Elimination of interferences is also feasible with this method. With careful optimisation of the temperature program it is possible to control the vaporization of interfering analytes so that they do not arrive at the plasma at the same time as the analyte under investigation, thus reducing the degree of interference. Figure 2 (a) and (b), demonstrate the removal of chlorine and hence elimination of the $^{36}\text{Ar}^{35}\text{Cl}^+$ interference on ^{76}Se .

Similar responses were observed when monitoring the bromine and sodium signals.

At 800°C both signals coincided with the Se signal, but on increasing the temperature to 1200°C vaporization of the interfering species was complete prior to that of the analyte of interest. With this procedure the interference free analysis of selenium using the ^{76}Se and ^{78}Se isotopes is now possible. Further development of the method to improve the accuracy and precision, was implemented by using the procedure of isotope dilution mass spectrometry (ID-MS).

The sample is spiked with a solution containing the enriched ^{76}Se isotope and the $^{76}\text{Se}/^{78}\text{Se}$ ratio is measured and used to calculate the concentration of selenium. Table 4 contains the results from the analysis of a bovine serum certified reference material (NIST 1598) by ETV-ICP-MS, both with and without isotope dilution.

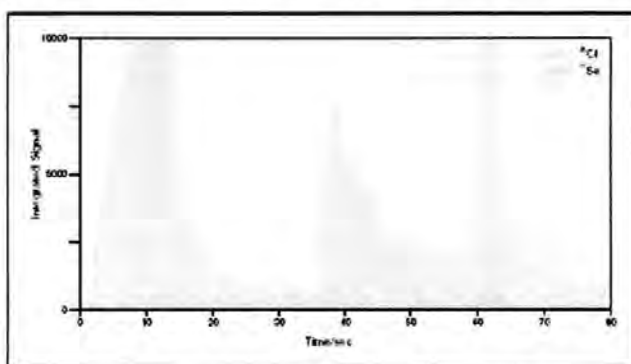


Figure 2 (a): Pyrolysis temperature of 800°C . Overlap of Cl and Se signals

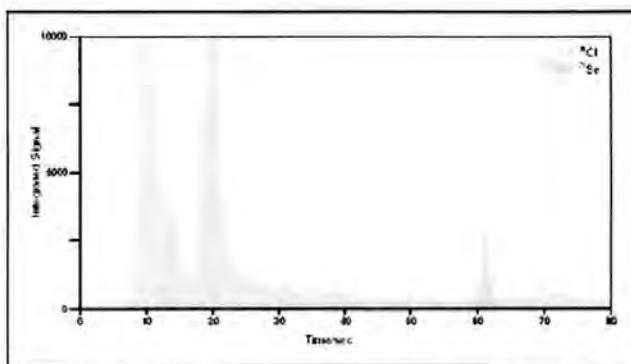


Figure 2 (b): Pyrolysis temperature of 1200°C . Removal of Cl interference

CONTRIBUTED ARTICLES

	Isotope	Concentration (ng g ⁻¹)					
		Replicate 1	Replicate 2	Replicate 3	Mean	SD	RSD %
ETV-ICP-MS	⁷⁷ Se	42.4	40.7	41.3	41.4	0.62	1.49
	⁷⁸ Se	40.4	41.3	40.7	40.8	0.37	0.92
ETV-ICP-ID-MS	⁷⁸ Se/ ⁷⁷ Se	40.85	40.89	40.91	40.88	0.02	0.06

Table 4: Results for the analysis of NIST 1598 bovine serum, containing a certified concentration of 42.4 ± 3.5 ng g⁻¹ selenium

The two procedures have produced very similar results, but the precision with the ETV-ICP-ID-MS method is an order of magnitude better than that achieved with the conventional ETV procedure.

Conclusions

This article has highlighted the importance of trace metal analysis in clinical and biomedical science, as well as the difficulties posed by measurement of trace metals in complex matrices, at biochemically significant levels.

The selenium work reported in this article was first presented in poster form at the European Winter Conference on Plasma Spectrochemistry, 1999, Pau, France. The analysis of whole blood was presented in poster form at the 6th International Conference on Plasma Source Mass Spectrometry, 1998, Durham, UK.

REFERENCES

- H G Sella, H Sigel and A Sigel (eds). *Handbook on Toxicity of Inorganic Compounds*, Marcel Dekker, New York, 1988.
- H Sigel and A Sigel (eds). *Concepts on Metal Ion Toxicity, Vol 20 of Metal Ions in Biological Systems*, Marcel Dekker, New York, 1986.
- H G Sella, H Sigel and A Sigel (eds). *Handbook on Metals in Clinical and Analytical Chemistry*, Marcel Dekker, New York, 1994.
- T W May and R H Wiedmeyer. *Atomic Spectroscopy*, 12 (5), 150-155.
- E Fujimori, Y Tomosue, and H Hariguchi. *Toxicol. J. Exp. Med.*, 1996, 178 (1), 63.
- E Barany, I A Bergdahl, A Shutz, S Skerfving, and A Oskarsson. *J. Anal. At. Spectrom.* 1997, 12, 1005.
- H T Delves, and C E Sieniawska. *J. Anal. At. Spectrom.*, 1997, 12, 987.
- J Riccardi, F Vanhaecke, L Moens and R Dams. *J. Anal. At. Spectrom.*, 1997, 12, 933.
- T Catterick, B Fairman, M Sargent and K Webb. *VAM Bulletin*, 17, 13-15, Autumn 1997.
- T Catterick and B Fairman. *VAM Bulletin*, 17, 16-17, Autumn 1997.
- T Catterick, B Fairman and C Harrington. *J. Anal. At. Spectrom.*, 1998, 13, 1009-1013.
- K Webb, D Carter and V J Barwick. *Metrologia*, in press 1999.
- R S Houk. *Anal. Chem.*, 1986, 58, 97A.
- M Rayman, F R Aboushakra and N I Ward. *J. Anal. At. Spectrom.*, 1996, 11, 61-68.